TRPC Channels in Sensory Systems

Kathryn Quick

A thesis submitted for the degree of Doctor of Philosophy to University College London

Wolfson Institute for Biomedical Sciences
University College London
2011

Declaration

I, Kathryn Quick, confirm that the work presented in this thesis is my own. Where information has been derived from other sources, I confirm that this has been indicated in the thesis.

Abstract

Transient receptor potential canonical (TRPC) channels are a family of non-selective cation channels which have a wide range of physiological functions. In this thesis we used genetic approaches to investigate functional roles of TRPC3, TRPC6

We used the Cre/*lox*P system to delete TRPC3 exclusively from nociceptive neurons, using Nav1.8Cre, and from all dorsal root ganglion (DRG) neurons, using Advillin Cre. Inflammatory pain behavior was attenuated in both TRPC3 conditional null animals but acute mechanical, cold and thermal pain behavior was not affected. Microarray analysis identified a number of dysregulated pathways in the nociceptors of the TRPC3 conditional null mice, providing insights into inflammatory pain pathways.

Given the similarity between TRPC channels we used a TRPC3/TRPC6 global double knockout to further investigate TRPC function. The TRPC3/TRPC6 double knockout mice were found to have attenuated mechanosensation specific to light touch, with no deficits in noxious mechanosensation, due to a reduction of rapidly adapting mechanically activated current in the small-medium DRG neurons. The TRPC3/TRPC6 double knockouts had no deficits in acute thermal or cold pain, or in neuropathic pain. The TRPC3/TRPC6 double knockouts were also behaviourally deaf, confirmed by auditory brainstem recordings. This work indicates a role for TRPC3 and TRPC6 in mechanosensation in sensory neurons and outer hair cells.

Funding

Publications

Papers

Raouf R, **Quick K**, Wood JN. (2010) Pain as a channelopathy. *J Clin Invest* 120(11):3745-52

Figures

xi

Tables

Abbreviations

5-HT	Serotonin
ABR	Auditory brainstem response
Amp	Ampicillin
ASIC	Acid sensing ion channel
ATP	Adenosine triphosphate
BAC	Bacterial Artificial chromosome
BDNF	Brain derived neurotrophic factor
BK	Bradykinin
CaMKI/II	Calmodulin Kinase I/II
cAMP	Cyclic adenosine monophosphate
CCI	Chronic constriction injury
CFA	Complete Freunds' adjuvant
CNS	Central nervous system
COX	Cyclooxygenase
Cre	Cyclization recombinase protein
Cre-deleter	Mouse line expressing Cre globally, including germline cells.
Ct	Cycle threshold
DAG	Diacylglycerol
DNase	Deoxyribonuclease
dNTPs	Deoxyribonucleotide triphosphate
DRG	Dorsal root ganglion
dsDNA	Double stranded DNA
DTA-Nav1.8Cre	Mouse line with ablation of Nav1.8+ve neurons by diphtheria toxin
EGF	Epidermal growth factor
EGTA	Ethylene glycol tetra-aceitc acid
ERK	Extracellular signal related kinases
ES cell	Embryonic stem cell
FSGCS	Focal segemental glomerulosclerosis
GDNF	Glia dervived neurotrophic factor
Gi	Inhibitory Gα protein
GPCR	G protein coupled receptor
Gq	Phospholipase C coupled GPCR pathway

Gs	Stimulatory G-protein
GsMTx-4	Grammostola spatulata toxin inhbiting SACs
GTP	Guanosine triphosphate
IP3	Inositol triphosphate
LTP	Long term potentiation
mGluR	Metabotropic glutamate receptor
mRNA	Messenger RNA
NE	Norepinephrine
Neo^r	Neomycin resistance
NGF	Nerve growth factor
NS	Nociceptive specific
NSAID	Non-steroidal anti-inflammatory drug
OAG	1-Oleoyl-2-acetyl-sn-glycerol (analogue of DAG)
PCR	Polymerase chain reaction
PI3K	Phosphoinositide 3-Kinase
PKC	Protein Kinase C
PLC	Phospholipase C
qRT-PCR	Quantitative reverse transcription PCR
ROC	Receptor operated channel
RVM	Rostral ventromedial medulla
SAC	Stretch-activated channel
SAP	Shrimp alkaline phosphatase
SNL	Spinal nerve ligation
SOC	Store operated channel
TK	Thymidine Kinase
TNFα	Tumour necrosis factor alpha
TRP Channel	Transient Receptor potential channel
TTX	Tetrodotoxin
VGCC	Voltage-gated calcium channel
VGSC	Voltage gated sodium channel
WDR	Wide dynamic range

Terminology for transgenic mouse lines

Abbreviation	Genetic modification
TRPC3 fl/fl	TRPC3 gene includes two loxP sites (no deletion)
TRPC3 fl/fl:Nav1.8Cre	Conditional knockout of TRPC3 in Nav1.8 positive neurons (nociceptors)
TRPC3 fl/fl:AdvCre	Conditional knockout of TRPC3 in Advillin positive neurons (all DRG neurons)
TRPC3$^{-/-}$:TRPC6$^{-/-}$	Global deletion of TRPC3 and TRPC6
TRPC3$^{-/-}$	Global deletion of TRPC3
TRPC6$^{-/-}$	Global deletion of TRPC6

Acknowledgements

Thank you to my supervisor, John Wood, for honest advice and supervision throughout my PhD.

I would like to thank all the members of the lab, both past and present, for their help and advice, particularly Dr Ramin Raouf, Dr Mohammed Nassar and Dr Jing Zhao who have been indispensible for practical help and advice along with motivational pep talks!

Thank you to Professor Jonathan Ashmore, Dr Ruth Taylor and Professor Andy Forge for their work on the auditory brainstem responses and Dr Francois Rugiero, Dr John Linley, Dr Niels Eijkelkamp and Dr James Cox for their relentless work on the TRPC3/TRPC6 double knockouts. Also, thanks to Dr Cruz Miguel Cendan for his early work on the TRPC3 mice and Dr Lucy Bee for excellent proof reading.

Special thanks go to my family and friends, especially Stephanie and Laura for their encouragement and Sam and Mike for keeping me in coffee.

Finally, I thank Tom for his emotional support during my PhD and for never letting me give up.

1 Introduction

1.1 Pain and nociception

Pain is defined by the International Association for the Study of Pain as "An unpleasant sensory and emotional experience associated with actual or potential tissue damage, or described in terms of such damage" (www.iasp-pain.org). Nociception is the process by which tissue-damaging stimuli activate ion channels within sensory neurons. Nociception is exclusively the presence of electrical activity within the relevant sensory neurons; it does not necessarily result in a conscious pain sensation, similarly pain may be experienced without nociception. Nociception is essential for survival, to avoid situations which could cause tissue damage and protect injuries, but pain can outlast the original injury developing into chronic pain.

The British Pain Society defines chronic pain as continuous, long-term, persistent pain extending beyond the time that would be expected for healing. Chronic pain is a major clinical problem; of nearly 50,000 people across 16 European countries 19% suffer chronic pain, of which 36% have inadequate pain control from medication (Gfk NOP British Pain Society Survey, 2005). Many existing analgesics are inadequately effective, as well as having side effects and abuse liabilities; efficacy is limited to making pain more manageable rather than controlling it. Over the past 20 years research for new analgesics has been limited to drugs acting on well-established targets such as cyclooxygenase inhibitors, local anesthetics and opioids. New targets are needed to avoid the side-effects and limitations of current analgesics.

1.2 Nociception and DRG primary afferent neurons

The primary afferent neurons of the somatosensory nervous system convey sensory information from their terminals in peripheral and visceral tissues to the spinal cord. The cell bodies of the primary afferent neurons are contained within the dorsal root ganglion (DRG). There are multiple subtypes of sensory neuron in the DRG which are broadly classified into three groups according to anatomical and functional features, Aβ-fibres, Aδ-fibres and C-fibres, which are further classified into nociceptive and non-nociceptive neurons.
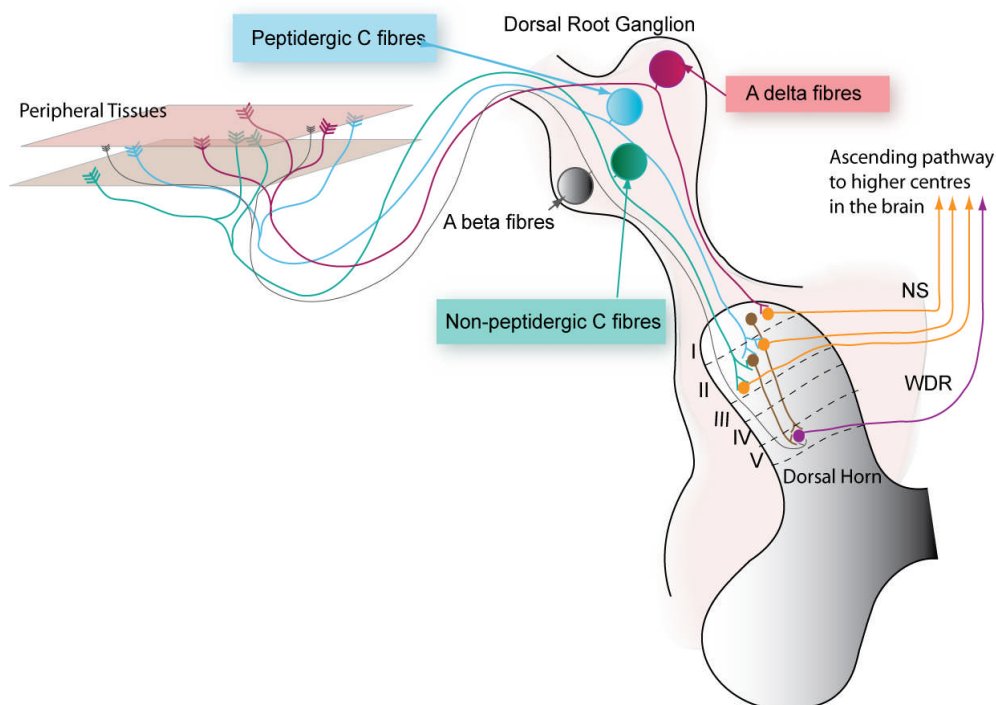
Figure 1.1 The primary sensory neurons and their terminations within the spinal cord.
Primary afferent fibres terminate in laminae I – V of the dorsal horn, synapsing with interneurons, nociceptive specific (NS) neurons and wide dynamic range (WDR) neurons. The laminae of the dorsal hornwhere sensory neurons terminate are labeled. Peptidergic and non-peptidergic C- fibres terminate in lamina II, Aδ-fibres terminare in lamina I and Aβ-fibres terminate in lamina V. The different classes of primary afferent neurons are discussed further in 1.2 (Nociception and DRG primary afferent neurons)

1.2.1 Non- nociceptors

1.2.1.1 Aβ-fibres

Aβ-fibres have nerve endings in the skin which are closely associated with Merkel cells and hair shafts which create highly touch-sensitive areas (see Figure 1.2). The Aβ-fibres terminate in laminas III and IV of the spinal cord and have a fast conduction velocity of 10-30m.sec^{-1}. Conduction velocity is determined by the diameter and degree of myelination of the neuron, hence the large diameter and thick myelination of Aβ-fibres underlies their fast conduction velocity. The majority of Aβ-fibres respond to innocuous stimuli such as light touch, although a small proportion of Aβ-fibres have been shown to transduce noxious stimuli (Lawson, 2002). They are unimodal and show adaptation in their response to a repeated stimulus, which therefore classifies them as non-nociceptive neurons.
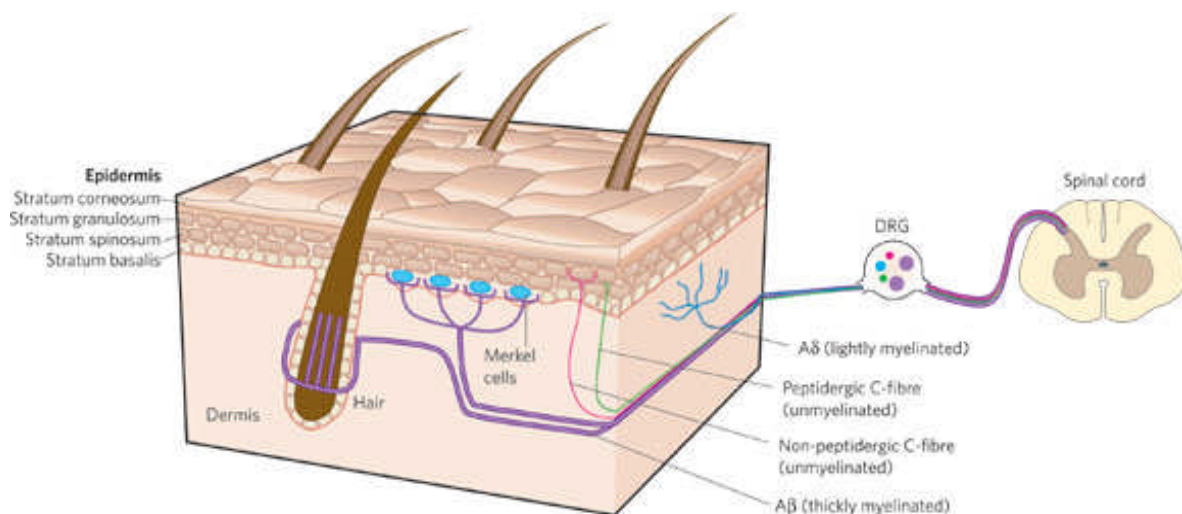
Figure 1.2 Innervation of the skin by somatosensory neurons.

Adapted from (Lumpkin and Caterina, 2007) .

The skin is innervated by Aβ-fibres, Aδ-fibres and C-fibres. Aβ-fibres innervate Merkel cells and hair shafts, Aδ-fibres terminate in the dermis and C-fibres in different epidermal layers. Transduction of the sensory stimulus, and hence the proteins and ion channels required, occur at the terminals of the sensory neurons, in the skin.

1.2.2 Nociceptors

The further two subtypes of sensory neuron are known as nociceptors because they respond to noxious stimuli. A noxious stimulus must be converted into an electrical signal by primary afferent neurons before it is transmitted to higher centres to be perceived as pain. Nociceptors respond to three types of noxious stimuli, mechanical, thermal and chemical which activate the free ending terminals which are mostly found in the skin (MacIver and Tanelian, 1993).

1.2.2.1 Aδ-fibres

Aδ-fibres are medium diameter, lightly myelinated neurons with a conduction velocity of 1.2-10m.sec^{-1}. Aδ-fibres terminate in laminas I and V of the spinal cord and respond to noxious mechanical, thermal and chemical stimuli. Their response to certain stimuli divides the Aδ-fibres into two further categories; Type I fibres are responsive to heat, mechanical and chemical stimuli with a fast conduction velocity and increase their response as the stimulus increases. Type II fibres respond only to thermal and chemical stimuli with a reduced conduction velocity and an adapting response to increased stimulus (Wall *et al.*, 2005).

1.2.2.2 C-fibres

C-fibres are small and unmyelinated, giving them the slowest conduction velocity of the primary afferent neurons at <1.2m.sec^{-1}. C-fibres terminate in laminae I and II of the spinal cord. Most C-fibres, like Aδ-fibres, are polymodal nociceptors responding to noxious mechanical, thermal and chemical stimuli. There is in addition a small subset of C-fibres which transduce only innocuous thermal information (Hunt and Mantyh, 2001).

1.2.3 Silent nociceptors

Nociceptors are classically defined as primary afferent neurons which respond to excessive mechanical or thermal stimuli outside the normal physiological range (Bessou and Perl, 1969;Burgess and Perl, 1967;Van and Gybels, 1972). There is also a sub-population of nociceptors which are typically unresponsive to noxious stimuli (Meyer *et al.*, 1991), the so called "silent" nociceptors (McMahon and Koltzenburg, 1990b). In an experimental model of arthritis initially unresponsive (silent) fibres gained mechanical sensitivity and new receptive

fields were found in the injured area (Schaible and Schmidt, 1988) showing that during ongoing pain states the silent nociceptors can be recruited to enhance the total nociceptive input and contribute to pain and hyperalgesia (McMahon and Koltzenburg, 1990a).

1.2.4 Gene expression in nociceptors

Nociceptors develop from the neural crest stem cells. Initially they all express the nerve growth factor (NGF) tyrosine kinase receptor TrkA and are dependent on NGF for survival (Crowley *et al.*, 1994), but during postnatal development TrkA is down-regulated in approximately 50% of nociceptors. These neurons now begin to express the tyrosine kinase receptor Ret, a component of the glial cell line-derived neurotrophic factor (GDNF) receptor (Molliver et al., 1997;Molliver and Snider, 1997). GDNF-sensitive C-fibres express cell surface glycoconjugates that bind the lectin IB4 and do not synthesise neuropeptides such as calcitonin gene-related peptide (CGRP). The NGF-sensitive C-fibres are peptidergic, synthesising CGRP and also substance P, and do not bind IB4.

The expression pattern of sensory channels and receptors within the peptidergic and non-peptidergic neurons is complex and regulated through a number of pathways. Runx1, a transcription factor, is required to activate expression of a large fraction of channels and receptors including the transient receptor potential channels TRPA1, TRPV1 and the adenosine triphosphate (ATP) gated channel P2X3 (Chen *et al.*, 2006). Runx1 dependent genes can be further divided into i) Ret-dependent, ii) Ret-independent and TrkA- dependent, iii) Ret-independent and TrkA-independent pathways.

The differential expression patterns produce functional differences between the two types of nociceptor. Non-peptidergic nociceptors are more responsive to capsaicin, protons and ATP activation (Dirajlal *et al.*, 2003;Burgard *et al.*, 1999) whereas peptidergic nociceptors have larger heat currents and have more tetrodotoxin (TTX) resistant current (Stucky and Lewin, 1999); TTX is a toxin originating from puffer fish that blocks a subpopulation of voltage-gated sodium channels.

1.2.5 Identification

The different subsets of sensory neurons may be identified using microscopy and immunohistochemistry. Aβ-fibres can be easily identified within the DRG as they are larger and have distinctive thick myelination. C-fibres and Aδ-fibres are not so easily distinguished on size alone but staining with Nissl causes C-fibres to appear as small and dark cells, whereas A-fibres are larger and lighter. Proteins unique to each cell type are also used for immunochemical identification, peripherin is unique to C-fibres and the neurofilament NF200 is unique to A-fibres.

1.2.6 Central projections

The spinal cord has 10 laminae identified by Rexed in 1952 (Rexed, 1952). The 5 most superficial laminae are involved in sensory transduction. Non-peptidergic nociceptors synapse in lamina I and outer lamina II (IIo), whereas peptidergic nociceptors synapse in inner lamina II (IIi). The distinct projection patterns of the two types of nociceptors may play a role in the differing mechanisms of inflammatory and neuropathic chronic pain states (Snider and McMahon, 1998).

1.3 Nociception

1.3.1 Mechanical

Aβ -fibres respond to innocuous mechanical stimuli such as light touch, whereas C-fibres and a subset of Aδ-fibres respond to noxious mechanical stimuli only. Noxious mechanotransduction does not require any specialized organs, instead the mechanically sensitive nociceptors terminate as free nerve endings in visceral organs or the skin, and tellingly, cultured DRG neurons retain their mechanosensitive properties (Drew *et al.*, 2002). Ion channels from several families have been suggested as the mechanosensor for noxious stimuli, including the TRP and epithelial sodium channel (ENaC) families. In culture, many nociceptors display a slowly inactivating current in response to mechanical stimulation (Drew *et al.*, 2004) that is consistent with the slowly adapting nature of primary afferent nociceptors (Lewin and Moshourab, 2004). This mechanically activated current is blocked by gadolinium (Kimitsuki *et al.*, 1996), FMI-43 (Drew and Wood, 2007) and by Ruthenium red (Caterina *et al.*, 1997).

6

Members of the TRP family have been investigated as putative mechanosensors. TRP channels share a number of characteristics with the mechanically-activated currents in DRG neurons. Both are inhibited by gadolinium and ruthenium red, sensitive to extracellular Ca^{2+}, and have non-selective cation permeability (Watanabe *et al.*, 2002;Drew *et al.*, 2002). TRPA1 is present in the inner ear and in small C-fibre nociceptors (Corey *et al.*, 2004;Kobayashi *et al.*, 2005). TRPA1 localises to the sensory endings and stereocilia (Nagata *et al.*, 2005) making it a good candidate for a mechanosensory channel. Corey et al showed that siRNA targeted to TRPA1 is able to decrease transduction currents (Corey *et al.*, 2004) but this is likely an off target effect since TRPA1$^{-/-}$ mice show no decrease in hair cell transduction and have normal hearing (Bautista *et al.*, 2006;Kwan *et al.*, 2006). TRPV4 is expressed in hair cells and Merkel cells (Liedtke *et al.*, 2000) and was originally cloned and implicated in mechanosensation due to its homology to the *Caenorhabditis elegans* mechanosensor OSM-9. Indeed, TRPV4 transcripts are able to reverse the loss of nose touch sensation in OSM-9 mutated *C. elegans* (Liedtke *et al.*, 2003). TRPV4$^{-/-}$ mice exhibit a reduced response to pressure on the tail but no change to von Frey withdrawal thresholds (Suzuki *et al.*, 2003). Although there is some evidence that TRPV4 may be mechanically gated it does not appear to be the only mechanosensor since mechanical sensation is not abolished in TRPV4$^{-/-}$ mice, and moreover TRPV4 appears to be present in only 11% of DRG neurons (Suzuki *et al.*, 2003).

MEC-4, MEC-6 and MEC-10 are members of the DEG/ENaC family and are required for light touch sensation in *C. elegans* (Chalfie and Sulston, 1981). Acid sensing ion channels (ASIC) also belong to this family, and as such, ASIC2 (Garcia-Anoveros *et al.*, 2001;Price *et al.*, 2000) and ASIC3 (Price *et al.*, 2001) are found in mammalian mechanosensory nerve endings. Location and homology to other mechanically sensitive channels has led to ASICs being implicated in mechanosensation, yet both ASIC3$^{-/-}$ and ASIC2$^{-/-}$ DRG neurons have normal mechanically activated currents in culture (Drew *et al.*, 2004). Behaviourally, ASIC3$^{-/-}$ mice have normal acute mechanical withdrawal thresholds assessed by von Frey hairs (Chen *et al.*, 2002;Price *et al.*, 2001). ASICs do not therefore appear to be involved in mechanotransduction in nociceptors but may have other roles in mechanosensation. An in

vitro skin nerve preparation of ASIC2 [-/-] mice showed reduced mechanical sensitivity in low-threshold fibres (Price *et al.*, 2000) suggesting ASIC2 may be involved in light touch sensation. ASIC3^{-/-} mice have reduced responses to high-intensity mechanical and thermal stimuli (Chen *et al.*, 2002), suggesting that ASIC3 could modulate high intensity pain regardless of the modality.

A number of accessory proteins that are essential for mechanotransduction have been identified. MEC-2 is a stomatin-related protein that is required for touch sensation in *C. elegans* but is not itself the mechanically sensitive channel. MEC-2 regulates MEC-4 and MEC-10 and is essential for their mechanical activity (Goodman *et al.*, 2002). Stomatin-Like-Protein 3 (SLP3), a mammalian homologue of MEC-2, appears to have a similar function in mice and as such. SLP3 mutants lose mechanical sensitivity in 35% of their skin mechanoreceptors (Wetzel *et al.*, 2007).

1.3.2 Thermal

1.3.2.1   Heat

There are two types of noxious heat responses that can be classified by their response thresholds. A subset of both C-and Aδ-fibres respond to a moderate threshold of ~43°C, the approximate temperature at which innocuous warmth becomes noxious heat. A smaller percentage of Aδ-fibres are high-threshold, responding to temperatures above 52°C.

Responsiveness to capsaicin is a pharmacological trait of the moderate threshold heat sensitive neurons and this was exploited to be used as part of a cDNA screening assay to identify VR1, later re-termed TRPV1, as a thermosensor (Caterina *et al.*, 1997) . TRPV1 is predominately expressed in trigeminal and dorsal root ganglia, within small – medium diameter neurons and can be activated by capsaicin and temperatures of ~ 45°C (Caterina *et al.*, 1997). TRPV1^{-/-} mice have deficient heat responses in culture and also behaviourally (Caterina *et al.*, 2000). Interestingly the behavioural differences occur with high-threshold noxious heat of >50°C and not at the moderate noxious threshold of ~45°C previously predicted.

Homology searches using the TRPV1 sequence found a second vanilloid receptor that is insensitive to capsaicin but responds to high threshold noxious heat with a threshold of ~52°C (Caterina *et al.*, 1999). This receptor was originally named VRL1 but later re-termed TRPV2. TRPV2 is found mainly in medium-large diameter neurons within the DRG (Caterina *et al.*, 1999), which are IB4 negative and therefore not C-fibres. These properties are consistent with the high thermal threshold Type I Aδ-fibres that Wall and Melzack described (Wall *et al.*, 2005).

Other members of the TRPV family are also implicated in thermosensation. TRPV3 is expressed in keratinocytes and is activated at temperatures above 33°C (Peier *et al.*, 2002b;Xu *et al.*, 2002;Guler *et al.*, 2002). TRPV3$^{-/-}$ mice do not have the preference for warm temperatures (30°C – 38°C) that is shown by wildtype mice (Moqrich *et al.*, 2005). Impaired thermosensation in this temperature range suggests a role for TRPV3 in sensing innocuous warmth. TRPV4 is also activated by warm temperatures in the range of 27°C – 34°C (Guler *et al.*, 2002).

1.3.2.2   Cold

Noxious cold activates Aδ fibres and a subset of C fibres (Simone and Kajander, 1997). Application of menthol to the skin causes a cooling sensation because these cold-sensitive fibres are sensitised or directly activated by menthol (Hensel and Zotterman, 1951). A number of different mechanisms have been proposed for cold transduction including direct activation of a non-selective cation channel, inhibition of background potassium conductance and inhibition of Na-K-ATPase.

Around 7% of cultured DRG neurons respond to cooling (Reid and Flonta, 2001b). These cold-responsive neurons possess a mixed-cation current that is potentiated by menthol, sensitive to extracellular Ca^{2+} and insensitive to amiloride (Reid and Flonta, 2001b). The identity of channels conferring cold sensitivity in DRG neurons were discovered by McKemy et al. using expression cloning and Ca^{2+} imaging (McKemy *et al.*, 2002). A cDNA library was constructed and transfected into HEK293 cells and subsequently calcium imaging was used to look at which cells responded to menthol and cold. A single cDNA was identified and termed CMR1, and this was found to be an orthologue to the TRPM8 channel in humans.

TRPM8 is found in small diameter neurons in the DRG, which agrees with previous data that the majority of noxious cold sensitive neurons are C-fibres (Leem *et al.*, 1993a;Leem *et al.*, 1993b). TRPM8^{-/-} mice have impaired cold sensation, having no strong preference for a warmer environment as opposed to an aversive cooler environment (Dhaka *et al.*, 2007). It has also been observed that nociceptive responses to cold are reduced, although not abolished in TRPM8^{-/-} mice (Dhaka *et al.*, 2007) suggesting that TRPM8 may also have a role in noxious cold.

TRPM8 was also identified as a cold sensor in DRG by Peier et al using a bioinformatic approach (Peier *et al.*, 2002a). The same group additionally identified another cold-sensitive TRP-like channel that is found in nociceptors, ANTKM1 (later termed TRPA1) (Story *et al.*, 2003). TRPA1 is mainly expressed in sensory neurons that are activated by capsaicin and are insensitive to menthol (Story *et al.*, 2003), indicating that TRPM8 and TRPA1 exist in two distinct populations of cold-sensitive neurons. Jordt et al found that TRPA1 can also be activated by mustard oil, however this study disputed the cold sensitivity of the channel (Jordt *et al.*, 2004). Two behavioural studies using TRPA1^{-/-} mice have failed to resolve this contention, with one group reporting no difference in cold sensitivity (Bautista *et al.*, 2006) and the other showing a small reduction in noxious cold responsiveness (Kwan *et al.*, 2006). It has been suggested that the reported cold sensitivity of TRPA1 is actually an indirect effect of the increased intracellular Ca^{2+} concentration upon cooling (Babes *et al.*, 2006;Zurborg *et al.*, 2007), however, Karashima et al have shown Ca^{2+} independent gating of TRPA1 by cold. This study also reported reduced behavioural responses to noxious cold in TRPA1^{-/-} mice (Karashima *et al.*, 2009).

From the current evidence it is suggested that TRPM8 is mainly involved in sensing innocuous cold and TRPA1 in noxious cold sensation. TRPM8 is activated at temperatures below 23°C which is in the cool, but not unpleasant, temperature range whereas TRPA1 is activated at around 17°C which is considered noxious cold. Furthermore, TRPV1, a marker for nociceptors, is co-expressed in 97% of TRPA1 neurons but in only 50% of TRPM8 neurons (Story *et al.*, 2003). In support of a potential role in noxious cold sensation TRPA1

has been found to be upregulated in inflammation and is thought to contribute to cold hyperalgesia (Obata *et al.*, 2005).

To further complicate the issue there are furthermore a number of cold sensitive peripheral neurons which express neither TRPM8 nor TRPA1 (Babes *et al.*, 2006;Munns *et al.*, 2007). Inhibition of potassium channels may also be involved in cold sensitivity, causing depolarization and activation of cold sensitive neurons (Reid and Flonta, 2001a;Viana et al., 2002). Using 4-AP to block voltage-gated potassium channels that may be acting as an 'excitability brake' can induce cold sensitivity in previously unresponsive DRG neurons (Munns *et al.*, 2007) providing a TRP-independent mechanism of cold transduction.

1.3.3 Inflammatory pain

Inflammation is a reaction to injury or irritation that is characterized by redness, pain and swelling. The tissue damage and inflammation causes the release of a large number of molecules both within the periphery and also centrally where they activate and sensitise peripheral neurons and central pain circuits. These pain mediators are responsible for the initiation and maintenance of thermal and mechanical hyperalgesia that accompanies, and sometimes outlasts, inflammation.

1.3.3.1　　　ATP

Levels of ATP and ATP gated receptors, P2X receptors, are increased after inflammation (Xu and Huang, 2002). Of the P2X receptors P2X3 is exclusively expressed in nociceptors (Chen *et al.*, 1995) where its homomeric form is the main type of ATP gated receptor (Souslova *et al.*, 2000) . P2X3$^{-/-}$ mice have reduced formalin induced pain behaviour in both the acute and inflammatory phases (Souslova *et al.*, 2000) suggesting a role of these receptors in inflammatory pain that has been confirmed by pharmacological block (Tsuda *et al.*, 1999;Zhong *et al.*, 2001).

1.3.3.2　　　Protons

Inflammation also causes a drop in pH, and the excess protons that result can activate a number of channels including ASICs. ASIC1b and ASIC3 subunits are almost exclusively expressed on peripheral sensory neurons (Waldmann *et al.*, 1997) and are up regulated in

inflammatory conditions (Duan *et al.*, 2007). ASIC antagonists reduce complete Freund's adjuvant (CFA) induced thermal and mechanical hyperalgesia, further supporting a role of these channels in inflammatory pain (Dube *et al.*, 2005). However, results from transgenic animal studies have produced conflicting results, with ASIC3$^{-/-}$ mice exhibiting increased, decreased or no change in hyperalgesia following inflammation (Price et al., 2001;Sluka et al., 2003;Staniland and McMahon, 2008). Low pH is also able to sensitise TRPV1 channels by shifting the temperature response curve such that TRPV1 is activated at physiological body temperature (Tominaga *et al.*, 1998). The pharmacological properties of the proton "activated" current cannot fully account for proton-evoked pain responses. Thus whilst ASICs and TRPV1 may play an important role in proton-evoked pain, this role is likely to be modulatory and/or not exclusive.

1.3.3.3 Bradykinin

Bradykinin (BK), a peptide that is released during inflammation, directly activates nociceptors via two G-protein coupled receptors (GPCRs) coupled to PLC, B1 and B2 (Inoue and Ueda, 2000). The B2 receptor is activated by BK itself whereas B1 is activated by des(arg)BG a major metabolite of BK. Activation of these receptors produces Inositol triphosphate (IP3) and diacylglycerol (DAG), leading to stimulation of protein kinase C (PKC) which phosphorylates cation channels, ultimately resulting in depolarization. B2 receptors are constitutively expressed in a wide range of tissues including sensory neurons, whereas B1 receptor expression increases following inflammation and tissue damage (Regoli and Barabe, 1980). The B1 and B2 receptor have different roles in inflammatory pain, B2 receptors are necessary for the development of thermal hyperalgesia following carrageenan-induced inflammation (a model of acute inflammatory pain) but has no effect on chronic/persistent forms of hyperalgesia (Boyce *et al.*, 1996). Conversely, B1$^{-/-}$ mice have attenuated hyperalgesia in CFA, confirmed by pharmacological techniques (Fox *et al.*, 2003;Pesquero *et al.*, 2000).

1.3.3.4 Neurotrophins

A number of neurotrophins are released during inflammation including NGF (Donnerer *et al.*, 1992;Woolf *et al.*, 1994). Administration of exogeonous NGF produces hyperalgesia further supporting a role in inflammatory pain (Lewin *et al.*, 1993;Lewin *et al.*, 1994). NGF acts

through TrkA receptors, activating intracellular signalling cascades including MAPK pathways. NGF is able to sensitise peripheral neurons and induce changes that lead to central sensitisation (Lewin *et al.*, 1993). NGF increases expression of substance P , CGRP and also TRPV1 causing thermal hyperalgesia (Bevan and Winter, 1995). Brain dervived neurotrophic factor, BDNF, is also upregulated in inflammatory pain states in an NGF dependent manner, however it's role in inflammatory pain is unclear.

1.3.3.5 Histamine

Histamine is released following the degranulation of mast cells during inflammation and can act as a neurotransmitter. H1, H2 and H3 receptors are activated by histamine and are expressed throughout the central nervous system (CNS). Knockout of H1 or H2 leads to higher pain thresholds in both basal and inflammatory states (Mobarakeh *et al.*, 2000;Mobarakeh *et al.*, 2006). Antagonists of H1 receptors have also been shown to decrease inflammatory pain (Olsen *et al.*, 2002). H3 activation, however, attenuates both nociceptive behaviours and oedma in inflammatory pain (Cannon *et al.*, 2007), conflicting with the actions of histamine on H1 and H2 receptors. It has been found that H3 is not activated during inflammatory pain models including the formalin test (Cannon *et al.*, 2007) which may explain these results.

1.3.3.6 Serotonin

Serotonin, also known as 5-HT, activates many different receptor subtypes including the 5HT3 receptor which is expressed along C and A- delta fibres. Injection of exogenous serotonin causes pain that can be attenuated by 5HT3 receptor antagonists, suggesting a possible role in nociception (Suzuki *et al.*, 2004). 5-HT3R$^{-/-}$ mice show reduced pain behaviours in some inflammatory pain models but not others (Zeitz *et al.*, 2002). The 5HT3R may therefore contribute to nociceptive processing in a modulatory role.

1.3.3.7 Substance P

Substance P is present in a sub-population of small sensory neurons and its release is increased in inflammation, sensitising sensory neurons (Lembeck *et al.*, 1981). Mice deficient in the substance P receptor, NK1, show reduced mechanical hyperalgesia and oedema during inflammation (Kidd *et al.*, 2003).

13

1.3.3.8 CGRP

CGRP is expressed in DRG neurons (Gibson *et al.*, 1984), and in a significant proportion it co-localises with substance P. Up-regulation of CGRP is characteristic of inflammatory diseases and has been shown in a number of inflammatory pain models (Smith *et al.*, 1992;Hanesch *et al.*, 1993). The number of CGRP positive neurons increases during inflammation, indicating not only increased CGRP synthesis but also activation of CGRP synthesis in neurons that would not normally produce this peptide (Hanesch *et al.*, 1993).

1.3.3.9 Prostglandins

Prostaglandins (PG) are synthesised from arachidonic acid, which is released upon tissue damage and inflammation, by COX- 1 and COX- 2. Inhibition of these enzymes is the dominant mechanism of analgesic action by non-steroidal anti-inflammatory drugs (NSAIDs). The prostaglandin receptors EP1 – 4 are G protein coupled receptors, acting through Gs to activate protein kinase A (PKA). Prostaglandins are able to sensitise peripheral neurons through sensitisation of TRPV1 (Moriyama *et al.*, 2005) and voltage-gated sodium-channels (VGSC). Prostaglandins also have central actions in the spinal cord, seen when PG are intrathecally administered (Uda *et al.*, 1990), the mechanisms of this central sensitisation are unclear.

1.3.3.10 Cytokines

Cytokines are released by immune cells and glial cells but also directly by sensory neurons during inflammation . The cytokine cascade initiated by the early generation of TNFα and IL-1β leads to production of further downstream cytokines and other mediators such as NO, ATP and the complement pathway. TNFα and IL1-β are able to produce pain in vivo in both animals and man (Sommer and Kress, 2004) acting directly on the peripheral terminals of nociceptors (Rueff and Mendell, 1996). Antisera not only to TNFα and IL1-β, but also to NGF, are able to block this hyperalgesia, suggesting a large proportion of their actions are mediated through NGF (Safieh-Garabedian et al., 1995;Woolf et al., 1997). The long-term changes in behaviour induced by cytokines require alterations in gene transcription and protein expression but TNFα and other upstream cytokines also produce very rapid changes in neuronal excitability which arise from direct effects on ion channel properties. For example, TNFα produces hyperalgesia by acting through TNFR1 (Sommer et al., 1998) to

activate a number of pathways, including p38 MAPK , leading to phosphorylation of TTX-resistant sodium channels and TRPV1 (Jin and Gereau, IV, 2006) which enhances the excitability of the peripheral nociceptors.

1.3.4 Neuropathic pain

Neuropathic pain is pain caused by disease, damage or dysfunction in the nervous system, usually in the periphery. Sufferers may experience spontaneous pain as well as hyperalgesia, increased sensitivity to a noxious stimulus, and allodynia, pain produced by a normally innocuous stimulus. Neuropathic pain leads to change in gene expression and neuron excitability in the spinal cord and peripheral nerves.

Nerve damage causes injured and uninjured primary afferents to fire ectopically resulting in an afferent barrage of inputs into the spinal cord (Chul Han *et al.*, 2000). This afferent barrage is the likely cause of spontaneous pain experiences and also the trigger for central changes in the spinal cord and the brain. The first event triggering the peripheral changes may include the loss of trophic support in the form of GDNF, NGF and other similar molecules. Trophic factors are usually taken up by sensory endings and retrogradely transported to the cell soma but this process is lost when nerve damage occurs. Growth factors are vital for neuronal development and are also thought to be neuroprotective (Huang and Reichardt, 2001). Administration of GDNF to the cell soma is able to reverse neuropathic pain and reduce related ectopic discharges in animal models of neuropathic pain (Boucher *et al.*, 2000) highlighting it's importance in normal neuronal function. The block of axonal trafficking also causes an accumulation of voltage gated sodium channels, which determine excitability, the excess channels are then able to insert in erroneous sites such as neuromas and areas of demyelination leading to hyperexcitability (Kretschmer T, 2002). Degeneration of nerves can occur at the injury site leading to release of cell contents including inflammatory mediators and other signalling molecules which can act not only on the injured afferent but also on adjacent non-injured neurons.

Novel signals, loss of trophic support and other changes result in alterations in neuron gene expression profiles (Costigan *et al.*, 2002). Genes involved in apoptosis, neurodegeneration and neuroinflammation are found to be up regulated in injured DRG cells, consistent with

15

increased apoptosis and cell death in the spinal cord and DRG after injury (Himes and Tessler, 1989).

A number of genes which are able to directly or indirectly alter excitability are also differentially regulated in injured DRGs and spinal cord. VGSCs are important in determining the excitability of a neuron and a number of VGSCs are found to have altered expression after nerve injury; Nav1.8 is found to be down-regulated and Nav1.3 upregulated as pain hypersensitivity in neuropathic pain develops (Black *et al.*, 1999;Dib-Hajj *et al.*, 1996). Nav1.3 shows faster recovery following inactivation which may facilitate repetitive firing at lower thresholds when it is expressed de novo in injured DRG neurons, leading to ectopic and spontaneous firing. *In vivo* treatment with antisense to Nav1.8 mRNA substantially reduced neuropathic pain (Lai *et al.*, 2002), however, knockout of Nav1.8 had no effect on neuropathic pain, nor complete deletion of Nav1.8 expressing neurons casting doubt on the involvement (Kerr *et al.*, 2001;Abrahamsen *et al.*, 2008).

The α2δ1 subunit of voltage gated calcium channels, which is important for function and expression of the channel, is upregulated in neuropathic pain models (Luo *et al.*, 2001). This upregulation is correlated with development and maintenance of allodynia (Li *et al.*, 2004). The α2δ1 subunit is also the binding site for gabapentin (Gee *et al.*, 1996). Gabapentin and analogues such as Pregabalin have analgesic properties in both the clinic and also animal models of neuropathic pain (Tanabe *et al.*, 2009;Tolle *et al.*, 2008;Field *et al.*, 2006) which further supports α2δ1 contribution to neuropathic allodynia .

Nerve injury will also result in an inflammatory reaction, either in response to the infection or autoimmune disorder causing the neuropathy or to the cellular debris resulting from cell death associated with neuropathy. The release of proinflammatory mediators plays a criticial role in the development and maintenance of neuopathic pain (Bennett, 1999;Schafers *et al.*, 2003;Cui *et al.*, 2000). Bradykinin is a potent inflammatory mediator which acts through the B1 or B2 receptors to increase intracellular Ca^{2+}. In nerve-injured mice B1 receptor expression increases and there is also a phenotypic switch of the cells responsible for BK signalling. In naive mice BK signalling occurs through non-myelinated fibres whereas after

nerve injury B1 receptors are laregely found on myelinated neurons and satellite cells (Rashid *et al.*, 2004).

1.3.5 Central Processing

Noxious stimuli are transmitted from primary afferent nociceptors to the brain via the dorsal horn of the spinal cord. The dorsal horn is divided into 6 laminae, labelled I – VI from outermost inwards. Most nociceptive Aδ-and C-fibres terminate in the superficial lamina I and lamina II whereas Aβ-fibres innervate the deeper laminae III-VI (Todd, 2002). The nociceptors can be further divided on the basis of their peptidergic content and site of termination with peptidergic C-fibres terminating in lamina I and outer lamina II, non-peptidergic C-fibres terminating in inner laminae II and finally Aδ-fibres terminating mainly in lamina I. The dorsal horn itself has a number of different neuronal cell types that the primary afferent fibres can synapse with; nociceptive-specific (NS) cells for example are mostly found superficially and synapse exclusively with Aδ- and C-fibres. NS cells respond only to high threshold stimuli. Proprioceptive cells receive input from Aβ cells only, and respond to touch. Wide dynamic range (WDR) neurones receive input from all three types of sensory fibre and hence respond to stimuli ranging from light touch to noxious pressure, heat and chemicals. Excitatory and inhibitory interneurons within the spinal cord can also act to increase or decrease the responses of NS and WDR cells.

Peripheral sensory neurons communicate with spinal neurons using a variety of neurotransmitters. Glutamate is the major excitatory neurotransmitter found throughout the nervous system and activates post-synaptic NMDA, AMPA and mGLuR receptors in the spinal cord. Other neurotransmitters include BDNF, which is released by Aδ-fibres and some C-fibres, substance P and CGRP, which are also released by C-fibres.

Output from the dorsal horn is transferred to higher centres of the brain by spinal projection neurones along several ascending pathways including the spinothalamic and spinoparabrachial. The spinobrachial pathway projects from the superficial lamina of the dorsal horn to the parabrachial area and periaqueductal grey whereas the spinothalamic tract originates in the deeper laminae and project predominantly to the thalamus.

17

Higher centres such as the rostroventral medulla (RVM) can modulate dorsal horn activity through descending inhibition and descending facilitation. Descending pathways from the RVM are predominantly facilitatory and act via the release of 5-HT onto 5-HT$_3$ receptors in the spinal cord. Depletion of spinal 5-HT attenuates the behavioural hypersensitivity normally seen after nerve ligation (Rahman *et al.*, 2006). Descending inhibition involves the release of norepinephrine (NE) in the spinal cord from brainstem nuclei. The NE acts mainly on α$_2$-adrenoceptors in the spinal cord and inhibits transmitter release from primary afferent terminals which suppresses the firing of the projection neurons in the dorsal horn (Fleetwood-Walker *et al.*, 1985). Descending modulatory pathways, be they inhibitory or facilitatory, can undergo plastic changes in chronic pain states. Studies after peripheral inflammation have shown an increase in descending noradrenergic inhibition (Stanfa and Dickenson, 1994) together with enhanced efficacy of α$_2$-adrenoceptor agonists (Mansikka and Pertovaara, 1995)

Nociceptor activity can induice plastic changes in the dorsal horn which plays an important role in inflammatory hyperalgesia and neuropathic pain. Repetitive firing of C fibres amplifies the dorsal horn response, a phenomenom known as wind-up which is dependent on the removal of the Mg^{2+} block from the pore of the NMDA receptor. NMDA receptor activation causes a large influx of Ca^{2+} ions into the neuron which initiates intracellular signalling cascades that activate various effectors. nNOS, CaMKI/II and ERK are a few of these effectors and can promote long-term potentiation (LTP) which is an abrupt and sustained increase in the efficiency of synaptic transmission and results in elevated responsiveness and activity of dorsal horn neurons, termed central sensitisation. LTP induces long lasting changes which, unlike wind-up, persist after the duration of the stimulus.

1.3.6 Voltage-gated sodium channels

Voltage-gated sodium channels (VGSC or Na$_v$) are transmembrane proteins that allow the rapid influx of sodium ions that underlie the depolarizing upstroke of action potentials (Catterall, 2000). VGSCs typically open rapidly in response to membrane depolarizations and also have a fast-inactivation caused by a cytoplasmic loop blocking the pore of the channel (West *et al.*, 1992). The functional unit of the VGSC is a 220-260kD α subunit which forms

the transmembrane helices, including the pore and voltage sensor. The α subunit alone is sufficient for functional sodium currents, however auxillary β subunits associated with and modulate the current and/or stabilization and localization of the α subunit (Isom, 2001).

VGSCs can be divided into two groups based on their sensitivity to tetrodotoxin (TTX). Na_v 1.1, 1.2, 1.3, 1.6 and 1.7 are TTX sensitive and $Na_v1.5$, Na_v 1.8 and $Na_v1.9$ are TTX resistant. Nine α subunits have been cloned in mammals ($Na_v1.1 – Na_v1.9$) and 4 auxillary β subunits. Na_v 1.7, 1.8 and 1.9 are expressed in sensory neurons where they play a role in nociception.

Na_v 1.7, a TTX-S channel, is expressed at high levels in rodent and human DRG and sympathetic ganglia, especially in C-fibres. Several pain conditions have been linked to Nav1.7 in humans which are reviewed in (Raouf *et al.*, 2010). A mutation in the SCN9A leading to a non-functional channel causes congenital insensitivity to pain, both thermal and mechanical (Cox *et al.*, 2006).Conversely, a gain of function mutation results in primary erythermalgia, a pain disorder characterised by severe burning pain of extremities (Yang *et al.*, 2004). In a nociceptor-specific knock-out of Na_v 1.7 the mice were found to have reduced mechanical and thermal pain in both acute and inflammatory conditions (Nassar *et al.*, 2004).

$Na_v1.8$, a TTX-R channel, is expressed almost exclusively in the subpopulation of small-diameter sensory neurons important in nociception (Akopian *et al.*, 1996) and is important in acute and inflammatory pain function shown by studies with $Na_v1.8$ null mice (Akopian *et al.*, 1999). The role of $Na_v1.8$ in neuropathic pain states remains controversial. Studies with $Na_v1.8$-null mice have concluded there is no role in neuropathic pain (Akopian *et al.*, 1999) but small interfering RNAs which knock-down $Na_v1.8$ are able to reverse the mechanical allodynia resulting from CCI in rats (Dong *et al.*, 2007).

$Na_v1.9$, another neuronal TTX-R channel, is also expressed in small-diameter DRG neurons (Tate *et al.*, 1998). $Na_v1.9$, like $Na_v1.7$ and $Na_v1.8$, appears to have a role in inflammatory pain shown by $Na_v1.9$ null mice (Priest *et al.*, 2005) but no role in neuropathic pain (Amaya *et al.*, 2006).

The role of a fourth neuronal Na_v channel in nociception has been proposed. $Na_v1.3$ is a TTX-S channel that is expressed in developing neurons but is down-regulated in mature neurons (Beckh *et al.*, 1989). Following axotomy or inflammation $Na_v1.3$ mRNA and protein are significantly up-regulated suggesting that this change of expression may contribute to altered neuron excitability. However, $Na_v1.3$ null mice exhibit normal pain behaviours in acute, inflammatory and neuropathic pain conditions (Nassar *et al.*, 2006).

1.4 TRP Channels

The transient receptor potential (TRP) channels are the second largest family of cation channels in mammals. TRP channels are expressed and function in a great variety of multicellular organisms, including worms, Drosophila, zebrafish, mice and humans. The discovery of this family of channels came from the study of Drosophila photoreceptors. A mutant fly had a transient receptor potential in the light-induced current and lacked a Ca^{2+} entry mechanism, the gene responsible for the phenotype was a channel protein, the TRP channel (Montell and Rubin, 1989;Harteneck et al., 2000). TRP channels are identified by sequence homology as their functions are disparate and often unknown. The TRP superfamily is broadly divided into groups 1 and 2, making 7 subfamilies of TRP channels in total. The composition of the TRP superfamily in worms, flies, mice and humans is shown in Table 1.1.

	Worms	Flies	Mice	Humans
TRPC	3	3	7	6[1]*
TRPV	5	2	6	6
TRPM	4	1	8	8
TRPA	2	4	1	1
TRPN	1	1	0	0
TRPP	1	1	3	3
TRPML	1	1	3	3
Total	**17**	**13**	**28**	**27**

Table 1.1 Composition of TRP superfamily in worms, flies, mice and humans

(*, TRPC2 is present but a pseudogene in humans)

The evolutionary tree for TRP channels is shown in Figure 1.3, sequence identity can be as low as 20% but all TRP channels form cation-permeable channels with six-transmembrane domains and polymodal activation properties. The TRPs include several notable sequence elements and domains, the largest region of sequence homology spans the 6 transmembrane segments, including the pore loop situated between the 5th and 6th transmembrane segments. TRPC, TRPM and TRPN channels also contain a 23-25 amino acid TRP domain at the C-terminal end with two highly conserved portions – TRP box 1 and TRP box 2 (Figure 1.3).
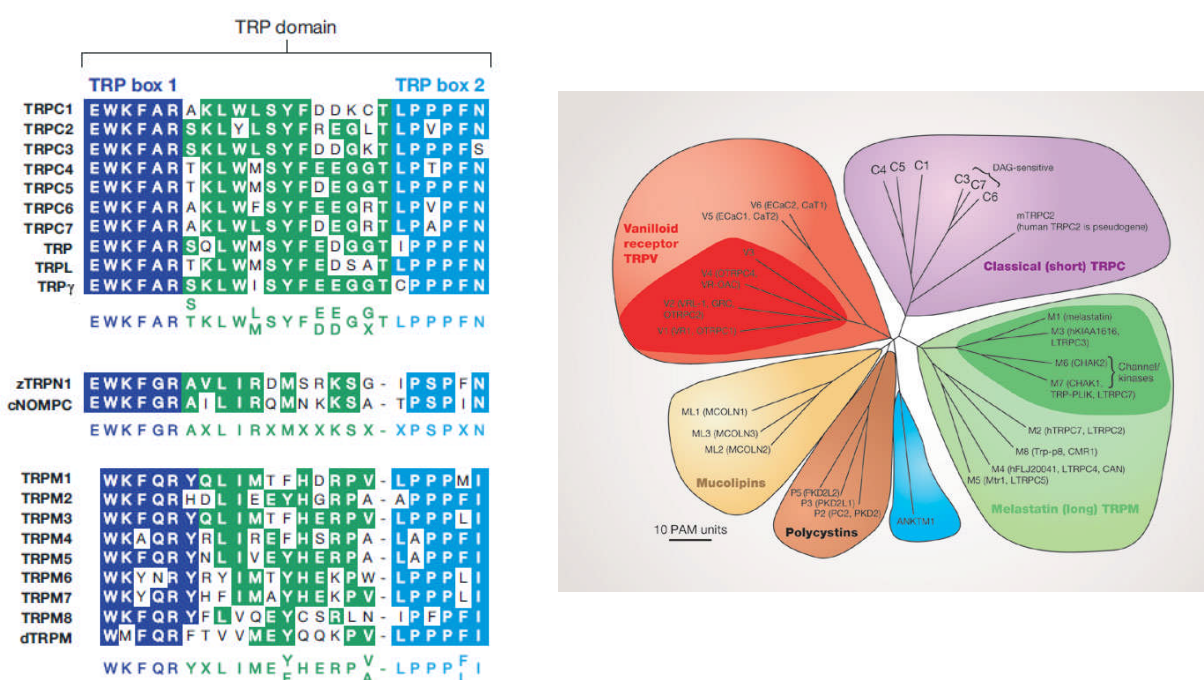
Figure 1.3 The TRP domain and evolutionary tree of mammalian TRP channels

The evolutionary distance is shown by the branch length is point accepted mutations (PAM) units, which is the mean number of substitutions per 100 residues.(Venkatachalam and Montell, 2007)

1.4.1 Structure of TRP channels

The structure of TRP channels has been elucidated using hydrophobicity analysis (Phillips *et al.*, 1992) and epitope immunocytochemistry (Vannier *et al.*, 1998). The channel has a tetrameric structure with each of the four subunits contributing to the channel functionality. The consensus structure of each subunit consists of six transmembrane domains, similar to that of voltage gated Ca^{2+} channels (VGCC), illustrated in Figure 1.4. Like a VGCC,

transmembrane domains 5 and 6 of the TRP channel is connected by a large loop which contains a motif essential to channel function, this is the proposed pore of the channel (Voets and Nilius, 2003). The N and C termini of the protein are intracellular and contain domains that are important for membrane trafficking and binding of modulators such as calmodulin (Tang *et al.*, 2001).
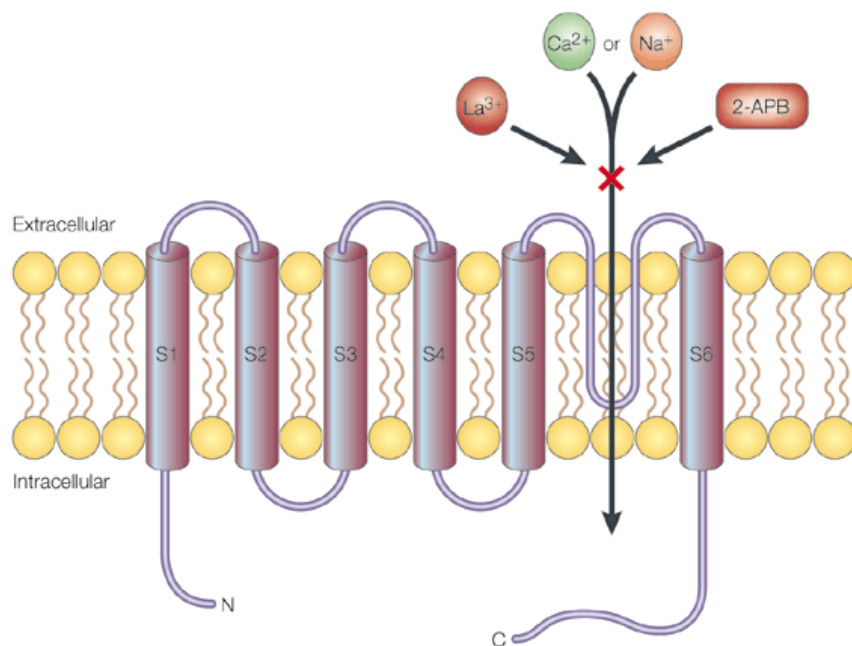
Figure 1.4 Structure of TRP channels

(Clapham et al., 2001;Clapham, 2003)

1.4.2 Transient Receptor Potential Canonical Channels

The TRPC family contains seven proteins that can be divided in to four subsets based on amino acid sequence similarity. The mammalian TRPCs include three to four ankyrin repeats at the N terminus. TRPC1 and TRPC2 form two individual groups, TRPC 3, 6 and 7 together forms a third group and the fourth and final group consists of TRPC4 and 5. Humans express only six TRPC proteins as TRPC2 is a pseudogene, in mice and rats TRPC2 has been linked to pheromone sensing (Hofmann *et al.*, 2002).

1.4.3 Properties of TRPC channels

Although some of the TRPC proteins, such as TRPC1, are ubiquitously expressed throughout all tissues all TRPC receptors are expressed at some level in the nervous system and some, for example TRPC3, are highly enriched in neurons. All TRPC channels are nonselective cation channels although there are differences in the permeabilities of Ca^{2+} relative to Na^+ and other cations, summarised in Table 1.2.

Gene Name	Selectivity $P_{Ca}:P_{Na}$	Proposed mode of activation	Expression	Function
TRPC1	Non-selective	SOC	Heart, brain, testis, ovaries	Ca^{2+} homeostasis, EPSC in purkinje cells
TRPC2	2.7	SOC, DAG	VNO, testis	Pheromone response, acrosome reaction
TRPC3	1.6	SOC, DAG, exocytosis	Brain, DRG, smooth muscle	I_{BDNF}, EPSC in purkinje cells,
TRPC4	7 (>100^3)	SOC	Brain, endothelia, adrenal gland, retina, testis	Vasorelaxation, neurotransmitter release
TRPC5	9.5	SOC	Brain	Neurite extension
TRPC6	5	DAG	Lung, brain, DRG, smooth muscle	Myogenic response,
TRPC7	1.9	SOC, DAG	Eye, heart, lung	Ca^{2+} signalling in keratinocytes

Table 1.2 Mammalian TRPC channel properties.

Adapted from (Montell, 2005).

SOC, store-operated channel, VNO, Vomeronasal organ, EPSC, excitatory postsynaptic potential.

23

TRPC channels are commonly activated through phospholipase C (PLC) dependent pathways, although the mechanisms thorough which stimulation of PLC leads to the activation of the different members of the TRPC family are not yet fully understood. It has been suggested that release of Ca^{2+} from internal stores, DAG production or an exocytotic mechanism may be responsible.

TRPC channels show a moderate selectivity for Ca^{2+} relative to Na^+, thus their activation may be able to modulate a host of secondary cascades and intracellular signalling in non-excitable cells, leading to cell depolarization. Under certain conditions, TRPC1, TRPC4 and TRPC5 can be activated by the emptying of intraceullular calcium stores mediated by IP3, whilst TRPC3, TRPC6 and TRPC7 are instead activated by DAG (Hofmann *et al.*, 1999).

1.4.4 Modulation of TRPC channels

The tetrameric structure of TRPC channels lends itself to multimerization hence ion channel properties become a function of their composition. Co-expression of TRPC channels and FRET analysis have shown that heteromeric channels form between two groups of TRPC channels, TRPC1, -4, -5 and TRPC -3, -6, -7 (Hofmann *et al.*, 2002;Goel *et al.*, 2002). However an interacting protein, STIM1, is able to promote cross-group heteromultimerizations (Yuan *et al.*, 2007). The same studies showed that TRPC2 does not interact with any other TRPC channels. Novel combinations of TRPC subunits have been found in embryonic brain involving more than two types of TRPC subunit (Strubing *et al.*, 2003). Multimerization is not restricted to the TRPC subunits, TRPC1 is able to form a heteromeric channel with another member of the TRP family, TRPP2 (Zhang *et al.*, 2009). The formation of many different channel types could be utilized to alter channel permeability and selectivity within different cell types depending on the composition of subunits present.

The role of TRPC channels within calcium signalling necessitates the interactions with Ca^{2+} signalling complexes that are assembled in plasma membrane microdomains. Homer proteins are scaffolds that bind Ca^{2+} signalling proteins and play a central role in Ca^{2+} signalling. TRPC channels have a Homer binding motif PPXF in their C terminus which mediates formation of a TRPC channel – Homer – IP_3R complex. The formation of this complex has been shown to regulate TRPC1 gating (Yuan *et al.*, 2003) and also translocation of TRPC

channels to the membrane (Kim *et al.*, 2006). Caveolin is also a scaffold protein that aids translocation of TRPC channels. TRPC1 is able to bind to caveolin at both the N and C terminus aiding the transport of TRPC1 to the plasma membrane (Brazer *et al.*, 2003).

In addition to this scaffolding role, protein- protein interactions of the TRPC family can also directly regulate channel activity, and particularly the Src kinase family have been implicated in the regulation of TRPC3 and TRPC6. Fyn, a Src kinase, interacts with TRPC6 and modulates TRPC6 activity via tyrosine phosphrylation (Hisatsune *et al.*, 2004) and Src kinase is obligatory for the activation of TRPC3 by muscarinic receptors (Vazquez *et al.*, 2004).

Another general regulatory mechanism of TRPC channels is exocytotic insertion and retrieval of the channels from the plasma membrane. TRPC3 interacts with the SNARE proteins VAMP2 and SNAP which aid the translocation of TRPC3 to the plasma membrane (Singh *et al.*, 2004). TRPC5 is translocated to the plasma membrane via a different mechanism, involving PI3K, Rac1 and PIP5K (Bezzerides *et al.*, 2004). TRPC6 is also reportedly regulated by exocytosis (Cayouette *et al.*, 2004), which may be linked to MxA a member of the dynamin family (Lussier *et al.*, 2005).

Calmodulin is important in TRP channel regulation in Drosophila where it negatively regulates TRP and TRPL channels. Calmodulin binds to the C-terminus of all TRPC channels (Tang *et al.*, 2001) and has been shown to regulate activation and inactivation of TRPC4 and TRPC1 respectively (Tang *et al.*, 2001;Singh *et al.*, 2002). Calmodulin is also able to interact with TRPC channels in coordination with other proteins such as Enkutin and PI3K.

1.4.5 The TRPC3/6/7 subfamily

The TRPC3/6/7 group of the TRPC family share 70-80% homology. Although TRPC3 is the most thoroughly characterised amongst the group of TRPC channels, initial studies into TRPC6 and TRPC7 showed very similar results suggesting that the group shares activation and functional properties.

All three members of the TRPC3/6/7 group are expressed to varying degrees in the CNS. TRPC3 is the most highly expressed and is found in distinct regions of the brain, namely purkinje cells (Huang *et al.*, 2007;Otsuka *et al.*, 1998) but also in non-neuronal cells, oligodendrocytes (Fusco *et al.*, 2004). TRPC6 is expressed in interneurons in the brain (Huang *et al.*, 2007) and also purkinje cells (Kunert-Keil *et al.*, 2006), but has higher levels of expression in peripheral tissues including lung, kidney and muscle (Riccio *et al.*, 2002b). TRPC7 has lower levels of expression than TRPC3 or TRPC6 but is found in the brain and other tissues including keratinocytes (Riccio *et al.*, 2002b). All TRPC channels are found within the DRG; TRPC3 is particularly highly expressed and is found exclusively in nonpeptidergic small diameter neurons (Elg *et al.*, 2007).

Co immunopreceiptation studies have shown that TRPC channels can form homomeric channels, as well as strictly defined heteromeric channels within the group but not between groups, both *in vitro* and *in vivo* (Hofmann *et al.*, 2002). However, novel subunit compositions have recently been found, for example together TRPC1/TRPC3 function as heteromeric channels in hippocampal cells (Wu *et al.*, 2004) and TRPC1/3/7 complexes in HEK cells (Zagranichnaya *et al.*, 2005). Immunohistochemistry studies have shown that TRPC3 co-localises with TRPC1, 4 and 5 rather than with TRPC6/7 in certain regions of the brain, suggesting that more heteromeric conformations may exist (Chung *et al.*, 2006).

The activation mechanisms of TRPC3, 6 and 7 channels have been investigated using various experimental approaches leading to conflicting results. Venkatachalam showed TRPC3 as a SOC when expressed in DT40 cells (Venkatachalam *et al.*, 2001), whereas the majority of other studies showed TRPC3 as a receptor activated channel when expressed in HEK293 cells. Variations in activation mechanisms in different cell lines (Trebak *et al.*, 2002) were ultimately linked to expression levels rather than a different cell environment (Vazquez *et al.*, 2003). A possibility for this difference could be that TRPC3 acts as a SOC only when interacting with other proteins that are in limited supply. TRPC3 is known to form heteromeric channels within the TRPC3/6/7 group and other interactions may well exist. When TRPC3 is over-expressed, more homomeric channels could form that may have different activation properties.

26

TRPC6 activation has always been less controversial. When originally cloned, Boulay showed TRPC6 acts as a receptor activated, but not store-operated, cation channel (Boulay *et al.*, 1997) and subsequent studies that showed insensitivity to depletion of internal stores have confirmed this (Hofmann *et al.*, 1999).

TRPC7 was originally shown to be receptor activated in a similar way to TRPC3 and 6 when expressed in HEK293 cells (Okada *et al.*, 1999) but Riccico showed that TRPC7 behaved as a SOC (Riccio *et al.*, 2002a). Confusingly, both of these studies were performed in the same HEK293 cell line which would in all probability have similar expression levels. Investigations by Lievremont et al showed that the mode of expression, transient or stable, was producing these conflicting results (Lievremont *et al.*, 2004).

The high homology shared between TRPC3, 6 and 7 is a likely reason why the three channels share many common biophysical properties, including within activation mechanisms. There are, however, striking difference between the constitutive activities of the channels. In HEK293 cells, TRPC3 and TRPC7 show significant constitutive activity (Okada *et al.*, 1999;Zhou *et al.*, 2008a), whereas constitutive activity of TRPC6 is negligible (Hofmann *et al.*, 1999).

Whether acting as receptor activated or SOCs the precise molecular mechanisms of activation and regulation of TRPC3/6/7 are not completely understood. Three main hypotheses have been proposed; conformational coupling with the IP3 receptor, a second messenger system, and an exocytosis-like mechanism.

All seven channels of the TRPC family can be activated downstream of PLC; PLC cleaves PIP2 into two molecules, IP3 and DAG. IP3 induces the emptying of intracellular stores by activating the IP3 receptor on the endoplasmic reticulum. Some TRPC channels can be activated as a consequence of this depletion by interacting with the IP3 receptor (Adebiyi *et al.*, 2010;Yuan *et al.*, 2003)

TRPC channels can also be activated by a PLC dependent mechanism that does not require store depletion. In the case of TRPC3/6/7 this receptor operated mode appears to involve activation by DAG. Direct activation of TRPC3/6/7 channels by OAG, a DAG analogue, has been shown in excised patches(Hofmann *et al.*, 1999;Okada *et al.*, 1999). Subsequent studies have not been able to replicate this direct activation of TRPC3/6/7 (Lemonnier *et al.*, 2008). An explanation may be that although activation was shown in excised patches, it is not direct, and other required factors are retained in the patch, but the retention can vary depending on the experimental set-up. This is supported by Smyth et al who showed that newly translocated TRPC3 channels lose the ability to be activated by OAG, suggesting other coupling factors are required that may be in limited supply (Smyth *et al.*, 2006).

It has also been suggested that TRPC channels may be activated by an exocytosis mechanism. TRPC6 levels at the plasma membrane are increased following activation of a PLC pathway and also directly by OAG. Store depletion is also able to increase TRPC6 levels at the membrane but in this case TRPC6 activation levels do not increase (Cayouette *et al.*, 2004). In contrast, TRPC3 is not externalized following PLC stimulation or OAG. TRPC3 is shown to be inserted into the membrane following activation by Epidermal growth factor, EGF, but there is no activation (Smyth *et al.*, 2006). Excoytosis mediated activation for TRPC channels appears to depend not only on the specific channel but also the signalling cascade which leads to the exocytosis.

TRPC7 has lower expression in the brain, and unlike TRPC3 and TRPC6 it is not found in smooth muscle cells. TRPC7 is expressed in keratinocytes where it acts as a receptor-operated channel mediating calcium influx signals that lead to differentiation and proliferation (Beck *et al.*, 2006).

1.4.5.1   Functions of TRPC3 and TRPC6

TRPC channels are able to form homo and heteromeric complexes which has made it difficult to unambiguously assign specific functions to one or the other TRPCs, especially within a subfamily with shared biophysical characteristics; in many cases it is likely that the functions of TRPCs overlap. In excitable cells, that are kept in a hyperpolarized state, the cation entry through TRPC channels would lead to membrane depolarization, activation of voltage gated

sodium and calcium channels. In both excitable and non-excitable cells the activation of TRPCs results in increases in intracellular Ca^{2+} concentration ($[Ca^{2+}]_i$) leading to a range of $[Ca^{2+}]_i$ responses which play pivotal roles in cellular and tissue functions. The complex set of molecular responses elicited from TRPC activation and the widespread distribution indicates their varying functional roles, some of which are outlined below. For a more detailed review see (Abramowitz and Birnbaumer, 2009).

Focal segmental glomerulosclerois

Focal segmental glomerulosclerosis (FSGS) is a cause of nephritc syndrome and kidney failure. A gain of function mutation in TRPC6 is responsible for a subset of forms of FSGS (Winn *et al.*, 2005). Overexpression of TRPC6 specifically in mouse podocytes (cells which respond to glomerular pressure), is sufficient to reproduce glomerular disease consistent with the human phenotype (Krall 2010). In podocytes, TRPC6 interacts with podocin (Huber *et al.*, 2006), a homologue of which contributes to mechanosensation in C. elegans which is proposed to alter the local lipid environment enabling TRPC6 to respond directly to the deformation of the plasma membrane (Huang *et al.*, 1995).

Myogenic response

The vasculature is exposed to frequently changing mechanical forces. Vascular smooth muscle cells respond to pressure causing constriction of arteries and arterioles which is known as the myogenic response. One proposed model for the myogenic response is the centralized model involving membrane ion channels which open in response to mechanical force. TRPC3 and TRPC6 are highly expressed in vascular smooth muscle (Dietrich *et al.*, 2005). Antisense TRPC6 decreased and TRPC6 protein expression greatly increased smooth muscle depolarization in response to mechanically induced stretching in ex vivo arteries (Welsh *et al.*, 2002). However, TRPC6$^{-/-}$ mice showed enhanced agonist-induced contractility in response to stretching of arterial segments (Dietrich *et al.*, 2005). It was found that TRPC3 mRNA expression was increased in the TRPC6$^{-/-}$ mice which may be able to account for this unusual result as TRPC3 has constitutive activity (Zhou *et al.*, 2008a). This theory is supported by the ability of TRPC3-specific small interference RNA to abolish the increased basal activity. These results implicate both TRPC3 and TRPC6 in the myogenic response.

Motor coordination

Within the brain TRPC3 is expressed highly in the cerebellum, particularly in Purkinje cells, and is required for synaptic transmission (Hartmann *et al.*, 2008). In TRPC3$^{-/-}$ mice, the slow EPSP following mGLuR1 activation is absent and as a result the mice lack motor coordination (Hartmann *et al.*, 2008). It has also been suggested that TRPC3, in coordination with Na$^+$ channels, are able to regulate basal neuronal activity of GABA neurons, since an antibody to TRPC3 decreases spontaneous firing and hyperpolarizes the cells (Zhou *et al.*, 2008a). In contrast, TRPC6 is involved in excitatory synapses where TRPC6 expression is enriched and contributes to spatial learning and memory tasks (Zhou *et al.*, 2008b).

Neuronal growth and development

Within the CNS, TRPC3 co-localises with TrkB, the receptor for the neurotrophin BDNF (Li *et al.*, 1999). BDNF evokes a nonselective cationic current in neurons, I$_{BDNF}$. I$_{BDNF}$ requires extracellular Ca^{2+}, but how BDNF regulates Ca^{2+} is not fully understood, since voltage dependent calcium channels are not essential so another channel by default must be responsible for the calcium influx. An antibody for a portion of TRPC3 was able to abolish I-$_{BDNF}$ in pontine neurons (Li *et al.*, 1999). Subsequently a study using siRNA against TRPC3 was able to support this finding, showing a similar result of a block on I$_{BDNF}$ (Amaral and Pozzo-Miller, 2007a). A known TRP channel blocker, SKF-96365, is also able to block I$_{BDNF}$ (Amaral and Pozzo-Miller, 2007a;Li et al., 2005) adding further weight to the supposition that the calcium influx evoked by BDNF is carried through TRPC3 channels. This calcium influx through TRPC3 induces dendritic spine formation (Amaral and Pozzo-Miller, 2007b) and growth cone turning in neurons (Li *et al.*, 2005). BDNF is proposed to increase Ca^{2+} influx through TRPC3 via two mechanisms, firstly as a store operated channel by activating PLCγ leading to emptying of intracellular stores (Li *et al.*, 2005), secondly by rapid vesicular insertion of TRPC3 channels into the plasma membrane by a PI3 kinase dependent mechanism (Amaral and Pozzo-Miller, 2007b). In addition to being involved in neuronal growth, TRPC3 may also be involved in CNS development. TRPC3 protein expression in the brain peaks during a narrow time window immediately before and after birth (Li *et al.*, 1999), and TRPC3 in tandem with TRPC1 are essential for differentiation of hippocampal cells *in vitro* (Wu *et al.*, 2004).

30

1.4.6 Targeted gene deletion by homologous recombination in embryonic stem cells

Homologous recombination provides a mechanism to introduce exogenous portions of DNA to create a knock-in transgene. The desired alteration is introduced into a cloned DNA sequence, which then recombines with the targeted sequence within the genome to transfer this alteration (Smithies *et al.*, 1985). In mammalian cells DNA generally integrates at random sites, making it difficult to target a specific gene. However, pluripotent embryonic stem cells (ES cells) can undergo homologous recombination *in vitro* when electroporated with DNA. ES cells can then be microinjected into a blastocyst and resume normal embryonic development. In the resulting chimeric mice, the ES cells contribute to the germ line as well as to the somatic tissues, enabling this system to be used as a way to generate transgenic animals.

1.4.7 Cre/loxP system

The production of knockout mouse lines is invaluable in elucidating gene function in mammalian tissues but global knockouts can lead to embryonic lethality in mice, obscuring the role of that gene in a target tissue or in the adult. Site-specific recombinases allow control of the targeted null mutation both spatially and temporally, avoiding lethality and also allowing investigation of just one tissue without the complications from knockout in other organs. The Cre recombinase of phage P1 catalyzes site-specific excision in mammalian cells and requires no other protein factors, making it an ideal tool for generating a conditional knockout (Sauer and Henderson, 1988).

The Cre-loxP system consists of the Cyclization Recombination protein (Cre) and its short DNA recognition sequence called *lox*P:

ATAACTTCGTATAATGTATGCTATACGAAGTTAT

The site-specific recombinase Cre will excise a sequence flanked by *lox*P sites that are placed in the same direction (Figure 1.5) or invert a sequence flanked by *lox*P in opposite directions. The Cre gene or the *lox*P sites are inserted into the genome using homologous recombination. Two lines of mouse are required, one with the expression of Cre limited to the tissue of interest, and one with the gene of interest flanked by *lox*P sites. When these two mouse lines are crossed the flanked sequence will be recombined and removed, but only in tissues that express Cre. The expression of the gene in other tissues will be normal.
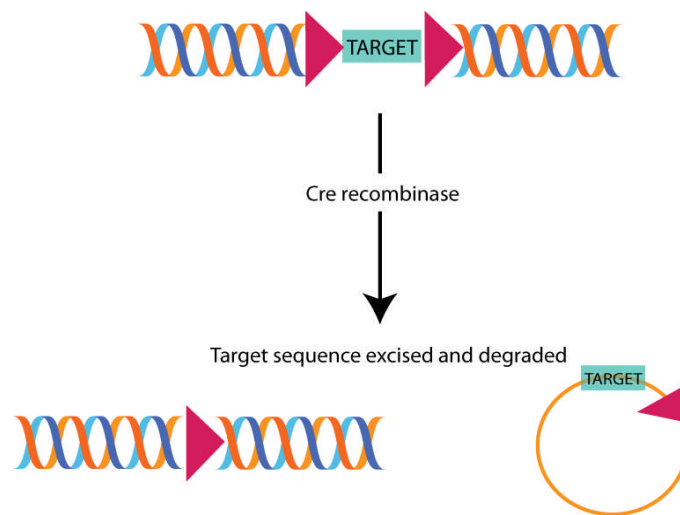
Figure 1.5 The Cre/loxP system

Cre recombinase excises the target sequence flanked by loxP sites (red triangles). The excised sequence is degraded.

1.4.8 Flp/FRT system

The Flp-FRT system also consists of a site specific recombinase and target sequences (Dymecki, 1996). Flp recombinase originates from the yeast *Saccharomyces cerevisiae* and the FRT target sites are similar to *loxP* sites but with the following sequence;

GAAGTTCCTATTCTCTAGAAAGTATAGGAACTTC

1.5 Aims

The aim of this thesis is to investigate the role of TRPC channels in sensory pathways, including the somatosensory and auditory/vestibular systems using tissue-specific and global knockout animals.

- Firstly, I looked at the effect of deletion of TRPC3 in DRG neurons on acute and inflammatory pain thresholds. I used Cre recombinase under the control of two different promoters to elucidate TRPC3's roles in nociceptors and non-nociceptors.

- Secondly, I investigated the changes in gene expression within the DRGs of TRPC3fl/fl:Nav1.8Cre mice using microarray technology.

- Next we examined the effect of global deletion of both TRPC3 and TRPC6 on touch, pain and auditory response thresholds.

- Lastly, I generated a construct to enable tissue-specific knockout of TRPC4 using Cre/*lox*P technology.

2 Materials and Methods

2.1 Molecular Biology

2.1.1 Gel electrophoresis

Agarose gel electrophoresis was used to separate DNA bands by size. 0.7-1 % agarose gels, depending on the size of the fragments, were prepared by dissolving agarose (Sigma, UK) in TAE 1X buffer (40mM Tris-acetate, 1mM EDTA). After cooling, ethidium bromide (EtBr) was added (0.5µg/ml) and then set into a gel tray. 1-3ul of 6X loading buffer was added to each sample before loading into the wells, alongside an appropriate molecular weight marker. A power pack supplying 80-120 volts was used to separate the bands which were then visualised using UV, UVP Biodoc-It^{TM} Systems, and a picture printed from a thermal printer.

2.1.2 Polymerase Chain Reaction (PCR)

Fragments of DNA were amplified for subcloning using PCR. Phusion High Fidelity PCR kit (Finnzymes) and Extended Long Template kit (Roche) were used for cloning purposes and Taq polymerase for genoytyping. The typical PCR protocol was as follows.

Phusion High Fidelity

10 ng   template DNA

4.0µl   5x HF buffer (includes MgCl$_2$)

0.4µl   dNTP (10mM)

1.0µl   of each primer (10µM)

0.2µl   DNA polymerase

^{dd}H$_2$O   up to 20µl

The PCR cycles were carried out using the DNA Engine DYAD. The PCR conditions were denaturation at 98ºC for 30 seconds, 20-30 cycles of 8 seconds at 98ºC, 20 seconds at 60-65ºC to anneal primers to the single strands and 2-3 minutes at 72ºC for extension of the DNA. Finally 10 minutes at 72ºC for further extension and then the reaction was cooled to 4ºC.

Extended Long Template

10 ng   template DNA

5.0µl   Buffer 1, 2 or 3 depending on size of product (includes $MgCl_2$)

1.0µl   dNTP (10mM)

2.0µl   of each primer (10µM)

0.75µl DNA polymerase

$^{dd}H_2O$ up to 50µl

The PCR cycles were carried out using DNA Engine DYAD. The PCR conditions were denaturation at 94ºC for 2 minutes, 10 cycles of 10 seconds at 94ºC, 30 seconds at 50-60ºC to anneal primers to the single strands and 5 minutes at 68ºC for extension of the DNA. A second set of PCR conditions with higher annealing temperatures was then used, 20 cycles of 15 seconds at 94ºC, 30 seconds at 60-65ºC to anneal primers to the single strands and 5- 6 minutes at 68ºC. Finally 10 minutes at 68ºC for further extension and then the reaction was cooled to 4ºC.

2.1.3 Gel extraction

After separation by agarose gel electrophoresis DNA fragments of the required size were excised from the gel and the QIAgen gel extraction kit was used to extract and purify the DNA.

2.1.4 DNA Digestions

Restriction enzyme digests of DNA were performed using the appropriate restriction enzymes and according to manufacturer's instructions. Restriction enzymes were obtained from New England Biolabs. Typically 3µg of DNA was digested for approximately 1 hour at 37ºC; the enzyme deactivated at 65ºC for 20 minutes followed by separation on an agarose gel.

2.1.5 Ligation of fragments into vectors

The vector was first cut using the appropriate restriction enzymes as previously described then treated with shrimp alkaline phosphatase, SAP, (30 minutes at 37ºC and then

deactivated at 65ºC for 15 minutes) to prevent re-ligation of an empty vector. The desired insert was cut with the same restriction enzymes to produce 'sticky' ends. Ligation was carried out using, where possible, a 1:3 ratio of vector to insert. The concentration of DNA was estimated by visualisation on an agarose gel or the nanodrop. 1µl of buffer and 1µl of T4 Ligase (Roche) was added and the volume adjusted to 10µl using purified water. The reaction was incubated at 16ºC overnight before transformation into bacterial cells took place.

2.1.6 Transformation

Transformation was carried out using DH5α heat activated competent cells, TOP10 competent cells or TSS competent cells.

TSS competent cells

DNA was added to 100µl of TSS cells and incubated on ice for 15 minutes. 900µl of pre-warmed SOC media was added and the samples were shaken at 37ºC for 1 hour. The cells were plated onto an LB+Amp agar plate with dilution and Xgal if necessary and incubated at 37ºC overnight.

TOP10 competent cells

5µl of DNA was added to 50µl of TOP10 cells and mixed gently before incubating on ice for 30 minutes. The cells were then heat shocked at 42ºC without shaking for exactly 30 seconds and then put back on ice for 2 minutes. 250µl of pre-warmed SOC media was added and the samples were shaken at 37ºC for 1 hour. The cells were plated onto an LB+Amp agar plate with dilution and Xgal if necessary and incubated at 37ºC overnight.

DH5α heat activated competent cells

5µl of DNA was added to 50µl of DH5α cells and mixed gently before incubating on ice for 30 minutes. The cells were then heat shocked at 42ºC without shaking for exactly 20 seconds and then put back on ice for 2 minutes. 950µl of pre-warmed SOC media was added and the samples were shaken at 37ºC for 1 hour. The cells were plated onto an LB+Amp agar plate with dilution and Xgal if necessary and incubated at 37ºC overnight.

2.1.7 Preparation of DNA

2.1.7.1 Mini-prep using QIAkit

From a Petri dish a single colony was inoculated in 2 ml of LB/Amp at 37ºC in a shaking incubator overnight. 600µl of media was spun down at 8,000RPM for 30 seconds. The supernatant was discarded and the pellet resuspended in 250µl P1 buffer, 250µl P2 buffer and 350µl N3 buffer. The mixture was spun at 13,000RPM for 10 minutes and the supernatant put into a QIAprep spin column which was then spun for 30-60 seconds and the flow-through discarded. The pellet was washed with PB buffer and PE buffer, and then the DNA was eluted in 30-60µl elution buffer.

2.1.7.2 Mini-prep using Solutions I, II, III

From a Petri dish a single colony was inoculated in 2 ml of LB/Amp at 37ºC in a shaking incubator overnight. 1.5ml of media was spun down at 8,000RPM for 30 seconds. The supernatant was discarded and the pellet resuspended in 100µl chilled Solution I (50nM glucose, 20mM Tris-HCl, pH 8.0, 10 mM EDTA, pH 8.0). Lysozyme was added (2.5mg/ml) and tubes were incubated on ice for 5 minutes. 200µl freshly prepared Solution II (0.2M NaOH, 1% SDS) and 150µl Solution III (3M Potassium acetate, pH 4.8) were added, mixing at each stage. The mixture was spun at 14,000RPM for 6 minutes and the supernatant put into a clean 1.5ml eppendorf with 1ml of ethanol and spun for a further 6 minutes. The supernatant was discarded and the pellet was air-dried. The pellet was then washed with 70% ethanol before being resuspended in 20µl elution buffer.

2.1.8 Sequencing

Sequencing was carried out using BigDye3.1 kit. A single sequence reaction containing 1.5µl BigDye Mix, 2.5µl BigDye buffer, 1µl 3.2µM primer, 2µl DNA and purified water up to 10µl was mixed. The sequencing reaction was carried out using the following cycle:

96ºC for 30 seconds

50ºC for 15 seconds

60ºC for 4 minutes

25 cycles and kept at 4ºC until purification.

Purification was performed by adding 2µl of 3M sodium acetate (pH 5.2) and 50 µl of 100% ethanol and incubated on ice for 10 minutes. The mix was then spun at 13,000RPM for 15 minutes and the supernatant discarded. The pellet was washed with 100µl of 70% room temperature ethanol and spun for 5 minutes at 13,000 rpm. The ethanol was carefully removed and the pellets air-dried on the bench. The sequencing reaction was performed at UCL sequencing facility (Stuart Martin).

2.1.9 Southern Hybridization

2.1.9.1 DNA separation and Blotting

Around 50ug of DNA from transfected ES cells was digested with at least 50 U of the appropriate restriction enzyme in a 50ul reaction volume. Digestion reactions were incubated at the appropriate temperature, usually 37ºC, overnight. The digestion products were separated by electrophoresis in a 0.6% agarose gel for approximately 4 hours. The gel was exposed to UV light for 1 minute to nick the DNA and then denatured in a denaturing solution (1.5M NaCl and 0.5M NaOH) for 45 - 90 minutes with agitation and subsequently incubated with agitation in neutralising solution (1.5M NaCl, 0.5M Tris pH 7.0) for 45 – 90 minutes. The DNA was transferred to a nylon membrane (Hybond-N+) overnight by capillary action using 10x SSPE (1.5M NaCl, 100mM NaH_2PO_4-H_2O, 10mM EDTA, pH 7.4) as the transfer buffer. DNA was fixed to the nylon membrane using the auto crosslink settting of the UV stratalinker which delivered 1200mJ.

2.1.9.2   Pre-Hybridization

Southern blot membranes were placed in hybridisation tubes (Hybaid) and incubated in hybridisation solution (Dextran sulphate, NaCl, SDS) at 65 C with rotation for at least 1 hour.

2.1.9.3   Oligoprobe labeling and Hybridisation

Labelled dsDNA probes were obtained by PCR amplification of genomic DNA followed by gel electrophoresis separation of the DNA fragment. The probes were between 300-500bp. The desired band was excised and melted in the minimum amount of water and stored at -20 C. The DNA fragment was labelled with alpha-^{32}P dATP (3000Ci/mMol, GE healthcare) using the Prime-it II random priming kit (Stratagen) according to the manufacturer's protocol. Briefly, 12ul of dissolved probe was added to 5ul of random 9-mer primers and heated at 95$^\textbf{o}$C for 5 minutes and 37$^\textbf{o}$C for 5 minutes. 5ul of buffer and 2.5ul of P^{32} was added followed by 0.5ul of Klenow enzyme followed by a 30 minute-1 hour incubation at 37$^\textbf{o}$C. The labelled DNA was purified from the non-incorporated nucleotides using the QIAquick nucleotide removal kit (Qiagen) according to the manufacturer's protocol.

The labelled dsDNA probe was mixed with 1mg of sheared salmon sperm DNA and denatured by incubating at 95$^\textbf{o}$C for 5 minutes and placed on ice for 2 minutes before being added to the hybridisation tubes containing the membrane and hybridisation solution and incubated at 65$^\textbf{o}$C with rotation overnight.

2.1.9.4   Membrane washing and imaging

The membranes were washed with 2xSSPE +0.1% SDS for 15-30 minutes at 65$^\textbf{o}$C and an optional wash of 0.2xSSPE +0.1%SDS for 1-5 minutes at 65$^\textbf{o}$C and exposed to X-ray film (Amersham) for 1-7 days at -80$^\textbf{o}$C.

2.1.10   Genotyping

Mice of at least 3 weeks of age were marked using an ear puncher and the tissue samples were then used for genotyping.

2.1.10.1 DNA extraction

Each sample was incubated with 30µl PCR lysis buffer at 55°C for 1 hour followed by 95°C for 5 minutes to inactivate the Proteinase K. The samples were vortexed briefly and spun for 1 minute. The supernatant was removed and stored at -20°C.

PCR lysis buffer: 3.6ml 10X GB, 0.72ml 25% TritonX-100, 0.36ml b-mecaptoethamol, 31.32ml H_2O. 1µl of 19.7mg/ml Proteinase K (Roche) was added to 475µl of PCR lysis buffer before use.

2.1.10.2 PCR Protocol

The following conditions for the PCR reactions were used

Components	uL	Final Conc.
H2O	17.7	
10x PCR Buffer	2.5	1x
25 mM MgCl2	1.5	1.5 mM
10 mM dNTPs	0.5	0.2 mM
10 µM Primer1	1.0	0.4 µM
10 µM Primer2	1.0	0.4 µM
DNA	0.5	1.0 ug/25 µl
Taq	0.3	1.5 U/25 µl
Volume	25	

Table 2.1 : PCR reaction quantities for genotyping

A typical PCR cycle was as follows:

Denaturation at 95°C for 2 min

Denaturation at 94 °C for 30 seconds

Annealing at 58 °C for 30 seconds

Extension of the product at 72 °C for 1 min

Steps 2-4 repeated 35 times

Additional extension step at 72 °C for 10 min

PCR product kept at 4 °C

The primers used to genotype each mouse strain are shown in Table 2.2.

Gene	Primer name	Sequence	WT	KO
TRPC3	TRPC3 F	GCTATGATTAATAGCTCATACCAAGAGATC	300	none
	TRPC3 R	GGTGGAGGTAACACAGACCTAAGCC		
	TRPC3 F2	GAATCCACCTGCTTACAACCATGTG	800	300
	TRPC3 R	GGTGGAGGTAACACAGACCTAAGCC		
TRPC6	E7F	CAGATCATCTCTGAAGGTCTTTATGC	234	none
	E7R	TGTGAATGCTTCATTCTGTTTTGCGCC		
	IFF	ACGAGACTAGTGAGACGTGCTACTTCC	none	339
	PgkR	GGGTTTAATGTCTGTATCACTAAAGCCTCC		
			Cre –ve	**Cre +ve**
Nav1.8 Cre	Sns13S	TGTAGATGGACTGCAGAGGATGGA		461
	Cre 5a	AAATGTTGCTGGATAGTTTTTACTGCC		
Adv Cre	Avil/003F	CCCTGTTCACTGTGAGTAGG	480	
	Avil/002B	AGTATCTGGTAGGTGCTTCCAG		
	Avil/003F	CCCTGTTCACTGTGAGTAGG	none	180
	Avil/001B	GCGATCCCTGAACATGTCCATC		

Table 2.2 : Genotyping primers

2.1.11 RNA Extraction

Mice were culled according to Home Office procedures and the DRG removed quickly on ice. DRGs were microdissected to remove the axons and placed into RNAlater. The RNA was extracted using QIAgen RNeasy mini kit within 48 hours. Briefly, 1 ml of Buffer RLT (with 2-mercaptoethanol) was added to the tissue samples. The tissue was homogenized using a glass homogenizer cleaned with distilled water, Ambion RNAzap® and diethylpyrocarbonate treated water followed by a single wash with Buffer RLT. The tissue was kept on ice throughout the homogenization process and tissue was homogenized for no longer than 2 minutes. The tissue samples were passed through a QIAshredder column (Qiagen, UK) and spun for 2 minutes at 13,000 rpm. The supernatant was transferred to a clean RNAase free tube and 1 volume of 70% ethanol was added and mixed. This mixture was passed through a RNaeasy column and spun briefly at 13,000 rpm. The column was washed with buffer RW1 once and RPE once. Finally the RNA was eluted with RNAase free water. RNA concentration was checked using nanodrop and quality was checked by agarose

gel electrophoresis, looking for two distinctive bands representing ribosomal RNA 28s and 18s subunits with a 1.5:1 ratio. RNA was stored at -80ºC

2.1.12   cDNA synthesis

cDNA was made using a Bio-Rad iscript cDNA synthesis kit according to manufacturer's instructions. Briefly, the following components were mixed and incubated for 60 minutes at 42ºC and 5 minutes at 85ºC. The cDNA was stored at -20ºC.

Components	Amount
5 x iScript select reaction mix (containing dNTPs, $MgCl_2$ and stabilizers	4µl
Oligo(dT)$_{20}$	2 µl
RNA sample	1µg
iScript reverse transcriptase	1 µl
Nuclease-free water	Variable
Total	20µl

Table 2.3 Reverse transcription reagents for cDNA synthesis

2.1.13   Reverse transcription Polymerase Chain Reaction

Confirmation of knockout of TRPC3 was performed using RT-PCR to check for a change in size of mRNA for the TRPC3 gene. A typical PCR cycle was performed as outlined above in Section 2.1.10.2 with the following primers (Table 2.4).

Gene	Primer name	Sequence	WT	KO
TRPC3	TRPC3F3	GGGCCAAAGTAAATCCTGCT	630bp	432bp
	TRPC3R3	GGCTGGAGATATCCTGCTTG		

Table 2.4 Primers for RT-PCR of TRPC3

2.1.14   Quantitative PCR

DRGs from 2 TRPC3fl/fl, 2 TRPC3fl/fl:Nav1.8Cre and 2 TRPC3$^{-/-}$ mice were excised and the RNA extracted as described above. The RNA was reverse transcribed into first strand cDNA and used for the qPCR. Reactions were performed in triplicate in 50 µl volume using

Bio-Rad iQ SYBR Green Supermix. Reaction mixtures were run using an Eppendorf RealPlex PCR machine, a typical programme was:-

Denaturation at 95ºC for 2 min

Denaturation at 95 ºC for 15 seconds

Annealing at 60 ºC for 15 seconds

Extension of the product at 72 ºC for seconds

Steps 2-4 repeated 40 times

Followed by a melt curve to check for one specific product.

Primer efficiency was measured using serial dilutions of cDNA and the efficiency, E, was calculated using the gradient of a graph of log [template] against C_t values. Efficiency is given by the formula $E = 10^{(-1/\text{gradient})} - 1$. Only primers with efficiencies of 90-110% were used for RNA quantification. The Pfaffl method (Pfaffl, 2001) was used for the relative quantification of cDNA levels. GAPDH was used as a reference gene.

	Primer name	Sequence
TRPC3	TRPC3S	AGCCGAGCCCCTGGAAAGACAC
	TRPC3AS	CCGATGGCGAGGAATGGAAGAC
GAPDH	GAPDHS	TGCGACTTCAACAGCAACTC
	GAPDHAS	CTTGCTCAGTGTCCTTGCTG

Table 2.5 qPCR primers

2.2 Behavioural phenotyping

Animals were tested between 6-8 weeks of age between 8am and 6pm. The investigator was unaware of the genotype of the animals at the time of testing. Animals were used for one test only unless the stimulus was considered innocuous, for example rotarod and von Frey tests were performed on the same animsls.

2.2.1 Rotarod

Mice were placed on a rod rotating at a constant 5 revolutions per minute (rpm) for 2 minutes. The speed of rotation was increased from 5 rpm to 40 rpm over 3 minutes and the time the mouse was able to remain on the rod from the beginning of acceleration was recorded. If the mouse made two full rotations this was considered a fall. Each mouse had three trials and the average was taken.

2.2.2 Mechanical sensitivity

Two methods of mechanical testing were employed to mimic innocuous, or light touch, and noxious, painful, mechanical stimuli.

2.2.2.1   von Frey monofilaments

Calibrated nylon filaments are used to deliver a graded mechanical force to the plantar surface of the hind paw to assess mechanical response threshold to an innocuous stimuli. The filament is applied perpendicular onto the paw's plantar surface until the filament slightly buckles and a constant force is thereafter applied for 3 seconds. A positive response is recorded if the mouse flinches, lifts or licks the paw whilst the stimulus is being applied, or if these responses occur immediately after withdrawal.

The up-down method described by Chaplan et al. was used to calculate the 50% withdrawal threshold with the minimum application of filaments to minimise discomfort of the animal and false positive results (Chaplan *et al.*, 1994). Briefly, a filament expected to give a positive withdrawal response 50% of the time is applied to the paw, if a response is recorded this is followed by application of a weaker strength. Alternatively, if no response to that filament occurs a stronger filament is applied. This is repeated until 6 responses are recorded.

The pattern of responses, together with the force of the last hair applied, is used to calculate algorithmically the 50% threshold as described in Chaplan et al 1994.

Mice were acclimatised in the apparatus for at least 90 minutes before testing. Mechanical sensitivity was tested using Ugo Basile automatic von Frey. The force at which the hindpaw was withdrawn was recorded. Each paw was tested 6 times with an interval of at least 2 minutes between each test. Mechanical sensitivity was tested on two non-consecutive days and the average taken.

2.2.2.2   Randall Selitto apparatus

The Randall Selitto apparatus applies an increasing mechanical pressure from a blunt probe to the tail of the mouse until a withdrawal response is observed. Withdrawal responses include vocalisation, writhing and flinching of the tail. The increasing pressure applied from a $3mm^2$ blunt probe activates high threshold mechanoreceptors in the C-fibres as a response to a noxious insult (Hogan, 2002;Takesue *et al.*, 1969).

The mouse was restrained in a Perspex tube and allowed to acclimatise for 5 minutes until settled. The tail was then placed on the apparatus and gradually increasing force was applied using the Ugo Basile analgesy meter the force at which the mouse moved the tail or struggled was recorded. Three trials were performed, each on different parts of the tail that were close together, and the average taken.

2.2.3 Thermal sensitivity

2.2.3.1   Hargreaves' apparatus

A radiant heat source is applied to the hind paw through a glass plate (Hargreaves *et al.*, 1988). The latency in seconds until the mouse responds to the heat, usually in the form of paw withdrawal, is recorded. The fast paw withdrawal is due to a spinal reflex.

Mice were acclimatised in the apparatus for at least 90 minutes before testing. The withdrawal latency to heat stimulation was tested by using a device of Hargreaves et al.

(1988) purchased from Ugo Basile (Comerio, Italy). The time until the animals reacted with withdrawal to the stimulation by a radiant heat source was determined automatically. Each testing period consisted of a maximum of three presentations for the each hind paw. Thermal sensitivity was tested on two non-consecutive days and the average taken.

2.2.3.2   Hot plate

The hot plate measures supra-spinal responses to temperatures between 45 – 55 ⁰C. The mouse is placed on a hot plate at a constant temperature and the latency to a pain response, such as licking, biting or flinching, is recorded (Jensen and Yaksh, 1984). In contrast to the Hargreaves' test, where a heat ramp is applied only to the paw, the hot plate exposes the whole mouse to a constant temperature.

Each animal was acclimatised for 5 minutes with the apparatus switched off and the plate at ambient temperature. For testing the plate was heated to the appropriate temperature and the mouse was placed on the plate and observed. The latency to the first pain behaviour, licking/biting/shaking of the hind paw or jumping, was recorded and the mouse removed immediately after this first behaviour. Three temperatures, 45ºC, 50ºC and 55ºC, were tested on three consecutive days.

2.2.4 Cold plate

Each animal was acclimatised for 5 minutes with the apparatus switched off and the plate at ambient temperature. The plate was cooled to 0ºC and the mouse was placed on the cold plate for 5 minutes. The latency to first pain response, licking/biting/shaking of the hind paw or jumping, was recorded and also the number of pain responses, licking, shaking, jumping, was counted over the 5 minutes.

2.2.5 Inflammatory pain models

2.2.5.1   CFA

Injection of complete Freund's adjuvant (CFA) into the hind paw has been used as a reliable model of persistant inflammatory hyperalgesia for several decades (Larson *et al.*, 1986). Thermal and mechanical hyperalgesia develops approximately 24 hours after injection and remains for up to 2 weeks. Hyperalgesia is linked to TNF α and cytokine release in the periphery (Cunha *et al.*, 1992), yet central changes in the dorsal horn of the spinal cord including increased expression of NMDA receptors, 5-HT receptors and increased PKC activity can also contribute (Igwe and Chronwall, 2001;Xu and Huang, 2002;Yang et al., 2009)

Prior to injections the baseline mechanical and thermal thresholds of each animal was measured on two days using the Hargreaves and von Frey apparatus. Mice received 20-30µl of CFA (Sigma) into the plantar surface of the left hindpaw. After the injection mice were tested at day 1, 3, 7 and 10. Oedema was also measured using a Mitutoyo Pocket Thickness Gage (Toolmix, UK).

2.2.5.2   Formalin

The formalin test allows assessment of continuous moderate pain, lasting around 1 hour in the absence of evoked stimuli. Typically 1-5% formalin is injected subcutaneously into the hind paw and the mice exhibits flinching, licking and shaking behaviours in two distinct phases; the first phase starts immediately after injection and last for approximately 5 minutes and this phase is due to direct chemical stimulation of C fibres, acting through the TRPA1 receptor (McNamara *et al.*, 2007). The second phase starts approximately 15-20 minutes after injection and lasts for 20-40 minutes. This phase involves central changes within the spinal cord and inflammatory molecules (Coderre *et al.*, 1990).

Animals were acclimatised individually in an observation chamber for 1 hour, until exploratory activity had ceased. 20µl of 5% formalin (40% formaldehyde) in saline was injected subcutaneously into the plantar region of the left hindpaw. The time spent engaging in nocifensive behaviour (licking, biting or shaking the injected paw) was recorded in 5

minute bins over a 1 hour period. The first phase (acute) is defined as 0-10 minutes after injection and the second phase (inflammatory) 10-60 minutes after injection.

2.2.5.3 Carrageenan induced mechanical hyperalgesia

The injection of carrageenan into the hind paw was originally developed as a model of inflammation for the screening of anti-inflammatory drugs (Crunkhorn and Meacock, 1971). Carrageenan causes oedema, which develops over 6 hours (Crunkhorn and Meacock, 1971), accompanied by mechanical and thermal hyperalgesia. Inflammatory hyperalgesia is dependent on TNFα activation of cytokine cascades (Cunha *et al.*, 1992) increased COX-2 expression in inflamed tissues and the spinal cord (Hay and de Belleroche, 1997).

Prior to injections, the baseline mechanical thresholds of each animal were measured on two days using the von Frey apparatus. 20µl of 2% Carrageenan dissolved in saline was injected into the plantar region of the left hindpaw as described previously. Mechanical withdrawal thresholds were measured 3 hours after injection.

2.2.5.4 Prostaglandin E2 induced mechanical hyperalgesia

Prostaglandin E2 is synthesised from arachidonic acid by COX-2 and PGE synthase enzymes. Incidentally, this pathway is the major site of action for NSAIDs which are known to be effective against inflammatory pain in humans and animals. Intraplantar administration of PGE2 causes a short lasting mechanical hyperalgesia (Taiwo *et al.*, 1987) by acting directly on primary afferent nociceptors to sensitise them (Southall and Vasko, 2000)

Prior to injection the baseline mechanical thresholds of each animal was measured on two days using the von Frey apparatus. 100ng of PGE2 dissolved in 2.5µl saline was injected intradermally into the plantar region of the left hindpaw. Mechanical withdrawal thresholds were measured 3 hours after administration of PGE2.

2.2.5.5 Bradykinin induced pain behaviour

Bradykinin is a major inflammatory mediator that produces severe spontaneous pain and mechanical and thermal hyperalgesia (Couture *et al.*, 2001). Hyperalgesia is caused by

sensitisation of sensory ion channels such as TRPV1(Chuang *et al.*, 2001) and TRPA1(Wang *et al.*, 2008) and the acute pain that is directly induced by BK is mediated via Gq/11 protein coupled receptors, PLC and release of calcium from intracellular stores (Liu *et al.*, 2010).

Animals were acclimatised individually in an observation chamber for 30 minutes, until exploratory activity had ceased. 10nmol of BK in a 10µl volume of saline was injected subcutaneously into the plantar region of the left hindpaw. The time spent engaging in nocifensive behaviour (licking, biting or shaking the injected paw) was recorded over a 30 minute period.

2.2.6 Neuropathic pain models

2.2.6.1   Chung/SNL model

The hyperalgesia, allodynia and tonic pain associated with peripheral neuropathies are due to changes in primary afferent neurons (Campbell *et al.*, 1992). Damaged primary afferents may experience changes in excitability, phenotype and/or develop ectopic activity (Noguchi *et al.*, 1995) moreover, in addition to injured afferents, uninjured afferents can also be affected by these changes. The spinal nerve ligation, SNL, model for peripheral neuropathy in animals was developed by Kim and Chung and allows study of the injured and uninjured afferents (Ho Kim and Mo Chung, 1992). This model involves the complete ligation of either the left L_5 or both L_5 and L_6 spinal nerves under anaesthesia. In my studies on neuropathic pain, only $L_5$was ligated. Spinal nerve ligation results in a long-lasting thermal hyperalgesia and mechanical allodynia on the affected hind paw. The model was developed in rats but also produces the same hyperalgesia and allodynia in mice (Honore *et al.*, 2000).
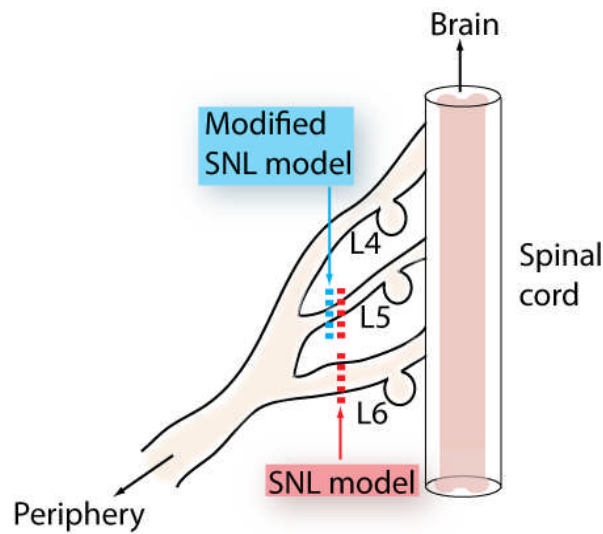
Figure 2.1 : Spinal nerve ligation (SNL) and modified spinal nerve ligation models.

Baseline measurements of mechanical thresholds were performed two days before surgery. Animals were anaesthetised using isofluorane. A midline incision was made in the skin of the back. The L5 transverse process was removed and the left L5 spinal nerve cut. Mechanical thresholds and weight bearing analysis was then performed up to 25 days after surgery.

2.2.7 Vestibular and hearing tests

2.2.8 Preyer reflex test

A custom built click-box (MRC Institute of Hearing Research) was held 30cm above the mouse and a calibrated 20kHz toneburst at an intensity of 90dB SPL was delivered. The presence or absence of an ear flick response (Preyer reflex) was recorded. If the animal responded well a score of 1.0 was given, it the animal did not respond at all a score of 0.0 was given. The Preyer reflex test was performed once on any given day to prevent habituation to the noise.

2.2.9 Air righting

The mouse was dropped onto a soft surface from a height of 30cm. A contact landing on all four paws was given a score of 1.0, a landing on its side or back was given a score of 0.0. The trial was repeated 5 times.

2.2.10 Reaching response

The mouse was held in the air by the tail 5cm away from a horizontal surface for 5 seconds. It the mouse reached out with its forelimbs towards the platform it received a score of 1.0. If the mouse curled towards its belly it received a score of 0.0. If the mouse curled only slightly it received a score of 0.5.

2.2.11 Swim test

A deep container was filled with at least 4 inches of 24-26°C water and the mouse carefully lowered into the water. The mouse was observed for a maximum of 1 minute and its swimming ability assessed. The swimming was scored as 3 = Swims, mouse body is elongated and tail propels in a flagella-like motion, head and back above water; 2.5 = ears under water, irregular swimming, which includes vertical swimming, swimming in a circle, swimming on side, swimming in an unbalanced manner; 2 = eyes at water level; 1 = Nose only above water; 0.5 = head under water; 0 = Underwater tumbling, mouse is unable to maintain a balanced body position and continuously tumbles. After 1 minute, or if a mouse displayed underwater tumbling, the mouse was rescued and placed under a heat lamp to dry.

3   Generation and phenotyping of TRPC3 Knockout mice

3.1 Introduction

3.1.1 TRPC3 channels in sensory neurons

As non-selective cation channels, the TRPCs have an important role in neurons as their activation and subsequent influx of cations may be sufficient to induce depolarization or neurotransmitter release, as well as the Ca^{2+} dependent intracellular signalling required for growth and development. Microarray analysis of DRGs from a mouse line with complete ablation of the nociceptor population shows a dramatic down regulation of TRPC3 (Abrahamsen *et al.*, 2008). TRPC3 has also been shown to co localise in neurons with TRPV1, an indicator of nociceptive neurons (Elg *et al.*, 2007). TRP channels are the landmarks of our sensory systems, responding to temperature, touch, pheromones and chemical stimuli so it is understandable that TRP channels are overrepresented in sensory neurons, however the sensory stimulus that TRPC3 responds to is not known.

TRPC3 is also expressed in the central nervous system and in smooth muscle. In order to look at the role of TRPC3 in the somatosensory system only we generated a conditional knockout using Nav1.8Cre to look at the role of TRPC3 in the nociception and Advillin Cre to look at the role of TRPC3 in all sensory neurons.

3.1.2 Na$_v$1.8 Cre

A "knock-in" mouse strain has been generated by expressing Cre recombinase under the control of the Na$_v$1.8 promotor (Stirling *et al.*, 2005). The coding sequence for Na$_v$1.8 was replaced by the gene for Cre but all regulatory elements controlling spatial and temporal expression patterns were retained. Since Na$_v$1.8 is expressed in a subset of sensory neurons, primarily nociceptors (Akopian *et al.*, 1996) , this is a very useful tool for investigating gene function in peripheral nociceptors. The expression pattern of Cre in the knock-ins was examined using ROSA26 reporter mice and found to match that of Na$_v$1.8 exactly. Expression of Cre began at embryonic day 14 in small diameter, unmyelinated neurons of DRG, trigeminal and nodose ganglia. Expression was also shown in a limited number of large

myelinated DRG neurons. CNS and non-neuronal cells were shown to have no Cre expression (Figure 3.1). $Na_v1.8$ Cre heterozygotes, expressing one functional copy of the $Na_v1.8$ channel, were found to have no deficits in sodium channel expression, motor function, acute pain thresholds nor inflammatory or neuropathic pain.

This makes the $Na_v1.8$ Cre mouse line a suitable tool for nociceptor specific deletion.

a.

b.
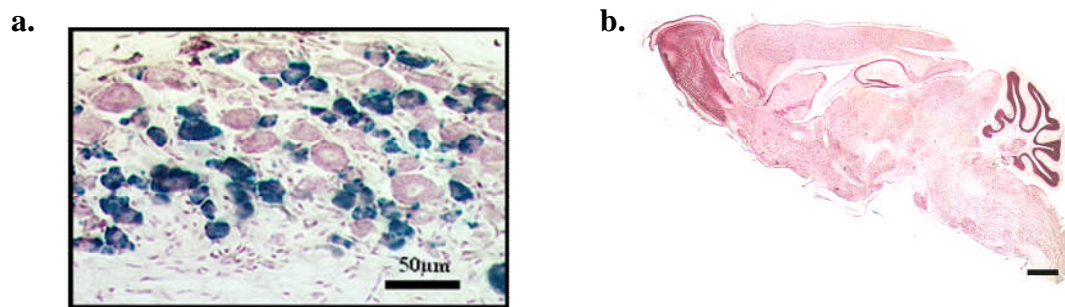
Figure 3.1 Expression of Nav1.8Cre in DRG and brain

Expression of Nav1.8Cre in mouse DRG **(a)** and brain **(b)** shown by crossing with ROSA26-lacZ reporter mice and staining with X-gal. (Stirling *et al.*, 2005). Blue cells represent expression of Nav1.8Cre (scale = 50µm)

3.1.3 Advillin Cre

Advillin is an actin binding protein involved in the organisation of the cytoskeleton which has been shown to be exclusively expressed in the DRG and TG from embryonic day12.5 with no expression in the brain or spinal cord. (Marks *et al.*, 1998;Shibata *et al.*, 2004;Ravenall *et al.*, 2002) Hasegawa et al also showed that Advillin is expressed in postmitotic sensory neurons and not in progenitor cells further proving the selective expression of Advillin in only DRG and TG sensory neurons (Hasegawa *et al.*, 2007). Wang et al generated a knock-in mouse line which expressed Cre under the control of the Advillin promoter enabling gene deletion in all sensory neurons without affecting other tissues, see Figure 3.2, (Zhou *et al.*, 2010). Advillin Cre heterozygotes, expressing one functional copy of Advillin, were found to have no deficits in neuronal function, motor function, acute pain thresholds or inflammatory pain (Minnet 2010, unpublished data)

This makes the Advillin Cre mouse line a suitable tool for sensory neuron specific deletion.

a.   b.
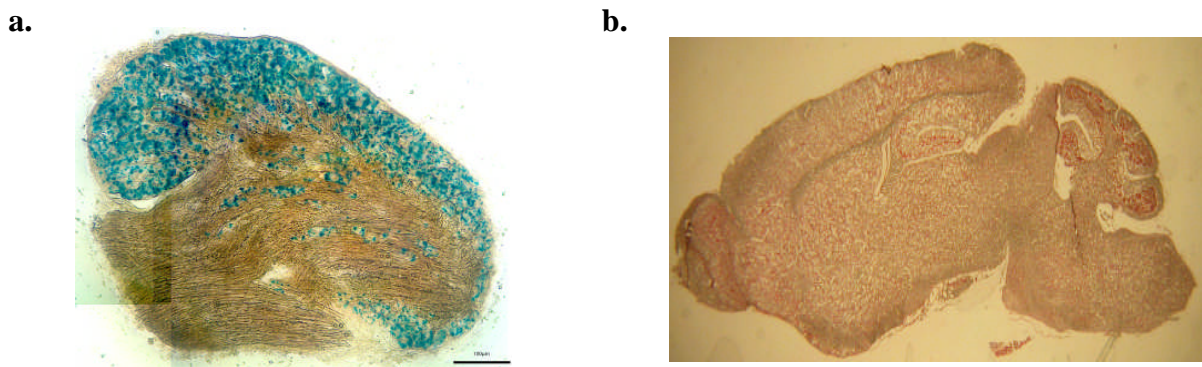
Figure 3.2 Expression of Advillin Cre in DRG and brain

Expression of AdvCre in mouse DRG **(a)** and brain **(b)** shown by crossing with ROSA26-lacZ
reporter mice and staining with X-gal. Blue cells represent expression of Advillin Cre
(scale = 100µm).

3.2 TRPC3fl/fl:Nav1.8Cre Phenotyping results

3.2.1 Targeting construct design

The design and manufacture of the floxed TRPC3 construct was performed by Birnbaumer et al (Hartmann *et al.*, 2008). The design and manufacture of the Nav1.8-cre mouse was performed by Mohammed Nassar (Stirling *et al.*, 2005). The intron-exon organisation of the *Mus musculus* TRPC3 gene and a diagram of the expected disruption of the gene is shown in Figure 3.3 along with the lengths of amplicons that will be used for genotyping.
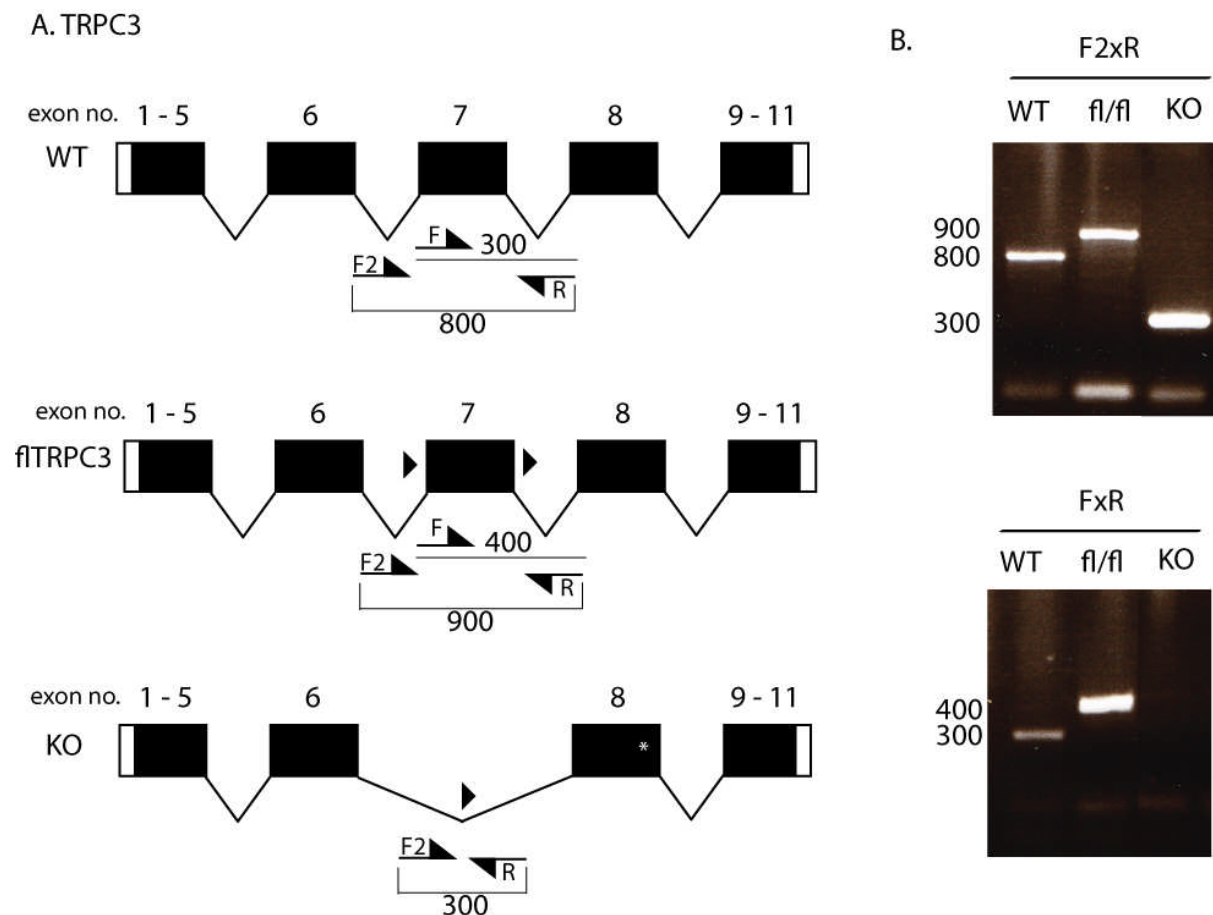
Figure 3.3 Intron-exon organization of *Mus musculus* TRPC3 gene

A. Diagram of intron-exon organization, triangles denote *loxP* sites, *, stop codon, boxes and lines represent exons and introns respectively, F (5' GCTATGATTAATAGCTCATACCAAGAGATC), F2 (5'GAATCCACCTGCTTACAACCATGTG), R (5'GGTGGAGGTAACACAGACCTAAGCC), primers. B. Migration of amplicons from wildtype (WT), floxed TRPC3 (fl/fl) and knockout after cre recombinase (KO) using primers indicated.

We chose to delete the TRPC3 gene using the Cre/*lox*P system. This system allows the deletion of a *loxP* flanked gene to be restricted to tissues expressing the Cre recombinase enzyme. This system has a number of advantages; firstly it allows the study of deletion of TRPC3 in the tissue of interest without affecting any role TRPC3 may play in development or other systems. Secondly it allows the generation of test and littermate control mice within a single litter without any unusable genotypes.

The Cre/*lox*P system is usually used to delete a portion of a gene rather than the whole gene which reduces the size of the targeting construct and also eliminates any possible reduction in efficiency of the Cre recombinase over large distances. Exon 7 of the TRPC3 gene was floxed. The resultant gene would encode a shorter protein of 606 amino acids lacking the C-terminal part downstream of the pore region (depicted in Figure 3.4). The deletion of exon 7 also induces a frame shift in the remaining exons, further reducing the chance of a functional protein being made. The deletion of exon 7 avoids any possibility of disrupting the promoter region of TRPC3, deletion of which is post-natally lethal (Rodriguez-Santiago *et al.*, 2007).
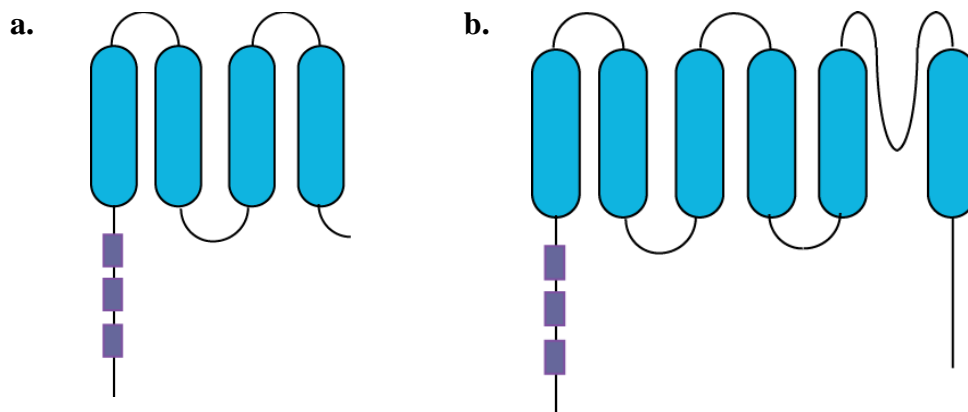
Figure 3.4 Illustration of the possible truncated protein encoded by TRPC3fl/fl mouse after deletion by Cre recombinase

a. After deletion the TRPC3 gene could encode a shorter protein comprising of the N terminus, three ankyrin repeats (purple boxes) and four transmembrane segments (blue cylinders). **b.** The full protein contains an N terminus, three ankyrin repeats, six transmembrane segments, a pore loop and C terminus.

3.2.2 Breeding strategy

The chimeras were crossed with C57BL/6 mice. This was followed by crossing to FLPe deleter mice to excise the positive selection cassette, neo resistance. These mice were then crossed to mice expressing Cre under the control of the Nav1.8 promotor. Finally, homozygous floxed mice and homozygous floxed mice heterozygous for Cre were crossed to generate conditional-null mutants and floxed littermate controls for analysis. This ensured an identical genetic background for conditional-null and control animals. Genotyping was performed on ear tissue as described in materials and methods.

3.2.3 Confirmation of TRPC3 knockout

The knockout of TRPC3 was confirmed with PCR of genomic DNA (see 8.1.1) and also reverse transcription PCR and quantitative RT-PCR of RNA. RT-PCR showed that TRPC3 RNA from the TRPC3$^{-/-}$ produced a smaller band, confirming excision of exon 7. Quantitative PCR showed a decrease of TRPC3 RNA in TRPC3fl/fl:Nav1.8Cre mice and a more substantial decrease of RNA in the TRPC3$^{-/-}$ mouse created by crossing the TRPC3fl/fl mouse with Cre deleter (see 5.2.1 for more details).
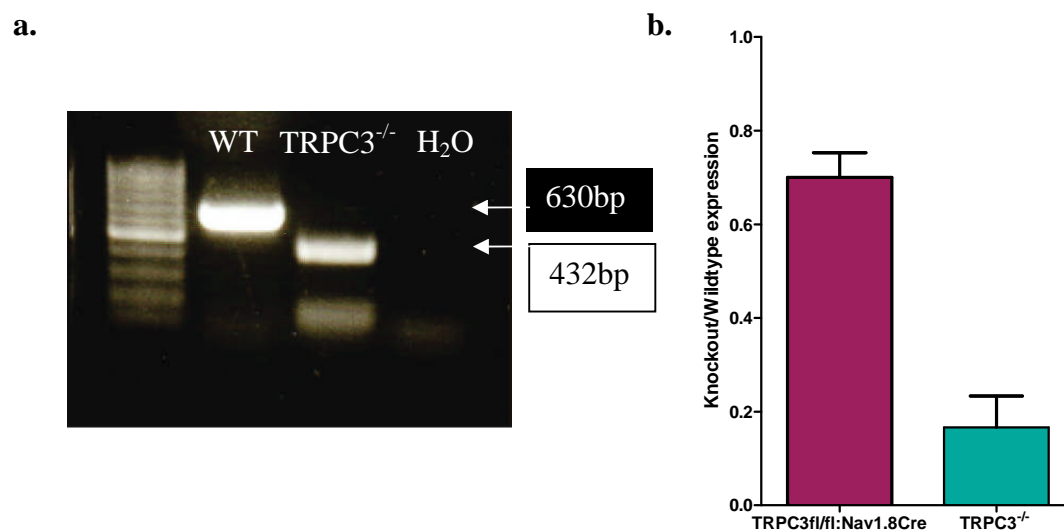
Figure 3.5 Confirmation of TRPC3 knockout at RNA level

a. RT-PCR of wildtype and TRPC3$^{-/-}$ cDNA showed ~200bp difference in band size, confirming the deletion of exon 7. **b.** Quantitative PCR showed a reduction in cDNA for both TRPC3fl/fl:Nav1.8Cre (0.7±0.05) and TRPC3$^{-/-}$ (0.2±0.05) animals. Expressed as a ratio knockout vs wildtype calculated using the Pfaffl method ±SEM.

3.2.4 TRPC3 fl/fl:Nav1.8Cre mice show no deficits in response to noxious cold

Behavioural responses to noxious cold were assessed using the cold plate set to 0ºC for 5 minutes. A pain behaviour was classified as a flinching, licking or shaking of the hind paw. The TRPC3 fl/fl:Nav1.8Cre animals were just as cold sensitive as control animals, with 17.9±1.23 behaviours in 5 minutes compared to 17.8±1.0 behaviours (Figure 3.6).
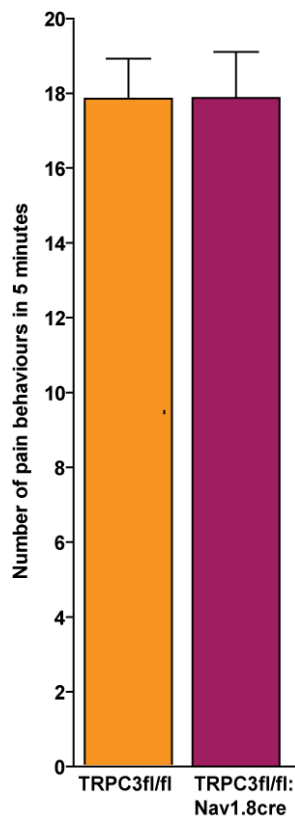
Figure 3.6 Acute cold pain behaviour in TRPC3 fl/fl:Nav1.8Cre and control (TRPC3 fl/fl) animals.
Noxious cold stimulation using cold plate at 0ºC. No significant difference seen between TRPC3 fl/fl littermate control (orange, n=5) and TRPC3 fl/fl:Nav1.8Cre (red, n=8) animals. All results shown as mean ±SEM.

3.2.5 TRPC3 fl/fl:Nav1.8Cre mice have attenuated inflammatory pain in some models

3.2.5.1 Carrageenan induced mechanical hyperalgesia

Mechanical responses were recorded from mice injected with carrageenan compared to baseline recordings made prior to the injections. The control mice developed a clear mechanical hyperalgesia, the 50% threshold dropping from 0.5 ± 0.03g to 0.1 ± 0.03g at 3 hours after carrageenan injection. The TRPC3 fl/fl:Nav1.8Cre mice developed a less severe mechanical hyperalgesia the threshold dropping from 0.6 ± 0.08g to 0.3 ± 0.03 g. (Figure 3.7) An unpaired t-test showed that there was a significant difference between the mechanical thresholds of TRPC3 fl/fl:Nav1.8Cre mice and the control mice post-carrageenan injection ($p = 0.0195$) confirming the result of the formalin test that TRPC3 is involved in inflammatory pain.
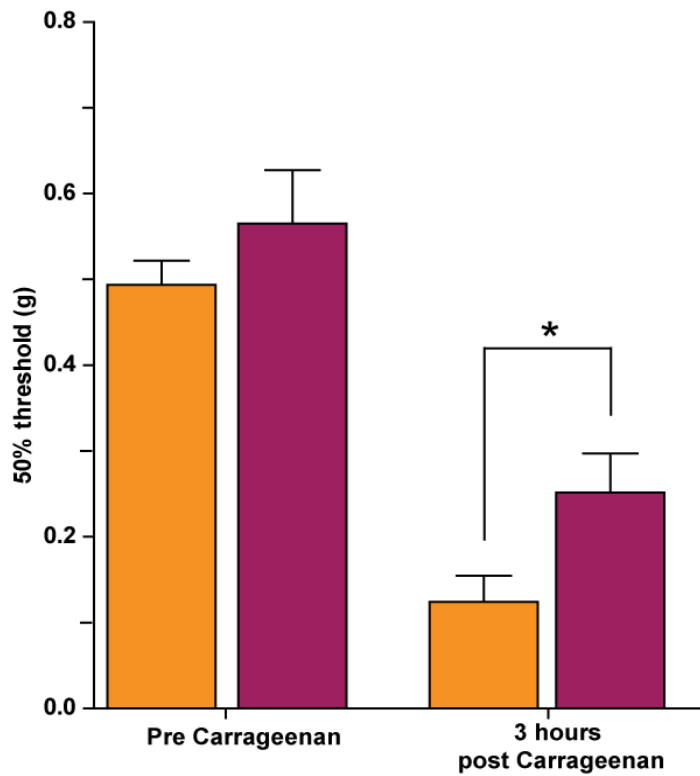
Figure 3.7 Carrageenan induced mechanical hyperalgesia in TRPC3 fl/fl:Nav1.8Cre and control (TRPC3fl/fl) animals.

Behaviour following injection of 20μl of 2% carrageenan. The 50% mechanical threshold was recorded using von Frey hairs on two days prior to injection and three hours post injection. TRPC3 fl/fl:Nav1.8Cre mice (orange, n = 4) have significantly attenuated mechanical hyperalgesia compared to littermate controls (red, n = 3). All results shown as mean ±SEM.

3.2.5.2   Complete Freund's adjuvant induced mechanical and thermal hyperalgesia

Mechanical (von Frey) and thermal (Hargreaves') thresholds were measured from 3 TRPC3 fl/fl:Nav1.8Cre   mice and 6 control mice following induction of inflammation by administration of 20µl of CFA and compared to baseline measurements. The same mice were used for both mechanical and thermal measurements on days 1, 3, 7 and 10 post injections. There was no difference between the mechanical hyperalgesia developed after CFA injection between the TRPC3 fl/fl:Nav1.8Cre   mice and the control mice at any of the time points measured (Figure 3.8a). Thermal hyperalgesia also developed in the TRPC3 fl/fl:Nav1.8Cre mice to the same extent as the control mice, although the TRPC3 fl/fl:Nav1.8Cre mice did appear to recover quicker. At day 7 there was a significant difference between the thermal hyperalgesia experienced by the control mice, 5.9±0.94 seconds, compared to the TRPC3 fl/fl:Nav1.8Cre   mice, 10.4±0.32 seconds, (p <0.01) (Figure 3.8b).
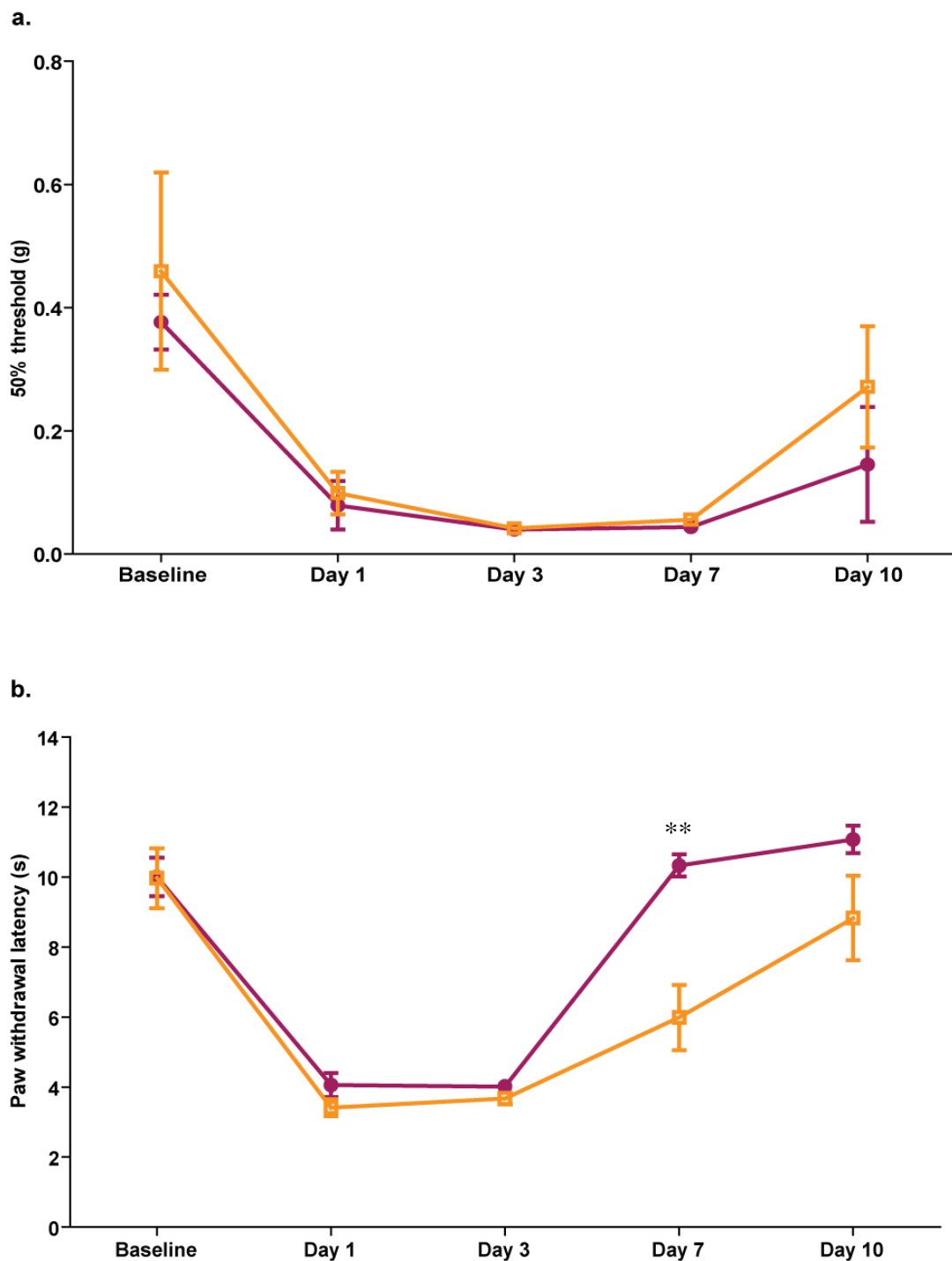
Figure 3.8 Complete Freunds' Adjuvant induced hyperalgesia in TRPC3 fl/fl:Nav1.8Cre and control (TRPC3fl/fl) animals.

Mechanical and thermal thresholds following injection of 20µl CFA. **a.** The 50% mechanical threshold was recorded using von Frey hairs prior to injection and on days 1, 3, 7 and 10 following injection. There is no significant difference between TRPC3 fl/fl:Nav1.8Cre mice (red, n = 3) and littermate controls (orange, n = 6). **b.** Paw withdrawal latency to a radiant heat source (Hargreaves') was measured prior to injection and on days 1, 3, 7 and 10 following injection. There was a significant difference between the thermal hyperalgesia between TRPC3 fl/fl:Nav1.8Cre mice (n = 3) and littermate controls (n = 6) on day 7 ($p < 0.01$, two-way ANOVA). All results shown as mean ±SEM.

62

3.2.5.3 Prostaglandin E2 induced mechanical hyperalgesia

Mechanical thresholds were measured from 5 TRPC3 fl/fl:Nav1.8Cre mice and 5 control mice 3 hours after administration of 100ng of PGE2 and compared to baseline measurements made on two non consecutive days previously. Both control and TRPC3 fl/fl:Nav1.8Cre mice developed mechanical hyperalgesia with thresholds dropping to 0.05 ± 0.004 grams and 0.1 ± 0.052 grams respectively (Figure 3.9).
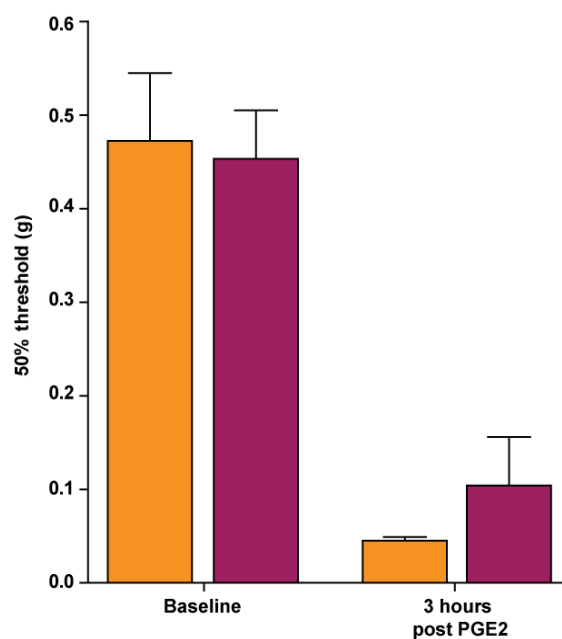
Figure 3.9: PGE2 induced mechanical hyperalgesia in TRPC3 fl/fl:Nav1.8Cre and control (TRPC3fl/fl) animals.

Mechanical and thermal thresholds following injection of 100ng PGE_2. There is no significant difference between **TRPC3 fl/fl:Nav1.8Cre** l mice (red, n = 5) and littermate controls (orange, n = 5). The 50% mechanical threshold was recorded using von Frey hairs prior to injection and 3 hours following injection.

3.2.5.4 Bradykinin induced pain behaviour

Behavioural responses from 7 TRPC3 fl/fl:Nav1.8Cre mice and 5 control mice were recorded for 30 minutes following administration of 10nmol of bradykinin in 10µl saline intraplantar into the left hind paw. TRPC3 fl/fl:Nav1.8Cre mice displayed 19±3.5 seconds of pain behaviours compared to 49±3.0 seconds for the littermate controls.
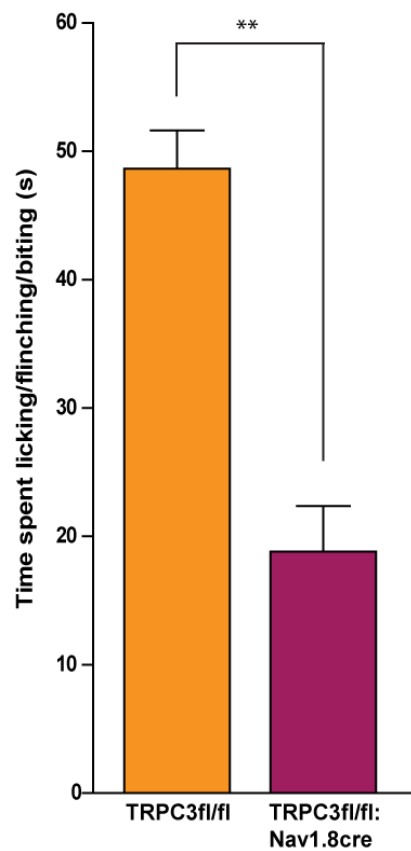
Figure 3.10: Behaviour following injection of 10nmol bradykinin.
TRPC3 fl/fl:Nav1.8Cre mice (red, n=4) had significantly attenuated pain behaviours (unpaired t-test, p = 0.0017) compared to littermate controls (orange, n = 3) following injection of bradykinin. All results shown as mean±SEM.

3.3 TRPC3 fl/-:AdvCre Phenotyping results

3.3.1 Breeding strategy

The breeding strategy was as previously described for the TRPC3 fl/fl:Nav1.8Cre mouse line, chimeras bred with C57BL/6 and the F1 crossed with FLPe deleter mice. But the homozygous floxed heterozygous Cre mice in the final breeding cross were required to be male as advillin Cre expression in female mice can be "leaky" and germ line cell transmission does not occur in all animals.

3.3.2 Confirmation of tissue specific knockout

The knockout of TRPC3 was confirmed with PCR using primers that flank exon 7 (Table 1.2). This enabled identification of a floxed exon 7 as an increase of 100bp of the PCR product and also the identification of a deleted exon 7 which would produce a smaller PCR product of 300bp.

Primer	Sequence	WT	fl/fl	Cre
TRPC3 F2	GAATCCACCTGCTTACAACCATGTG	800bp	900bp	300bp
TRPC3 R	GGTGGAGGTAACACAGACCTAAGCC			
TRPC3 F	GCTATGATTAATAGCTCATACCAAGAGATC	300bp	400bp	none

Table 3.1 PCR primers for confirmation of knockout of TRPC3

Tissue was collected from the ears, tail and DRG of TRPC3$^{fl/fl}$ mice and TRPC3 fl/-:AdvCre mice and the DNA extracted. PCRs using primers TRPC3F2 x TRPC3R and TRPC3F x TRPC3R were performed and the results shown in Figure 3.11. The PCR product showed the floxed band to be present in all tissues of the TRPC3$^{fl/fl}$ animals and also in the ear and tail of the TRPC3 fl/-:AdvCre mice. A strong knockout band of 300bp was present in the DNA from the DRG of the TRPC3 fl/-:AdvCre mouse along with a faint band at 900bp indicating the presence of the floxed TRPC3 gene in the small amount of non-neuronal cells within the DRG. However, the knockout band was also present in all of the other tissues, along with the floxed TRPC3 band. This indicates that all of the mice were global heterozygotes for the TRPC3 gene and the Advillin Cre had acted to excise the one remaining copy of TRPC3 in

the DRG cells only. This was also confirmed by using a primer within exon 7 (TRPC3F) which gave a band in all tissues of the TRPC3$^{fl/fl}$ mouse proving that there is one copy of the TRPC3 gene in all tissues that do not express Cre. The TRPC3 fl/-:AdvCre mouse gave a faint band in the DRG, from non-neuronal cells, and a strong band in the ear and tail (Figure 3.11b). The TRPC3$^{fl/-}$ mice which did not have the Advillin Cre gene were used as littermate controls for all behavioural experiments.

3.3.3
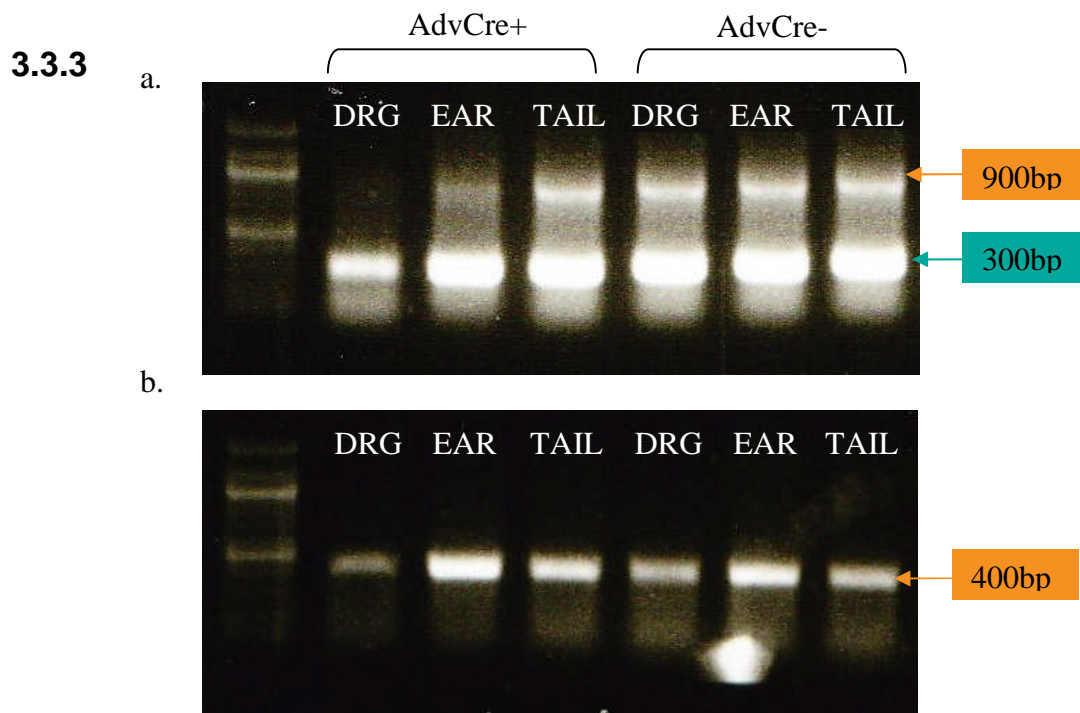
Figure 3.11 Confirmation of tissue specific knockout of TRPC3 in DRG neurons
a. PCR of ear, tail and DRG DNA from a AdvCre+ and AdvCre- mouse using primers TRPC3F2 and TRPC3R. **b.** PCR of same ear, tail and DRG DNA using primers TRPC3F and TRPC3R

TRPC3 fl/-:AdvCre mice show no deficits in motor coordination

Motor coordination was judged using an accelerating rotarod. There was no difference in the motor ability of the TRPC3 conditional null mice (160±19 seconds) compared with control animals (138±34 seconds) (Figure 3.12).
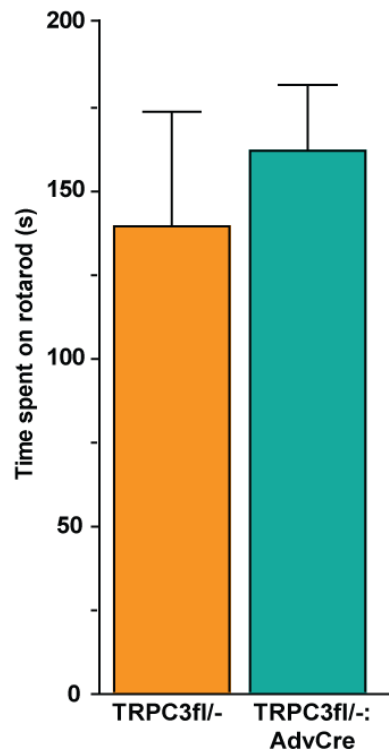
Figure 3.12 Motor coordination of TRPC3 fl/-:AdvCre and control animals.

There was no difference in motor coordination between TRPC3fl/- littermate control (orange, n=4) and TRPC3 fl/-:AdvCre (green, n=7) animals. All results shown as mean ±SEM.

3.3.4 TRPC3 fl/-:AdvCre mice do not show behavioural deficits in mechanosensation

Behavioural responses to mechanical stimulus were measured using von Frey hairs and the Randall Selitto test. No difference in withdrawal threshold to von Frey hairs was observed between TRPC3 fl/-:AdvCre, 0.4±0.04g, and control animals, 0.4±0.03g (Figure 3.13a). The Randall Selitto test showed there was also no difference in behavioural responses to noxious blunt stimulation of the tail between TRPC3 fl/-:AdvCre mice, 116±11g, and control animals, 128±4.4g (Figure 3.13b).
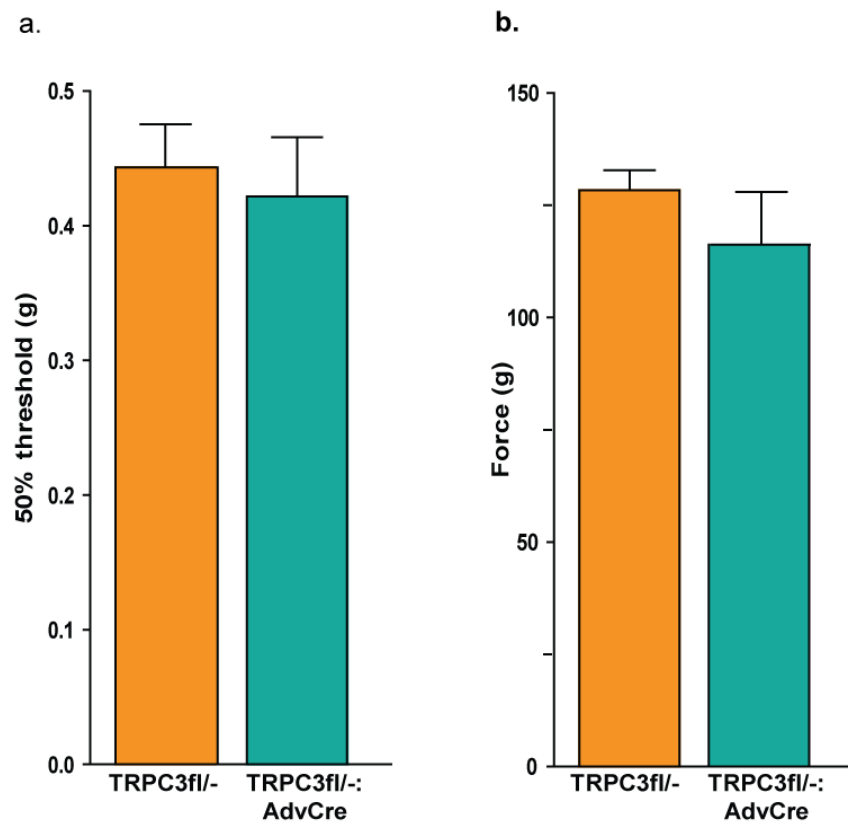
Figure 3.13 Acute mechanical pain behaviour in TRPC3 fl/-:AdvCre and control animals

a. Response to mechanical stimulation with von Frey hairs was not significantly different between TRPC3fl/- littermate control (orange, n=4) and TRPC3 conditional null (green, n=7) animals. **b.** Response to blunt mechanical stimulation of the tail in the Randall Selitto test was not significantly different between TRPC3fl/- littermate control (orange, n=3) and TRPC3 fl/-:AdvCre (green, n=4) animals. All results shown as mean ±SEM.

3.3.5 TRPC3 fl/-:AdvCre mice do not show behavioural deficits in noxious thermosensation

Behavioural responses to noxious thermal stimuli were measured using the Hargreaves' apparatus and the hot plate test. Paw withdrawal latency in Hargreaves' test was not altered in the TRPC3 fl/-:AdvCre mice, 8±1 second, compared to control animals, 8 ±0.9 seconds (Figure 3.14a). There was also no difference in latency of behavioural responses on the hot plate at 45ºC, 50ºC or 55ºC (Figure 3.14b).
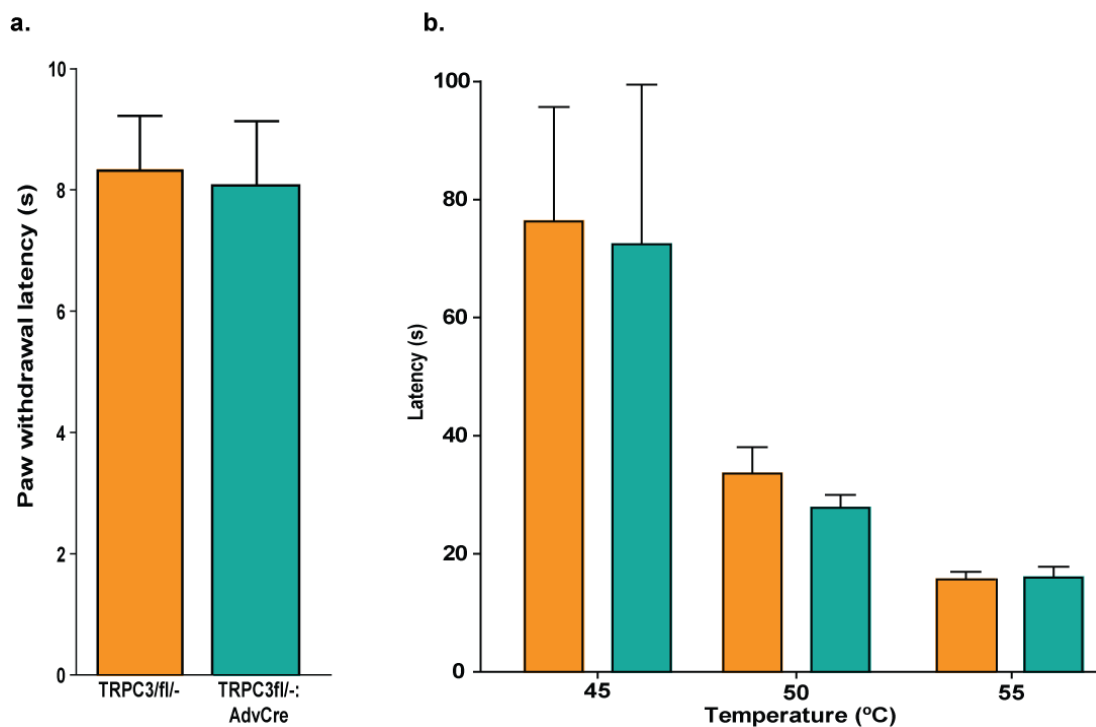
Figure 3.14 Acute thermal pain behaviour in TRPC3 fl/-:AdvCre and control animals.

a. Noxious thermal stimulation using Hargreaves' apparatus. No significant difference was observed between TRPC3fl/- littermate control (orange, n=4) and TRPC3 fl/-:AdvCre (green, n=7) animals. **b.** Response to noxious thermal stimulation using the hot plate test was not significantly different between TRPC3fl/- littermate control (orange, n=6) and TRPC3 fl/-:AdvCre (green, n=5) animals at 45ºC, 50ºC or 55ºC. All results shown as mean ±SEM.

3.3.6 TRPC3 fl/-:AdvCre mice show no deficits in cold sensing

Behavioural responses to noxious cold were assessed using the cold plate set to 0°C for 5 minutes. A pain behaviour was classified as a flinching, licking or shaking of the hind paw. The TRPC3 fl/-:AdvCre animals had the same number of pain behaviours in 5 minutes 14 ±2.7 as control animals, 14±1.3. Innocuous cold sensation was also assessed in the TRPC3 fl/-:AdvCre animals using acetone evaporation, again there was found to be no difference between the time spent licking, flinching or biting, 4±0.74, compared to the control animals, 4±0.50 seconds.
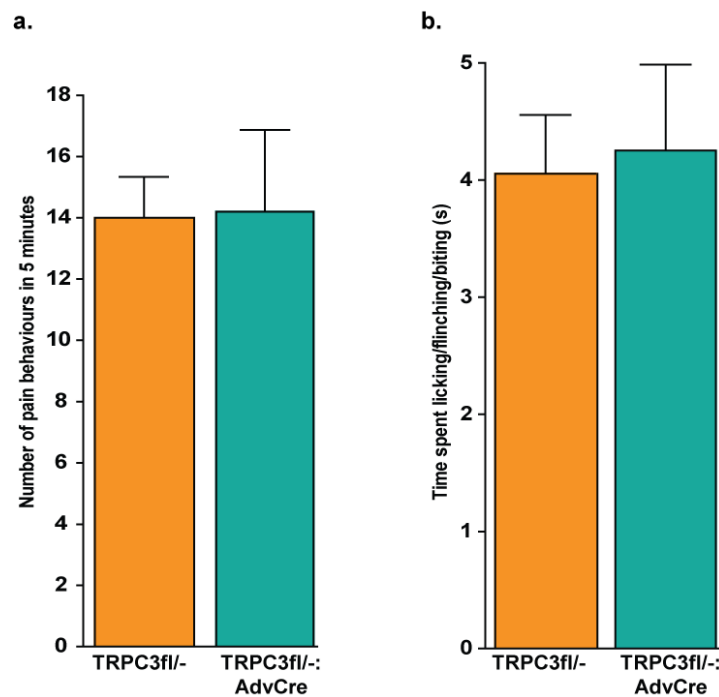
Figure 3.15 Acute cold pain behaviour in TRPC3 fl/-:AdvCre and control animals.

a. Noxious cold stimulation using cold plate at 0°C. No significant difference seen between TRPC3fl/- littermate control (orange, n=6) and TRPC3 fl/-:AdvCre (green, n=5) animals. **b.** Innocuous cold stimulation from evaporation of acetone. No significant difference seen between TRPC3fl/-littermate control (orange, n=9) and TRPC3 fl/-:AdvCre (green, n=10) animals. All results shown as mean ±SEM.

3.3.7 TRPC3 fl/-:AdvCre mice display reduced inflammatory pain behaviour

3.3.7.1 **Formalin test**

Behavioural responses from 4 TRPC3 conditional null mice and 3 control mice in the two distinct phases were recorded. In the first phase, 0-10 minutes, the TRPC3 fl/-:AdvCre mice displayed 135±18 seconds of pain behaviour compared with 172±16 seconds for the control mice. There was no significant difference between the two groups. In contrast the TRPC3 fl/-:AdvCre mice showed attenuated pain behaviours in the second phase, from 10-60 minutes, displaying just 275±14 seconds compared with 450±62 seconds for the control mice. This was shown to be significant using an unpaired 2-tailed t-test (p = 0.0243). (Figure 3.16)

Figure 3.16b shows the time course of the formalin response and demonstrates that the TRPC3 fl/-:AdvCre mice displayed reduced pain behaviours at nearly every 5 minute interval within the second, inflammatory, phase with significant differences at 10-15 and 25-30 minutes found using a 2-way ANOVA.
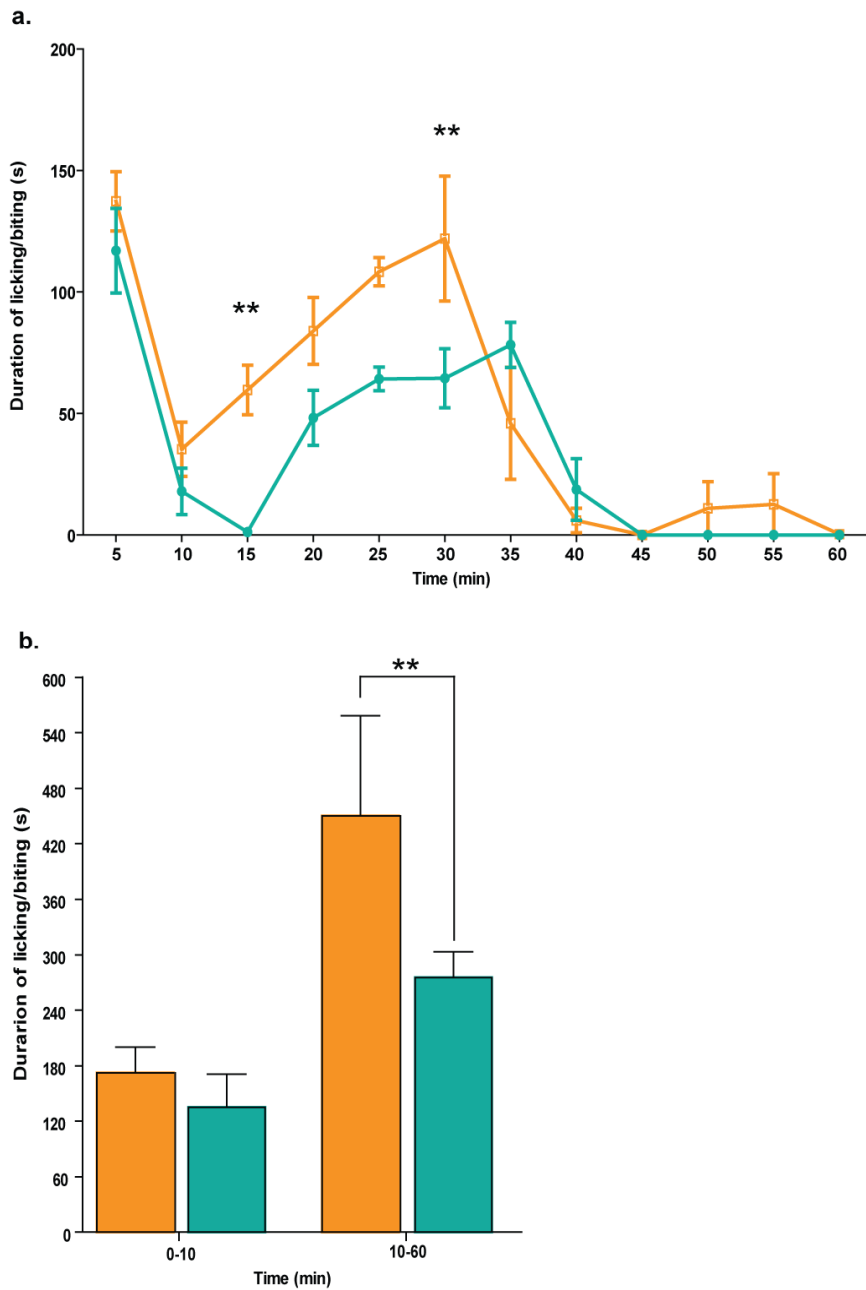
Figure 3.16 Formalin induced pain behaviours in TRPC3 fl/-:AdvCre and control mice

Behaviour following injection of 20µl of 5% formalin. **a.** Time spent licking/flinching/biting the hind paw was recorded in 5 minute sections. No significant reduction in pain behaviours was seen in Phase I (0-10 minutes) however in Phase II (10-60 minutes) TRPC3 fl/-:AdvCre mice (green, n=4) have significantly attenuated pain behaviours compared to littermate controls (orange, n=3). b. Time course of the formalin test. A traditional biphasic response was observed with the attenuated pain behaviour of TRPC3 fl/-:AdvCre mice apparent in the second phase. All results shown as mean ±SEM.

3.3.7.2 Carrageenan induced mechanical hyperalgesia.

Mechanical responses were recorded from mice injected with carrageenan compared to baseline recordings made prior to the injections. The control mice developed a clear mechanical hyperalgesia, the 50% threshold dropping from 0.5±0.04g to 0.07±0.01g at 3 hours after carrageenan injection. The TRPC3 fl/-:AdvCre mice developed a less severe mechanical hyperalgesia the threshold dropping from 0.5±0.01g to 0.2±0.04 g. (Figure 3.7) An unpaired t-test showed that there was a significant difference between the mechanical thresholds of TRPC3 fl/-:AdvCre mice and the control mice post-carrageenan injection (p = 0.0127) confirming the result of the formalin test that TRPC3 is involved in inflammatory pain.
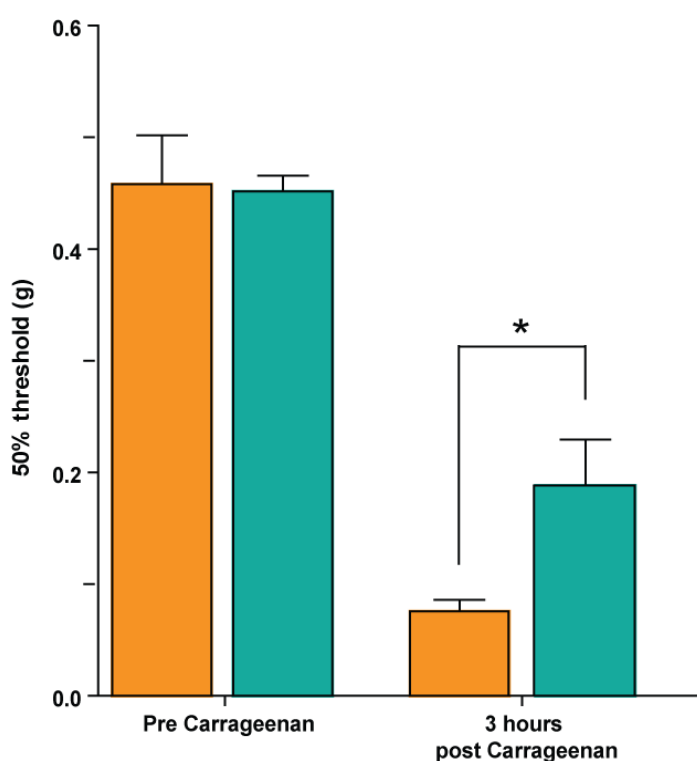
Figure 3.17 Carrageenan induced mechanical hyperalgesia in TRPC3 fl/-:AdvCre and control animals.

Behaviour following injection of 20µl of 2% carrageenan. The 50% mechanical threshold was recorded using von Frey hairs on two days prior to injection and three hours post injection. TRPC3 fl/-:AdvCre mice (green, n =5) have significantly attenuated mechanical hyperalgesia (unpaired t-test, p = 0.0127) compared to littermate controls (orange, n =6). All results shown as mean ±SEM.

3.3.7.3 Complete Freund's adjuvant induced thermal and mechanical hyperalgesia.

Mechanical (von Frey) and thermal (Hargreaves') thresholds were measured from 7 TRPC3 TRPC3 fl/-:AdvCre mice and 3 control mice following induction of inflammation by administration of 20µl of CFA and compared to baseline measurements. The same mice were used for both mechanical and thermal measurements on days 1, 3, 5, 7 and 10 post injections. Both control and TRPC3 fl/-:AdvCre mice developed mechanical hyperalgesia from day 1 post injection of CFA, on day 5 it appeared that the TRPC3 fl/-:AdvCre mice had attenuated mechanical hyperalgesia but this difference was not found to be significant (Figure 3.18a). Thermal hyperalgesia developed in both the TRPC3 fl/-:AdvCre mice and the control mice with no significant difference (Figure 3.18b).
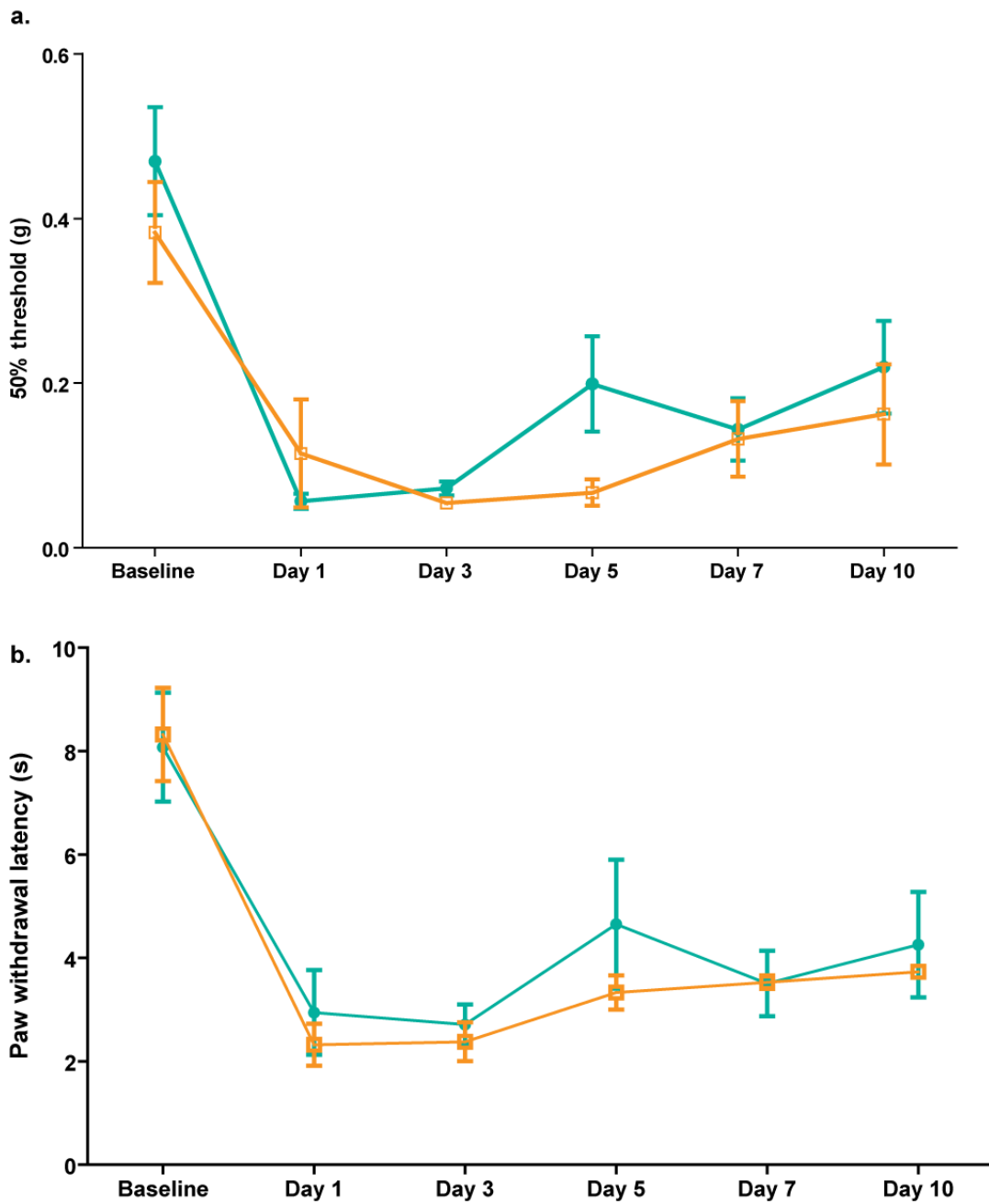
Figure 3.18 Complete Freunds' Adjuvant induced hyperalgesia in TRPC3 fl/-:AdvCre and control animals.

Mechanical and thermal thresholds following injection of 20µl CFA. There is no significant difference between TRPC3 fl/-:AdvCre mice (green, n = 7) and littermate controls (orange, n = 4). **a.** The 50% mechanical threshold was recorded using von Frey hairs prior to injection and on days 1, 3, 7 and 10 following injection. b. Paw withdrawal latency to a radiant heat source (Hargreaves') was measured prior to injection and on days 1, 3, 7 and 10 following injection. All results shown as mean±SEM.

3.3.7.4 Prostaglandin E2 induced mechanical hyperalgesia.

Mechanical thresholds were measured from 5 TRPC3 fl/-:AdvCre mice and 3 control mice 3 hours after administration of 100ng of PGE2 and compared to baseline measurements made on two non consecutive days previously. Both control and TRPC3 fl/-:AdvCre mice developed mechanical hyperalgesia with no significant difference, with 50% thresholds both dropping to 0.14g (Figure 3.19).
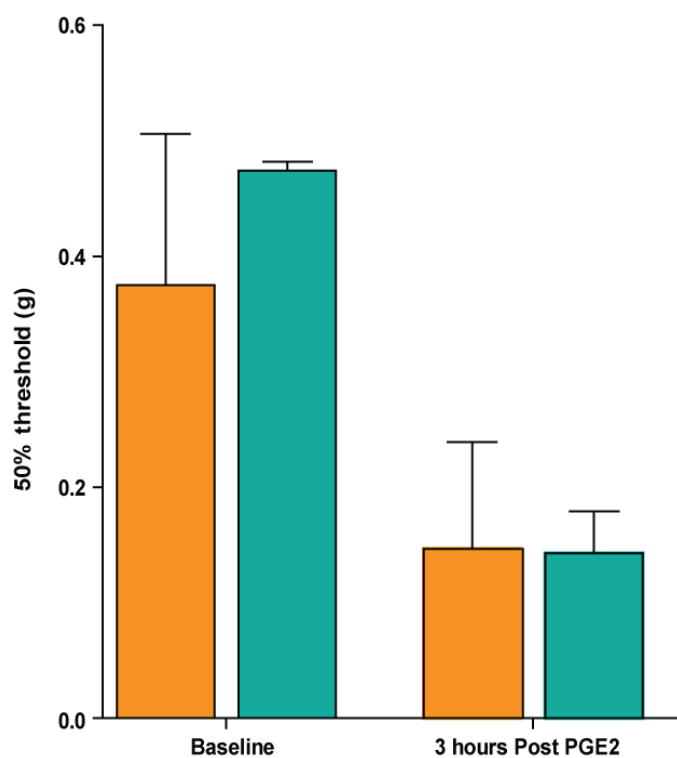
Figure 3.19 PGE2 induced mechanical hyperalgesia in TRPC3 fl/-:AdvCre and animals.

Mechanical and thermal thresholds following injection of 100ng PGE$_2$. There is no significant difference between TRPC3 fl/-:AdvCre mice (green, n = 5) and littermate controls (orange, n = 3). The 50% mechanical threshold was recorded using von Frey hairs prior to injection and 3 hours following injection. All results shown as mean±SEM.

3.3.7.5 Bradykinin induced pain behaviour

Behavioural responses from 5 TRPC3 fl/-:AdvCre mice and 4 control mice were recorded for 30 minutes following administration of 10nmol of bradykinin in 10µl saline intraplantar into the left hind paw. TRPC3 fl/-:AdvCre mice displayed 20±9 seconds of pain behaviours compared to 54±5 seconds for the littermate controls.
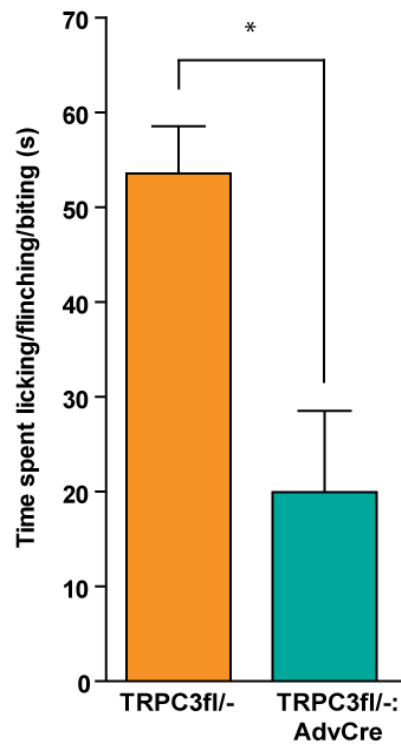
Figure 3.20 Bradykinin induced pain behaviours in TRPC3 fl/-:AdvCre **and control animals**

Behavior following injection of 10nmol bradykinin. TRPC3 fl/-:AdvCre mice (green, n=5) had significantly attenuated pain behaviours (unpaired t-test, p=0.016) compared to littermate controls (orange, n=4). All results shown as mean±SEM.

3.4 Discussion

3.4.1 TRPC3 conditional null mice develop normally.

Before any experiments were performed the fitness of the TRPC3fl/fl:Nav1.8Cre and TRPC3fl/-:AdvCre mice strains were assessed. There were no differences in weight gain, motor function, fertility or general behaviour. The size of litters produced was within expected range and the ratio of male/female progeny was close to 1:1. The Cre+ and Cre-progeny ratio was also close to 1:1 as expected.

3.4.2 Advillin Cre can produce a heterozygous global deletion sporadically

The TRPC3fl/fl:AdvCre mice were found to have a heterozygous global deletion that was also present in TRPC3fl/fl mice. During the breeding strategy the presence of floxed TRPC3, wildtype TRPC3 and advillin Cre gene were checked in order to set up the next round of breeding. The Advillin Cre gene had been shown to be "leaky" in females so only male carriers of advillin Cre were used for breeding. The stages of the breeding and the expected genotypes of progeny are shown in Table 3.2.

	Female		Male		Genotypes of progeny					
	TRPC3	Cre	TRPC3	Cre						
F1	fl/fl	+/+	+/+	Cre/+	fl/+, cre/+	fl/+, +/+				
F2	fl/+	+/+	fl/+	Cre/+	fl/fl, cre/+	fl/fl, +/+	+/+, cre/+	+/+, +/+	fl/+, cre/+	fl/+, +/+
F3	fl/fl	+/+	fl/fl	Cre/+	fl/fl, cre/+	fl/fl, +/+				

Table 3.2 Resulting genotypes from TRPC3fl/fl:AdvCre breeding strategy.

The genotypes of each mouse were checked at each generation. To look for the fl/fl mouse primers TRPC3F and TRPC3R were used to produce a single band at 400bp that we presume represents the amplification of two copies of the floxed exon7 of TRPC3. A non-floxed

TRPC3 gene would give a PCR product of 300bp, these primers were chosen as the size and separation of the bands is clear and easily identifiable. The non-quantitative nature of traditional PCR means that using these primers it is not possible to conclusively prove the presence of two copies of the floxed gene. Some of the progeny from the F2 breeding pairs may have had spontaneous expression of Advillin Cre leading to a deletion of both copies of TRPC3 that would produce a heterozygous zygote. This would lead to a proportion of TRPC3 fl/- mice in the progeny which would still give a single PCR product of 400bp. In the future it would be possible to identify the erroneous knockout of TRPC3 using primers TRPC3F2 and TRPC3R for genotyping alongside TRPC3F and TRPC3R.

The loss of one copy of TRPC3 does not affect the pain thresholds or development of inflammatory pain as throughout all of the behavioural studies the control mice used, TRPC3fl/-, were found to have comparable results to the TRPC3fl/fl mice from the Nav1.8Cre strain and also to wildtype mice from other studies conducted in the lab (see Figure 3.8 and Figure 3.18 for baseline mechanical and thermal thresholds). For this reason it was decided not to repeat the behavioural experiments using littermate floxed TRPC3 mice to reduce the number of animals used unnecessarily.

3.4.3 TRPC3 is not involved in acute mechanical sensation.

Mechanosensation was tested using three different methods, von Frey hairs, automated von Frey and Randall Selitto. Automated von Frey and von Frey hairs test for thresholds to dynamic light touch and Randall Selitto tests the threshold for noxious mechanical pressure. Previous studies showed that Nav1.8 neurons are essential for noxious mechanical pressure sensation but not required for light touch sensation (Abrahamsen *et al.*, 2008). The TRPC3fl/fl:Nav1.8Cre showed no deficit in light touch sensation but also no deficit in noxious mechanical pressure proving TRPC3 is not a high threshold mechanosensor in Nav1.8 neurons.

The TRPC3fl/-:AdvCre mouse had a knockout of TRPC3 in all DRG neurons, including the subset that must be responsible for transducing light touch signals. This knockout also had no effect on the animal's ability to sense light touch.

When investigating the contribution of TRPC6 to the myogenic response Dietrich et al found that instead of a reduced response the knockout actually had an increased sensitivity (Dietrich *et al.*, 2005). Upregulation of TRPC3, which has constitutive activity, was found to be responsible for this erroneous result. TRPC6 is also shown to be mechanically sensitive and could be acting in conjunction with TRPC3 in DRG neurons as it is also expressed in these cells. The knockout of TRPC3 at an early time point, from embryonic day 12-14, could lead to an upregulation of TRPC6 either at a protein level or increased availability or activity at the membrane.

3.4.4 TRPC3 is not involved in acute noxious heat sensation

Thermosensation was tested using two different models, the Hot plate and the Hargreaves' apparatus. The thermal stimulation provided by the hot plate test causes voluntary behaviour requiring supraspinal responses. There was no difference in the response to the hotplate test between the control mice and either the TRPC3fl/fl:Nav1.8Cre knockout or the TRPC3fl/-:AdvCre knockout. The Hargreaves' apparatus provokes a reflex withdrawal in response to a radiant heat. There was no difference found between withdrawal reflex time between control mice and the TRPC3fl/fl:Nav1.8Cre or the TRPC3fl/-:AdvCre.

Previous use of Nav1.8 Cre to knock out Nav1.7 or BDNF in the nociceptors has produced a significant thermal deficit in either the Hargreaves' or the hotplate test (Nassar *et al.*, 2004;Zhao *et al.*, 2006) suggesting that this subset of neurons and proteins are important for thermal sensation. However, complete ablation of the Nav1.8 expressing neurons produced only a small thermal deficit (Abrahamsen *et al.*, 2008) casting doubt on their involvement. Subsets of fibres have been identified with different response thresholds and conduction velocity (Treede *et al.*, 1995). It is possible that complete ablation of one population of noxious heat responsive fibres led to compensation from another subset.

Members of the transient receptor protein superfamily have been reported as the mammalian heat sensors, all of these heat sensors are within the TRPV family. TRPV1 was the first TRP

to be proposed as a heat sensor, being activated at ~45°C in vitro (Caterina *et al.*, 1997). TRPV1 is found in a subset of peptidergic and IB4+ DRG neurons, the lack of response to capsaicin both *in vitro* and *in vivo* in the DTA-CRE mouse showed that this subset is almost completely overlapping with Nav1.8 expressing neurons (Abrahamsen *et al.*, 2008). TRPV1 was proposed to be the moderate heat sensor, a theory confirmed by data from the knockout mouse showing increased thermal thresholds to the hotplate and tail immersion test (Caterina *et al.*, 2000). However, heat sensing was not completely abolished and further studies on the TRPV1$^{-/-}$ mouse failed to find a difference in acute thermal sensation, although inflammatory thermal hyperalgesia was affected (Davis *et al.*, 2000).

As the Nav1.8-expressing neurons have been shown not to be solely responsible for transducing noxious heat we used advillin cre to produce a conditional knockout in all DRG neurons allowing us to fully investigate the involvement of TRPC3 in heat sensing. Neither the hot plate or the Hargreaves' apparatus showed any differences between the control and TRPC3fl/-:AdvCre mice proving that TRPC3 has no involvement in acute heat sensing. This was not surprising as TRPC channels are not closely related to the TRPV family and have not been shown to be activated by heat *in vitro* or *in vivo*.

3.4.5 TRPC3 is not involved in sensing of noxious or innocuous cold

Response to noxious cold was tested using a cold plate at 0° C, well below the 10° C threshold for cold pain previously described in rats (Allchorne *et al.*, 2005), to ensure a noxious stimulus. There was no difference in the number of pain behaviours observed in the TRPC3fl/fl:Nav1.8Cre or TRPC3fl/-:AdvCre mouse compared to control animals.

Nav1.8 is essential for noxious cold sensation (Zimmermann *et al.*, 2007) suggesting that the cold sensor is expressed within the Nav1.8 + neurons; this was confirmed by the DTA mouse which is resistant to the noxious cold experienced on the cold plate (Abrahamsen *et al.*, 2008). TRPM8 has been suggested as the cold sensor but is not co-localised with Nav1.8 and is thought to be responsible for sensing of innocuous cold (Jordt *et al.*, 2004;Dhaka *et al.*, 2007). Another ion channel must be responsible for noxious cold sensation.

As noxious cold is sensed by the Nav1.8+ neurons if TRPC3 was important for noxious cold sensation the TRPC3fl/fl:Nav1.8Cre mouse would be resistant to noxious cold, Figure 3.6 shows this is not the case. The TRPC3fl/-:AdvCre mouse also shows no resistance to noxious cold confirming this result. Innocuous cold is thought to be transmitted by TRPM8 expressing neurons, which are Nav1.8-ve. The sensitivity of TRPC3fl/-:AdvCre mice to innocuous cold was tested using the acetone test and showed no difference between wildtype and knockout mice, Figure 3.15. This confirms that TRPC3 is not involved in noxious or innocuous cold sensation.

3.4.6 TRPC3 has an important role in inflammatory pain

Inflammatory pain requires the peripheral and/or central sensitization of DRG neurons. The release of inflammatory mediators linked to this sensitization requires ion channels and receptors expressed at the termini of the primary sensory neurons.

Both the nociceptor-specific and pan-DRG knockout of TRPC3 showed reduced inflammatory pain in the formalin and carrageenan tests, and the pan-DRG TRPC3 knockout had an attenutated phenotype in the bradykinin test. It is not possible to directly compare the phenotype of TRPC3fl/-:AdvCre mice with the phenotype observed previously in the TRPC3fl/fl:Nav1.8Cre mice as the formalin test is highly sensitive to external environmental factors (Rosland, 1991) and also subjectivity of the experimenter. However, as shown in Figure 3.16, pain behaviours are not completely abolished in the inflammatory phase, suggesting that additional deletion of TRPC3 from the large diameter neurons has no further effect on the attenuated inflammatory phenotype. This fact, together with previous work showing the importance of the Nav1.8+ve neurons in inflammatory pain, suggests that the role of TRPC3 in inflammatory pain is mainly within the small-medium nociceptors.

The first phase of formalin induced pain behaviours was unaffected by the knockout of TRPC3, this was expected as this phase is known to be directly mediated through TRPA1 (McNamara *et al.*, 2007). The second phase of formalin is mediated through a variety of inflammatory mediators causing peripheral and central sensitisation by enhancing excitability of neurons. NMDA receptors are fundamental for the central sensitisation, excitatory amino acids released from peripheral neurons act on post-synaptic NMDA receptors in the dorsal

horn leading to calcium entry and an increase in intracellular signalling cascades (Coderre and Melzack, 1992). Phosphorylation of NMDA receptors increases calcium entry and correlates with the second phase of formalin (Zhao *et al.*, 2006). This synaptic plasticity is regulated by presynaptic molecules such as BDNF and Ephrin-B2 that are increased in inflammatory pain states (Zhao *et al.*, 2010;Zhao *et al.*, 2006).

Many inflammatory mediators signal through GPCRs, which are found on both peripheral and central neurons. Phospholipase C is downstream of a number of GPCRs and is essential for the second phase of formalin, PLC inhibitors can block the second phase without affecting the first phase (Coderre, 1992) . PLC is part of a second messenger cascade that also involves arachidonic acid, PGE2 and PKC. PKC inhibitors and COX-2 inhibitors, preventing the formation of PGE2, are able to attenuate the pain behaviours in the second phase of formalin but not abolish them (Coderre and Yashpal, 1994) .

TRPC3 can be activated by PLC, via the production of DAG, which leads to an influx of cations which increases excitability, releases secondary mediators and phosphorylates other channels. To investigate whether the attenuated inflammatory phenotype seen in the TRPC3 fl/fl:Nav1.8Cre mice is specifically linked to PLC signalling we looked at the induction of inflammatory pain directly through two different G proteins. There are three main G-protein-mediated signalling pathways, mediated by four subclasses of G-proteins, Gs, Gi/o, Gq/11, G12/13. Most GPCRs are capable of activating more than one subtype of G protein but show a strong preference for one over another. BK receptors are Gq protein coupled receptors and cause activation of PLC. PGE2 acts through four EP receptors, EP1 coupled to Gq, EP2 and 4are Gs protein coupled receptors causing the activation of adenylate cyclase and EP3 is coupled to Gi causing inhibition of cAMP. The TRPC3 fl/fl:Nav1.8Cre mice had attenuated inflammatory pain in the BK model but not with PGE2 suggesting that it's involvement in inflammatory pain is restricted to the Gq/11 signalling pathways.

TRPC3 fl/fl:Nav1.8Cre mice also have reduced carrageenan induced mechanical hyperalgesia. In a similar way to formalin, carrageenen leads to the production of many inflammatory mediators which act to sensitise the peripheral neurons, reducing the threshold

and increasing the excitability. An important molecule for inflammatory hyperalgesia is TNFα which initiates a cascade of pro-inflammatory cytokines, antisera to TNFα is able to abolish carrageenan induced thermal and mechanical hyperalgesia (Cunha *et al.*, 1992). Recently the association of TRPC3 with cytokines has been investigated in human monocytes and found to be positively correlated with TNFα and IL1 (Thilo *et al.*, 2008). Furthermore, TNFα has been shown to increase mRNA and protein levels of TRPC3 in human airway smooth muscle cells (HASMCs) (White *et al.*, 2006). The increased levels of TRPC3 are thought to be responsible for the TNFα induced increase in intracellular Ca2+ levels which control a number of cellular responses in HASMCs including contractility. A similar upregulation of TRPC3, and resulting rise in intracellular Ca2+, in neurons as a response to pro-inflammatory cytokines could trigger intracellular signalling pathways leading to sensitisation.

As the knockout of TRPC3 did not produce a complete abolition of pain behaviours in any of these inflammatory models there are obviously other inflammatory mediator pathways that are still intact, which may explain the lack of phenotype in the CFA model. TRPC3 fl/fl:Nav1.8Cre mice showed no attenuation of mechanical or thermal hyperalgesia from day 1 to day 10 after CFA injection. The other inflammatory models studied were of a shorter duration so it is possible that TRPC3 is involved in the early stages of hyperalgesia initiation. However, another explanation may be functional differences between the models. Whereas carrageenan and formalin provoke an innate immune response the CFA model produces an adaptive immune response which includes T-cell activation. This would lead to a different profile of inflammatory mediators being released, activating different pathways which may eclipse the deficient PLC pathway outlined above.

In conclusion, TRPC3 plays a role in the PLC signalling pathway downstream of Gq/11 coupled receptors acting to sensitise peripheral nociceptors in acute inflammatory pain conditions. TRPC3 may be coupled to a specific GPCR, i.e. BK, or to a range of GPCRs of the Gq/11 subtype. Further investigations with different inflammatory mediators and G protein inhibitors could help to find this out. TRPC3 expression may also be increased by TNFα, or downstream cytokines, increasing intracellular Ca^{2+}.

Test	Modality	TRPC3fl/fl: Nav1.8Cre	TRPC3fl/-: AdvCre
Von Frey hairs	Light touch	No phenotype	No phenotype
Automatic von Frey	Touch	No phenotype	No phenotype
Randall Selitto	Noxious pressure	No phenotype	No phenotype
Hot plate	Noxious thermal	No phenotype	No phenotype
Hargreaves	Noxious thermal	No phenotype	No phenotype
Cold plate	Noxious cold	No phenotype	No phenotype
Acetone	Innocuous Cold	N/A	No phenotype
Formalin	Spontaneous acute pain behaviours	No phenotype	No phenotype
	Spontaneous inflammatory pain behaviours	**Attenuated**	**Attenuated**
Carrageenan	Mechanical hyperalgesia (inflammation)	**Attenuated**	**Attenuated**
CFA	Thermal (inflammation)	No phenotype	No phenotype
	Mechanical (inflammation)	No phenotype	No phenotype
PGE2	Mechanical hyperalgesia (inflammation)	No phenotype	No phenotype
Bradykinin	Spontaneous inflammatory pain behaviours	**Attenuated**	**Attenuated**

Table 3.3 Summary of phenotypes in TRPC3 fl/fl:Nav1.8Cre and TRPC3 fl/-:AdvCre mice

4 Effects of nociceptor TRPC3 deletion on gene expression

4.1 Introduction

The deletion of a gene, such as TRPC3 does not just have an effect on the single protein. The complex molecular pathways and networks within a cell can all be affected by the deficit especially when the gene is knocked out early on in development. Redundancy within a large family such as the TRP channel superfamily can lead to upregulation of similar channels to compensate for the deficit (Selli *et al.*, 2008). TRPC3, 6 and 7 are highly homologous, furthermore it has been shown that in the global knockout of TRPC6 there was an upregulation of TRPC3 (Dietrich *et al.*, 2005).

The TRPC3fl/fl:Nav1.8Cre mouse line have attenuated inflammatory hyperalgesia in the formalin, bradykinin and carrageenan tests. The inflammatory hyperalgesia, which develops rapidly in these models, is linked to the release of cytokines and activation of signalling cascades sensitising the nociceptors. Although TRPC3 may be activated directly by inflammatory mediators, such as substance P (Ben-Mabrouk and Tryba, 2010), it is also possible that the deletion of TRPC3 may have a secondary effect on the expression of proteins which are involved in the generation of inflammatory hyperalgesia.

DNA microarrays allow the investigation of thousands of genes simultaneously allowing us to gain a complex and integrated view of the molecular events taking place within a cell. Microarrays can be used to look at the differences in gene expression between a wildtype and knockout mouse by determining the amount of mRNA present. Affymetrix uses the photolithographic method to synthesise oligonucleotides representing the entire mouse genome in situ directly onto a silica slide. Labelled cRNA, made from cDNA synthesised from mRNA, obtained from samples with different conditions, in this case wildtype and knockout, are hybridised to the chip. The labelled cDNA fragments hybridise with their corresponding oligonucleotides and the resulting fluorescent readout shows the abundance of each specific nucleotide sequence present in each sample. A comparison can be made

between the wildtype and knockout samples and a list of up- or downregulated genes can be generated. The resulting transcriptional profile is very informative and can show adjustments of the cell to protein functional disruption. As well as providing a list of individual genes which are up or down regulated further analysis can look at pathways and biological gene networks allowing detection of small, but consistent, changes in expression of a group of genes with a related function. This can lead to elucidation of biological aspects and trends that would be hidden in a gene-by-gene analysis. A microarray cannot detect any difference in the translation of mRNA into functional protein, a Western blot would need to be used for this purpose.

4.2 Results

4.2.1 Microarray analysis

Around 7,500 genes were found to be significantly dysregulated ($p < 0.05$) between the TRPC3 fl/fl:Nav1.8Cre and control mice. Gene ontology enrichment analysis using Partek software grouped the genes according to the gene product properties. The most biologically relevant groups are displayed in Table 4.1. Pathway analysis using DAVID mapped the genes onto known pathways to determine which pathways were overrepresented in the dysregulated gene list.

Function	Enrichment score	% of genes in group that are present
G –protein coupled receptor activity	77.44	10.15
G-protein couple receptor protein signalling pathway	63.68	11.75
Ribonucleotide binding	20.90	34.26
Protein kinase activity (MAPK, PI3K)	19.03	40.87
Protein binding (Cytokines)	18.83	29.78

Table 4.1 Gene ontology enrichment analysis

The dysregulated genes grouped by gene properties and functions are displayed in alphabetical order in Table 4.2 to Table 4.4. Genes are listed in alphabetical order: shaded lines are downregulated and unshaded lines are upregulated genes in the TRPC3 fl/fl:Nav1.8Cre mice.

G-Protein Receptor Signalling Proteins

Gene Symbol	Gene Name	Fold-change	p-value
Adora2b	adenosine A2b receptor	-1.39862	0.0498
Adora3	adenosine A3 receptor	-1.28955	0.02182
Adra1b	adrenergic receptor, alpha 1b	-1.35294	0.02711
Adrb3	adrenergic receptor, beta 3	-1.3506	0.03755
Bai1	brain-specific angiogenesis inhibitor 1; similar to brain-specific angiogenesis inhibitor 1	1.51744	0.04948
C3ar1	complement component 3a receptor 1	1.26338	0.03156
Calcr	calcitonin receptor	1.83535	0.02937
Cckbr	cholecystokinin B receptor	-1.68023	0.02282
Ccr6	chemokine (C-C motif) receptor 6	-1.33221	0.04759
Ccrl2	chemokine (C-C motif) receptor-like 2	-1.60451	0.00955
Celsr1	cadherin, EGF LAG seven-pass G-type receptor 1 (flamingo homolog, Drosophila)	-1.60572	0.04362
Celsr2	cadherin, EGF LAG seven-pass G-type receptor 2 (flamingo homolog, Drosophila)	-1.53368	0.03087
Celsr3	cadherin, EGF LAG seven-pass G-type receptor 3 (flamingo homolog, Drosophila)	-1.50139	0.03334
Cmklr1	chemokine-like receptor 1	-1.47397	0.03241
Cnr2	cannabinoid receptor 2 (macrophage)	-1.63407	0.04627
Cxcr6	chemokine (C-X-C motif) receptor 6	-1.51509	0.01187
Drd2	dopamine receptor 2	1.27574	0.0452
Drd5	dopamine receptor 5	1.24028	0.02296
Ednrb	endothelin receptor type B	1.5803	0.00971
Eltd1	EGF, latrophilin seven transmembrane domain containing 1	1.43492	0.0378
Emr4	EGF-like module containing, mucin-like, hormone receptor-like sequence 4	1.86491	0.0302
F2r	coagulation factor II (thrombin) receptor	1.20442	0.02004
Fshr	follicle stimulating hormone receptor	-1.59003	0.03584
Fzd4	frizzled homolog 4 (Drosophila)	3.11054	0.02144
Galr2	galanin receptor 2	1.52444	0.03829
Ghrhr	growth hormone releasing hormone receptor	-2.27873	0.02827
Glp1r	glucagon-like peptide 1 receptor; similar to glucagon-like	2.445	0.02257

	peptide-1 receptor		
Gpbar1	G protein-coupled bile acid receptor 1	-1.1183	0.02552
Gpr1	G protein-coupled receptor 1	1.21718	0.01611
Gpr112	G protein-coupled receptor 112	-1.21938	0.01166
Gpr123	G protein-coupled receptor 123	-1.23449	0.03623
Gpr132	G protein-coupled receptor 132	2.29839	0.0145
Gpr139	G protein-coupled receptor 139	1.18112	0.0049
Gpr156	G protein-coupled receptor 156	1.4024	0.03699
Gpr56	G protein-coupled receptor 56	1.50256	0.04203
Gpr64	G protein-coupled receptor 64	1.5002	0.00309
Gpr84	G protein-coupled receptor 84	-1.2254	0.01348
Gpr98	G protein-coupled receptor 98	2.16921	0.04429
Gprc5b	G protein-coupled receptor, family C, group 5, member B	-1.22433	0.03126
Gprc5c	G protein-coupled receptor, family C, group 5, member C; similar to G protein-coupled receptor, family C, group 5, member C	1.76189	0.02467
Grm5	glutamate receptor, metabotropic 5	-1.72125	0.03304
Grm7	glutamate receptor, metabotropic 7	1.31024	0.04433
Gucy2g	guanylate cyclase 2g	1.29511	0.04955
Hcrtr1	similar to Hypocretin (orexin) receptor 1; hypocretin (orexin) receptor 1	-2.0562	0.03784
Lgr4	leucine-rich repeat-containing G protein-coupled receptor 4	1.312	0.02199
Lgr6	leucine-rich repeat-containing G protein-coupled receptor 6	-1.77361	0.03154
Lhcgr	luteinizing hormone/choriogonadotropin receptor	1.48492	0.04447
Lpar1	lysophosphatidic acid receptor 1	-1.29522	0.03467
Lpar6	purinergic receptor P2Y, G-protein coupled, 5	1.40968	0.00661
Lphn3	latrophilin 3	-2.94302	0.0232
Ltb4r1	leukotriene B4 receptor 1	-1.554	0.00575
Mc3r	melanocortin 3 receptor	1.84627	0.01805
Mrgpra4	predicted gene 5734; predicted gene 5733; MAS-related GPR, member A4; MAS-related GPR, member A8; predicted gene 9717	1.39821	0.00267
Mrgprg	MAS-related GPR, member G	-1.37152	0.00463
Mtnr1a	melatonin receptor 1A	1.3149	0.04505
Nmur2	neuromedin U receptor 2	-1.27556	0.0351
Npy6r	neuropeptide Y receptor Y6	-1.07549	0.01538
Olfr1002	olfactory receptor 1002	-1.0669	0.01168

Olfr1039	olfactory receptor 1039	-1.17109	0.02747
Olfr1082	olfactory receptor 1082	-1.14074	0.03594
Olfr112	olfactory receptor 112	-1.45858	0.03297
Olfr1135	olfactory receptor 1135	1.03294	0.01789
Olfr1138	olfactory receptor 1138	-1.10808	0.03582
Olfr1140	olfactory receptor 1140	1.78285	0.0026
Olfr1151	olfactory receptor 1151	1.09939	0.02736
Olfr119	olfactory receptor 119	-1.47475	0.02202
Olfr1199	olfactory receptor 1199	1.07442	0.04212
Olfr1200	olfactory receptor 1200	1.20037	0.03061
Olfr1203	olfactory receptor 1203	1.12851	0.03731
Olfr1252	olfactory receptor 1252	-1.28163	0.00755
Olfr1256	olfactory receptor 1256	1.07715	0.03025
Olfr1264	olfactory receptor 1264	-1.16247	0.00902
Olfr128	olfactory receptor 128	1.16926	0.02222
Olfr1289	olfactory receptor 1289	-1.08937	0.04964
Olfr1294	olfactory receptor 1294	-1.13056	0.04198
Olfr1295	olfactory receptor 1295	-1.49532	0.03737
Olfr1298	olfactory receptor 1298	-1.51931	0.00911
Olfr1321	olfactory receptor 1321	-1.25539	0.03042
Olfr1349	olfactory receptor 1349	-1.04691	0.02528
Olfr1357	olfactory receptor 1357	-1.05694	0.01939
Olfr1387	olfactory receptor 1387	1.19039	0.03126
Olfr1395	olfactory receptor 1395	-1.16074	0.04742
Olfr1404	olfactory receptor 1404	-1.07483	0.00218
Olfr142	olfactory receptor 142	-1.07319	0.03702
Olfr1420	olfactory receptor 1420	-1.30721	0.00742
Olfr1426	olfactory receptor 1426	1.11218	0.03386
Olfr1499	olfactory receptor 1499	-1.13539	0.02131
Olfr1501	olfactory receptor 1501	1.21514	0.02869
Olfr1506	olfactory receptor 1274; olfactory receptor 1506; predicted gene 13766	-1.07363	0.04916
Olfr1510	olfactory receptor 1510	1.17054	0.03715
Olfr191	olfactory receptor 191	1.1055	0.00639
Olfr205	olfactory receptor 205	-1.08197	0.02819
Olfr208	similar to olfactory receptor 208; olfactory receptor 209; olfactory receptor 208; olfactory receptor 207	-1.11276	0.04891

Olfr24	olfactory receptor 24	-1.25452	0.00915
Olfr272	olfactory receptor 272	1.1604	0.0332
Olfr283	olfactory receptor 283	-1.61662	0.04072
Olfr351	olfactory receptor 351	-1.13665	0.02628
Olfr402	olfactory receptor 402	-1.22236	0.03355
Olfr419	olfactory receptor 419	-1.10526	0.02873
Olfr421	olfactory receptor 421	-1.58137	0.04336
Olfr456	olfactory receptor 456	-1.08026	0.03008
Olfr461	olfactory receptor 461	-1.10063	0.02684
Olfr513	olfactory receptor 513	-1.04814	0.03732
Olfr514	olfactory receptor 514	-1.14504	0.01493
Olfr544	olfactory receptor 544	-1.14698	0.02092
Olfr56	olfactory receptor 56	-1.35927	0.03464
Olfr582	olfactory receptor 582	-1.17023	0.00814
Olfr59	olfactory receptor 59	-1.28268	0.02644
Olfr61	olfactory receptor 61	-1.12722	0.03203
Olfr655	olfactory receptor 655	-1.08031	0.01581
Olfr659	olfactory receptor 659	1.14756	0.03777
Olfr669	olfactory receptor 669	1.0987	0.04151
Olfr676	olfactory receptor 676	1.14361	0.03054
Olfr683	olfactory receptor 683	-1.10152	0.02605
Olfr689	olfactory receptor 689	1.05886	0.02492
Olfr70	olfactory receptor 70	1.4977	0.02179
Olfr706	olfactory receptor 706	-1.10886	0.03437
Olfr714	olfactory receptor 714	-1.32792	0.02346
Olfr731	olfactory receptor 731	1.13099	0.0133
Olfr74	olfactory receptor 74	-1.11298	0.04499
Olfr748	olfactory receptor 748	1.20363	0.0347
Olfr76	olfactory receptor 76	-1.1374	0.00042
Olfr761	olfactory receptor 761	1.13	0.04204
Olfr776	olfactory receptor 1518; olfactory receptor 776; olfactory receptor 774	-1.09671	0.00152
Olfr782	olfactory receptor 782	1.12587	0.03962
Olfr813	olfactory receptor 813	-1.08656	0.03615
Olfr818	olfactory receptor 818	1.11669	0.031
Olfr829	olfactory receptor 829	-1.17185	0.02352
Olfr859	olfactory receptor 857; olfactory receptor 859; olfactory	1.34349	0.01911

	receptor 58		
Olfr926	olfactory receptor 926	-1.2012	0.02845
Olfr935	olfactory receptor 935	-1.09106	0.04787
Olfr99	olfactory receptor 99	1.13175	0.00502
Opn1mw	opsin 1 (cone pigments), medium-wave-sensitive (color blindness, deutan)	1.60474	0.03302
Opn1sw	opsin 1 (cone pigments), short-wave-sensitive (color blindness, tritan)	1.40117	0.02584
Opn5	opsin 5	1.40368	0.03455
Oprl1	opioid receptor-like 1	1.58561	0.00772
Oprm1	opioid receptor, mu 1	-2.64743	0.04067
Prlhr	prolactin releasing hormone receptor	-1.51821	0.03085
Ptger1	prostaglandin E receptor 1 (subtype EP1)	-1.67613	0.0176
Ptger2	prostaglandin E receptor 2 (subtype EP2)	1.39571	0.00916
Ptger3	prostaglandin E receptor 3 (subtype EP3)	1.66151	0.00401
Pth1r	parathyroid hormone 1 receptor	1.46914	0.04052
Pth2r	parathyroid hormone 2 receptor	1.42525	0.0106
Rxfp1	relaxin/insulin-like family peptide receptor 1	2.76272	0.0457
Sstr3	somatostatin receptor 3	-1.29761	0.01776
Sucnr1	succinate receptor 1	1.26105	0.01758
Tas1r2	taste receptor, type 1, member 2	-2.22575	0.03892
Trhr2	thyrotropin releasing hormone receptor 2	1.48953	0.00624
Tshr	thyroid stimulating hormone receptor	-1.16878	0.01205
Vipr1	vasoactive intestinal peptide receptor 1	1.65673	0.02443
Vipr2	vasoactive intestinal peptide receptor 2	1.22358	0.00731

Table 4.2 G-protein receptor signaling proteins dysregulated in TRPC3 fl/fl:Nav1.8Cre mice

PI3K Signalling Pathway

Gene Symbol	Gene Name	Fold-change	p-value
Cds2	CDP-diacylglycerol synthase (phosphatidate cytidylyltransferase) 2	-1.14669	0.013879
Dgki	diacylglycerol kinase, iota	-1.35829	0.047392
Itpr1	inositol 1,4,5-triphosphate receptor 1	-2.62009	0.013892
Itpr2	inositol 1,4,5-triphosphate receptor 2	-2.00108	0.032144
Itpr3	inositol 1,4,5-triphosphate receptor 3	1.29266	0.022612
Inpp4a	inositol polyphosphate-4-phosphatase, type I	-1.26067	0.049702
Inpp5a	inositol polyphosphate-5-phosphatase A	-1.12735	0.019539
Inpp5d	inositol polyphosphate-5-phosphatase D	-1.8362	0.025926
Inpp5e	inositol polyphosphate-5-phosphatase E	-1.34082	0.033357
Inpp5f	inositol polyphosphate-5-phosphatase F	-1.27	0.003589
Pik3r3	phosphatidylinositol 3 kinase, regulatory subunit, polypeptide 3 (p55)	1.18656	0.031314
Pik3cd	phosphatidylinositol 3-kinase catalytic delta polypeptide; RIKEN cDNA 2610208K16 gene	-1.5837	0.015683
Pik3c2a	phosphatidylinositol 3-kinase, C2 domain containing, alpha polypeptide	1.53673	0.012696
Pik3c2g	phosphatidylinositol 3-kinase, C2 domain containing, gamma polypeptide	-1.8824	0.025506
Pik3cb	phosphatidylinositol 3-kinase, catalytic, beta polypeptide	1.38045	0.002054
Pik3r1	phosphatidylinositol 3-kinase, regulatory subunit, polypeptide 1 (p85 alpha)	-1.17062	0.001974
Pip5k1b	phosphatidylinositol-4-phosphate 5-kinase, type 1 beta;	1.41511	0.022619
Pip5k1c	phosphatidylinositol-4-phosphate 5-kinase, type 1 gamma	-1.22606	0.043822
Pik3ap1	phosphoinositide-3-kinase adaptor protein 1	-1.74252	0.016098
Pik3ip1	phosphoinositide-3-kinase interacting protein 1	1.2579	0.018488
Pik3cg	phosphoinositide-3-kinase, catalytic, gamma polypeptide	-2.72543	0.042276
Pik3c2b	phosphoinositide-3-kinase, class 2, beta polypeptide	-1.59959	0.026033
Pik3r6	phosphoinositide-3-kinase, regulatory subunit 6	1.64621	0.015919
Plcb4	phospholipase C, beta 4	-1.45394	0.034925
Plcd1	phospholipase C, delta 1	-1.55796	0.029271
Plcg2	phospholipase C, gamma 2	1.42275	0.009242
Plcz1	phospholipase C, zeta 1	-2.53562	0.036422

Table 4.3 PI3K signaling proteins dysregulated in TRPC3 fl/fl:Nav1.8Cre mice

MAPK Signalling Pathway

Gene Symbol	Gene Name	Fold-change	p-value
Cacna1a	calcium channel, voltage-dependent, P/Q type, alpha 1A subunit	-3.01242	0.2999
Cacna1b	calcium channel, voltage-dependent, N type, alpha 1B subunit	-1.29064	0.033873
Cacna1c	calcium channel, voltage-dependent, L type, alpha 1C subunit	2.27069	0.048964
Cacna1d	calcium channel, voltage-dependent, L type, alpha 1D subunit	2.27069	0.048964
Cacna1e	calcium channel, voltage-dependent, R type, alpha 1E subunit	-1.30304	0.044397
Cacna1f	calcium channel, voltage-dependent, alpha 1F subunit	-2.19039	0.010133
Cacna1g	calcium channel, voltage-dependent, T type, alpha 1G subunit	-1.32601	0.038265
Cacna1h	calcium channel, voltage-dependent, T type, alpha 1H subunit	-1.19875	0.007808
Cacna1i	calcium channel, voltage-dependent, alpha 1I subunit	-1.70664	0.029454
Cacna1s	calcium channel, voltage-dependent, L type, alpha 1S subunit	2.38838	0.023724
Cacna2d2	calcium channel, voltage-dependent, alpha 2/delta subunit 2; similar to Cacna2d2 protein	1.99894	0.047296
Cacna2d4	calcium channel, voltage-dependent, alpha 2/delta subunit 4	-3.38467	0.007552
Cacnb3	calcium channel, voltage-dependent, beta 3 subunit	-1.38103	0.02486
Dusp10	dual specificity phosphatase 10	1.95411	0.042402
Fas	Fas (TNF receptor superfamily member 6)	-1.93293	0.014972
Fgf18	fibroblast growth factor 18	-1.2977	0.025489
Fgf6	fibroblast growth factor 6	-1.81101	0.021649
Fgf9	fibroblast growth factor 9	-1.57222	0.014944
Fgfr1	fibroblast growth factor receptor 1	-1.47564	0.04324
Fgfr3	fibroblast growth factor receptor 3	-1.32813	0.017987
Fgfr4	fibroblast growth factor receptor 4	-2.05918	0.005423
Flna	filamin, alpha	2.30043	0.04151
Flnb	filamin, beta	-2.59033	0.042665
Flnc	filamin C, gamma	1.49663	0.020983
Hspa8	similar to heat shock protein 8; heat shock protein 8	2.15725	0.046987

Il1a	interleukin 1 alpha	-1.68167	0.037311
Il1b	interleukin 1 beta	-1.45757	0.010813
Il1r1	interleukin 1 receptor, type I	1.41169	0.04951
Jmjd7, Pla2g4b	phospholipase A2, group IVB (cytosolic); jumonji domain containing 7	-1.79936	0.001136
Map2k5	mitogen-activated protein kinase kinase 5	1.32356	0.042167
Map2k6	mitogen-activated protein kinase kinase 6	-1.68971	0.038545
Map3k10	mitogen-activated protein kinase kinase kinase 10	-1.24805	0.027814
Map3k14	mitogen-activated protein kinase kinase kinase 14	-3.35982	0.000949
Map3k15	mitogen-activated protein kinase kinase kinase 15	-3.21509	0.044432
Map3k2	mitogen-activated protein kinase kinase kinase 2	1.10891	0.0081
Map3k5	mitogen-activated protein kinase kinase kinase 5	-1.29092	0.031118
Map3k6	mitogen-activated protein kinase kinase kinase 6	-2.61658	0.049409
Map4k2	mitogen-activated protein kinase kinase kinase kinase 2	-1.41688	0.024496
Map4k4	mitogen-activated protein kinase kinase kinase kinase 4	-1.33711	0.035203
Map4k5	mitogen-activated protein kinase kinase kinase kinase 5	1.20557	0.014635
Mapk1	mitogen-activated protein kinase 1	1.07803	0.014384
Mapk12	mitogen-activated protein kinase 12	2.47187	0.009211
Mapk14	mitogen-activated protein kinase 14	-1.38381	0.030209
Mapk4	mitogen-activated protein kinase 4	1.66141	0.002742
Mapk8ip1	mitogen-activated protein kinase 8 interacting protein 1	2.16785	0.032464
Mapkap1	mitogen-activated protein kinase associated protein 1	-1.16248	0.012883
Mapkapk2	MAP kinase-activated protein kinase 2	1.11854	0.027234
Mapkapk3	mitogen-activated protein kinase-activated protein kinase 3	-1.97475	0.00608
Mapkapk5	MAP kinase-activated protein kinase 5; similar to MK-5 type 2	1.18366	0.022651
Mapkbp1	mitogen-activated protein kinase binding protein 1	-2.91122	0.014916
Mknk1	MAP kinase-interacting serine/threonine kinase 1	-1.34666	0.041772
Ngf	nerve growth factor	-1.38703	0.041977
Nlk	nemo like kinase; similar to nemo-like kinase	1.13698	0.039565
Pla2g12b	phospholipase A2, group XIIB	-1.69136	0.045898
Pla2g2d	phospholipase A2, group IID	-1.41167	0.005237
Pla2g4a	phospholipase A2, group IVA (cytosolic, calcium-dependent)	-1.90122	0.009625
Pla2g4e	phospholipase A2, group IVE	-1.76591	0.020157
Pla2g7	phospholipase A2, group VII	11.1518	0.020251
Pla2r1	phospholipase A2 receptor 1	2.1758	0.002845
Plac1	placental specific protein 1	2.37659	0.000835

Plag1	pleiomorphic adenoma gene 1	1.46279	0.027824
Rap1b	RAS related protein 1b; similar to GTP-binding protein (smg p21B)	1.05826	0.032762
Rapgef2	Rap guanine nucleotide exchange factor (GEF) 2	1.21705	0.02585
Rasa2	RAS p21 protein activator 2	1.30517	0.043228
Rasgrf1	RAS protein-specific guanine nucleotide-releasing factor 1	1.45261	0.047802
Rasgrp2	RAS, guanyl releasing protein 2	-1.9529	0.021783
Rasgrp4	RAS guanyl releasing protein 4	-1.34799	0.02518
Taok2	TAO kinase 2	-1.14029	0.04993
Taok3	TAO kinase 3	1.16228	0.045618
Traf2	TNF receptor-associated factor 2	-1.8359	0.029042
Traf5	TNF receptor-associated factor 5	1.91994	0.039169
Traf6	TNF receptor-associated factor 6	-1.27159	0.041114

Table 4.4 MAPK signaling pathway proteins dysregulated in TRPC3 fl/fl:Nav1.8Cre mice

4.3 Discussion

TRPC3 fl/fl:Nav1.8Cre mice have an attenuated inflammatory phenotype which is likely due to a decrease in sensitisation of peripheral afferents. Sensitisation occurs from enhanced activity of nociceptor ion channels which leads to a decrease of threshold at which an action potential is fired. The gene list from the microarray analysis did not show any significant change in expression of any ion channels themselves so the decreased sensitisation in the TRPC3 fl/fl:Nav1.8Cre mice may be caused by a downregulation of the molecules leading to the enhanced activity of ion channels or an upregulation of inhibitory molecules.

Gene ontology (GO) analysis allows identification of functionally related gene groups within the microarray gene list to enable increased understanding of the biological meaning. Although the most up and down regulated proteins in the TRPC3 fl/fl:Nav1.8Cre mice were cytoskeletal proteins and some ATP linked enzymes the GO analysis shows that a large number of signalling pathways such as GPCRs, MAPK and cytokines are dysregulated which is more biologically relevant given the attenuated inflammatory phenotype of these animals.

4.3.1 Technical considerations

A microarray compares only the mRNA for known genes, there can be no analysis of novel transcripts and the amount of message can only give an indication of the amount of protein made. Trafficking, phosphorylation and other modulations and alternative splicing can also affect the amount of functional protein but these are not detected in a microarray. Affymetrix technology does allow some analysis of splice variants but this type of array was not chosen due to expense and time considerations. To minimise false positives each sample has three biological replicates but qPCR is also recommended to validate specific targets of biological importance.

4.3.2 G-protein coupled receptor activity and signalling are dysregulated in TRPC3fl/fl:Nav1.8Cre mice

The gene ontology group that was most represented in the gene list was GPCR activity and signalling. TRPC3 is known to be activated downstream of phospholipase C, PLC, which is activated by GPCRs. GPCRs are a large family of receptors that are ligand activated and

activate intracellular signalling pathways. Many inflammatory mediators such as BK, PGE2 and complement signal through GPCRs from the Gq/11,Gs, Go/i sub types.

Prostaglandin E receptor subtypes 2 and 3 were identified in the gene list as being up regulated in the TRPC3 fl/fl:Nav1.8Cre mouse, however subtype 1 was slightly down regulated (Table 4.2). The PGE2 receptors, EP1-4, signal through three types of GPCR. EP1 couples to Gq, EP2 and 4 to Gs and EP3 to Gi. The TRPC3 fl/fl:Nav1.8Cre mice had no deficits in PGE2 induced mechanical hyperalgesia (Figure 3.9) and it is possible that upregulation of the Gs and Gi coupled receptors in the TRPC3 fl/fl:Nav1.8Cre mice is compensating for the deficit in the Gq pathway discussed previously. Complement component 3a receptor 1 binds to the C3a and C4a components of the complement system and is slightly upregulated in the TRPC3 fl/fl:Nav1.8Cre mice (Table 4.2). C3AR1 is a GPCR coupled to G-alpha 16 or G-alpha o/i (Settmacher *et al.*, 2003), not the Gq pathway that appears to be affected by the TRPC3 knockout. These compensation mechanisms may, in part, explain why the TRPC3 fl/fl:Nav1.8Cre mouse line has no attenutated inflammatory phenotype in CFA induced hyperalgesia. Even though CFA initiates an inflammatory signalling cascade including Gq proteins and PLC the other pathways that are activated, including Gs and Gi/o, are up regulated and the neurons are still sensitised to the same extent.

Interestingly, there are also up and down regulations in the metabotropic glutamate receptor (mGluR) genes. GRM5 is a Group I mGluR and is able to activate PLC (linked to Gq), and is pro-nociceptive in inflammatory pain states (Sharpe *et al.*, 2002;Zhu *et al.*, 2004). GRM7 is a Group III mGluR that inhibits cAMP production and is hence anti-nociceptive (Zhang *et al.*, 2002;Kumar *et al.*, 2010). GRM5 is down-regulated and GRM7 in upregulated in the TRPC3 fl/fl:Nav1.8Cre mice. The mGluR receptors regulate glutamate release in the spinal cord in both inflammatory and neuropathic pain states, (Kumar *et al.*, 2010), and are also important in the periphery where mGluR5 mediates inflammatory induced nociceptive behaviour (Lee *et al.*, 2006).

The dysregulation of the GPCR signalling pathway, and specifically the upregulation of some Gs and Gi/o protein coupled receptors, substantiates the theory that TRPC3 is downstream of

Gq protein coupled receptors. As no single GPCR is especially up or down regulated in the TRPC3 fl/fl:Nav1.8Cre mice it is not clear if TRPC3 is coupled to a specific GPCR or if it is downstream of a number of different receptors.

4.3.3 MAP Kinase and PI3 Kinase pathways are dysregulated in TRPC3fl/fl:Nav1.8Cre mice

Pathway analysis using DAVID identified a large number of genes from the phosphatidylinositol signalling pathway. 27 genes in total were significantly up or down regulated which represents around 32% of the number of genes known to be involved in this signalling pathway. Phosphatidylinositol signalling includes both the MAP Kinase and PI3 Kinase pathways which cause phosphorylation of ion channels leading to enhanced excitability and sensitisation of nociceptors. The MAPK and PI3K pathways are activated downstream of inflammatory mediators via GPCRs and receptor tyrosine kinases. Reduced signalling via these pathways would lead to a reduction of sensitisation and associated hyperalgesia in response to inflammatory mediators.

4.3.4 TRPC channel expression is not upregulated in TRPC3fl/fl:Nav1.8Cre mice

TRPC3 was not present in the microarray downregulated list, despite gene deletion being confirmed previously (Figure 8.1). The design of this mouse strain results in the deletion of exon 7, a partial length mRNA may still be made which would be picked up in the microarray even though this would not be translated into a functional protein. There would also be full-length TRPC3 mRNA present from Nav1.8 negative neurons within the DRG and non-neuronal cells.

TRPC6 was not present in the list of significantly up or down regulated genes in the TRPC3fl/fl:Nav1.8Cre mouse. However, this does not prove that TRPC6 is not compensating for the lack of TRPC3. The microarray detects only the change in messenger RNA, not the levels of functional protein. Although the level of mRNA for TRPC6 does not change it is possible that the compensation is acting through a different mechanism. TRPC6 is regulated by an exocytotic mechanism that controls levels of the ion channel within the plasma membrane. There are also a number of auxillary proteins such as Src Kinase that modulate

channel activity. An increased level of TRPC6 at the plasma membrane of increased activity could only be detected by immunohistochemistry, using an antibody to look at the location of TRPC6 and also to see whether it is phosphorylated.

4.3.5 Further work

The microarray was performed using three biological replicates to minimise false positives however qPCR was not used to validate the results. The original gene list of significantly up or down regulated genes contained over 7,500 genes. The most up-regulated and most down-regulated genes did not appear to have any obvious biological relevance to TRPC3 or the attenuated inflammatory phenotype. Pathway analysis did show some interesting targets, however individually each of the genes contained within the pathway lists were not massively up or down regulated. This doesn't invalidate the results but means that an extensive list of genes would need to be investigated with qPCR before any follow up experiments performed.

It would also be interesting to look at the gene expression profile of wildtype and knockout mice after inflammatory insults such as formalin and carrageenan.

5 Phenotyping TRPC3$^{-/-}$:TRPC6$^{-/-}$ mice

5.1 Introduction

TRPC3 and TRPC6 are in the same sub-group of the TRPC family, along with TRPC7. This gives them a high degree of sequence homology and also similarities in activation, expression and functional properties. Knockout or knockdown of genes can lead to other, related, genes compensating for the deficit, concealing the true phenotype. For these reasons we used a double knockout of TRPC3 and TRPC6 to minimise compensation and redundancy. A global knockout of both TRPC3 and TRPC6 also allowed us to look at other tissues where mechanically activated channels are known to be important. Global knockout, including germline cells, of a gene flanked with *loxP* sites can be achieved using a Cre-deleter mouse strain. This Cre-deleter mouse uses human cytomegalovirus promoter to control expression of Cre which together with a nuclear localization signal and addition of splicing and polyadenylation signals to increase Cre recombinase efficacy lead to global deletion or the floxed region (Schwenk *et al.*, 1995).

5.1.1 Mechanotransduction in sensory neurons

The molecular transduction mechanisms mediating the detection of mechanical stimuli in the somatosensory and auditory/vestibular systems remain undefined. The vast majority of DRG neurons are mechanosensitive but the sensitivity and pattern of firing varies (Lewin and Moshourab, 2004), determined by the position of the termini and the complement of voltage gated ion channels and primary mechanotransducers. DRG neurons respond to mechanical stimuli, either low threshold, innocuous touch sensation, or high threshold, noxious pressure sensation. The currents mediated by the mechanosensitive ion channels can be separated by their decay kinetics, rapidly adapting (RA) currents decline very quickly (<20 ms), slowly adapting (SA) currents decline in around 100 ms and the third population are intermediately adapting (IA). SA and IA currents are the major mechanically activated currents in nociceptors, whereas RA form the majority of the mechanically activated currents in large mechanosensitive neurons.

The two types of mechanical stimuli are transduced by distinct populations of neurons which show different properties. Nociceptors respond to high threshold stimuli and ablation of these neurons abolishes noxious mechanosensation *in vivo* without affecting innocuous touch sensation (Abrahamsen *et al.*, 2008). A subset of TRPV1 negative neurons respond to lower thresholds but with larger, RA, currents than nociceptors (Drew *et al.*, 2002). The noxious mechanosensation blocker 1, or NMB-1, also abolishes noxious mechanosensation *in vivo* by selectively inhibiting slowly adapting (SA) mechanically active currents (Drew *et al.*, 2007), suggesting there are also pharmacologically distinct mechanically gated receptors in mammalian sensory neurons. These data suggests that the RA currents are mainly activated by light touch and the SA currents by noxious mechanical stimuli.

5.1.2 Mechanotransduction in hair cells

Hearing and balance are dependent on hair cells within the inner ear and vestibule that are able to detect mechanical stimuli and therefore allow sensitive detection of sound and head movement. The mechanically sensitive part of the hair cell is its stereociliary bundle, consisting of 50-100 individual sterocilia. Mechanical stimuli cause a small displacement of the bundle mediating the opening of mechanically activated channels producing a receptor potential and subsequent depolaraization of the hair cell. Hearing loss is the most common form of sensory impairment and is frequently of genetic origin. Only a fraction of the affected genes have been identified which include cytoskeletal components and transcription factors but not, as yet, the mechanically activated channel.

Hair cells are arranged along the length of the cochlea and vary in their frequency sensitivity with highest frequencies found at the base of the cochlea. The kinetics of the mechanically activated channels also varies with an increase in activation speed and conductance accompanying higher frequency sensitivity. The mechanically activated channels have high calcium permeability, linked to their Ca^{2+} dependent adaptation, and can be blocked by Gd^{3+}, ruthenium red, and amiloride (Nagata *et al.*, 2005). Mechanically gated ion channels in various organisms have been identified as TRP channels, additionally the block of mechanically activated channels in hair cells by Gd^{3+} and RR make the TRPs obvious candidates for the hair cell mechanotransducer. Several TRPs have been investigated for

involvement in hair cell mechanotransduction and subsequently eliminated including TRPV4, TRPA1 and TRPML3

TRP channels were first implicated in mechanosensation in the ear when a genetic screen in Drosophila revealed a new ion channel family, "nomp" (Kernan *et al.*, 1994), which were later shown to have homologues in vertebrates, renamed TRPN, (Sidi *et al.*, 2003) . Zebrafish TRPN1 mutants showed auditory and vestibular dysfunction but cannot be part of the transduction channel in all vertebrates as TRPN1 is entirely absent in mammals and birds. TRPV4 was also identified as a candidate in a genetic screen in *C elegans*. TRPV4 is mechanically sensitive (Liedtke *et al.*, 2003) and found in the ear, although mainly in the stria (Shen *et al.*, 2006) and TRPV4 knockout mice have a late-onset hearing deficit (Tabuchi *et al.*, 2005). However an osmoregulatory role is more likely due to expression in the stria rather than hair cells and slow activation that isn't conducive to transduction. Variant waddler mice exhibit deafness and circling behaviour along with other deficits such as pigmentation. The mutant gene was mapped to TRPML3 (Di *et al.*, 2002) and loss of function causes disorganization of hair cell stereocilia (Cable and Steel, 1998;Di et al., 2002) due to abnormal organgelle trafficking, likely ruling out TRPML3 as a transduction channel. TRPA1 is expressed in the sensory epithelium of the mouse utricle and has large numbers of ankyrin repeats that are attractive as a gating spring, but activators of TRPA1 have no affect on hair cell transduction and TRPA1 knockout mice have no hearing deficits (Bautista *et al.*, 2006;Kwan *et al.*, 2006).

TRPC channels have not yet been investigated for hair cell mechanotransduction. As mentioned previously, TRPC channels are calcium permeable and can be blocked by gadolinium and ruthenium red and TRPC3 is found in the cochlea, in the hair cells (Tadros *et al.*, 2010) . TRP channels are known to heteromultimerize, this could produce a number of mechanically gated channels with different kinetic properties to explain the variation in mechanically activated channel properties at different locations along the cochlea. Additionally, the redundancy among the pore-forming subunits in a heteromer could account for the lack of an ion channel mutation in the human deafness or ENU mice screens.
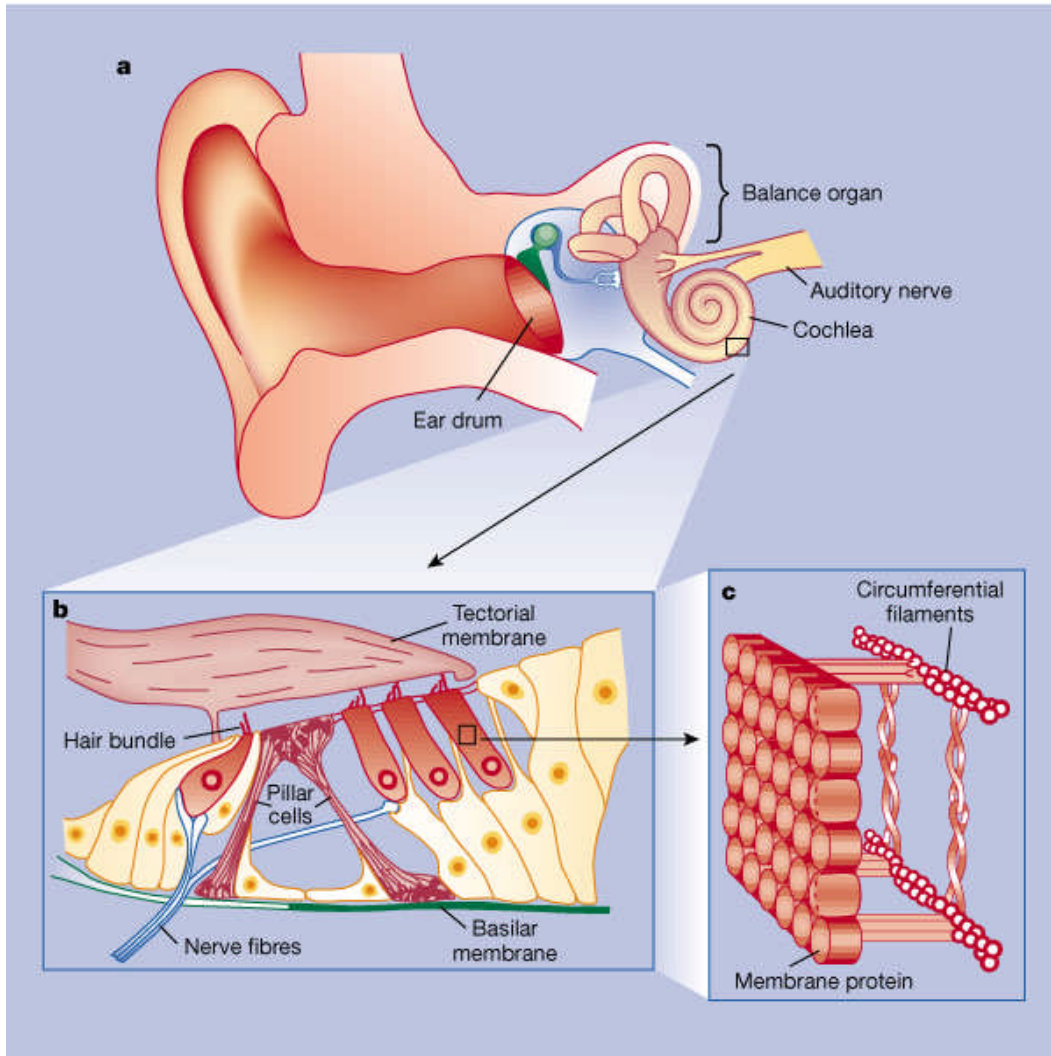
Figure 5.1 The ear and cochlea.

(adapted from (Holley, 2000))

a The cochlea. Sound enters the outer ear canal, vibrates the eardrum and is transmitted to the cochlea by the middle ear bones. **b.** Inside the cochlea, the organ of Corti sits upon the basilar membrane, which is covered by the tectorial membrane. Vibration of the basilar membrane leads to lateral displacements of the mechanosensory bundles on the hair cells (coloured orange). Inner hair cells form a row to one side of two rows of specialized supporting cells (pillar cells); outer hair cells form three rows on the other side. Inner hair cells are connected mainly to afferent nerve fibres and so are responsible for sending sensory information to the brain. Outer hair cells are connected to relatively few afferent fibres and are located above the most flexible region of the basilar membrane, where they can more easily influence its mechanical responses. **c,** The plasma membrane of outer hair cells contains a high density of membrane proteins embedded within the lipid layer.

105

5.1.3 Evidence for a role for TRPC3 and TRPC6 in mechanosensation

When TRPC6 is expressed in HEK293 cells they are able to be activated by mechanically- or osmotically-induced stretch (Spassova *et al.*, 2006). This stretch-activated current is blocked by GsMTx-4, a tarantuala toxin known to specifically inhibit mechanosensitive channels, and is PLC independent (Spassova *et al.*, 2006;Suchyna *et al.*, 2004;Suchyna *et al.*, 2000). Additionally TRPC6 shares many other biophysical properties of stretch activated channels including activation by DAG, high divalent cation permeability and blockade by Gd^{3+} (Setoguchi *et al.*, 1997;Welsh *et al.*, 2000;Inoue *et al.*, 2001).

TRPC3 and TRPC6 are also able to be mechanically activated in vivo. As described earlier TRPC3 and TRPC6 are highly expressed in vascular smooth muscle where they are mechanically activated, contributing to the myogenic response. TRPC6 has been implicated in the mechanosensory complexes found in the kidney as the PHB domain membrane protein podocin associates with and regulates TRPC6 as part of a complex that also includes Neph1, Neph2, Nephrin, and CD2AP which may act to sense glomerular pressure (Huber *et al.*, 2006). All seven TRPC channels are found within the inner ear where they may contribute to the sensory transduction process (Takumida and Anniko, 2009). The developmental regulation of TRPC3 coincides with the development of the sensory and neural tissues of the ear (Phan *et al.*, 2010) .

TRPC3 and TRPC6 are also highly expressed in DRG (Elg *et al.*, 2007) where stretch-activated channels (SAC) participate in mechanical stimulus detection (McCarter et al., 1999;Hu and Lewin, 2006). The SAC blocker, GsMTx-4, is able to block inflammatory induced mechanical hyperalgesia in vivo (Alessandri-Haber *et al.*, 2009). GsMTx-4 blocks both TRPC1 and TRPC6 but the mechanical hyperalgesia can be attributed to TRPC6 as only antisense to TRPC6 but not TRPC1-antisense is able to block the hyperalgesia (Alessandri-Haber *et al.*, 2009). TRPV4 plays a role in mechanical hyperalgesia (Alessandri-Haber *et al.*, 2006) but does not itself appear to be gated by mechanical stretch (Strotmann *et al.*,

2000).TRPV4 is frequently coexpressed with TRPC6 so could be contributing to mechanical transduction by functional coupling with this SAC.

As well as being expressed in tissues which have physiologically relevant mechanosensitive functions such as smooth muscle, kidney and the cochlea, TRPC channels also associate with a number of proteins that have a role in mechanosensation. Caveolae, which are found in many cell types including endothelial cells, are 50-100nm invaginations that facilitate interactions between proteins and are involved in endocytosis. Mechanical forces have been shown to increase translocation of signalling molecules and activation of secondary messenger pathways specifically at caveolae. TRPC6 in particular translocates to caveolae where it mediates Ca^{2+} facilitation (Cayouette *et al.*, 2004).

Both in vitro and in vivo evidence both suggest a role for TRPC3 and TRPC6 as mechanically sensitive channels but do these channels fit into what is currently known about the mechanisms of mechanotransduction?

There are two main theories for how mechanically activated channels are opened, namely the membrane model and the tether model. The membrane model proposes that mechanical force causes a change in the lipid bilayer inducing exposure and/or conformational change of the channel resulting in an open state. Chemicals which disrupt the lipid bilayer are able to activate mechanically sensitive channels supporting this theory. The tether model suggests that specific proteins are responsible for inducing a conformational change in the channel allowing it to open. These proteins could be cytoskeletal elements, diffusible messenger proteins or part of the channel itself. Many putative mechanosensors have elements which have the right properties to act as a tether, sometimes termed the "gating spring". These two mechanisms may however not be mutually exclusive; each could be acting in different tissues or in response to different mechanical stimuli.

TRPC3 and TRPC6 are both activated by DAG, a small-headed lipid produced from the breakdown of PIP_2 molecules located within the membrane bilayer. The breakdown of PIP_2 into a smaller molecule could result in increased membrane stress similar to that produced by stretch. This mechanism, proposed by Spassova et al, provides a common mechanism of

107

action for the stretch activated and receptor operated functions of TRPC3 and TRPC6 (Spassova *et al.*, 2006).

The evidence for the TRPC channels playing a critical role in mechanotransduction does not necessarily mean that the TRPC channels themselves are the direct sensors of mechanical stimuli, instead they may be indirectly activated downstream of other molecules. For example, Gudermann et al showed that membrane stretch activation of TRPC6 in HEK cells may be due to $G_{q/11}$ – coupled receptors acting as mechanosensors, independent of ligand, and in turn activating TRPC6 (Schnitzler *et al.*, 2008). It appears that many GPCRs are able to be mechanically activated which are found ubiquitously, yet specialised mechanotransduction occurs only in certain tissues such as primary afferent neurons and outer hair cells; if GPCRs are mechanosensors they must undergo some kind of conformational coupling to infer selectivity.

Translocation of ion channels could confer another mechanism leading to TRP channels' mechanosensitive properties. Mechanical forces are able to initiate rapid translocation of TRP channels to the plasma membrane, for example TRPM7, TRPV2 and TRPV4 have been shown to be translocated to the plasma membrane following mechanical forces applied to endothelial cells or myocytes (Oancea *et al.*, 2006;Iwata *et al.*, 2003;Loot *et al.*, 2008). A number of TRPC channels are also translocated to the plasma membrane following stimulation. TRPC3 interacts with VAMP2, a SNARE protein found in neuronal tissues, to insert into the plasma membrane in response to carbachol (Singh *et al.*, 2004). TRPC6 is also inserted into the plasma membrane following GPCR activation (Cayouette *et al.*, 2004). These translocations could also occur in response to mechanical stimulation as is the case for other members of the TRP family.

5.2 Results

5.2.1 Targeting construct design

Flockerzi et al generated the TRPC3$^{-/-}$:TRPC6$^{-/-}$ global knock out . The intron-exon organization of the TRPC3 and TRPC6 genes and the expected disruptions caused by the knockout are shown in Figure 5.2.
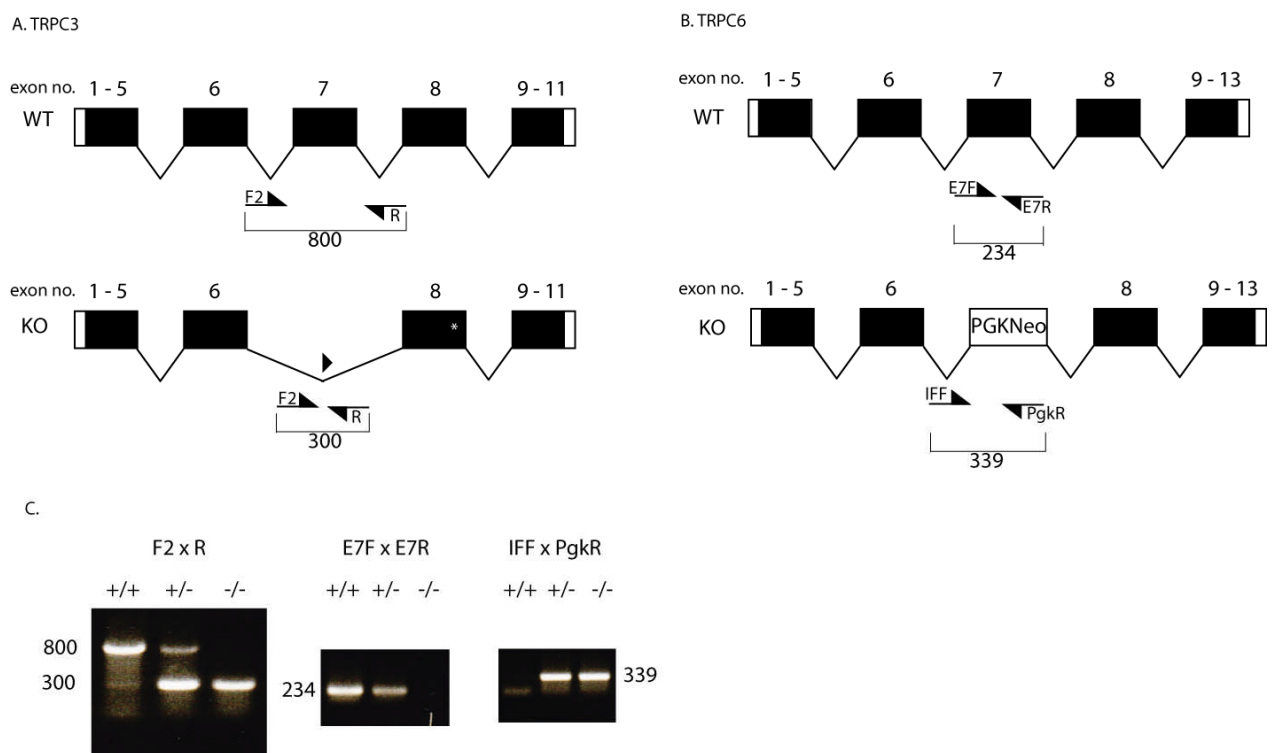
Figure 5.2 Generation of TRPC3$^{-/-}$:TRPC6$^{-/-}$ mouse

A. (Top) Diagram of the intron-exon organisation of the Mus musculus TRPC3 gene. The lengths of the amplicons, including primers, are depicted. F2 (5' GAATCCACCTGCTTACAACCATGTG) and R (5' GGTGGAGGTAACACAGACCTAAGCC), PCR primers, *, stop codon, black triangle denotes *loxP* site. (Bottom) Diagram of the expected disruption after excision of exon 7 by the action of Cre recombinase. **B.** (Top) Diagram of the intron-exon organisation of the Mus musculus TRPC6 gene. The lengths of the amplicons, including primers, are depicted. E7F (5' CAGATCATCTCTGAAGGTCTTTATGC), E7R (5' TGTGAATGCTTCATTCTGTTTTGCGCC), IFF (5' ACGAGACTAGTGAGACGTGCTACTTCC) and PgkR (5' GGGTTTAATGTCTGTATCACTAAAGCCTCC), PCR primers. (Bottom) Diagram of the TRPC6 gene after targeted disruption by the PGKNeo cassette. **C.** Image of the electrophoretic migration in an agarose gel of the amplicons obtained using the indicated primers

A floxed TRPC3 mouse, obtained from Birnbaumer as before, was crossed with Cre deleter as described in (Schwenk *et al.*, 1995). The offspring of homozygous floxed, heterozygous cre will have a global deletion of TRPC3. A TRPC6 global knockout mouse was generated using a "knock-in" targeting construct, replacing exon 7 of the TRPC6 gene with a pgk NEO^r cassette to create a non-functional gene. These two mouse lines, TRPC3-null and TRPC6-null, were crossed to create a double knockout of both TRPC3 and TRPC6 in all tissues.

5.2.2 Breeding strategy

A double knockout was crossed with a C57BL/6 to generate heterozygous null-TRPC3; heterozygous null-TRPC6 animals. Heterozygotes were then crossed together to create a number of genotypes, including TRPC3$^{-/-}$:TRPC6$^{-/-}$, TRPC3$^{-/-}$; TRPC6$^{-/-}$ and littermate wildtype controls.

In order to reduce the number of animals needed a non-littermate control was used where possible. This was obtained either by crossing a 129 strain with a C57BL/6 to create a strain with as similar genetic background to the double knockouts as possible or using floxed TRPC3 mice which also have a mixed 129/C57Bl6 background.

5.2.3 TRPC3$^{-/-}$:TRPC6$^{-/-}$ mice have normal development and fertility

TRPC3$^{-/-}$:TRPC6$^{-/-}$ mice developed normally and survived to ages within the normal mortality range. Litters from the double knockout x double knockout cross were of expected size. Litters from the heterozygous x heterozygous were also of normal size and weight (Figure 5.3) and the ratios of all genotypes were as expected (1:1:1:1:2:2:2:2:4), illustrated in Table 5.1.

	Observed	Expected
TRPC3-/-TRPC6-/-	42	36.625
TRPC3-/-TRPC6-/+	80	73.25
TRPC3-/+TRPC6-/-	71	73.25
TRPC3-/+TRPC6-/+	145	146.5
TRPC3-/-TRPC6+/+	33	36.625
TRPC3+/+TRPC6-/-	38	36.625
TRPC3+/+TRPC6-/+	74	73.25
TRPC3-/+TRPC6+/+	71	73.25
TRPC3+/+TRPC6+/+	32	36.625
Chi squared value	2.567	
p = 0.9586	Not statistically significant	

Table 5.1 Observed genotypes from double heterozygote x double heterozygote cross

('+' indicates wildtype allele, '-' indicates knockout allele)
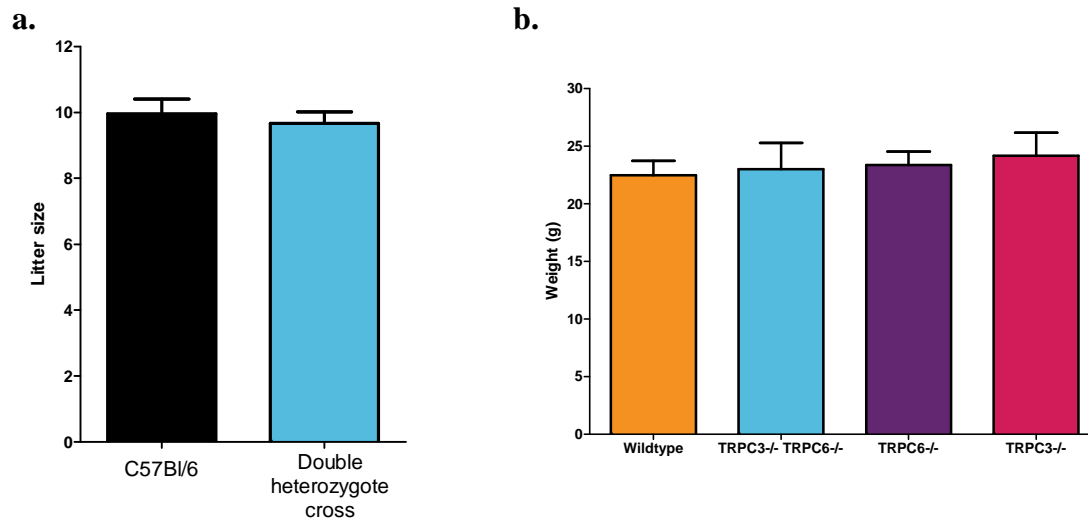
Figure 5.3 Litter sizes and weights of TRPC3$^{-/-}$TRPC6$^{-/-}$ mice.

a. Average litter size from 25 C57Bl/6 breeding pairs compare with 25 litters from TRPC3$^{-/+}$TRPC6$^{-/+}$ breeding pairs. **b.** Average weight of 8 week old mice (6 mice in each group). All results expressed as mean ±SEM.

5.2.4 TRPC3$^{-/-}$:TRPC6$^{-/-}$ mice show no deficits in locomotion

Motor coordination was judged using an accelerating rotarod. There was no difference in the motor ability of the TRPC3$^{-/-}$:TRPC6$^{-/-}$ mice compared with control animals or TRPC3$^{-/-}$ or TRPC6$^{-/-}$ animals (Figure 5.4).
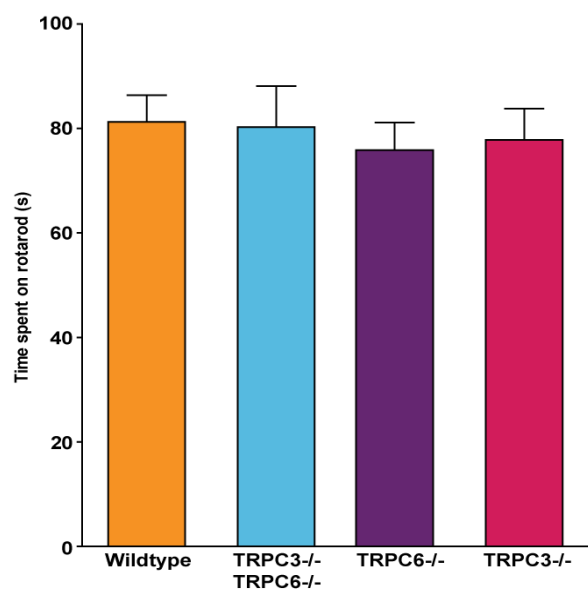
Figure 5.4 Motor coordination of TRPC3-/-:TRPC6-/-, TRPC3-/-, TRPC6-/- and wildtype control animals.

There was no difference in motor coordination between wildtype control (orange, n=6) and TRPC3$^{-/-}$:TRPC6$^{-/-}$ (blue, n=5), TRPC6$^{-/-}$ (purple, n=5) and TRPC3$^{-/-}$ (red, n = 6) animals. All results expressed as mean ±SEM.

5.2.5 TRPC3$^{-/-}$:TRPC6$^{-/-}$ mice do not show behavioural deficits in noxious mechanosensation

Behavioural responses to noxious mechanical stimuli were measured using the Randall Selitto test. There was no difference in behavioural responses to noxious blunt stimulation of the tail between TRPC3$^{-/-}$:TRPC6$^{-/-}$ and control animals (Figure 5.5). Results expressed as mean threshold±SEM are as follows, TRPC3$^{-/-}$:TRPC6$^{-/-}$, 143.1±3.2g, TRPC3$^{-/-}$, 147±11, TRPC6$^{-/-}$, 136±6, control mice 140±9g.
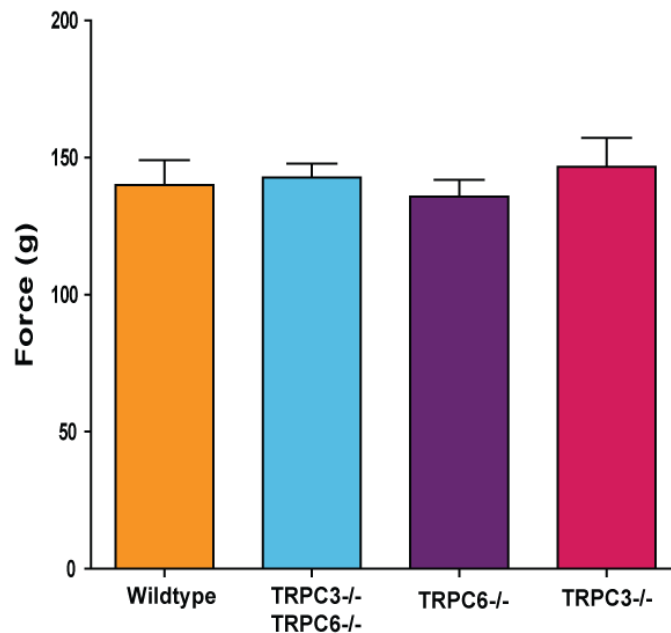
Figure 5.5 Acute mechanical pain behaviour in TRPC3-/-:TRPC6-/- , TRPC3-/-, TRPC6-/- and wildtype control animals.

Response to blunt mechanical stimulation of the tail in the Randal Selitto test was not significantly different between wildtype control animals (orange, n=4) and TRPC3$^{-/-}$:TRPC6$^{-/-}$ animals (blue, n=9), TRPC6$^{-/-}$ (purple, n=7) and TRPC3$^{-/-}$ (red, n = 6) animals. All results expressed as mean±SEM.

5.2.6 TRPC3$^{-/-}$:TRPC6$^{-/-}$ mice have a behavioural deficit in light touch sensation.

Behavioural responses to light touch were assessed using von Frey hairs and the up-down method. TRPC3$^{-/-}$:TRPC6$^{-/-}$ mice had an increased mechanical threshold (0.6 ± 0.04g) compared to wildtype controls (0.3 ± 0.03g) which was statistically significant (one-way ANOVA with post-hoc Bonferroni test, p = 0.01). TRPC3$^{-/-}$ and TRPC6$^{-/-}$ mice did not have increased mechanical thresholds, 0.04 ± 0.03g and 0.38 ± 0.03g respectively.
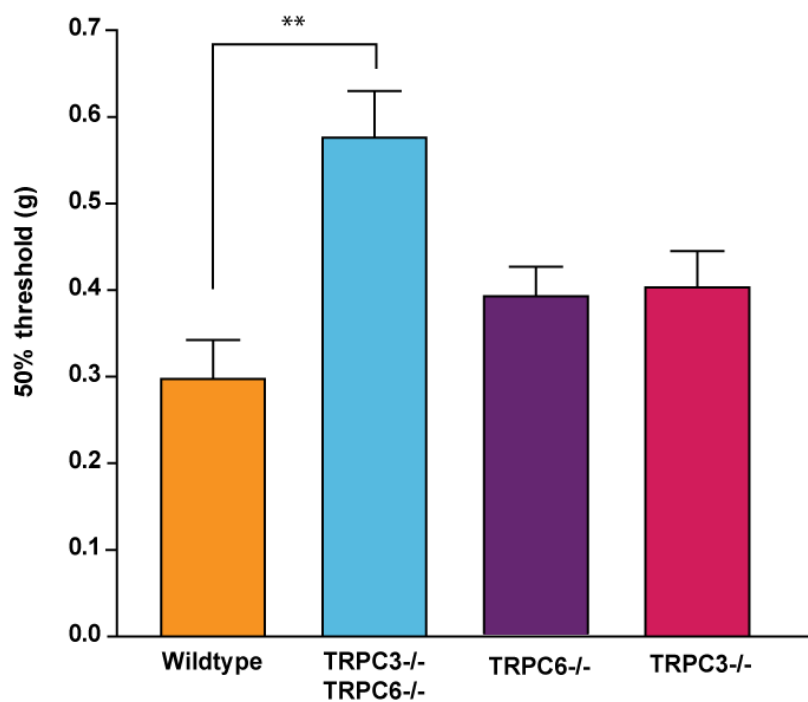
Figure 5.6 Light touch sensation in TRPC3-/-:TRPC6-/- and littermate control animals assessed using von Frey hairs.

Response to mechanical stimulation with von Frey hairs was significantly different between littermate control (orange, n=5) and TRPC3$^{-/-}$:TRPC6$^{-/-}$ (blue, n=6) animals (p = 0.01). TRPC6$^{-/-}$ (purple, n=12) and TRPC3$^{-/-}$ (red, n=6) animals were not significantly different from control animals. All results expressed as mean±SEM.

5.2.7 TRPC3$^{-/-}$:TRPC6$^{-/-}$ mice do not show behavioural deficits in noxious thermosensation

Behavioural responses to noxious thermal stimuli were measured using the Hargreaves' apparatus and the hot plate test. Paw withdrawal latency in Hargreaves' test was not altered in the TRPC3$^{-/-}$:TRPC6$^{-/-}$, TRPC6$^{-/-}$ not TRPC3$^{-/-}$ animals compared with littermate control animals (Figure 5.7a). Results expressed as mean latency±SEM are as follows, TRPC3$^{-/-}$:TRPC6$^{-/-}$ mice 8.5±0.8 seconds, TRPC6$^{-/-}$ mice 8±1.2 seconds, TRPC3$^{-/-}$ mice 6.5±0.5 seconds and control mice 9.5±2.8 seconds. There was also no difference in latency of behavioural responses on the hot plate at 45°C, 50°C or 55°C. TRPC3$^{-/-}$:TRPC6$^{-/-}$ responding on average 133±23 seconds compared to 120±30 seconds for floxed TRPC3 controls at 45°C, 32±4 seconds compared to 34±6 seconds at 50°C and 16±1 seconds compared to 13±1 seconds at 55°C (Figure 5.7b).
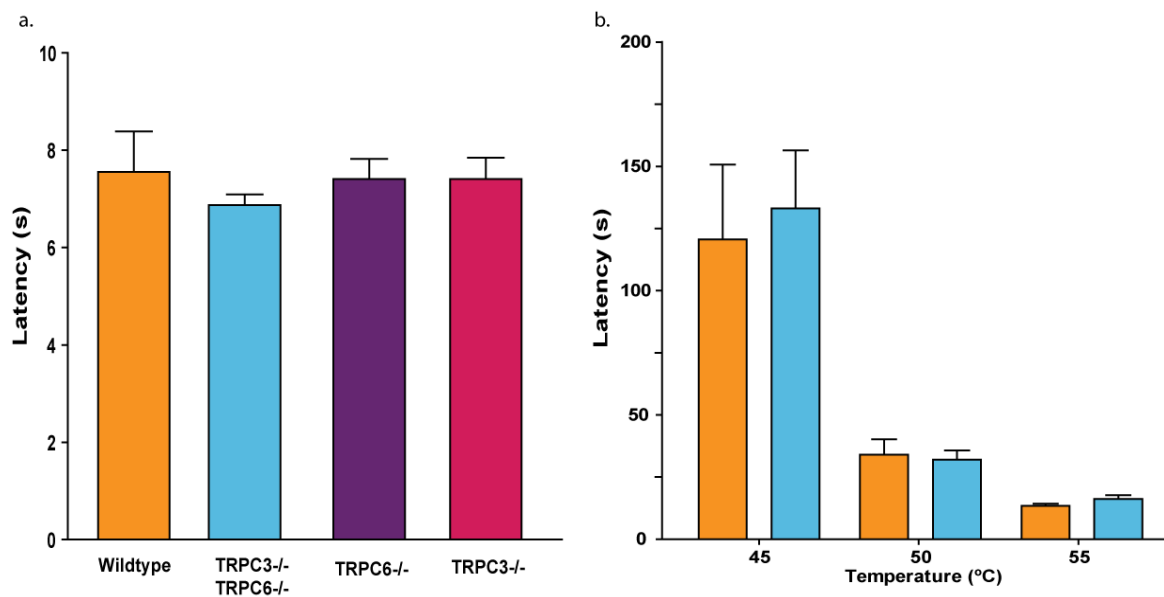
Figure 5.7 Acute thermal pain behaviour in TRPC3$^{-/-}$:TRPC6$^{-/-}$ and control animals

a. Noxious thermal stimulation using Hargreaves' apparatus. No significant difference was observed between littermate control (orange, n=3) and TRPC3$^{-/-}$:TRPC6$^{-/-}$ (blue, n=3), TRPC6$^{-/-}$ (purple, n=4), nor TRPC3$^{-/-}$- (red, n=4) animals. **b.** Response to noxious thermal stimulation using the hot plate test was not significantly different between TRPC3fl/fl control (orange, n=7) and TRPC3$^{-/-}$:TRPC6$^{-/-}$ (blue, n=8) animals at 45ºC, 50ºC or 55ºC. All results shown as mean ±SEM.

5.2.8 TRPC3$^{-/-}$:TRPC6$^{-/-}$ mice show no deficits in response to noxious cold

Behavioural responses to noxious cold were assessed using the cold plate set to 0ºC for 5 minutes. There was no significant difference in the behavioural responses in the TRPC3$^{-/-}$:TRPC6$^{-/-}$ mice, 13.9±1 behaviours, compared to control TRPC3fl/fl animals, 13±2.3 behaviours, (Figure 5.8).
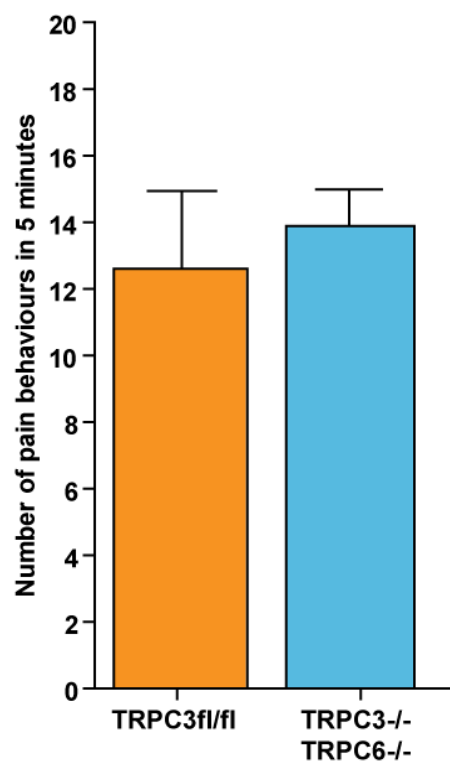
Figure 5.8 Acute cold pain behaviour in TRPC3$^{-/-}$:TRPC6$^{-/-}$ and control (TRPC3fl/fl) animals.
Noxious cold stimulation using cold plate at 0ºC. No significant difference seen between TRPC3fl/fl control (orange, n=5) and TRPC3$^{-/-}$:TRPC6$^{-/-}$ (blue, n=8) animals. All results expressed as mean±SEM.

5.2.9 TRPC3$^{-/-}$:TRPC6$^{-/-}$ mice display reduced inflammatory pain behaviour

5.2.9.1   Formalin Test

Behavioural responses from 4 TRPC3$^{-/-}$:TRPC6$^{-/-}$ mice and 4 control mice in the two distinct phases were recorded. In the first phase, 0-10 minutes, the TRPC3$^{-/-}$:TRPC6$^{-/-}$ mice displayed 127±13.3 seconds of pain behaviour compared with 128.5±11 seconds for the control mice. There was no significant difference between the two groups.

In contrast the TRPC3$^{-/-}$:TRPC6$^{-/-}$ mice showed attenuated pain behaviours in the second phase, from 10-60 minutes, displaying just 194±22 seconds compared with 564±77 seconds for the control mice. This was shown to be statistically significant using an unpaired 2-tailed t-test, p = 0.0035, (Figure 5.9a).

Figure 5.9b shows the time course of the formalin response and demonstrates that the TRPC3$^{-/-}$:TRPC6$^{-/-}$ mice displayed reduced pain behaviours at each 5 minute interval within the second, inflammatory, phase with significant differences found at the time points between 15-35 minutes using a 2-way ANOVA with Bonferroni post test.
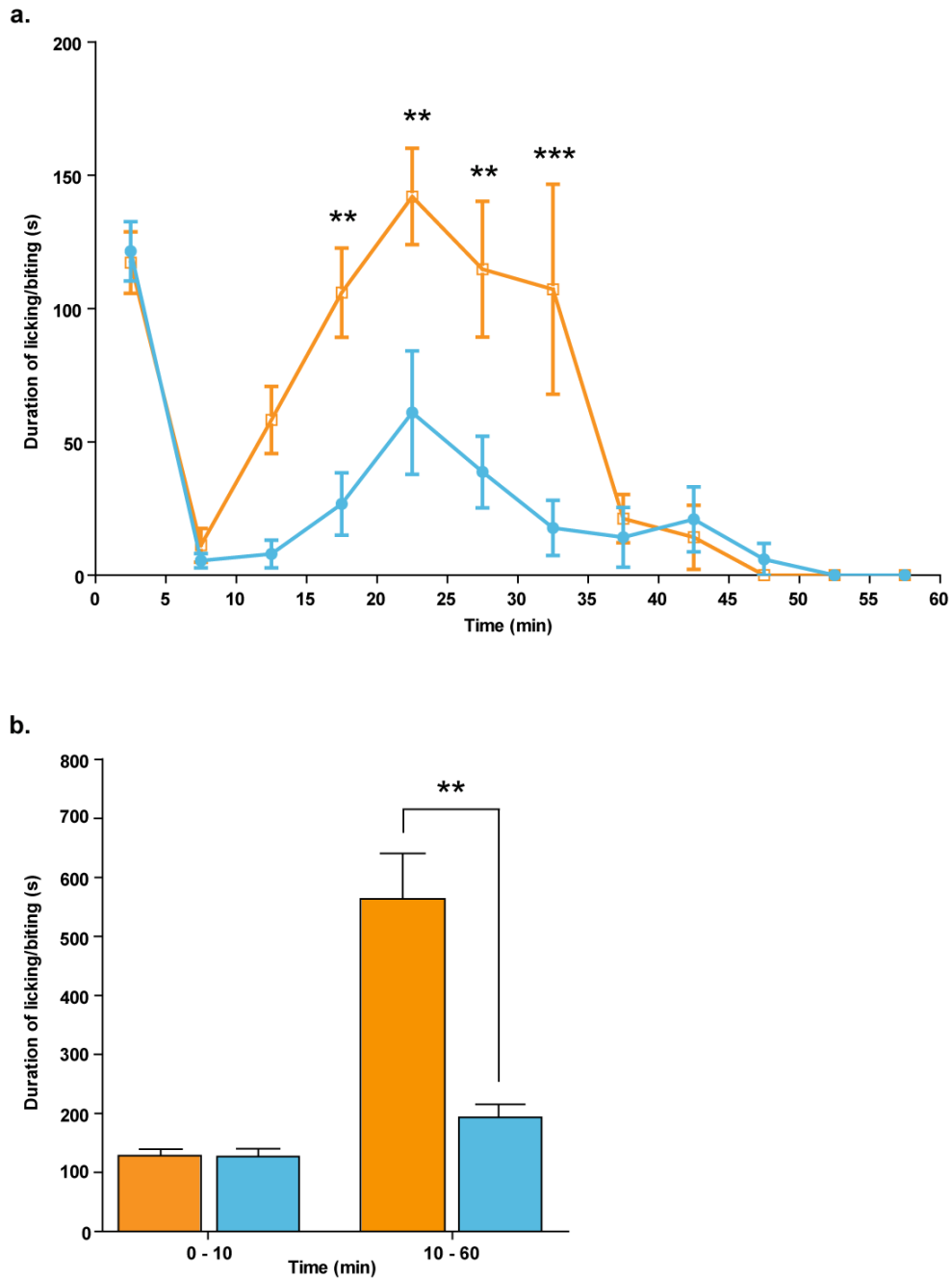
Figure 5.9 Formalin-induced inflammatory pain behaviour in TRPC3$^{-/-}$:TRPC6$^{-/-}$ and control (129sv/Bl/6) animals.

Behaviour following injection of 20µl of 5% formalin. **a.** Time spent licking/flinching/biting the hind paw was recorded in 5 minute sections. No significant reduction in pain behaviours was seen in Phase I (0-10 minutes) however in Phase II (10-60 minutes) TRPC3$^{-/-}$:TRPC6$^{-/-}$ mice (blue, n=4) have significantly attenuated pain behaviours compared to littermate controls (orange, n=4) (p = 0.0035, unpaired t-test). b. Time course of the formalin test. A traditional biphasic response was observed with the attenuated pain behaviour of TRPC3$^{-/-}$:TRPC6$^{-/-}$ mice apparent in the second phase (2-way ANOVA). All results expressed as mean±SEM.

118

5.2.9.2   Carrageenan induced mechanical hyperalgesia

Mechanical responses were recorded from mice injected with carrageenan compared to baseline recordings made prior to the injections. The control mice developed a clear mechanical hyperalgesia, the 50% threshold dropping from 0.5 ± 0.03g to 0.1 ± 0.03g at 3 hours after carrageenan injection. The TRPC3$^{-/-}$:TRPC6$^{-/-}$ mice had a significantly higher baseline mechanical threshold, and developed a less severe mechanical hyperalgesia with the threshold dropping from 0.7 ± 0.04g to 0.4 ± 0.08 g, $p < 0.01$, (Figure 5.10).
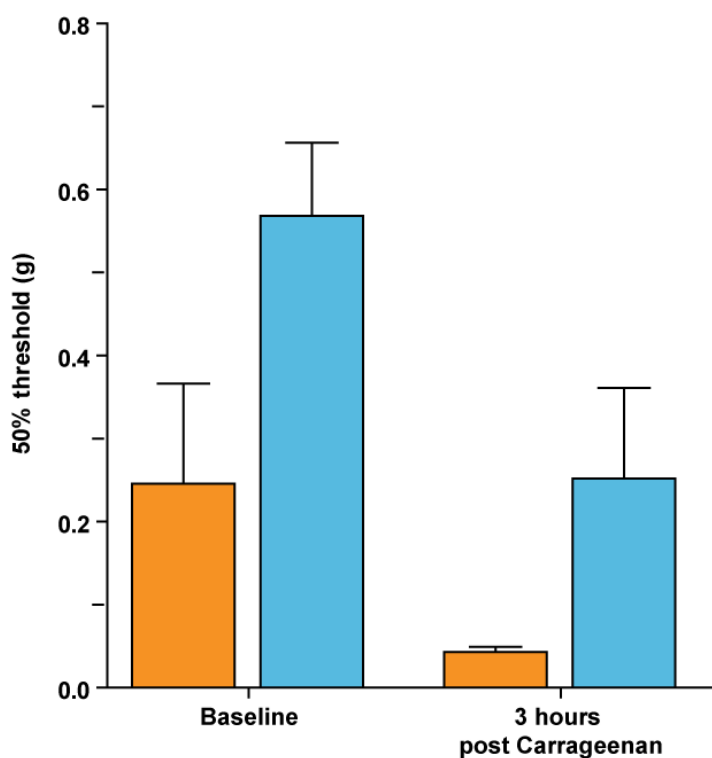
Figure 5.10 Carrageenan induced mechanical hyperalgesia in TRPC3$^{-/-}$:TRPC6$^{-/-}$ and control (TRPC3fl/fl) animals.

Behaviour following injection of 20µl of 2% carrageenan. The 50% mechanical threshold was recorded using von Frey hairs on two days prior to injection and three hours post injection. TRPC3$^{-/-}$:TRPC6$^{-/-}$ mice (blue, n = 4) have significantly attenuated mechanical hyperalgesia compared to floxed TRPC3 controls (orange, n = 3). All results expressed as mean±SEM.

5.2.9.3 Complete Freunds' Adjuvant induced hyperalgesia

Mechanical (von Frey) and thermal (Hargreaves') thresholds were measured from 6 TRPC3$^{-/-}$:TRPC6$^{-/-}$ mice and 6 control mice following induction of inflammation by administration of 20µl of CFA and compared to baseline measurements. The same mice were used for both mechanical and thermal measurements on days 1, 3, 5, 7 and 10 post injections. Both control and TRPC3$^{-/-}$:TRPC6$^{-/-}$ mice developed mechanical hyperalgesia from day 1 post injection of CFA, on day 3 the TRPC3$^{-/-}$:TRPC6$^{-/-}$ mice had significantly attenuated mechanical hyperalgesia, $p < 0.05$, 2-way ANOVA (Figure 5.11a). Thermal hyperalgesia developed in both the TRPC3$^{-/-}$:TRPC6$^{-/-}$ mice and the control mice with no significant difference at any timepoint (Figure 5.11b).
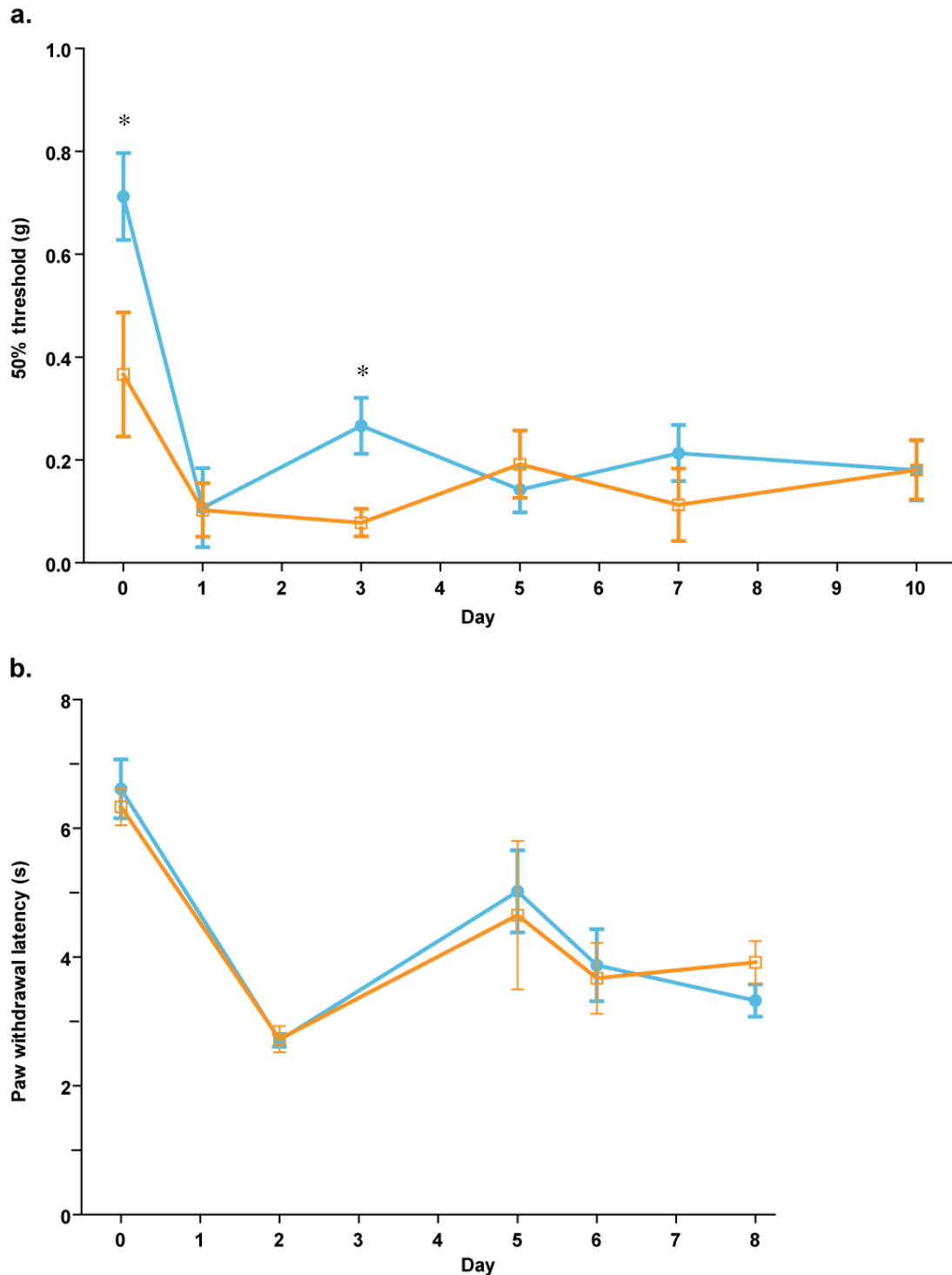
Figure 5.11 Complete Freunds' Adjuvant induced hyperalgesia in TRPC3$^{-/-}$;TRPC6$^{-/-}$ and control (TRPC3fl/fl) animals.

Mechanical and thermal thresholds following injection of 20µl CFA. a. The 50% mechanical threshold was recorded using von Frey hairs prior to injection and on days 1, 3, 7 and 10 following injection. b. Paw withdrawal latency to a radiant heat source (Hargreaves') was measured prior to injection and on days 1, 3, 7 and 10 following injection. No significant difference was seen between TRPC3$^{-/-}$;TRPC6$^{-/-}$ (blue, n=6) and control TRPC3fl/fl animals (orange, n=6). All results expressed as mean±SEM.

121

5.2.10 TRPC3$^{-/-}$:TRPC6$^{-/-}$ mice do not have any deficits in neuropathic mechanical allodynia

To test the effect of TRPC3 and TRPC6 knockout on neuropathic pain 5 TRPC3$^{-/-}$:TRPC6$^{-/-}$ and 5 wildtype mice underwent spinal nerve ligation. Thresholds to von Frey filaments were recorded before and after surgery. Both TRPC3$^{-/-}$:TRPC6$^{-/-}$ and wildtype controls developed mechanical allodynia to the same extent.
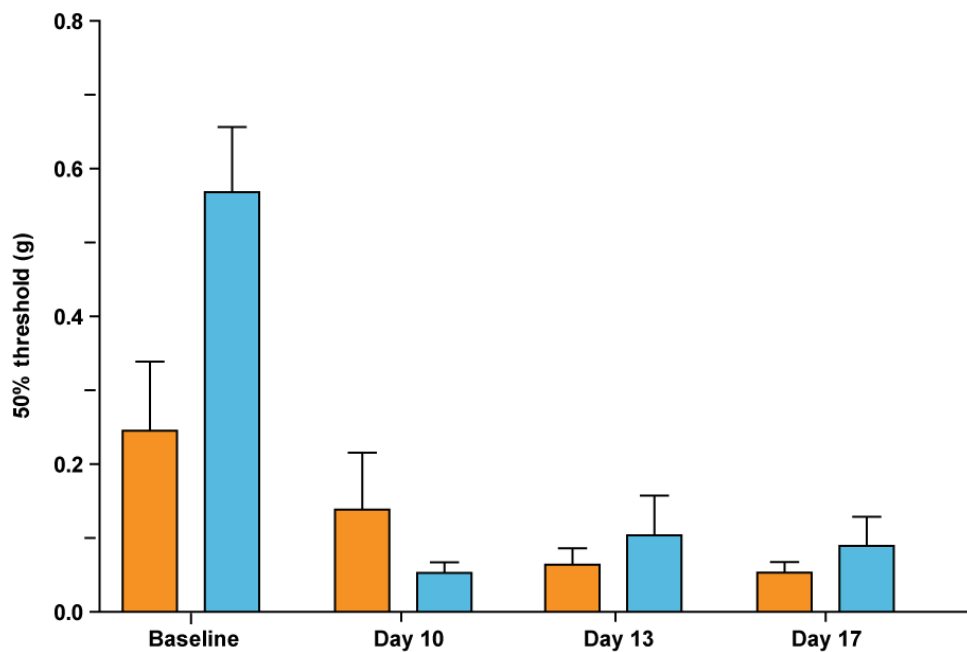
Figure 5.12 Mechanical allodynia following spinal nerve ligation in TRPC3$^{-/-}$:TRPC6$^{-/-}$ and control (TRPC3fl/fl) animals

Mechanical thresholds before and after SNL surgery. No significant difference was seen between TRPC3$^{-/-}$:TRPC6$^{-/-}$ (blue, n = 5) and control (orange, n = 5) animals. All results expressed as mean±SEM.

5.2.11 TRPC3$^{-/-}$:TRPC6$^{-/-}$ mice show behavioural signs of vestibular and auditory dysfunction

A number of tests were used to measure vestibular function, which enables a mouse to balance and control head movements. The TRPC3$^{-/-}$:TRPC6$^{-/-}$ mice are able to right themselves in the air and are also able to swim (Figure 5.15). The TRPC3$^{-/-}$:TRPC6$^{-/-}$ mice were slow to begin swimming and alternated between left and right sides, appearing to have trouble staying afloat, these behaviours were not seen in wildtype animals. The typical swimming positions of the wildtype and TRPC3$^{-/-}$:TRPC6$^{-/-}$ animals are shown in (Figure 5.13). However, the scores of the swim test (as described in the methods) were not different between the TRPC3$^{-/-}$:TRPC6$^{-/-}$ and the wildtype mice (Figure 5.15).

a.

b.
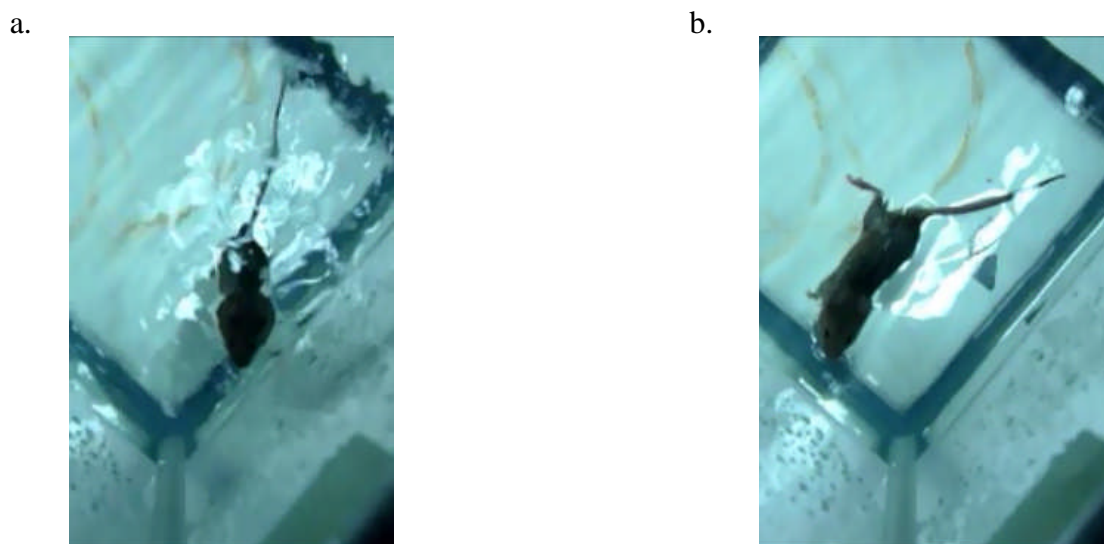
Figure 5.13 : Swimming positions of TRPC3$^{-/-}$:TRPC6$^{-/-}$ and control mice.

a. A wildtype mouse swimming with an elongated body, using the tail to propel and steer through the water.

b. TRPC3$^{-/-}$:TRPC6$^{-/-}$ mice are unbalanced and swim irregularly. (Also see video for more information)

The TRPC3$^{-/-}$:TRPC6$^{-/-}$ mice showed an abnormal reaching response in the trunk curl test. When held 5cm away from a surface the TRPC3$^{-/-}$:TRPC6$^{-/-}$ curled upwards instead of reaching forward and down with both forelimbs like the wildtype mice (Figure 5.14 and Figure 5.15). The TRPC3$^{-/-}$ and TRPC6$^{-/-}$ mice appeared to show a slight trunk curl but this was not significant (Figure 5.15).
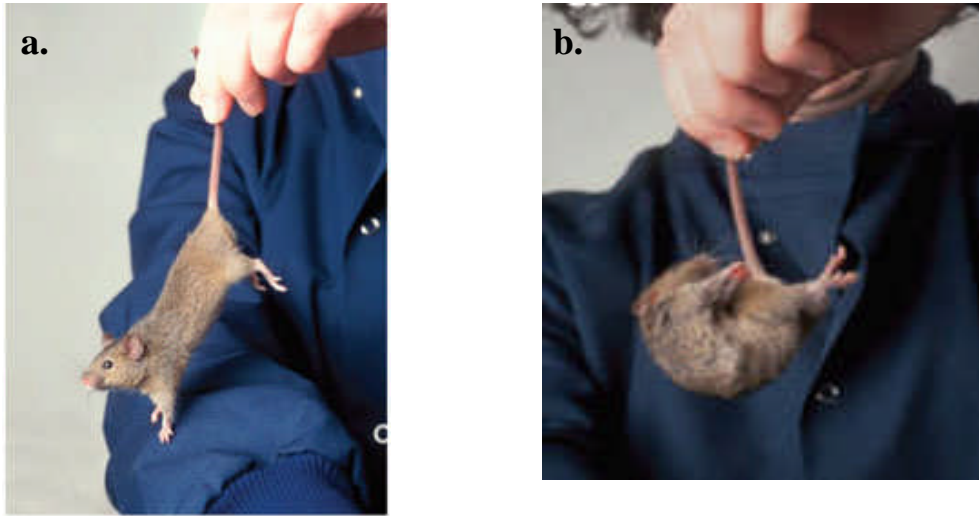
Figure 5.14 Reaching responses of wildtype and TRPC3$^{-/-}$:TRPC6$^{-/-}$ mice

Wildtype mice reach forwards and down when held 5cm away from a surface (**a**) whereas TRPC3$^{-/-}$:TRPC6$^{-/-}$ mice curl upwards towards their tail (**b**). (example pictures adapted from (Hardisty-Hughes *et al.*, 2010)

The auditory function was tested using a clickbox, the wildtype, TRPC3$^{-/-}$ and TRPC6$^{-/-}$ mice all displayed a strong Preyer reflex in response to the 20kHz toneburst but the TRPC3$^{-/-}$:TRPC6$^{-/-}$ mice did not (Figure 5.15).
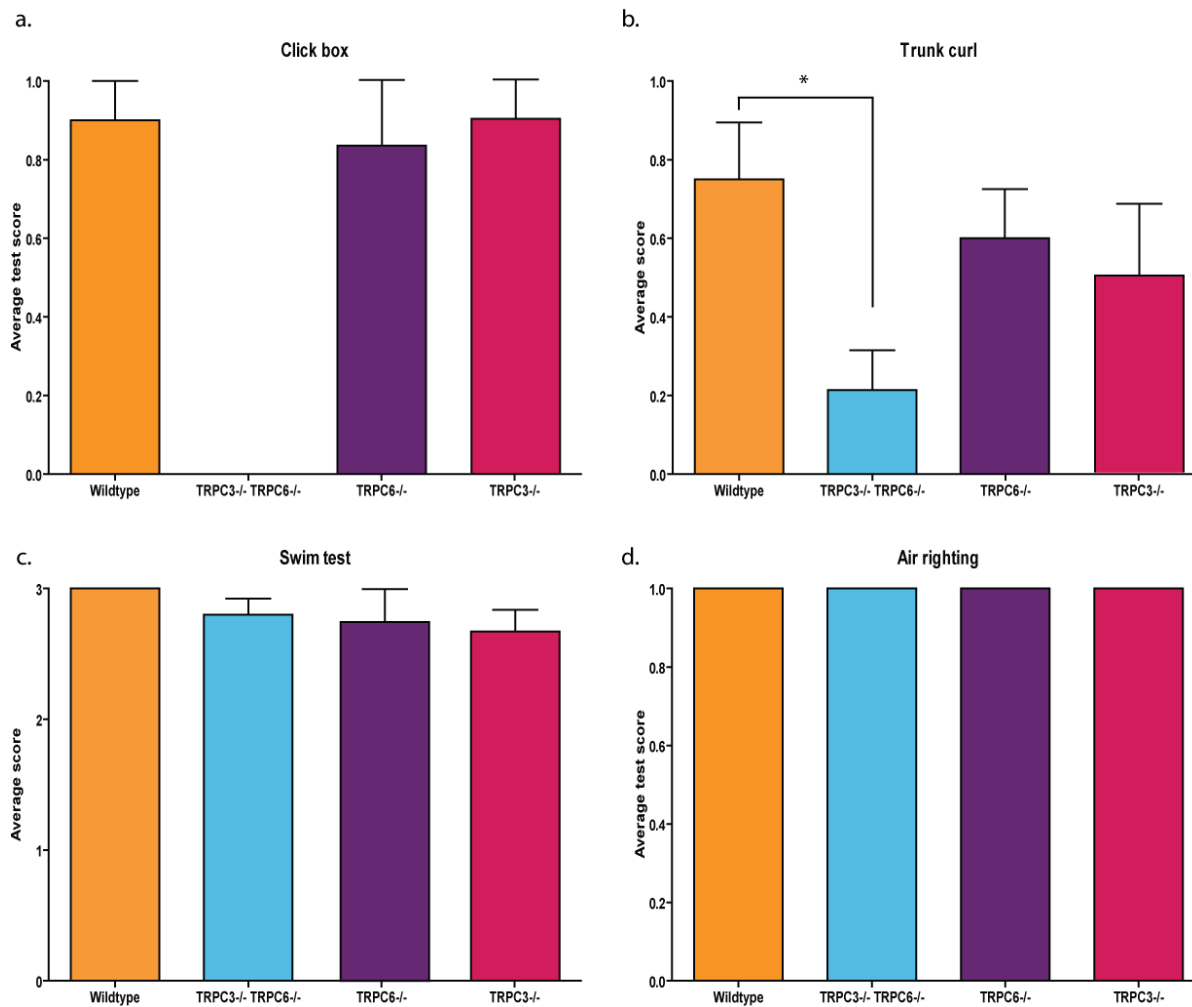
Figure 5.15 Vestibular and auditory testing in TRPC3$^{-/-}$:TRPC6$^{-/-}$ mice and littermate controls.
a. TRPC3/TRPC6 null mice do not exhibit a Preyer reflex in response to a 20kHz toneburst at 90dSB (Mann-Whitney test, p <0.0001) . **b.** TRPC3/TRPC6 null mice show an abnormal reaching response compared to wildtype littermate controls, TRPC3$^{-/-}$ and TRPC6$^{-/-}$ animals (Mann-Whitney test, p<0.05) **c.** and **d.** TRPC3$^{-/-}$:TRPC6$^{-/-}$ mice, TRPC3$^{-/-}$ and TRPC6$^{-/-}$ mice are able to swim and have a normal air righting response. All results expressed as mean ± SEM. TRPC3$^{-/-}$:TRPC6$^{-/-}$; blue, n = 6, TRPC3$^{-/-}$; red, n = 6, TRPC6$^{-/-}$;purple, n = 10, wildtype; orange, n = 7.

5.3 Discussion

5.3.1 TRPC3$^{-/-}$:TRPC6$^{-/-}$ mice develop normally

Before any experiments were performed the fitness of the TRPC3$^{-/-}$:TRPC6$^{-/-}$ mice strains were assessed. The size of litters produced with a TRPC3$^{-/-}$:TRPC6$^{-/-}$ x TRPC3$^{-/-}$:TRPC6$^{-/-}$ cross was within expected range and the ratio of male/female progeny was close to 1:1. When heterozygotes, TRPC3$^{+/-}$:TRPC6$^{+/-}$ were crossed together the litters were also of an expected size and with the correct mendelian ratios. There were no differences in weight gain, motor function, fertility or general behaviour between the various genotypes produced from any of the breeding crosses.

A gain-of-function mutation in TRPC3 has been attributed to the motor deficit in moonwalker mice (Becker *et al.*, 2009) and a motor coordination defect was also noted in the global TRPC3$^{-/-}$ mice (Hartmann *et al.*, 2008). Despite these previous results we found no deficits in motor ability using the accelerating rotarod test. The primary reason for performing the rotarod test is to ensure the mice do not have motor defects which would prevent the withdrawal responses for the pain threshold tests. It was observed that the double knockout mice had an unusual technique on the rotarod that was different to wildtype mice. We have not performed more elaborate motor ability tests such as an irregularly spaced ladder or gait analysis, if we were to do so it is likely that the double knockouts would have a similar phenotype to that of the TRPC3$^{-/-}$ mice.

5.3.2 TRPC3$^{-/-}$:TRPC6$^{-/-}$ mice have vestibular and auditory dysfunction

The vestibular apparatus provides information about the location and movement of the head and body which, along with the visual, proprioceptive and somatosensory systems, enables an upright position to be maintained. Rodents rely much less on vision than humans so as a result a vestibular defect can cause severe phenotypes due to inadequate compensation from the proprioceptive and somatosensory systems. The swim test removes proprioceptive input from gravity acting on the mouse and also lack of contact with the floor removes somatosensory input which highlights vestibulopathy. The TRPC3$^{-/-}$:TRPC6$^{-/-}$ mice displayed irregular swimming which indicates an element of vestibular dysfunction. The reaching

response exploits a mouse's instinct to reach for the ground, a stable, solid surface. In the air, without the somatosensory inputs, the mouse relies on the vestibular system to determine which way is up and its relative position. Wildtype mice extended both paws towards the ground whereas TRPC3$^{-/-}$:TRPC6$^{-/-}$ mice curled up and twisted their bodies aimlessly. TRPC3 has been implicated in motor coordination which could be contributing to the swimming phenotype, however the TRPC3$^{-/-}$:TRPC6$^{-/-}$ mice moved all four limbs whilst swimming which indicates this is unlikely.

TRPC3$^{-/-}$:TRPC6$^{-/-}$ mice have a severe hearing deficit at the high frequency range. The mice do not exhibit a Preyer reflex in response to a click box, and have an increased threshold to tones above 32kHz in ABR. The outer hair cells (OHCs) along the corti membrane responsible for transducing sounds contain mechanosensors. There was no loss of OHCs in the TRPC3$^{-/-}$:TRPC6$^{-/-}$ mice to explain the deafness, suggesting the transduction mechanism has been affected rather than any problems during development. The frequencies transmitted by the hair cells form a gradient with the lowest frequencies at the apex and highest frequencies at the basal of the cochlea. Single-cell recordings from apical and basal hair cells have different conductances (Marcotti *et al.*, 1999) suggesting differences between the mechanically gated channels. Our work supports this theory as the loss of TRPC3 and TRPC6 renders the basal hair cells unable to sense mechanical stimulation, however the apical hair cells function normally.

5.3.3 TRPC3 and TRPC6 are part of the mechanosensory complex

Mechanosensation was tested using two different methods, von Frey hairs and Randall Selitto, The TRPC3$^{-/-}$, TRPC6$^{-/-}$ or the TRPC3$^{-/-}$:TRPC6$^{-/-}$ mice had no deficit in the sensation of noxious mechanical pressure as tested using Randall Selitto. However, the TRPC3$^{-/-}$:TRPC6$^{-/-}$ mice had an increased threshold to innocuous touch tested using von Frey hairs; the TRPC3$^{-/-}$ and TRPC6$^{-/-}$ mice had normal innocuous touch thresholds.

Sensory neurons can be distinguished by their responses to mechanical pressure, either classed as high-threshold, low-threshold or non-responsive. The ion channel composition of these different sub populations of neurons differs, suggesting there are distinct high-threshold and low-threshold mechanoreceptors. We know that the high threshold mechanoreceptor is

predominantly expressed in the small diameter, Nav1.8+ve neurons as the DTA-CRE mouse had no noxious mechanical pain. The low-threshold mechanoreceptor remains more of a mystery. A range of sensory neurons respond to innocuous touch, including Aβ-fibres and a proportion of small diameter Nav1.8-ve neurons. TRPC3 and TRPC6 are predominantly expressed in small diameter neurons, where they could be responsible for a proportion of innocuous touch sensation. As the touch deficit observed in the double knockouts is not complete, sensory neurons where TRPC3 and TRPC6 are not highly expressed, such as Aβ-fibres, may contain different mechanosensitive channels.

The total number and proportion of each subpopulation of sensory neuron in the DRG of the TRPC3/TRPC6 null mice did not differ from the wildtype animals showing that developmental or neuronal survival cannot explain the decreased sensitivity to touch (Figure 10.4). We looked at the mechanosensitive properties of cultured DRG neurons from the TRPC3$^{-/-}$:TRPC6$^{-/-}$ mice compared to TRPC3$^{-/-}$, TRPC6$^{-/-}$ and wildtype mice (Figure 10.3). The large neurons had no differences in amplitude or threshold of the mechanically sensitive current. As discussed previously, TRPC3 and TRPC6 are not largely expressed in these large neurons so it is unsurprising that the knockout had no effect. However, the mechanically sensitive currents in the small neurons of the TRPC3$^{-/-}$:TRPC6$^{-/-}$ mice show differences which correspond with the behavioural data. The DRG neurons from TRPC3$^{-/-}$:TRPC6$^{-/-}$ mice had a larger proportion of non-responders, a 15% increase, and a comparable decrease of RA currents compared to TRPC3$^{-/-}$, TRPC6$^{-/-}$ and wildtype DRGs. The total number of mechanically sensitive neurons was the same for TRPC3$^{-/-}$, TRPC6$^{-/-}$ and wildtype DRGs but TRPC3$^{-/-}$ mice showed some change in kinetics. A decrease in the RA currents in TRPC3$^{-/-}$ appeared to have been compensated by an increase in IA currents.

The motor response to move the hind paw in reaction to the sensing of the von Frey hair is a spinal reflex. The decrease of neurons able to be activated by mechanical stimulation would decrease the input into the spinal cord so a larger mechanical stimulus is required to sense the von Frey hair and elicit a motor reflex response. There is no difference in touch threshold for the TRPC3$^{-/-}$ mice, therefore the compensation from IA mechanically activated currents appears sufficient to retain the normal amount of touch sensitivity.

Heteromultimerization has been shown not only in members of the same TRP subfamily but also between subfamily groups; for example TRPP2 has been shown to form multimers with TRPC1 or TRPV4 (Kottgen *et al.*, 2008;Kobori *et al.*, 2009). The large number of subunits that could participate in a TRP heterotetramer provides countless permutations of cation channels. The differing biophysical properties of these heterotetramers would confer a range of mechanically sensitive channels with different thresholds of activation. It would be expected that some element of redundancy and overlap may occur in this system to preserve the evolutionary important mechanical sensitivity that is vital for touch, hearing, kidney function and vasculature.

These results provide evidence that TRPC3 and TRPC6 play a role in mechanotransduction, but does not prove they are directly gated by mechanical stimuli. TRPC3 and TRPC6 could be activated indirectly via coupling to mechanosensitive GPCRs which release DAG, similar to how the angiotensin receptor activates TRPC6 in myocytes (Saleh *et al.*, 2006).

5.3.4 Thermal sensation is not dependent on TRPC3 or TRPC6

Thermosensation was tested using the Hargreaves' and hot plate apparatus (see page 115). TRPC3 conditional-null animals showed no deficit in heat sensation and neither TRPC3 nor TRPC6 have been shown to be thermosensitive *in vitro* hence this result was expected. Noxious cold sensation was tested using the cold plate as above. We did not expect to see any difference in cold sensation as neither TRPC3 conditional null animals showed any deficit and TRPC6 has also not been suggested to be cold sensitive either *in vivo* or *in vitro*.

The presence of normal nociceptive behaviour in response to heat and cold pain indicates the sensory pathways are intact, for thermosensation at least; this also proves TRPC3$^{-/-}$:TRPC6$^{-/-}$ animals have unimpaired motor reflex activity.

5.3.5 TRPC3 and TRPC6 are not involved in neuropathic pain

The mechanisms of neuropathic pain are not fully understood. It is known that the small Nav1.8 expressing neurons are not required (Abrahamsen *et al.*, 2008), this suggests that Aβ-fibres are important in neuropathic pain. TRPC3 and TRPC6 are mainly expressed in the small neurons, shown by immunohistochemistry (Elg *et al.*, 2007), and microarray analysis of

the DTA-Nav1.8 Cre mouse (Abrahamsen *et al.*, 2008). No differences in mechanical allodynia after nerve injury were found in the TRPC3$^{-/-}$:TRPC6$^{-/-}$ mice compared with control mice suggesting TRPC3 or TRPC6 are not involved. Electrophysiology of cultured DRG neurons from TRPC3$^{-/-}$:TRPC6$^{-/-}$ mice show that there is no effect on the large neurons which are important for mechanical allodynia (Figure 10.4d).

Test	Modality	TRPC3$^{-/-}$:TRPC6$^{-/-}$	TRPC3$^{-/-}$	TRPC6$^{-/-}$
Von Frey hairs	Light touch	**Attenuated**	No phenotype	No phenotype
Randall Selitto	Noxious pressure	No phenotype	No phenotype	No phenotype
Hot plate	Noxious thermal	No phenotype	No phenotype	No phenotype
Hargreaves	Noxous thermal	No phenotype	No phenotype	No phenotype
Cold plate	Noxious cold	No phenotype	No phenotype	No phenotype
Formain	Spontaneous acute pain behaviours	No phenotype	N/A	N/A
	Spontaneous inflammatory pain behaviours	**Attenuated**	**N/A**	**N/A**
Carrageenan	Mechanical hyperalgesia (inflammation)	**Attenuated**	**N/A**	**N/A**
CFA	Thermal (inflammation)	No phenotype	N/A	N/A
	Mechanical (inflammation)	No phenotype	N/A	N/A
Trunk Curl	Vestibular function	**Attenuated**	No phenotype	No phenotype
Swim test	Vestibular function	No phenotype	No phenotype	No phenotype
Click box	Hearing function	**Abolished**	No phenotype	No phenotype
Air righting	Vestibular function	No phenotype	No phenotype	No phenotype
SNL	Neuropathic pain	No phenotype	**N/A**	**N/A**

Table 5.2 Summary of phenotypes of TRPC3$^{-/-}$:TRPC6$^{-/-}$, TRPC3$^{-/-}$ and TRPC6$^{-/-}$ mice

6 Generation of TRPC4 targeting construct

6.1 Introduction

6.1.1 The TRPC4/5 subfamily

TRPC4 and TRPC5 share 65% sequence homology and are also closely related to TRPC1, and are therefore often placed in the same sub group (Ramsey *et al.*, 2006). TRPC4 and TRPC5 form ion channels that are mainly permeable to Ca^{2+} (Philipp *et al.*, 1996;Philipp *et al.*, 1998). Calcium signalling has been described in a variety of cells and has been attributed to basic and specific cell functions such as cell growth, differentiation and transmitter release.

TRPC4 is expressed throughout the CNS and is also found in a number of peripheral tissues including bone (Riccio *et al.*, 2002b). TRPC4 and TRPC5 have overlapping distribution within the CNS and are able to form heteromeric channels (Strubing *et al.*, 2003). TRPC1 is also able to form heteromeric channels with TRPC5 (Strubing *et al.*, 2001) although this interaction has not been shown for TRPC4.

The activation mechanism for the TRPC4/5 family remains controversial. The first characterization of TRPC4 channels reported that bovine TRPC4 can act as a store operated channel (SOC) when expressed in HEK cells, demonstrated by thapsigargin mediated store depletion (Philipp *et al.*, 1996) . A similar methodology was used to characterize mTRPC5 as a SOC (Philipp *et al.*, 1998). Adding to the evidence for TRPC4 and 5 as SOCs is the discovery that STIM1 is a sensor of intracellular calcium stores and interacts with a number of TRPC channels (Worley *et al.*, 2007). Although these studies suggest TRPC4 is vital for store operated calcium entry, in cell lines at least, it is not known whether TRPC4 is a channel forming subunit in this complex or an essential constituent. However, both TRPC4 and TRPC5 have also been proposed to be receptor activated channels activated through a PLC dependent mechanism (Schaefer *et al.*, 2000). The exact mechanism of this activation is not known, but unlike the TRPC3/6/7 family, neither TRPC4 or 5 can be activated by DAG (Schaefer *et al.*, 2000).

There are no specific blockers for the TRPC channels, which makes characterization difficult. Attempts to clarify activation mechanisms have used genetic manipulation of TRPC genes. TRPC4$^{-/-}$ mice have almost completely attenuated store-operated calcium currents in endothelial cells (Freichel *et al.*, 2001) , and in addition, antisense knockdown of TRPC4 reduces store operated currents in adrenal cells (Philipp *et al.*, 2000).

6.1.2 TRPC4 in sensory neurons

TRPC4 is important for endothelial permeability, which studies in TRPC4 knockout mice have shown, requires TRPC4 dependent intracellular Ca^{2+} signalling (Tiruppathi *et al.*, 2002), but its function in other tissues is not known. TRPC4 is found in peripheral afferent fibres, both peripherin positive and peripherin negative, indicating that TRPC4 is found within nociceptors and non-nociceptors within the DRG (Buniel *et al.*, 2003).

In neuronal cells both TRPC4 and TRPC5 appear to have a role in growth. A recent report showed TRPC4 mRNA and protein was significantly increased following nerve injury and is present in neurite growth cones (Wu *et al.*, 2007) . Inhibiting TRPC4 with shRNA prevents neurite outgrowth, which can be reversed by over-expressing hTRPC4 (Wu *et al.*, 2007). As TRPC4 and TRPC5 are closely related and able to form heteromeric channels, the function of TRPC5 may also give insight into the function of TRPC4. Greka et al. showed that TRPC5 generates instructive intracellular Ca^{2+} signals in growth cones which control neurite length and growth cone morphology (Greka *et al.*, 2003). TRPC5 is also upregulated in growth cones that are under the control of BDNF, with a rapid increase of membrane insertion (Bezzerides *et al.*, 2004).

Many other TRP channels have sensory functions, and TRPC channels are implicated in a number of sensory functions including chemosensing in the carotid body (Buniel *et al.*, 2003) and blood pressure regulation (Sharif-Naeini, 2008). TRPC4 is expressed in sensory neurons, including small diameter nociceptors, where it possibly plays a role in nociception. As there are no specific blockers or activators of TRPC4, a conditional knock-out mouse is the ideal way to investigate the properties of TRPC4 in sensory neurons.

6.1.3 Strategy for generation of conditional TRPC4 knock-out mice

A TRPC4$^{-/-}$ mouse was produced by Friechel et al in 2001 in order to investigate the role of TRPC4 in the endothelium (Freichel *et al.*, 2001). The TRPC4$^{-/-}$ mice were found to be essential for store-operated and agonist-activated Ca^{2+} entry in endothelial cells (Freichel *et al.*, 2001;Tiruppathi *et al.*, 2002). Additionally, in TRPC4$^{-/-}$ mice the 5-HT-induced increase in GABA release from thalamic interneurons is largely reduced (Munsch *et al.*, 2003). TRPC4 could therefore be contributing to the state-dependent processing of visual information in the thalamic network. The role of TRPC4 within sensory neurons has not been investigated, and since TRPC4 is expressed in a variety of tissues within the central nervous system including the olfactory bulb, septal nuclei, hippocampus, cortex and cerebellum, then the global knockout could have a number of central nervous system defects that would complicate any conclusions from *in vivo* behavioural tests. For this reason we chose to generate a floxed TRPC4 mouse which could then be crossed with a number of neuronal Cre lines for further analysis to enable tissue specific gene deletion. Use of the Cre/*lox*P system also minimises the potential problems that global deletion poses such as reduced fitness.

We chose to flank exon 4 with *loxP* sites as this will produce a frameshift upon deletion and lead to a truncated protein. The targeting construct was designed to contain positive and negative selection markers and two arms of homology, each approximately 5kbp in length. The targeting construct was obtained by polymerase chain reaction, or PCR, of BAC clones from a 129sv database and genomic DNA. The strategy of subcloning steps is shown in full in Figure 6.1.
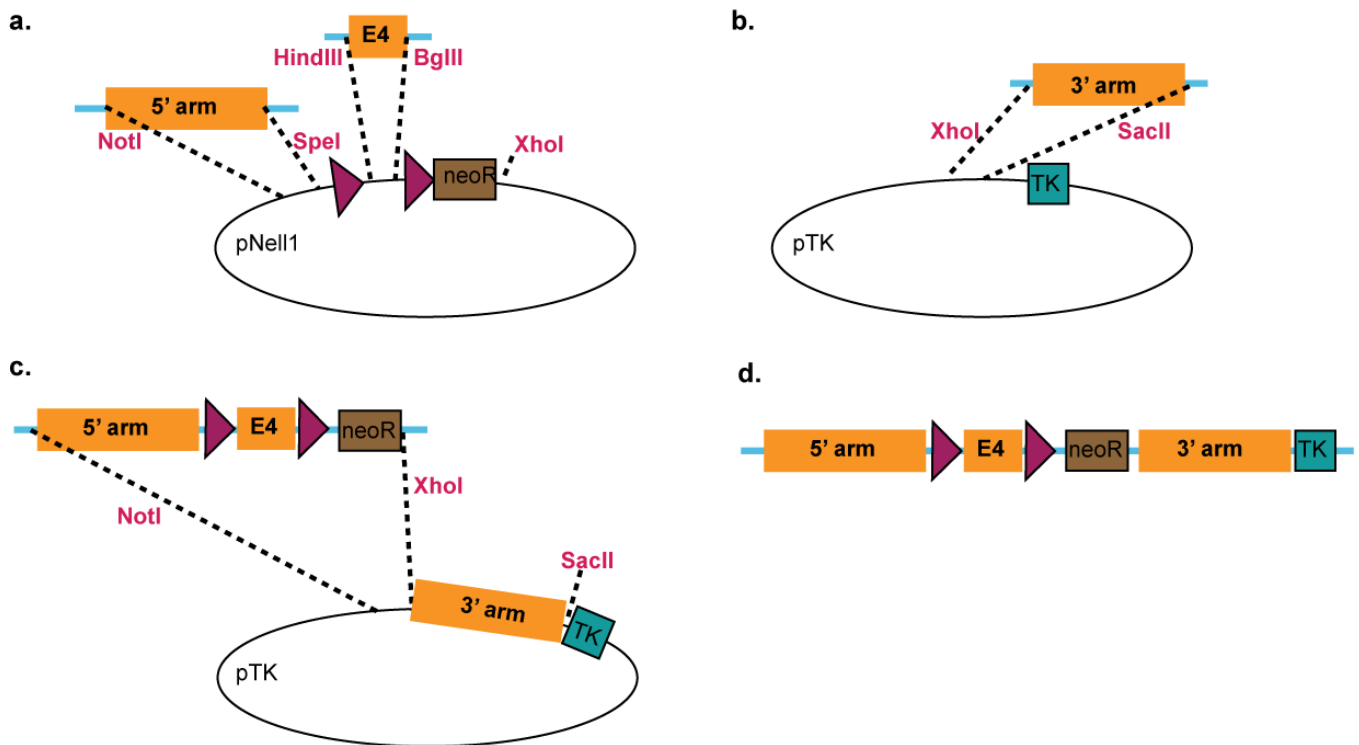
Figure 6.1 Subcloning strategy for generation of targeting construct for TRPC4 gene.
a. The 5'arm and exon 4 will be obtained using PCR and ligated into vectors and sequenced before insertion into a pre-existing construct (pNell1) containing the *loxP* sites and a cassette conferring neomycin resistance. **b.** The 3' arm will also be obtained using PCR and sequenced before insertion into a vector (pTK) containing the thymidine kinase gene. **c.** Finally the 5'-loxP-E4-loxP-neoR fragment will be inserted into the TK vector to obtain the final 17.kb construct (**d**). Red triangles denote loxP sites in same orientation

6.2 Results

6.2.1 PCR amplification of homologous fragments

The homologous portions of the construct were obtained by PCR of the appropriate BAC clones or genomic DNA. The 3' arm was obtained from BMQ 429J2 using the extended long template kit. The PCR primers used were:

XhoI 11165   GTTCTCGAGGTTAACTTCAAAACTGAGAGGAGTC
SacII 16056AS   TAACCGCGGCTGAGTAGAGTGTCTGGAA

The 4.9kb PCR product was visualised with ethidium bromide on an agarose gel and purified using the QIAgen gel extraction kit.

Exon 4 was obtained from genomic 129 strain DNA using the high fidelity PCR kit. The PCR primers used were:

TrpC4-H/K9357   AGCAAGCTTGGTACCGGGCATTTTCTAAATTGCTAATTTAG
TC4-BglII-11165AS   CCCAAGCAGATCTCCTGAGATTAGG

The 1.8kb PCR product was visualized with ethidium bromide on an agarose gel and purified using the QIAgen gel extraction kit.

The 5' arm was obtained from genomic 129 strain DNA using the high fidelity PCR kit. The PCR primers used were:

TC4-NotI-4338   ATCGCGGCCGCCATCATGTGCTGTCA
TC4-SpeI-9360AS   CCCACTAGTGCCCAACAGACATTCCCA

The 5.0kb PCR product was visualized with ethidium bromide on an agarose gel and purified using the QIAgen gel extraction kit.

All of the PCR fragments were transformed into empty vectors to allow amplification of the product and sequencing to ensure the sequence was correct. The vectors used were floxed, pNell1 and pTK.

6.2.2 Ligation into vectors containing positive and negative selection markers

The vector containing exon 4 flanked with *loxp* sites (flE4) and the vector containing the positive selection marker, neo resistance, (pNellI) were digested with BglII and HindIII . The restriction digest products were run on an agarose gel and the appropriate fragments excised and purified as before. The pNell1 vector was treated with SAP before ligation with flE4 and transformation into TSS cells. DNA was extracted from the colonies using the QIAgen miniprep kit and double digested with HindIII and BglII to confirm correct insertion of E4 (Figure 6.2).
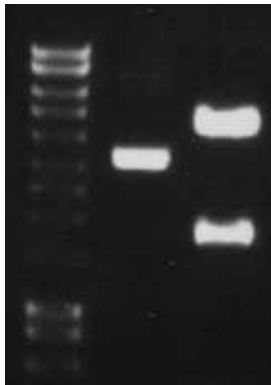
Figure 6.2 Restriction enzyme analysis of E4-pNel1 ligation
Double digestion with HindIII and BglII confirms correct insertion of exon 4 into pNel1 vector. 1.8kb band is floxed exon 4, 6.2kb band is pNel1. Digestion of the empty vector would give just one band at approximately 6.2kb.

The vector containing the 5'arm and pNell1-E4 were digested with NotI and SpeI and the appropriate fragments excised and purified as before. pNell1 was treated with SAP before ligation with the 5' arm and transformation into TSS cells. DNA was extracted from the colonies as before and singly digested with BamHI and HindIII to confirm correct insertion of the 5' arm (Figure 6.3).
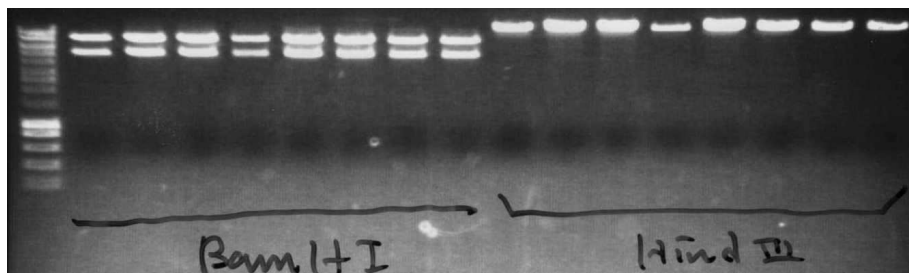
Figure 6.3 Restriction enzyme analysis of 5'-E4-pNel1- ligation

Digestion with BamHI or HindIII confirms correct insertion of 5' arm into E4-pNel1 construct.

The purified 3' arm fragment and the vector containing the negative selection cassette, thymidine kinase, (pTK) were double digested with XhoI and SacII and the appropriate fragments excised and purified as before. pTK was treated with SAP before ligation with the 3' arm and transformation into TOP10 cells. DNA was extracted from the colonies as before and double digested with BamHI and XhoI to confirm correct insertion of the 3' arm (Figure 6.4).
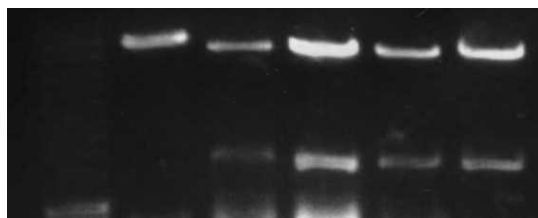
Figure 6.4 Restriction enzyme analysis of 3'-pTK ligation

Double digestion with BamHI and XhoI confirms correct insertion of 3' arm into pTK vector.

The 3'-pTK construct and the 5'-E4-pNel1 construct were both double digested with XhoI and NotI and the appropriate fragments excised and purified as before. The 3'-pTK construct was treated with SAP before ligation with 5'-E4-neo construct and transformation into TOP10 cells. DNA was extracted from the colonies as before digestion with a number of restriction enzymes confirmed correct insertion of the 5'-E4-neo construct (Figure 6.5)

138
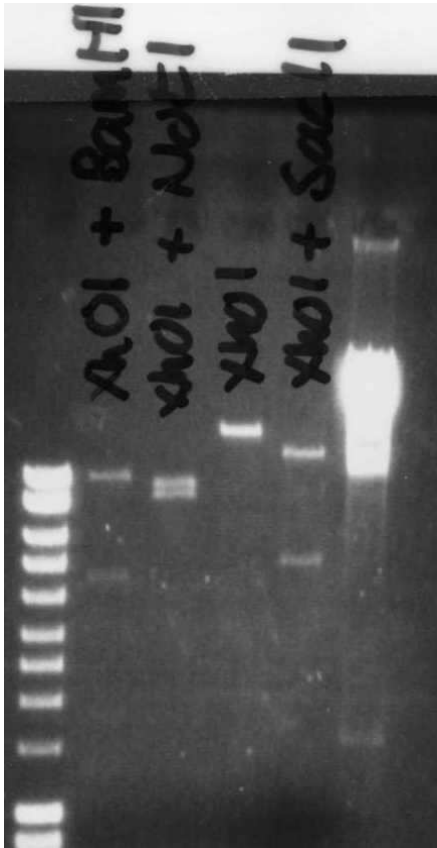
Figure 6.5 Restriction enzyme analysis of the final construct, 5'-E4-neo-3'-TK.

6.2.3 Confirmation of correct sequence

Sequencing primers were designed approximately every 500bp and sequenced using the BigDye kit at either the UCL sequencing facility or WIBR sequencing service. The sequences were compared to genomic 129 strain sequence of TRPC4 obtained from the Ensembl database using BLAST2seq (NCBI).

6.2.4 Embryonic stem cell transfection

The final construct was linearized with NotI and electroporated into 129 derived embryonic stem cells, ES cells, by Monica Mendelsohn at Columbia University, NYC. ES cells were selected for neomycin resistance and gangcylovir insensitivity and DNA extracted for Southern hybridization screening.

6.2.5 Screening for positive ES cells using Southern hybridization

ES cell DNA was screened for targeted insertion of the flTRPC4 construct by Southern hybridization. 168 samples were singly digested with KpNI or BSTXI and run on a 0.8% agarose gel. The digested DNA was transferred to a nitrous cellulose membrane and hybridised to an external probe specific to either the 3' or 5' region which had been radiolabelled with p32αATP. The strategy for the Southern hybridization screening is outlined in Figure 6.6.
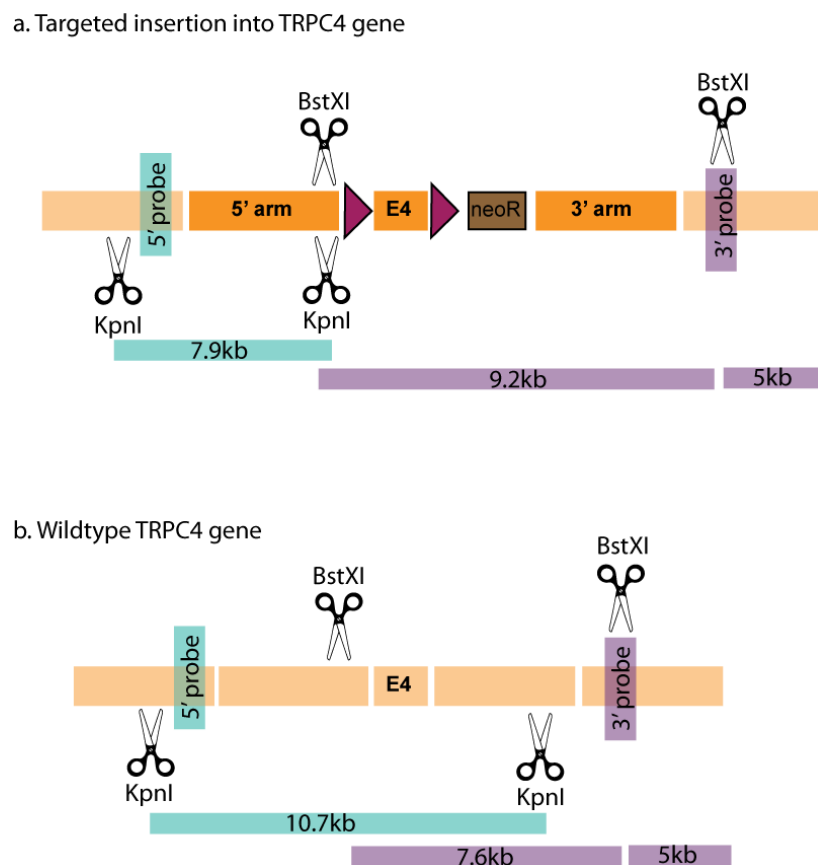
Figure 6.6 Strategy for Southern hybridization screening.

Location of probe binding and restriction enzyme sites in the targeted and wildtype TRPC4 gene.

a. Targeted insertion produces a 7.9kb band with KpnI digestion and 5' probe, and two bands at 9.2kb and 5kb with BstXI digestion and 3' probe. **b.** The wildytpe gene produces a 10.7kb band with KpnI digestion and 5' probe, and two bands at 7.6kb and 5kb with BstXI digestion and 3' probe

The screen for the 5' end of the targeting construct found one ES cell positive for correct insertion. This sample shows two bands, one at 10.7kb and one at 7.9kb (Figure 6.7) indicating one copy of the wildtype TRPC4 gene and one copy of the flTRPC4 targeted gene.

The screen for the 3' end of the targeting construct found no ES cells positive for correct insertion. All of the samples showed two bands at 7.6kb and 5kb indicating copies of the wildtype TRPC4 gene only (Figure 6.8).

The membranes were stripped and hybridized with an internal probe specific for the neo resistance cassette. All of the samples showed a positive band for neo but the size of the fragment was extremely variable (Figure 6.9).

None of the 168 clones were positive for the targeted insertion of the flTRPC4 construct
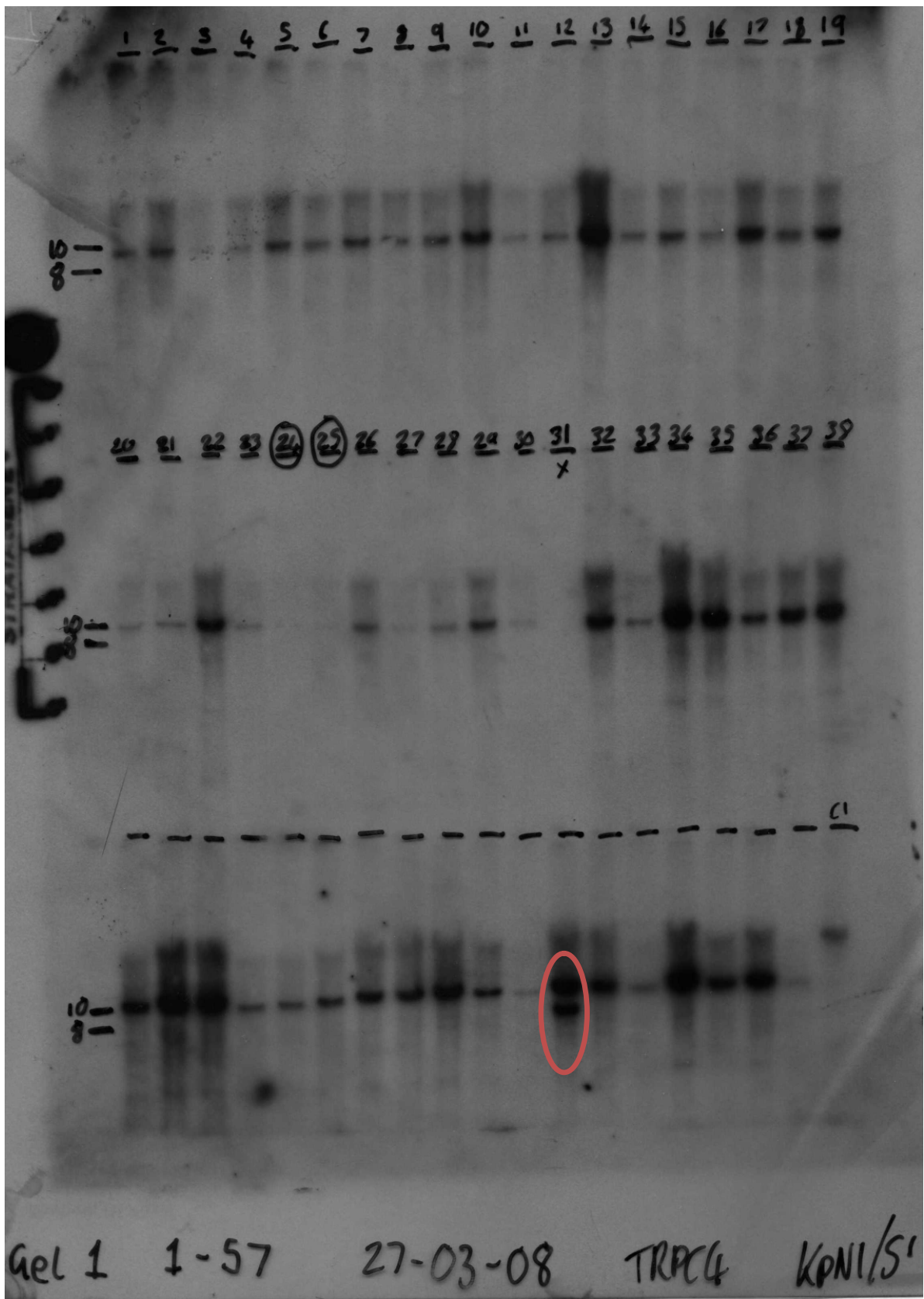
Figure 6.7 Southern hybridization analysis using 5' probe and digestion with KpnI

The single recombinant found is indicated by a red circle.
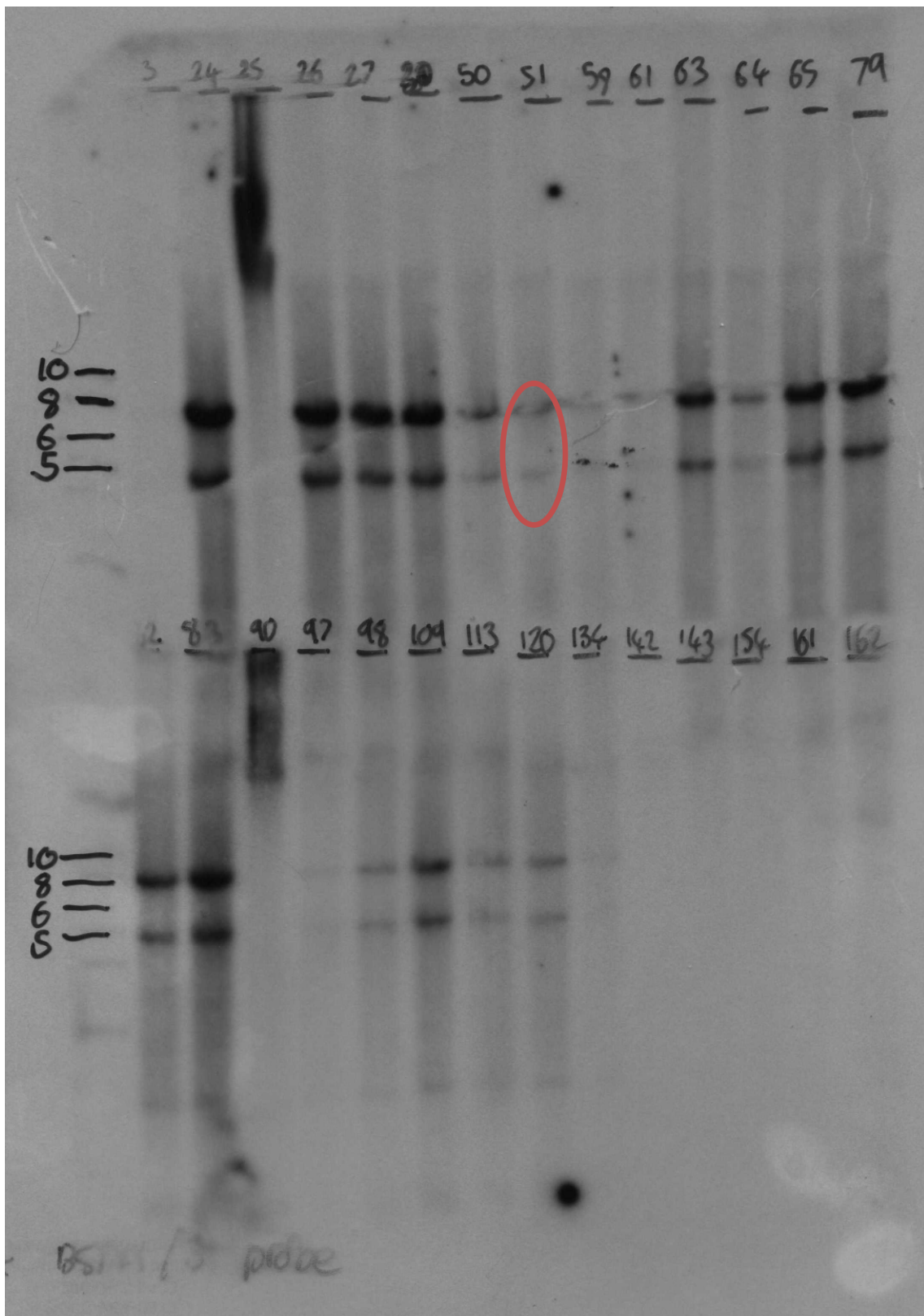
Figure 6.8 Southern hybridization analysis using 3' probe and digestion with BstXI

The clone positive at the 5' arm is indicated by a red circle, and is negative for recombination at the 3' arm.

143
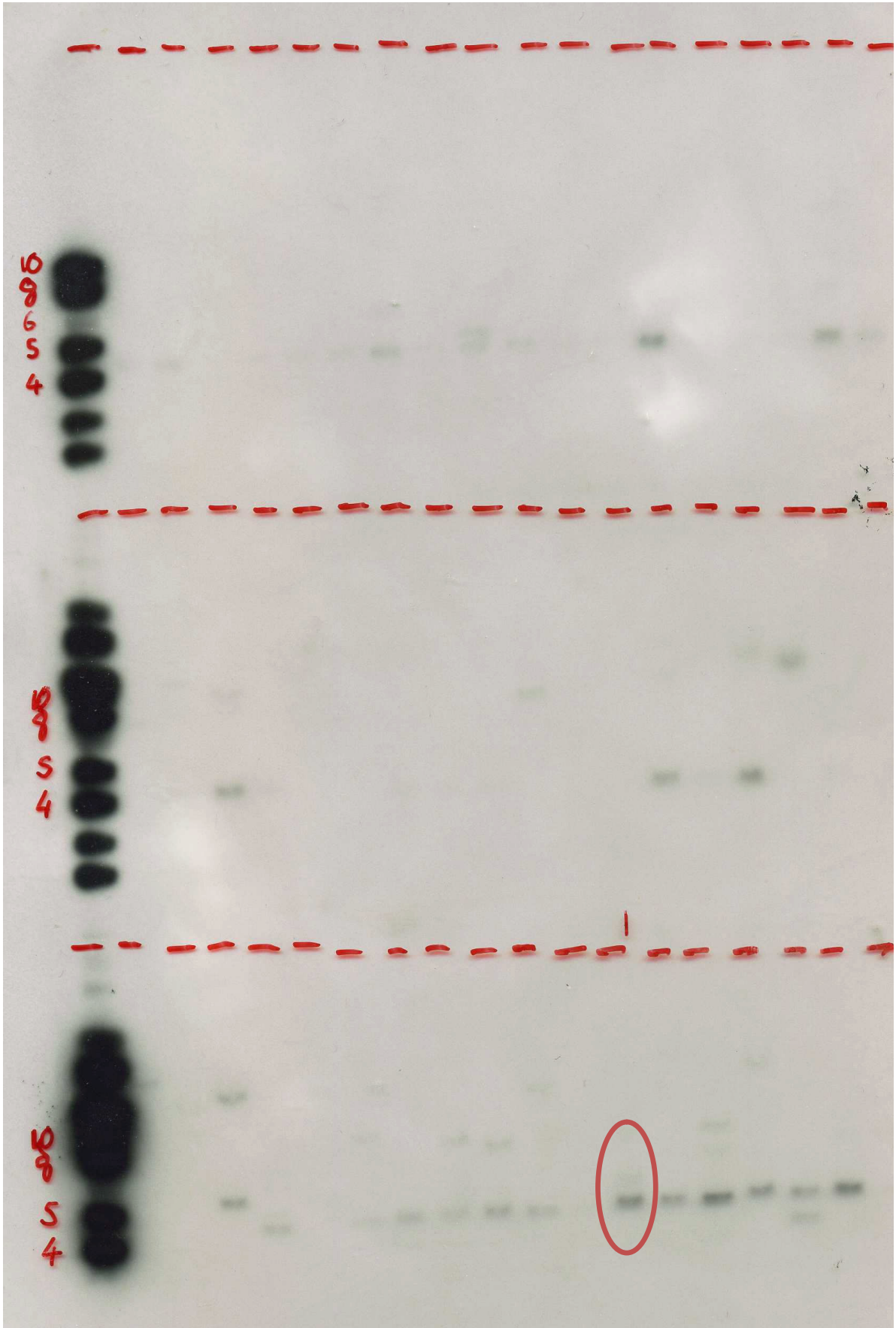
Figure 6.9 Southern hybridization analysis using Neo probe and digestion with BstXI

144

6.3 Discussion

6.3.1 Cloning of the targeting construct was successful

The targeting construct was cloned in 3 separate steps using 129 strain DNA from either genomic or BAC sources. In order to obtain the greatest degree of homology we initially used genomic DNA extracted from the same ES cell line which would be used for transfection. It was possible to amplify the 5' arm and exon 4 from the genomic DNA, however PCR of the 3' arm proved problematic. PCR of large fragments from genomic DNA can be difficult due to variable quality and complexity. However, PCR from Bacterial Artificial Chromosomes, BACs, is generally easier than from genomic DNA and enables a higher concentration of amplification fragments to be generated. BACs are plasmids which are modified to contain a large segment of exogenous DNA which can be transformed into bacteria allowing the DNA fragment to be amplified. The BAC library used was from an end-sequenced 129 strain which has previously been shown to produce targeting vectors with up to 35% targeting efficiency in 129 derived ES cells (Adams *et al.*, 2005). PCR amplification of the 3' arm from BAC BMQ429J2 was successful.

6.3.2 Southern hybridization screening was capable of identifying targeted and wildtype events.

The Southern hybridization produced specific bands at the appropriate size for each probe with no background or nonspecific binding, proving that the screening method was capable of detecting recombinants.

6.3.3 Embryonic stem cells did not undergo targeted homologous recombination.

The Southern screening found that no ES cells had the correct targeted insertion of the construct. One ES cell appeared to have the 5' end of the construct inserted, but this cell did not have a positive result at the 3' end. This result could be due to partial insertion of the construct, with the second crossover occurring before the 3' arm of homology or random

insertion of the entire construct, including the TK cassette. There are a number of reasons that could have prevented the targeted insertion:

1.   DNA is mutated and not isogenic

Homologous recombination within mammalian cells is rare, occurring in approximately 1 in 10^6 cells (Reid *et al.*, 1991). Studies of the mechanism of homologous recombination have identified several factors that affect the frequency of homologous recombination. The extent of homology between the targeting vector and target locus is extremely important with isogenic (identical) sequences giving maximum targeting efficiency. For this reason we chose to make the targeting construct from 129 genomic DNA and a library of BAC clones derived from 129sv mice (Adams *et al.*, 2005). 129sv mice are commonly used for embryonic stem cell transfection as they are more reliable at colonizing germline cells in chimeric animals. The targeting construct was periodically sequenced to screen for spontaneous mutations and compared to the most up to date 129sv genomic sequence. Non-isogenic targeting has previously been shown to reduce homologous recombination 15-fold with only 2% divergence between targeting vector and targeting locus sequences (Zhou *et al.*, 2001). A small mistake in the sequence database, or the sequencing data from the targeting vector, would have greatly reduced the number of homologous recombination events. The construct was resequenced after the failed transfection and no errors were found in the sequence, therefore non-isogenic sequences were not the cause of the low frequency of homologous recombination.

2.   Homologous recombination occurred in the short floxed arm

Homologous recombination can occur between any isogenic sequences. The correct targeting event would require two crossovers, one within the 3' arm of homology and one within the 5' arm of homology. The targeting construct we designed contained a third, much smaller, area of homology between the *loxP* sites. Thomas and Capecchi originally showed an increase in targeting rate with an increase in targeting arm size (Thomas and Capecchi, 1987) but a study targeting the β-globin locus found the size of the targeting arm made no difference (Lu *et al.*, 2003). Therefore, although the region of homology within the floxed region is small a

crossover could theoretically take place and prevent full insertion of the targeting vector. If homologous recombination had occurred in the floxed region the band identified by digestion with KpnI and 5' probe would be 7.9kb as expected for a targeted insertion as the additional KpnI site will have been inserted at the end of the 5' arm. However, the largest band identified with the 3' probe and digestion with BstXI would have been approximately 7.6kb, as expected for a wildtype gene, since the large 9.2kb band observed with targeted insertion arises from the addition of the Neo cassette and two *loxP* sites between the two endogenous BSTXI sites. A crossover in the floxed region would lead to the addition of just one *loxP* site which would not lead to a considerable size difference in the digested fragment.

3.   **TRPC4 has a lower than average recombination frequency**

The efficiency of targeted insertion of a vector varies at different chromosomal loci (Hasty *et al.*, 1994). Changes in chromatin structure along the length of a chromosome can affect DNA accessibility leading to recombination "hot spots" and "cold spots" (Petes, 2001). If the TRPC4 gene is within a "cold" spot for recombination this would reduce the chances of chiasmata forming and reduce the probability of homologous recombination between the targeting vector and the targeted locus.

6.3.4 Future work

A low homologous recombination frequency would require a large number of ES cells to be screened in order to find a positive targeted event. We screened just 168 ES cell clones which should be increased to improve our chances of finding a correct recombinant.

7 Summary

The work presented in the thesis demonstrates the importance of TRPC channels in sensory systems. The Cre/*lox*P system was used to delete TRPC3 exclusively from sensory neurons in the mouse, allowing the investigation of TRPC3 function without confounding effects from deletion in other tissues. This mouse line displayed deficits in inflammatory pain, which could be due to dysregulated inflammatory signalling cascades in the TRPC3 conditional null animals revealed with microarray analysis.

A global deletion of TRPC3 together with TRPC6 exposed further sensory functions of TRPC channels. This mouse line displayed deficits in touch sensation and hearing, implicating TRPC3 and TRPC6 in mechanical sensation. The reduced mechanical sensitivity was found to be due to a reduction in mechanically sensitive DRG neurons, particularly the subpopulation characterised by small diameter and rapidly adapting currents. The hearing deficit was localised to the high frequency ranges between 32-40kHz as assessed by auditory brainstem responses. This evidence alludes to a range of mechanically sensitive channels, including TRPC3 and TRPC6, which may form heteromers with different activation thresholds and properties dependent not only on subunit identity but also modulatory proteins. Direct recordings from hair cells and sensory neurons could help to determine if TRPC3 and TRPC6 are themselves mechanically gated or if they are indirectly activated by other molecules such as GPCRs.

The generation of a floxed TRPC4 construct would allow us to look at the functions of TRPC4 limited to certain tissues of interest, in light of the functions of TRPC3 and TRPC6 this may include sensory neurons and also the outer hair cells.

8 Appendix A

8.1 Additional results for Chapter 3 : Generation and phenotyping of TRPC3 Knockout mice

8.1.1 Confirmation of tissue-specific knockout

The confirmation of tissue-specific knockout was performed by Dr Jing Zhao.

The knockout of TRPC3 was confirmed with PCR using primers that flank exon 7. This enabled identification of a floxed exon 7 as an increase of 100bp of the PCR product and also the identification of a deleted exon 7 which would produce a smaller PCR product of 300bp.
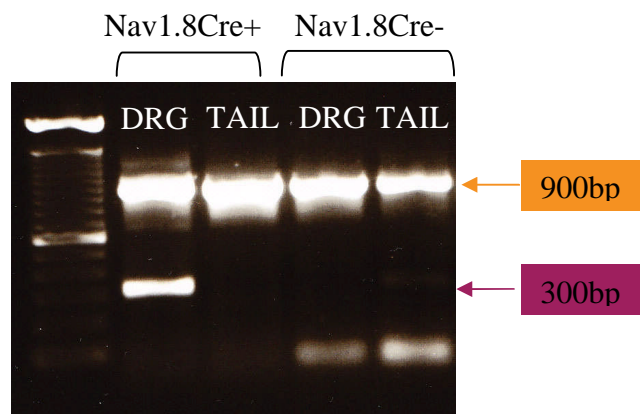
Figure 8.1 Confirmation of tissue specific knockout of TRPC3 in DRG neurons.
PCR of tail and DRG DNA from a Nav1.8Cre+ and Nav1.8Cre- mouse using primers TRPC3F2 and TRPC3R. Floxed TRPC3; 900bp, KO TRPC3; 300bp.

Tissue was collected from the tail and DRG of TRPC3fl/fl mice and TRPC3fl/fl:Nav1.8Cre mice and the DNA extracted. PCRs using primers TRPC3F2 x TRPC3R were performed and the results shown in Figure 8.1.

8.1.2 TRPC3fl/fl:Nav1.8Cre mice show no deficits in motor coordination

The rotarod test was performed by Dr Cruz Miguel Cendan

Motor coordination was judged using an accelerating rotarod. There was no difference in the motor ability of the TRPC3fl/fl:Nav1.8Cre mice compared with control animals (Figure 8.2). TRPC3fl/fl:Nav1.8Cre mice were able to carry out normal motor responses such as paw withdrawal, flinching and shaking in response to the stimuli presented in the other behavioural tests. Results, expressed as mean time spent on accelerating rotarod ±SEM, were as follows: TRPC3fl/fl:Nav1.8Cre mice, 218±16 seconds, control animals, 222±16 seconds.
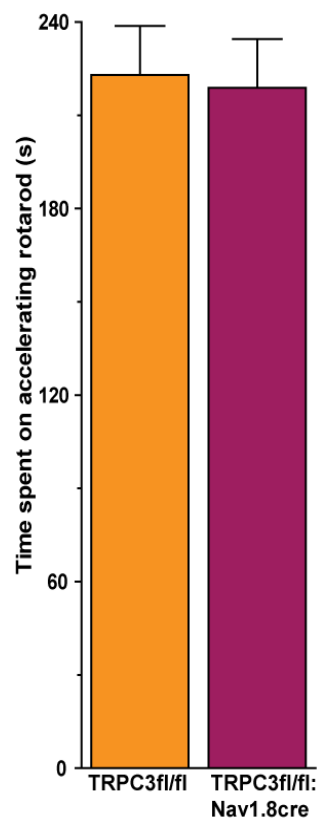
Figure 8.2 Motor coordination of TRPC3fl/fl:Nav1.8Cre and control (TRPC3fl/fl) animals.

There was no difference in motor coordination between TRPC3fl/fl littermate control (orange, n=14) and TRPC3fl/fl:Nav1.8Cre (red, n=13) animals. All results shown as mean ±SEM.

8.1.3 TRPC3fl/fl:Nav1.8Cre mice do not show behavioural deficits in mechanosensation

The Randall Selitto test was performed by Dr Cruz Miguel Cendan

Behavioural responses to mechanical stimulus were measured using von Frey hairs and the Randall Selitto test. No difference in the 50% withdrawal threshold to von Frey hairs was observed between TRPC3fl/fl:Nav1.8Cre, 0.45±0.05g, and control animals, 0.47±0.07g (Figure 8.3a). The Randall Selitto test showed there was also no difference in behavioural responses to noxious blunt stimulation of the tail between TRPC3fl/fl:Nav1.8Cre mice and control animals (Figure 8.3b). Results expressed as mean threshold±SEM are as follows, TRPC3fl/fl:Nav1.8Cre mice, 258±37g, control mice, 287±39g.
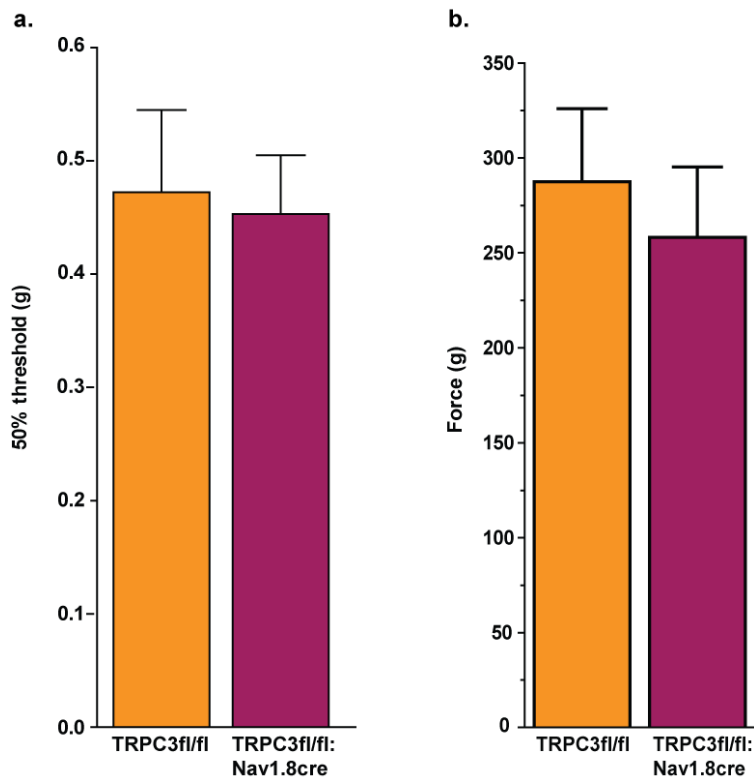
Figure 8.3 Acute mechanical sensation in TRPC3fl/fl:Nav1.8Cre and control (TRPC3fl/fl) animals
a. Response to mechanical stimulation with von Frey hairs was not significantly different between TRPC3fl/fl littermate control (orange, n=5) and TRPC3fl/fl:Nav1.8Cre (red, n=5) animals. **b.** Response to blunt mechanical stimulation of the tail in the Randal Selitto test was not significantly different between floxed TRPC3 littermate control (orange, n=14) and TRPC3fl/fl:Nav1.8Cre (red, n=14) animals. All results shown as mean ±SEM.

8.1.4 TRPC3fl/fl:Nav1.8Cre mice do not show behavioural deficits in noxious thermosensation

The Hargreaves' and hot plate tests were performed by Dr Cruz Miguel Cendan

Behavioural responses to noxious thermal stimuli were measured using the Hargreaves' apparatus and the hot plate test. Paw withdrawal latency in Hargreaves' test was not altered in the TRPC3fl/fl:Nav1.8Cre mice compared to control animals (Figure 8.4a). Results expressed as mean latency±SEM are as follows, TRPC3fl/fl:Nav1.8Cre mice 10±0.6 seconds, control mice 11.1±0.6 seconds. There was also no difference in latency of behavioural responses on the hot plate at either 50ºC, TRPC3fl/fl:Nav1.8Cre mice responding on average in 50±2.7seconds compared to 48±4 seconds for control mice, or 55ºC, TRPC3fl/fl:Nav1.8Cre mice responding on average in 25±1.2 seconds and control mice in 24±1.6 seconds (Figure 8.4b).
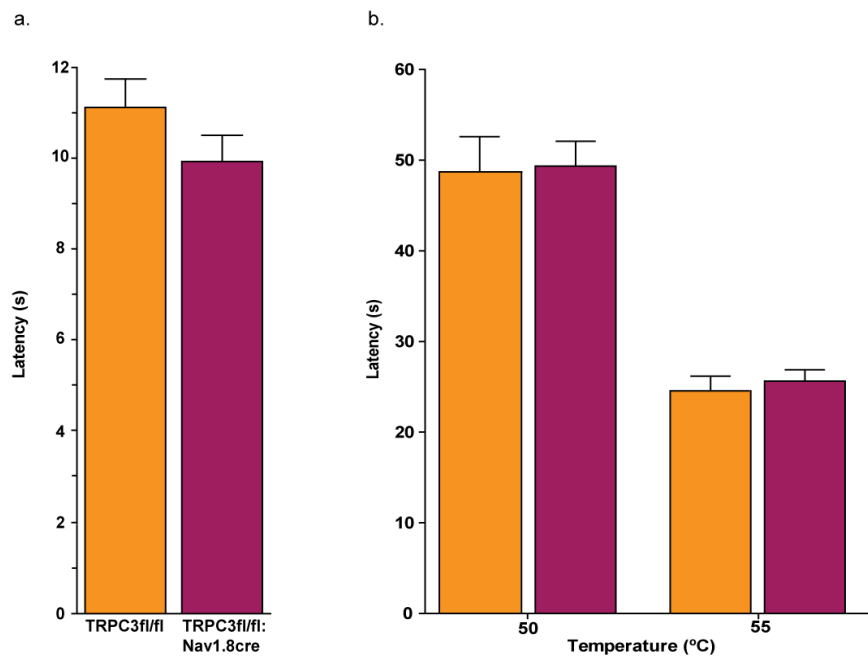
Figure 8.4 Acute thermal pain behaviour in TRPC3fl/fl:Nav1.8Cre and control (TRPC3fl/fl) animals.
a. Noxious thermal stimulation using Hargreaves' apparatus. No significant difference was observed between littermate control (orange, n=14) and TRPC3fl/fl:Nav1.8Cre (red, n=14) animals. **b.** Response to noxious thermal stimulation using the hot plate test was not significantly different between littermate control (orange, n=14) and TRPC3fl/fl:Nav1.8Cre (red, n=14) animals at either 50ºC or 55ºC. All results shown as mean ±SEM.

8.1.5 TRPC3fl/fl:Nav1.8Cre mice display reduced inflammatory pain behaviour

8.1.5.1　　　Formalin test

The formalin test was performed by Dr Cruz Miguel Cendan

Behavioural responses from 11 TRPC3fl/fl:Nav1.8Cre mice and 11 control mice in the two distinct phases were recorded. In the first phase, 0-10 minutes, the TRPC3fl/fl:Nav1.8Cre mice displayed 62±6 seconds of pain behaviour compared with 72±5 seconds for the control mice. There was no significant difference between the two groups. In contrast the TRPC3fl/fl:Nav1.8Cre mice showed attenuated pain behaviours in the second phase, from 10-60 minutes, displaying just 56.5±17 seconds compared with 124±25 seconds for the control mice. This was shown to be significant using an unpaired 2-tailed t-test ($p = 0.0423$).

Figure 8.5b shows the time course of the formalin response and demonstrates that the TRPC3fl/fl:Nav1.8Cre mice displayed reduced pain behaviours at each 5 minute interval within the second, inflammatory, phase although a significant difference was found only at 15-20 minutes ($p < 0.001$).
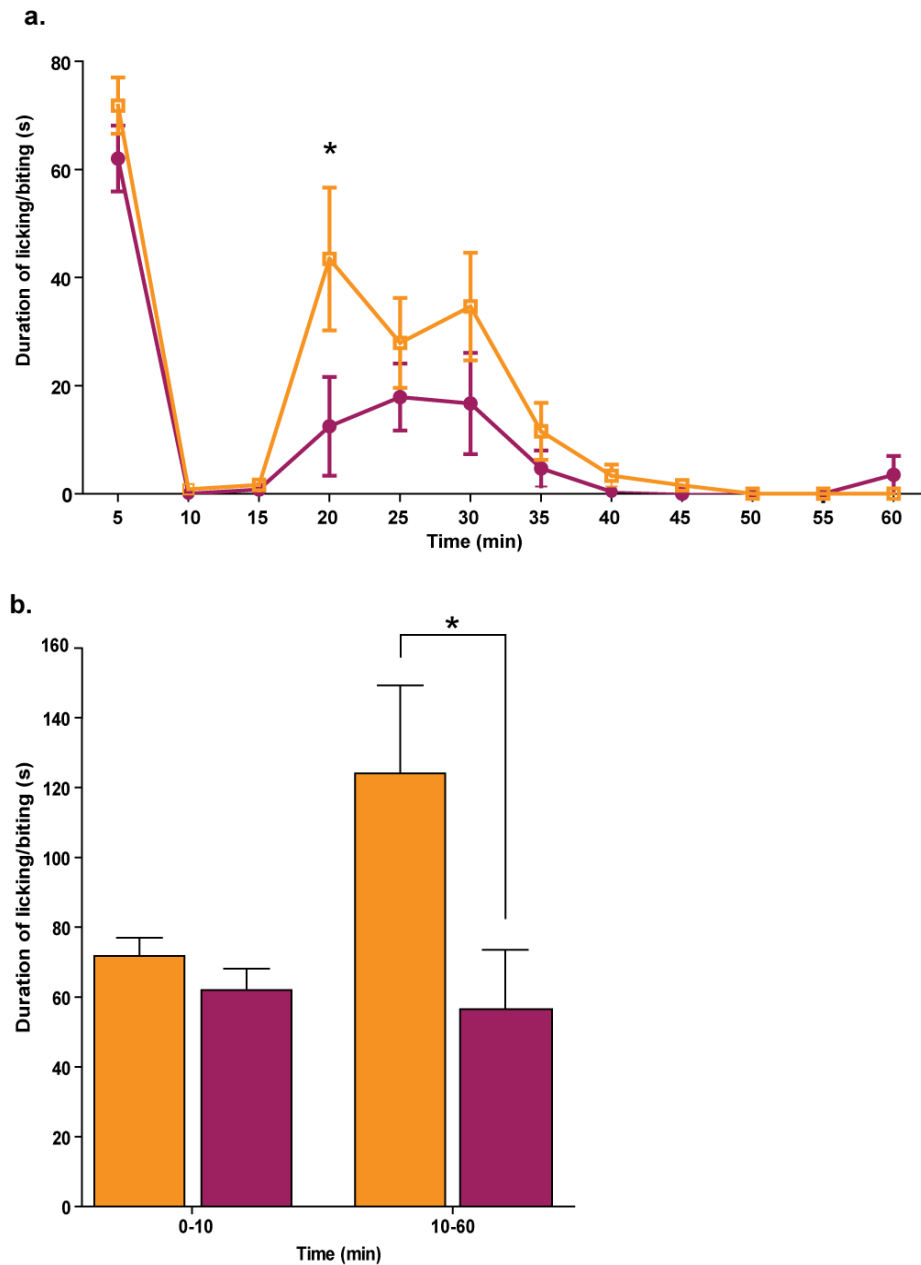
Figure 8.5 Formalin-induced inflammatory pain behaviour in TRPC3fl/fl:Nav1.8Cre and control (TRPC3fl/fl) animals.

Behaviour following injection of 20µl of 5% formalin. **a.** Time spent licking/flinching/biting the hind paw was recorded in 5 minute sections. No significant reduction in pain behaviours was seen in Phase I (0-10 minutes) however in Phase II (10-60 minutes) TRPC3fl/fl:Nav1.8Cre mice (red, n=11) have significantly attenuated pain behaviours compared to littermate controls (orange, n=11). b. Time course of the formalin test. A traditional biphasic response was observed with the attenuated pain behaviour of TRPC3fl/fl:Nav1.8Cre mice apparent in the second phase. All results shown as mean ±SEM.

9 Appendix B

9.1 Additional methods for Chapter 4 : Effects of nociceptor TRPC3 deletion on gene expression

9.1.1 Methods for Microarray

The preparation of the samples and initial microarray data analysis was performed by Priya Banerjee and Simone Sharma.

The DRGs from three TRPC3fl/fl:Nav1.8Cre and three TRPC3fl/fl (control) mice were excised and the RNA was extracted as described above. The samples were kept separate to ensure three biological replicates for each genotype. RNA concentration and quality was checked using Nanodrop and Agilent Bioanalyser.

NuGen 3' Applause kit with Encore Biotin Module was used for first and second strand cDNA synthesis and labeling.

9.1.1.1 First strand synthesis

To each RNA sample of 200ng, 2ul of Buffer A1 (containing a chimeric DNA/RNA chimeric primer) was added and incubated at 65⁰C for 5 minutes. 3ul of First Strand Master Mix, containing a reverse transcriptase, was added and the First Strand Synthesis programme was run for, 4⁰C for 1 minute, 48⁰C for 60 seconds, 70⁰C for 15 seconds, cool to 4⁰C.

9.1.1.2 Second strand synthesis

10ul of Second Strand Master Mix, containing DNA polymerase and DNA primers, was added to each First Strand reaction tube and the Second Strand Synthesis programme run, 4⁰C for 1 minute, 25⁰C for 10 minutes, 50⁰C for 30 minutes, 70⁰C for 5 minutes, cool to 4⁰C.

9.1.1.3 Single Primer Isothermal Amplification (SPIA)

5ul of SPIA buffer, DNA polymerase, RNase H and SPIA DNA/RNA chimeric primers master mix were added to each Second Strand reaction and run on the following program, 47⁰C for 90 minutes, 95⁰C for 5 minutes, cool to 4⁰C. The RNase degrades the DNA/RNA

heteroduplex at the end of the cDNA strand which allows the hybridization of a second SPIA DNA/RNA chimeric primer. DNA polymerase initiates synthesis at the 3' end of the primer, displacing the existing strand and the RNA portion at the 5' end is again removed by RNase. This results in rapid accumulation of cDNA with a sequence complementary to the original mRNA.

SPIA cDNA was purified using QIAGEN's MinElute Reaction Cleanup Kit. Adding 300ul of high-salt, binding buffer was added and the sample was applied to the MinElute spin column where DNA adsorbs to the silica membrane. Flow-through was discarded and the column washed with buffer PE to remove impurities before eluting with nuclease-free water.

9.1.1.4 Biotin Labelling

7ul of Fragmentation Master Mix (containing fragmentation enzyme and buffer) was added to 25ul of SPIA cDNA and placed into a thermal cycler running the following programme, 37°C for 30 minutes, 95°C for 2 minutes, cool to 4°C.

1.5ul Biotin Reagent, 1.5ul Labeling enzyme and 15ul Labeling buffer were added to each fragmented cDNA sample and the following programme run, 37°C for 60 minutes, 70°C for 10 minutes, cool to 4°C.

Sample preparation and the microarray scanning was performed at UCL Genomics centre.

9.1.1.5 Microarray data analysis

Initial microarray data analysis was performed by UCL Genomics which included cluster analysis to check the biological replicates were similar and ANOVA analysis to determine which genes were significantly up or down regulated in the knockout animals. Partek software was used to further analyse the gene list and perform gene ontology enrichment analysis. Pathway analysis was also performed using the Database for Annotation, Visualization and Integrated Discovery (DAVID).

10   Appendix C

10.1 Additional methods and results for Chapter 5 : Phenotyping TRPC3$^{-/-}$:TRPC6$^{-/-}$ mice

10.1.1   Patch clamp electrophysiology

Patch clamp electrophysiology is a way of investigating ion channels by recording electrophysiological characteristics from either small numbers of ion channels in the cell membrane or from the whole cell. The cell membrane consists of a bilayer of phospholipids that form a barrier to charged molecules; the flow of ions across the plasma membrane is facilitated by specialised proteins, ion channels, transporters and pumps. These proteins act to maintain the differences in osmolarity of the intracellular and extracellular media that many physiological processes depend on, the distribution of the main ions is shown in Table 10.1.

Ion	Intracellular range	Extracellular range
Na$^+$	5-20mM	130-160mM
K$^+$	130-160mM	4-8mM
Ca^{2+}	50-1000nM	1.2-4mM
Mg^{2+}	10-20mM	1-5mM
Cl$^-$	1-60mM	100-140mM
HCO$_3^-$	1-3mM	20-30mM

Table 10.1 Intracellular and extracellular distribution of main ions

The membrane potential is the difference in voltage between the interior and exterior of the cell and the resting membrane potential of a cell is determined by the permeability of the membrane to ions that produce this electrical potential difference. In most neurons the resting membrane potential is around -70mV. Each ion will have a characteristic reversal potential dependent on the concentrations inside and outside and the permeability of the cell membrane to the particular ion. Diffusion down their electrochemical gradients through ion channels will move the membrane potential closer to their reversal potential. The resulting resting

membrane potential would be a weighted average of all the permeable ions reversal potentials. Ion transporters however can work against the electrochemical gradients. The particularly important high intracellular potassium and low sodium concentration is maintained by an Na^+/K^+ pump, which transports out $3Na^+$ ions for every $2 K^+$ ions in at the cost of one ATP molecule, makes the cytoplasm negatively charged relative to the extracellular space.

When ion channels open in response to a stimulus, or the extracellular solution, cations flow down the electrochemical gradient into the cell making the membrane potential more positive. Voltage gated sodium channels are opened in response to the change in membrane potential causing a rapid influx of Na^+ ions, which depolarizes the membrane leading to an action potential. Following the action potential K^+ channels restore the membrane potential to the negative resting potential (also see Figure 10.1).
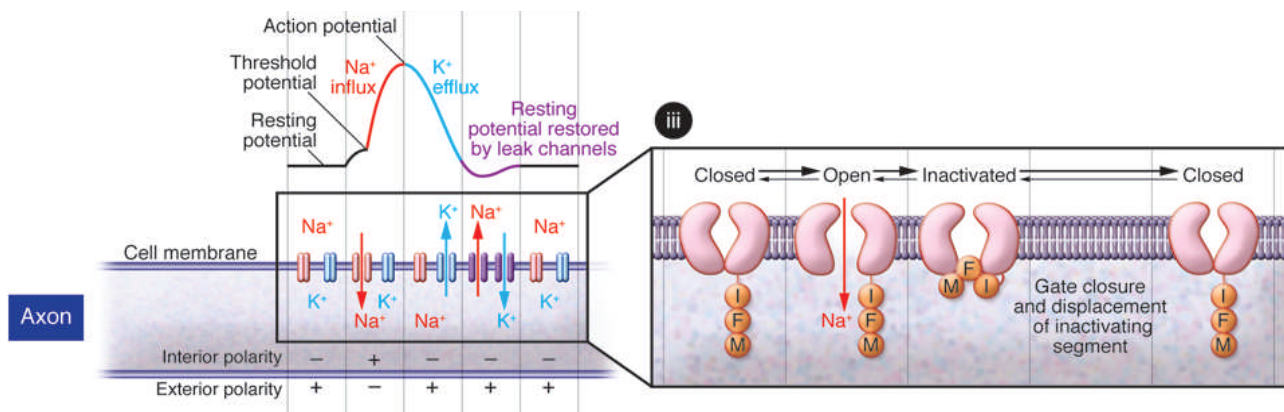
Figure 10.1 Phases of the action potential and inactivation of voltage gated sodium channels
When a defined threshold of depolarization is reached, voltage-gated sodium channels are activated and an action potential is generated. During an action potential, an IFM-inactivating segment moves to block the channel within 0.5–1 ms. In this inactivated state, the channel cannot be opened. Meanwhile, potassium channels open, acting to repolarize the membrane. As the membrane repolarizes, the sodium channel gate is closed and inactivating segment is displaced, returning the sodium channel to a resting closed state adapted from (Raouf et al.,

Patch clamp electrophysiology can elucidate the properties of the ion channels responding to heat, chemical and mechanical stimuli. This transduction occurs at the peripheral terminals of sensory neurons *in vivo* but receptors normally found on peripheral terminals are present on

the cell bodies of cultured sensory neurons allowing these cells to be used as a model for the study of transduction (Cesare and McNaughton, 1996).

10.1.1.1   Electrophysiological recordings

DRG Culture

Mice were sacrificed by CO2 inhalation followed by cervical dislocation in accordance with the UK Animals Scientific Procedures Act 1986. All efforts were made to minimize animal suffering and to reduce the number of animals used. Dorsal root ganglia were removed, collected in ice-cold medium (Ca2+- and Mg2+-free HBSS supplemented with 5 mM HEPES and 10 mM Glucose) and subsequently digested in an enzyme mixture containing Ca2+- and Mg2+-free HBSS, 5 mM HEPES, 10 mM Glucose, Collagenase type XI (5 mg ml−1), Dispase (10 mg ml−1) for 1 hour prior to mechanical trituration in Dulbecco's modified Eagle's Medium (DMEM) + 10% Heat-inactivated Foetal Bovine Serum (FBS). Cells were then centrifuged for 5 min at 800 rpm and resuspended in DMEM containing 4.5 g l−1 glucose, 4 mM l-glutamine, 110 mg l−1 sodium pyruvate, 10% FBS, 1% penicillin–streptomycin (10 000 i.u. ml−1), 1% Glutamax, 125 ng ml−1 nerve growth factor (NGF) and 50 ng ml−1 Neurotrophin-4 (NT-4) and plated on 35 mm dishes coated with poly-l-lysine (0.01 mg ml−1) and laminin (0.02 mg ml−1). Cultures were kept at 37 °C in 5% CO2. Neurons were used up to 2 days after plating.

Whole cell perforated patch recordings

Voltage-clamp recordings from cultured DRG neurons were carried out at a holding potential of -60mV using an Axopatch 200B amplifier (Axon Instruments, Inc). Pipettes were pulled from borosilicate glass capillaries with a P-97 puller (Sutter Instrument Co.) and exhibited resistances of 1-3MΩ. Currents were digitized with a Digidata 1322A data acquisition system (Axon Instruments Inc.). Data was recorded and stored using Clamps 8.1 (Axon Instruments Inc.). Currents were low pass-filtered at 2kHz and sampled at 11kHz. Capacity transients were cancelled, and series resistance was compensated by 80% minimum. Voltages were not corrected for liquid junction potential. Recordings were performed at room temperature. Off-line analysis and statistics were performed using Clampfit 9.0 (Graphpad software). Values

were expressed as means±SEM. The standard pipette solution contained 140mM KCl, 5mM NaCl, 2mM $MgCl_2$, 5 mM EGTA and 10mM HEPES (pH 7.3). The standard external solution contained 140mM KCl, 5mM NaCl, 2mM $MgCl_2$, and 10mM HEPES (pH 7.4). Amphothericin-B was added to the pipette solution to perforate the cell membrane.

Mechanical stimulation of DRG neurons

A heat-polished glass pipette, a tip diameter of ~5-6µm, was used to stimulate the neurons mechanically at an angle of ~60° to the surface of the culture dish. The probe was connected to a computer-controlled piezo-electric crystal drive (Burleigh) and positioned such that a 10µm movement did not visibly contact the cell but an 11µm stimulus produced an observable membrane deflection. A 1µm stimulus was attributed to a probe movement of 11µm stimulation, a 2µm stimulus to a 12µm movement and so on. The probe moved at a speed of 0.5µm/ms and the stimulus duration was 200ms. The correlation between action potential properties and DRG neuronal phenotype that exists in adult animals was used to distinguish between mechanoreceptive (low threshold) neurons and nociceptive (high threshold) neurons. IB4 staining was used to distinguish between peptidergic and non-peptidergic $IB4^+$ small neurons.

10.1.2 Auditory Brainstem Response

Mice were anesthetized with ketamine-medetomidine cocktail (50mg ketamine, 0.415mg medetomidine in 4.1ml saline), 0.01ml/g body weight. Electrodes were placed at the vertex and the mastoid, with a ground near the tail. TDT System 3 equipment was used to generate the stimuli and acquire the evoked response. Tone pips were presented through a closed field speaker at 25 s^{-1} at each frequency. Pure tone stimuli was generated at 8, 12, 24, 32 and 40KHz. Sound pressure level was varied in 5 dB steps from 10 to 90 relative dB. The data was converted using Matlab and evoked potential wave forms were visually inspected to obtain a threshold value.

10.1.3 Fluorescence microscopy

Mice were sacrificed directly after functional testing and cochleae excised from bullae. Fixative was perfused directly into the cochlea by creating a small opening at the apex of the cochlea and rupturing the bone between the round and oval window. Cochleae were fixed in

4% paraformaldehyde for 90 minutes and then decalcified in 4.13% EDTA (pH 7.3). Organ of Corti strips (1/2 turns) were carefully dissected, categorised into apical or basal, and incubated in 0.5% Triton X-100 for 20 minutes to permeabilise plasma membranes. Tissue was then incubated in phalloidin conjugated to rhodamine fluorophore 1μg/ml in PBS with 0.15% Triton X-100 for 80 minutes at room temperature. Wholemounts were PBS washed x4 and mounted on multispot slides with Vectashield containing DAPI to counterstain nuclei. Preparations were examined and imaged using a Zeiss Meta confocal laser scanning microscope. Digital images were exported as TIFF or JPEG files.

10.1.4 Immunohistochemical analysis

To prepare the DRG sections for lectin IB4 (IB4) and calcitonin gene-related peptide (CGRP) staining, Wild-type control and TRPC3$^{-/-}$:TRPC6$^{-/-}$ mice were deeply anesthetised with pentobarbital (140 mg/kg) and transcardially perfused with heparinised saline (0.9% NaCl) followed by 4% paraformaldehyde (PFA) in 0.1 M phosphate buffer (PB), pH7.4. The lumbar DRGs were dissected and post-fixed in 4% PFA overnight at 4°C. The tissue was transferred into 20% sucrose in 0.1 M PB for 24 hours at 4°C and then embedded in O.C.T. compound (BDH Essex, UK) on dry ice. Cryostat sections (thickness, 11μm) were cut and collected on Superfrost plus slides. For Peripherin and Neurofilament 200 (NF200) immunostaining, fresh unperfused Lumber 4 (L4) DRGs from wild-type control (n = 3) and TRPC3/6 DKO mice (n = 3) were dissected and embedded in O.C.T. compound. Cryostat sections (thickness, 11μm) were serially cut. Every 8th section throughout the L4 DRG was collected. All the slides were dried over night at room temperature after sectioning. The sections for Peripherin and NF200 staining were fixed with fresh prepared 4% PFA at room temperature for 7 minutes, and then washed three times for 5 minutes each with 1x PBS containing 0.3% Triton X-100 (PBST). All the sections for immunostaining were incubated in blocking buffer (PBST containing 10% goat serum, Sigma G9023) at room temperature for 1 hour and then were incubated with diluted primary antibodies overnight at 4°C. After three times washes for 10 minutes each with PBST, bound primary antibodies were detected by incubating with diluted secondary antibodies at room temperature for 2 hours. The slides were washed with PBST for three times 10 minutes each and then mounted using VECTASHIELD HardSet Mounting Medium (Vector Labs, H-1400). The staining sections were visualized using a fluorescent Leica microscope. Images were taken using Hamamatsu Camera and HC Image Live software. The

same setup of acquisition was used to acquire the pictures of both groups of mice. The number of DRG neurons was counted as described[1]. Briefly, the number of peripherin-positive (green), NF200-positive (red) and double-positive (yellow) neurons were counted blind in all sections from L4 DRG in each animal. The total number of L4 DRG neurons was calculated by adding Peripherin-, NF200- and double-positive neuron numbers together. Mean and SEM of percentages and number of L4 DRG neurons were evaluated for wild-type and mutant groups. The following primary antibodies were diluted in blocking buffer: rabbit anti-CGRP (1:4000, Sigma C8198); mouse anti-Peripherin (1:500, Sigma, P5117); rabbit anti-Neurofilament 200 (1:200, Sigma, UK, N4142). lectin IB4-biotin (1:500, Sigma, L2140) was diluted in PBS containing 0.1 mM $MnCl_2$, 0.1 mM $MgCl_2$, and 0.1 mM $CaCl_2$. The following secondary antibodies were diluted in blocking buffer: goat anti-mouse IgG Alexa fluor 488 (1:1000, Invitrogen, A11017); goat anti-rabbit IgG Alexa fluor 594 (1:1000, Invitrogen, A11037) and Alexa Fluor 488-conjugated streptavidin (1:200, Invitrogen, S11223).

10.1.5   TRPC3^{-/-}:TRPC6^{-/-} mice have severe hearing loss

The following work was performed by Professor Jonathan Ashmore amd Dr Ruth Taylor

The TRPC3$^{-/-}$:TRPC6$^{-/-}$ mice do not show a Preyer reflex response to a 20kHz toneburst at 90dSB delivered by a custom built clickbox (see Supplementary video and Figure 5.15a). Auditory function was further tested using auditory brainstem responses. The dB threshold at which a brainstem response was seen in response to pure tone stimuli was assessed by eye. The TRPC3$^{-/-}$:TRPC6$^{-/-}$ had a hearing deficit at 32kHz and above compared to age-matched wildtype controls (Figure 10.2).
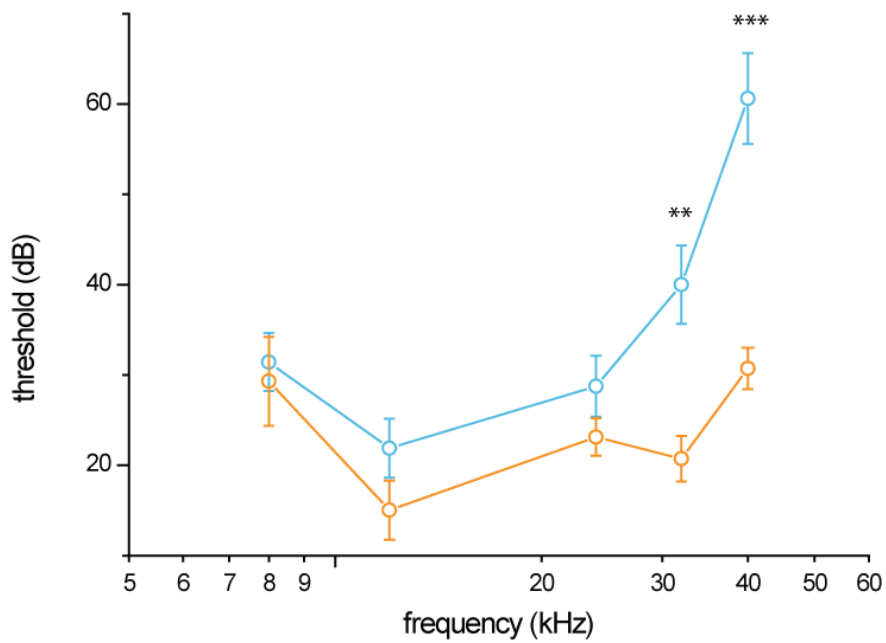
Figure 10.2 Auditory brainstem response TRPC3$^{-/-}$:TRPC6$^{-/-}$ mice and wildtype controls

TRPC3$^{-/-}$:TRPC6$^{-/-}$ mice (blue, n=9) had significantly increased thresholds at 32kHz (p<0.01) and 40kHz (p<0.001) compared to wildtype controls (orange, n=8). Two-way ANOVA with Bonferroni post test. Results expressed as mean±SEM.

10.1.6 TRPC3^{-/--}:TRPC6^{-/-} null mice have reduced rapidly adapting currents in large diameter DRG neurons

The following work was performed by Dr. Francois Rugiero and Dr. John Linley.

Three types of mechanically activated currents are seen in DRG neurons, slowly adapting (SA), intermediately adapting (IA) and rapidly adapting (RA) (Figure 10.3a), a proportion of DRG neurons are non responsive to mechanical stimulus. All three types of current were seen in TRPC3/TRPC6 null, TRPC3$^{-/-}$ and TRPC6$^{-/-}$ mice and the magnitude of currents evoked by mechanical stimulus did not differ (Figure 10.3c). When looking at the subpopulations of neurons no difference was found in mechanically evoked currents in the large diameter neurons (Figure 10.3d). However, in the small diameter neurons there was an increase in the numbers of non-responsive cells by 15% and a decrease of rapidly adapting current in the TRPC3/TRPC6 double knockout by a similar amount compared to the wildtype controls (Figure 10.3b). TRPC3$^{-/-}$ also displayed a decrease of RA currents but an increase of IA currents meant the overall number of mechanically sensitive neurons remained the same as wildtype animals.
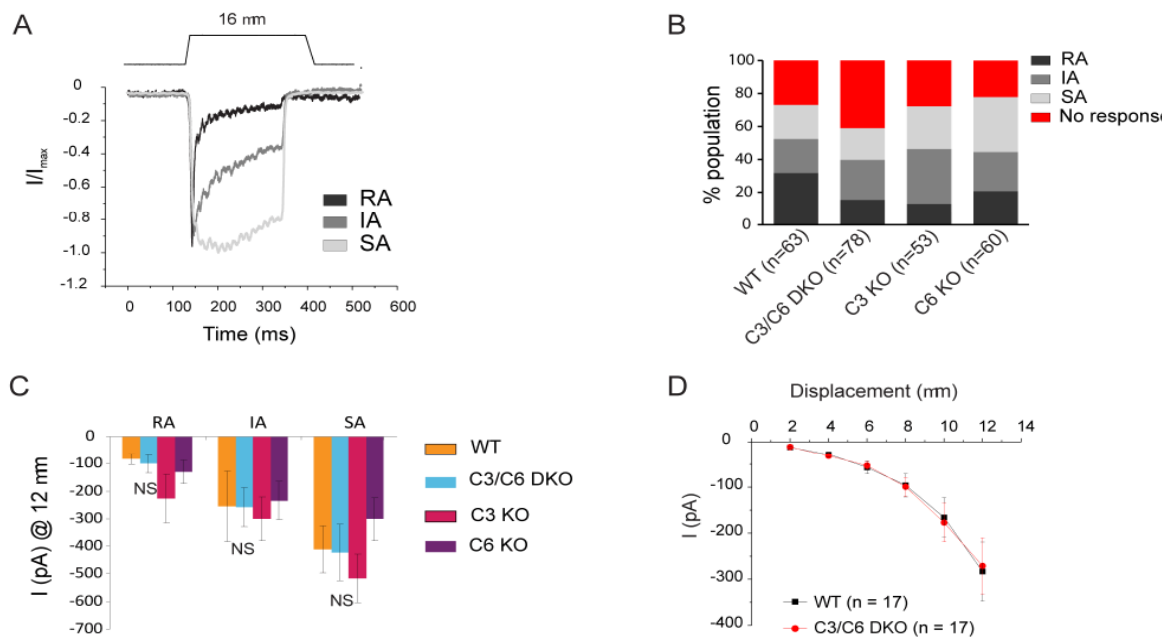
Figure 10.3 Mechanosensitive currents in DRG neurons from TRPC3/TRPC6 double knockout, TRPC3^{-/-}, TRPC6^{-/-} and wildtype controls.

A. Mechanically evoked currents from small diameter mouse DRG neurons normalised to peak were classified based on kinetic of adaptation; Rapidly adapting (RA) Intermediately adapting (IA), Slowly adapting (SA). **B.** Proportion of small diameter mouse DRG neurons expressing each current type from wild type mice (WT) TRPC3/6 double knockout mice (DKO), TRPC3 single KO mice (C3 KO) and TRPC6 single KO mice (C6 KO). **C.** Magnitude of currents evoked by a 12 um stimulus in mouse DRG cultures. No significant difference was found between genotypes (ANOVA, $p>0.05$). (**D**) Mechanically evoked currents from large diameter mouse DRG neurons with action potential widths <1 ms. No significant difference was seen between genotypes (unpaired t-test, $p>0.05$, n = 17).

10.1.7 TRPC3$^{-/-}$:TRPC6$^{-/-}$ null mice have normal cochlea and DRG neurons

The following work was performed by Dr Zing Zhao

The sensory neurons of the TRPC3$^{-/-}$:TRPC6$^{-/-}$ mice were quantified and characterised using immunohistochemistry. Sections of DRG were stained with anti-peripherin, anti-neurofilament, anti-IB4 and anti-CGRP; The TRPC3$^{-/-}$:TRPC6$^{-/-}$ (DKO) mice show the similar expression pattern of the four markers compared to littermate wild-type control (WT) mice (Figure 10.4a). The wild-type control and TRPC3$^{-/-}$:TRPC6$^{-/-}$ mice also have similar percentage of Peripherin (64.0 ± 1.0%, 64.2 ± 1.0%), NF200 (27.5 ± 1.8%, 26.2 ± 0.7%) and Peripherin+NF200 (8.5 ± 0.8%, 9.6 ± 0.4%) positive DRG neurons (P > 0.05, Student's *t*-test). TRPC3$^{-/-}$:TRPC6$^{-/-}$ mice have no deficits in any subpopulations of DRG neurons (Figure 10.4b-c).

The following work was performed by Dr Ruth Taylor

Cochlea from a wildtype and TRPC3$^{-/-}$:TRPC6$^{-/-}$ mice were examined with fluorescence microscopy. There was little evidence of hair cell loss except where the occasional scar formation, derived from the expansion of supporting cells apices, could be seen in the region of outer hair cell loss (<0.1% of outer hair cells). Additionally, hair cell loss could be identified by the absence of nuclei in the apical layer of the tissue. Pillar cells and inner hair cells were readily recognised with phalloidin labelling and all had normal morphology (Figure 10.4d).
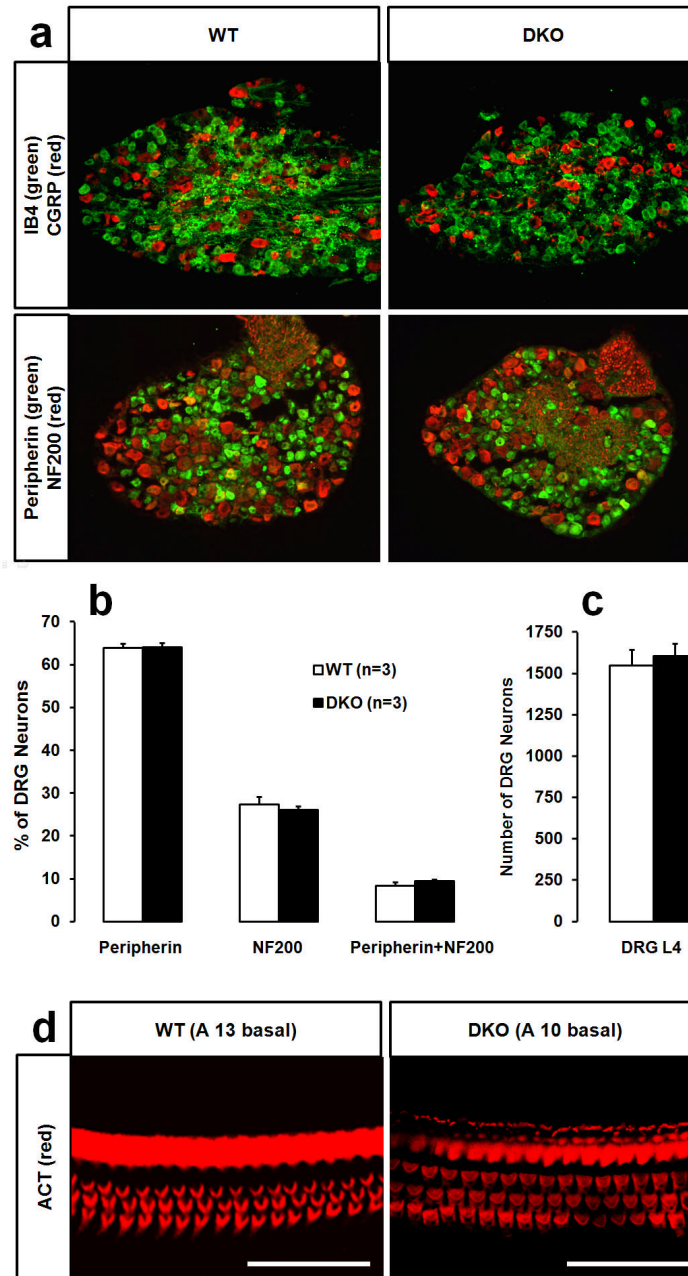
Figure 10.4 No significant neuronal marker changes and neuron losses in DRG, no cell losses in organ of Corti in TRPC3$^{-/-}$:TRPC6$^{-/-}$ (DKO) mice.

a, Subpopulation sensory neuron markers IB4 (green, top) and CGRP (red, top), Peripherin (green, bottom) and Neurofilament 200 (NF200) (red, bottom) were detected in DRG sections by immunohistochemistry. **b,** The percentage of Peripherin and NF200 positive DRG neurons was calculated after immunohistochemistry. The positive cells were counted on every 8th cross section from DRG Lumber 4 (L4). c, The total number of DRG neurons were calculated on above sections by adding Peripherin positive (+), NF200+ and double-positive neuron numbers together. There is no significant difference in DRG neuron numbers between WT and TRPC3$^{-/-}$:TRPC6$^{-/-}$ (1550 ± 93, 1607 ± 72; P > 0.05, Student's *t*-test). d, Comparison surface confocal sections of organ of Corti from WT and TRPC3$^{-/-}$:TRPC6$^{-/-}$ from same litter. Rhodamine-phalloidin stained shows actin-containing stereocilia (ACT, red) from basal turn. The three rows of outer hair cells are intact in both cases. The rows of pillar cells show up as strongly labelled upper band. Mice age is 10.7 weeks. Scale bar = 50 µm.

Reference List

Abrahamsen B, Zhao J, Asante CO, Cendan CM, Marsh S, Martinez-Barbera JP, Nassar MA, Dickenson AH, Wood JN (2008) The Cell and Molecular Basis of Mechanical, Cold, and Inflammatory Pain. Science 321:702-705.

Abramowitz J, Birnbaumer L (2009) Physiology and pathophysiology of canonical transient receptor potential channels. The FASEB Journal 23:297-328.

Adams DJ, Quail MA, Cox T, van der Weyden L, Gorick BD, Su Q, Chan Wi, Davies R, Bonfield JK, Law F, Humphray S, Plumb B, Liu P, Rogers J, Bradley A (2005) A genome-wide, end-sequenced 129Sv BAC library resource for targeting vector construction. Genomics 86:753-758.

Adebiyi A, Zhao G, Narayanan D, Thomas-Gatewood CM, Bannister JP, Jaggar JH (2010) Isoform-Selective Physical Coupling of TRPC3 Channels to IP3 Receptors in Smooth Muscle Cells Regulates Arterial Contractility. Circulation Research 106:1603-1612.

Akopian AN, Sivilotti L, Wood JN (1996) A tetrodotoxin-resistant voltage-gated sodium channel expressed by sensory neurons. Nature 379(6562):257-62.

Akopian AN, Souslova V, England S, Okuse K, Ogata N, Ure J, Smith A, Kerr BJ, McMahon SB, Boyce S, Hill R, Stanfa LC, Dickenson AH, Wood JN (1999) The tetrodotoxin-resistant sodium channel SNS has a specialized function in pain pathways. Nat Neurosci 2:541-548.

Alessandri-Haber N, Dina OA, Chen X, Levine JD (2009) TRPC1 and TRPC6 channels cooperate with TRPV4 to mediate mechanical hyperalgesia and nociceptor sensitization. J Neurosci 29:6217-6228.

Alessandri-Haber N, Dina OA, Joseph EK, Reichling D, Levine JD (2006) A transient receptor potential vanilloid 4-dependent mechanism of hyperalgesia is engaged by concerted action of inflammatory mediators. J Neurosci 26:3864-3874.

Allchorne A, Broom D, Woolf C (2005) Detection of cold pain, cold allodynia and cold hyperalgesia in freely behaving rats. Molecular Pain 1:36.

Amaral MD, Pozzo-Miller L (2007a) BDNF induces calcium elevations associated with IBDNF, a nonselective cationic current mediated by TRPC channels. Journal of Neurophysiology 98(4):2476-82.

Amaral MD, Pozzo-Miller L (2007b) TRPC3 channels are necessary for brain-derived neurotrophic factor to activate a nonselective cationic current and to induce dendritic spine formation. Journal of Neuroscience 27(19):5179-89.

Amaya F, Wang H, Costigan M, Allchorne AJ, Hatcher JP, Egerton J, Stean T, Morisset V, Grose D, Gunthorpe MJ, Chessell IP, Tate S, Green PJ, Woolf CJ (2006) The voltage-gated

sodium channel Na(v)1.9 is an effector of peripheral inflammatory pain hypersensitivity. J Neurosci 26:12852-12860.

Babes A, Zorzon D, Reid G (2006) A novel type of cold-sensitive neuron in rat dorsal root ganglia with rapid adaptation to cooling stimuli. Eur J Neurosci 24:691-698.

Bautista DM, Jordt SE, Nikai T, Tsuruda PR, Read AJ, Poblete J, Yamoah EN, Basbaum AI, Julius D (2006) TRPA1 mediates the inflammatory actions of environmental irritants and proalgesic agents. Cell 124:1269-1282.

Beck B, Zholos A, Sydorenko V, Roudbaraki M, Lehen'kyi V, Bordat P, Prevarskaya N, Skryma R (2006) TRPC7 is a receptor-operated DAG-activated channel in human keratinocytes. Journal of Investigative Dermatology 126(9):1982-93.

Becker EBE, Oliver PL, Glitsch MD, Banks GT, Achilli F, Hardy A, Nolan PM, Fisher EMC, Davies KE (2009) A point mutation in TRPC3 causes abnormal Purkinje cell development and cerebellar ataxia in moonwalker mice. Proceedings of the National Academy of Sciences 106:6706-6711.

Beckh S, Noda M, Lubbert H, Numa S (1989) Differential regulation of three sodium channel messenger RNAs in the rat central nervous system during development. EMBO J 8:3611-3616.

Ben-Mabrouk F, Tryba AK (2010) Substance P modulation of TRPC3/7 channels improves respiratory rhythm regularity and ICAN-dependent pacemaker activity. Eur J Neurosci 31:1219-1232.

Bennett GJ (1999) Does a neuroimmune interaction contribute to the genesis of painful peripheral neuropathies? Proceedings of the National Academy of Sciences of the United States of America 96:7737-7738.

Bessou P, Perl ER (1969) Response of cutaneous sensory units with unmyelinated fibers to noxious stimuli. J Neurophysiol 32:1025-1043.

Bevan S, Winter J (1995) Nerve growth factor (NGF) differentially regulates the chemosensitivity of adult rat cultured sensory neurons. J Neurosci 15:4918-4926.

Bezzerides VJ, Ramsey IS, Kotecha S, Greka A, Clapham DE (2004) Rapid vesicular translocation and insertion of TRP channels. Nat Cell Biol 6:709-720.

Black JA, Cummins TR, Plumpton C, Chen YH, Hormuzdiar W, Clare JJ, Waxman SG (1999) Upregulation of a Silent Sodium Channel After Peripheral, but not Central, Nerve Injury in DRG Neurons. J Neurophysiol 82:2776-2785.

Boucher TJ, Okuse K, Bennett DLH, Munson JB, Wood JN, McMahon SB (2000) Potent Analgesic Effects of GDNF in Neuropathic Pain States. Science 290:124-127.

Boulay G, Zhu X, Peyton M, Jiang M, Hurst R, Stefani E, Birnbaumer L (1997) Cloning and Expression of a Novel Mammalian Homolog of Drosophila Transient Receptor Potential (Trp) Involved in Calcium Entry Secondary to Activation of Receptors Coupled by the Gq Class of G Protein. J Biol Chem 272:29672-29680.

Boyce S, Rupniak NM, Carlson EJ, Webb J, Borkowski JA, Hess JF, Strader CD, Hill RG (1996) Nociception and inflammatory hyperalgesia in B2 bradykinin receptor knockout mice. Immunopharmacology 33:333-335.

Brazer Sc, Singh BB, Liu X, Swaim W, Ambudkar IS (2003) Caveolin-1 Contributes to Assembly of Store-operated Ca2+ Influx Channels by Regulating Plasma Membrane Localization of TRPC1. Journal of Biological Chemistry 278:27208-27215.

Buniel MC, Schilling WP, Kunze DL (2003) Distribution of transient receptor potential channels in the rat carotid chemosensory pathway. J Comp Neurol 464:404-413.

Burgard EC, Niforatos W, van Biesen T, Lynch KJ, Touma E, Metzger RE, Kowaluk EA, Jarvis MF (1999) P2X Receptor-Mediated Ionic Currents in Dorsal Root Ganglion Neurons. J Neurophysiol 82:1590-1598.

Burgess PR, Perl ER (1967) Myelinated afferent fibres responding specifically to noxious stimulation of the skin. J Physiol 190:541-562.

Cable J, Steel KP (1998) Combined cochleo-saccular and neuroepithelial abnormalities in the Varitint-waddler-J (VaJ) mouse. Hear Res 123:125-136.

Campbell JN, Meyer RA, Raja SN (1992) Is nociceptor activation by alpha-1 adrenoreceptors the culprit in sympathetically maintained pain? APS Journal 1:3-11.

Cannon KE, Leurs R, Hough LB (2007) Activation of peripheral and spinal histamine H3 receptors inhibits formalin-induced inflammation and nociception, respectively. Pharmacology Biochemistry and Behavior 88:122-129.

Caterina MJ, Leffler A, Malmberg AB, Martin WJ, Trafton J, Petersen-Zeitz KR, Koltzenburg M, Basbaum AI, Julius D (2000) Impaired nociception and pain sensation in mice lacking the capsaicin receptor.[see comment]. Science 288(5464):306-13.

Caterina MJ, Rosen TA, Tominaga M, Brake AJ, Julius D (1999) A capsaicin-receptor homologue with a high threshold for noxious heat. Nature 398:436-441.

Caterina MJ, Schumacher MA, Tominaga M, Rosen TA, Levine JD, Julius D (1997) The capsaicin receptor: a heat-activated ion channel in the pain pathway. Nature 389:816-824.

Catterall WA (2000) Structure and regulation of voltage-gated Ca2+ channels. Annu Rev Cell Dev Biol 16:521-555.

Cayouette S, Lussier MP, Mathieu EL, Bousquet SM, Boulay G (2004) Exocytotic insertion of TRPC6 channel into the plasma membrane upon Gq protein-coupled receptor activation. Journal of Biological Chemistry 279(8):7241-6.

Cesare P, McNaughton P (1996) A novel heat-activated current in nociceptive neurons and its sensitization by bradykinin. Proc Natl Acad Sci U S A 93:15435-15439.

Chalfie M, Sulston J (1981) Developmental genetics of the mechanosensory neurons of Caenorhabditis elegans. Developmental Biology 82:358-370.

Chaplan SR, Bach FW, Pogrel JW, Chung JM, Yaksh TL (1994) Quantitative assessment of tactile allodynia in the rat paw. Journal of Neuroscience Methods 53:55-63.

Chen CC, Akopian A, Sivilottit L, Colquhoun D, Burnstock G, Wood J (1995) A P2X purinoceptor expressed by a subset of sensory neurons. Nature 377:428-431.

Chen CC, Zimmer A, Sun WH, Hall J, Brownstein MJ, Zimmer A (2002) A role for ASIC3 in the modulation of high-intensity pain stimuli. Proceedings of the National Academy of Sciences of the United States of America 99:8992-8997.

Chen CL, Broom DC, Liu Y, de Nooij JC, Li Z, Cen C, Samad OA, Jessell TM, Woolf CJ, Ma Q (2006) Runx1 Determines Nociceptive Sensory Neuron Phenotype and Is Required for Thermal and Neuropathic Pain. Neuron 49:365-377.

Chuang Hh, Prescott ED, Kong H, Shields S, Jordt SE, Basbaum AI, Chao MV, Julius D (2001) Bradykinin and nerve growth factor release the capsaicin receptor from PtdIns(4,5)P2-mediated inhibition. Nature 411:957-962.

Chul Han H, Hyun Lee D, Mo Chung J (2000) Characteristics of ectopic discharges in a rat neuropathic pain model. Pain 84:253-261.

Chung YH, Sun AH, Kim D, Hoon SD, Su KS, Yong KK, Bok LW, Ik CC (2006) Immunohistochemical study on the distribution of TRPC channels in the rat hippocampus. Brain Research 1085(1):132-7.

Clapham DE (2003) TRP channels as cellular sensors. Nature 426:517-524.

Clapham DE, Runnels LW, Strubing C (2001) The trp ion channel family. Nat Rev Neurosci 2:387-396.

Coderre TJ (1992) Contribution of protein kinase C to central sensitization and persistent pain following tissue injury. Neurosci Lett 140:181-184.

Coderre TJ, Melzack R (1992) The contribution of excitatory amino acids to central sensitization and persistent nociception after formalin-induced tissue injury. J Neurosci 12:3665-3670.

Coderre TJ, Vaccarino AL, Melzack R (1990) Central nervous system plasticity in the tonic pain response to subcutaneous formalin injection. Brain Res 535:155-158.

Coderre TJ, Yashpal K (1994) Intracellular messengers contributing to persistent nociception and hyperalgesia induced by L-glutamate and substance P in the rat formalin pain model. Eur J Neurosci 6:1328-1334.

Corey DP, Garcia-Anoveros J, Holt JR, Kwan KY, Lin SY, Vollrath MA, Amalfitano A, Cheung ELM, Derfler BH, Duggan A, Geleoc GSG, Gray PA, Hoffman MP, Rehm HL, Tamasauskas D, Zhang DS (2004) TRPA1 is a candidate for the mechanosensitive transduction channel of vertebrate hair cells. Nature 432:723-730.

Costigan M, Befort K, Karchewski L, Griffin R, D'Urso D, Allchorne A, Sitarski J, Mannion J, Pratt R, Woolf C (2002) Replicate high-density rat genome oligonucleotide microarrays reveal hundreds of regulated genes in the dorsal root ganglion after peripheral nerve injury. BMC Neuroscience 3:16.

Couture R, Harrisson M, Vianna RM, Cloutier F (2001) Kinin receptors in pain and inflammation. European Journal of Pharmacology 429:161-176.

Cox JJ, Reimann F, Nicholas AK, Thornton G, Roberts E, Springell K, Karbani G, Jafri H, Mannan J, Raashid Y, Al-Gazali L, Hamamy H, Valente EM, Gorman S, Williams R, McHale DP, Wood JN, Gribble FM, Woods CG (2006) An SCN9A channelopathy causes congenital inability to experience pain. Nature 444:894-898.

Crowley C, Spencer SD, Nishimura MC, Chen KS, Pitts-Meek S, Armaninl MP, Ling LH, McMahon SB, Shelton DL, Levinson AD, Phillips HS (1994) Mice lacking nerve growth factor display perinatal loss of sensory and sympathetic neurons yet develop basal forebrain cholinergic neurons. Cell 76:1001-1011.

Crunkhorn P, Meacock SC (1971) Mediators of the inflammation induced in the rat paw by carrageenin. Br J Pharmacol 42:392-402.

Cui JG, Holmin S, Mathiesen T, Meyerson BA, Linderoth B (2000) Possible role of inflammatory mediators in tactile hypersensitivity in rat models of mononeuropathy. Pain 88:239-248.

Cunha FQ, Poole S, Lorenzetti BB, Ferreira SH (1992) The pivotal role of tumour necrosis factor alpha in the development of inflammatory hyperalgesia. Br J Pharmacol 107:660-664.

Davis JB, Gray J, Gunthorpe MJ, Hatcher JP, Davey PT, Overend P, Harries MH, Latcham J, Clapham C, Atkinson K, Hughes SA, Rance K, Grau E, Harper AJ, Pugh PL, Rogers DC, Bingham S, Randall A, Sheardown SA (2000) Vanilloid receptor-1 is essential for inflammatory thermal hyperalgesia. Nature 405:183-187.

Dhaka A, Murray AN, Mathur J, Earley TJ, Petrus MJ, Patapoutian A (2007) TRPM8 is required for cold sensation in mice. Neuron 54:371-378.

Di PF, Belyantseva IA, Kim HJ, Vogt TF, Kachar B, Noben-Trauth K (2002) Mutations in Mcoln3 associated with deafness and pigmentation defects in varitint-waddler (Va) mice. Proc Natl Acad Sci U S A 99:14994-14999.

Dib-Hajj S, Black JA, Felts P, Waxman SG (1996) Down-regulation of transcripts for Na channel alpha-SNS in spinal sensory neurons following axotomy. Proc Natl Acad Sci U S A 93:14950-14954.

Dietrich A, Mederos YS, Gollasch M, Gross V, Storch U, Dubrovska G, Obst M, Yildirim E, Salanova B, Kalwa H, Essin K, Pinkenburg O, Luft FC, Gudermann T, Birnbaumer L (2005) Increased vascular smooth muscle contractility in TRPC6-/- mice.[erratum appears in Mol Cell Biol. 2005 Dec;25(24):11191]. Molecular & Cellular Biology 25(16):6980-9.

Dirajlal S, Pauers LE, Stucky CL (2003) Differential Response Properties of IB4-Positive and -Negative Unmyelinated Sensory Neurons to Protons and Capsaicin. J Neurophysiol 89:513-524.

Dong XW, Goregoaker S, Engler H, Zhou X, Mark L, Crona J, Terry R, Hunter J, Priestley T (2007) Small interfering RNA-mediated selective knockdown of Na(V)1.8 tetrodotoxin-resistant sodium channel reverses mechanical allodynia in neuropathic rats. Neuroscience 146:812-821.

Donnerer J, Schuligoi R, Stein C (1992) Increased content and transport of substance P and calcitonin gene-related peptide in sensory nerves innervating inflamed tissue: evidence for a regulatory function of nerve growth factor in vivo. Neuroscience 49:693-698.

Drew LJ, Rohrer DK, Price MP, Blaver KE, Cockayne DA, Cesare P, Wood JN (2004) Acid-sensing ion channels ASIC2 and ASIC3 do not contribute to mechanically activated currents in mammalian sensory neurones. J Physiol 556:691-710.

Drew LJ, Rugiero F, Cesare P, Gale JE, Abrahamsen B, Bowden S, Heinzmann S, Robinson M, Brust A, Colless B, Lewis RJ, Wood JN (2007) High-threshold mechanosensitive ion channels blocked by a novel conopeptide mediate pressure-evoked pain. PLoS One 2:e515.

Drew LJ, Wood JN (2007) FM1-43 is a permeant blocker of mechanosensitive ion channels in sensory neurons and inhibits behavioural responses to mechanical stimuli. Mol Pain 3:1.

Drew LJ, Wood JN, Cesare P (2002) Distinct mechanosensitive properties of capsaicin-sensitive and -insensitive sensory neurons. J Neurosci 22:RC228.

Duan B, Wu LJ, Yu YQ, Ding Y, Jing L, Xu L, Chen J, Xu TL (2007) Upregulation of acid-sensing ion channel ASIC1a in spinal dorsal horn neurons contributes to inflammatory pain hypersensitivity. J Neurosci 27:11139-11148.

Dube GR, Lehto SG, Breese NM, Baker SJ, Wang X, Matulenko MA, Honore P, Stewart AO, Moreland RB, Brioni JD (2005) Electrophysiological and in vivo characterization of A-317567, a novel blocker of acid sensing ion channels. Pain 117:88-96.

Dymecki SM (1996) Flp recombinase promotes site-specific DNA recombination in embryonic stem cells and transgenic mice. Proceedings of the National Academy of Sciences of the United States of America 93:6191-6196.

Elg S, Marmigere F, Mattsson JP, Ernfors P (2007) Cellular subtype distribution and developmental regulation of TRPC channel members in the mouse dorsal root ganglion. Journal of Comparative Neurology 503(1):35-46.

Field MJ, Cox PJ, Stott E, Melrose H, Offord J, Su TZ, Bramwell S, Corradini L, England S, Winks J, Kinloch RA, Hendrich J, Dolphin AC, Webb T, Williams D (2006) Identification of the alpha2-delta-1 subunit of voltage-dependent calcium channels as a molecular target for pain mediating the analgesic actions of pregabalin. Proc Natl Acad Sci U S A 103:17537-17542.

Fleetwood-Walker SM, Mitchell R, Hope PJ, Molony V, Iggo A (1985) An [alpha]2 receptor mediates the selective inhibition by noradrenaline of nociceptive responses of identified dorsal horn neurones. Brain Research 334:243-254.

Fox A, Wotherspoon G, McNair K, Hudson L, Patel S, Gentry C, Winter J (2003) Regulation and function of spinal and peripheral neuronal B1 bradykinin receptors in inflammatory mechanical hyperalgesia. Pain 104:683-691.

Freichel M, Suh SH, Pfeifer A, Schweig U, Trost C, Weissgerber P, Biel M, Philipp S, Freise D, Droogmans G, Hofmann F, Flockerzi V, Nilius B (2001) Lack of an endothelial store-operated Ca2+ current impairs agonist-dependent vasorelaxation in TRP4-/- mice. Nat Cell Biol 3:121-127.

Fusco FR, Martorana A, Giampa C, De MZ, Vacca F, Tozzi A, Longone P, Piccirilli S, Paolucci S, Sancesario G, Mercuri NB, Bernardi G (2004) Cellular localization of TRPC3 channel in rat brain: preferential distribution to oligodendrocytes. Neuroscience Letters 365(2):137-42.

Garcia-Anoveros J, Samad TA, Zuvela-Jelaska L, Woolf CJ, Corey DP (2001) Transport and localization of the DEG/ENaC ion channel BNaC1alpha to peripheral mechanosensory terminals of dorsal root ganglia neurons. J Neurosci 21:2678-2686.

Gee NS, Brown JP, Dissanayake VUK, Offord J, Thurlow R, Woodruff GN (1996) The Novel Anticonvulsant Drug, Gabapentin (Neurontin), Binds to the Subunit of a Calcium Channel. J Biol Chem 271:5768-5776.

Gibson SJ, Polak JM, Bloom SR, Sabate IM, Mulderry PM, Ghatei MA, McGregor GP, Morrison JF, Kelly JS, Evans RM (1984) Calcitonin gene-related peptide immunoreactivity in the spinal cord of man and of eight other species. J Neurosci 4:3101-3111.

Goel M, Sinkins WG, Schilling WP (2002) Selective Association of TRPC Channel Subunits in Rat Brain Synaptosomes . Journal of Biological Chemistry 277:48303-48310.

Goodman MB, Ernstrom GG, Chelur DS, O'Hagan R, Yao CA, Chalfie M (2002) MEC-2 regulates C. elegans DEG/ENaC channels needed for mechanosensation. Nature 415:1039-1042.

Greka A, Navarro B, Oancea E, Duggan A, Clapham DE (2003) TRPC5 is a regulator of hippocampal neurite length and growth cone morphology. Nature Neuroscience 6(8):837-45.

Guler AD, Lee H, Iida T, Shimizu I, Tominaga M, Caterina M (2002) Heat-evoked activation of the ion channel, TRPV4. Journal of Neuroscience 22(15):6408-14.

Hanesch U, Pfrommer U, Grubb BD, Schaible HG (1993) Acute and chronic phases of unilateral inflammation in rat's ankle are associated with an increase in the proportion of calcitonin gene-related peptide-immunoreactive dorsal root ganglion cells. Eur J Neurosci 5:154-161.

Hardisty-Hughes RE, Parker A, Brown SDM (2010) A hearing and vestibular phenotyping pipeline to identify mouse mutants with hearing impairment. Nat Protocols 5:177-190.

Hargreaves K, Dubner R, Brown F, Flores C, Joris J (1988) A new and sensitive method for measuring thermal nociception in cutaneous hyperalgesia. Pain 32:77-88.

Harteneck C, Plant TD, Schultz G (2000) From worm to man: three subfamilies of TRP channels. Trends in Neurosciences 23:159-166.

Hartmann J, Dragicevic E, Adelsberger H, Henning HA, Sumser M, Abramowitz J, Blum R, Dietrich A, Freichel M, Flockerzi V, Birnbaumer L, Konnerth A (2008) TRPC3 channels are required for synaptic transmission and motor coordination. Neuron 59(3):392-8.

Hasegawa H, Abbott S, Han BX, Qi Y, Wang F (2007) Analyzing Somatosensory Axon Projections with the Sensory Neuron-Specific Advillin Gene. Journal of Neuroscience 27:14404-14414.

Hasty P, Crist M, Grompe M, Bradley A (1994) Efficiency of insertion versus replacement vector targeting varies at different chromosomal loci. Mol Cell Biol 14:8385-8390.

Hay C, de Belleroche J (1997) Carrageenan-induced hyperalgesia is associated with increased cyclo-oxygenase-2 expression in spinal cord. [Miscellaneous Article]. Neuroreport 8:1249-1251.

Hensel H, Zotterman Y (1951) The effect of menthol on the thermoreceptors. Acta Physiol Scand 24:27-34.

Himes BT, Tessler A (1989) Death of some dorsal root ganglion neurons and plasticity of others following sciatic nerve section in adult and neonatal rats. J Comp Neurol 284:215-230.

Hisatsune C, Kuroda Y, Nakamura K, Inoue T, Nakamura T, Michikawa T, Mizutani A, Mikoshiba K (2004) Regulation of TRPC6 Channel Activity by Tyrosine Phosphorylation. Journal of Biological Chemistry 279:18887-18894.

Ho Kim S, Mo Chung J (1992) An experimental model for peripheral neuropathy produced by segmental spinal nerve ligation in the rat. Pain 50:355-363.

Hofmann T, Obukhov AG, Schaefer M, Harteneck C, Gudermann T, Schultz G (1999) Direct activation of human TRPC6 and TRPC3 channels by diacylglycerol. Nature 397(6716):259-63.

Hofmann T, Schaefer M, Schultz G+, Gudermann T (2002) Subunit composition of mammalian transient receptor potential channels in living cells. Proceedings of the National Academy of Sciences of the United States of America 99:7461-7466.

Hogan Q (2002) Animal pain models. Reg Anesth Pain Med 27:385-401.

Holley M (2000) Hearing: Tuning in with motor proteins. Nature 405:130-133.

Honore P, Rogers SD, Schwei MJ, Salak-Johnson JL, Luger NM, Sabino MC, Clohisy DR, Mantyh PW (2000) Murine models of inflammatory, neuropathic and cancer pain each generates a unique set of neurochemical changes in the spinal cord and sensory neurons. Neuroscience 98:585-598.

Hu J, Lewin GR (2006) Mechanosensitive currents in the neurites of cultured mouse sensory neurones. The Journal of Physiology 577:815-828.

Huang EJ, Reichardt LF (2001) Neurotrophins: roles in neuronal development and function. Annu Rev Neurosci 24:677-736.

Huang M, Gu G, Ferguson EL, Chalfie M (1995) A stomatin-like protein necessary for mechanosensation in C. elegans. Nature 378:292-295.

Huang WC, Young JS, Glitsch MD (2007) Changes in TRPC channel expression during postnatal development of cerebellar neurons. Cell Calcium 42(1):1-10.

Huber TB, Schermer B, Muller RU, Hohne M, Bartram M, Calixto A, Hagmann H, Reinhardt C, Koos F, Kunzelmann K, Shirokova E, Krautwurst D, Harteneck C, Simons M, Pavenstadt H, Kerjaschki D, Thiele C, Walz G, Chalfie M, Benzing T (2006) Podocin and MEC-2 bind cholesterol to regulate the activity of associated ion channels. Proceedings of the National Academy of Sciences of the United States of America 103(46):17079-86.

Hunt SP, Mantyh PW (2001) The molecular dynamics of pain control. [Review] [98 refs]. Nature Reviews Neuroscience 2(2):83-91.

Igwe OJ, Chronwall BM (2001) Hyperalgesia induced by peripheral inflammation is mediated by protein kinase C betaII isozyme in the rat spinal cord. Neuroscience 104:875-890.

Inoue M, Ueda H (2000) Protein kinase C-mediated acute tolerance to peripheral mu-opioid analgesia in the bradykinin-nociception test in mice. J Pharmacol Exp Ther 293:662-669.

Inoue R, Okada T, Onoue H, Hara Y, Shimizu S, Naitoh S, Ito Y, Mori Y (2001) The transient receptor potential protein homologue TRP6 is the essential component of vascular

alpha(1)-adrenoceptor-activated Ca(2+)-permeable cation channel.[see comment]. Circulation Research 88(3):325-32.

Isom LL (2001) Sodium channel beta subunits: anything but auxiliary. Neuroscientist 7:42-54.

Iwata Y, Katanosaka Y, Arai Y, Komamura K, Miyatake K, Shigekawa M (2003) A novel mechanism of myocyte degeneration involving the Ca2+-permeable growth factorΓÇôregulated channel. The Journal of Cell Biology 161:957-967.

Jensen TS, Yaksh TL (1984) Effects of an intrathecal dopamine agonist, apomorphine, on thermal and chemical evoked noxious responses in rats. Brain Res 296:285-293.

Jin X, Gereau RW, IV (2006) Acute p38-Mediated Modulation of Tetrodotoxin-Resistant Sodium Channels in Mouse Sensory Neurons by Tumor Necrosis Factor-{alpha}. Journal of Neuroscience 26:246-255.

Jordt SE, Bautista DM, Chuang HH, McKemy DD, Zygmunt PM, Hogestatt ED, Meng ID, Julius D (2004) Mustard oils and cannabinoids excite sensory nerve fibres through the TRP channel ANKTM1. Nature 427:260-265.

Karashima Y, Talavera K, Everaerts W, Janssens A, Kwan KY, Vennekens R, Nilius B, Voets T (2009) TRPA1 acts as a cold sensor in vitro and in vivo. Proceedings of the National Academy of Sciences 106:1273-1278.

Kernan M, Cowan D, Zuker C (1994) Genetic dissection of mechanosensory transduction: mechanoreception-defective mutations of Drosophila. Neuron 12:1195-1206.

Kerr BJ, Souslova V, McMahon SB, Wood JN (2001) A role for the TTX-resistant sodium channel Nav 1.8 in NGF-induced hyperalgesia, but not neuropathic pain. Neuroreport 12:3077-3080.

Kidd BLC, Inglis JJ, Vetsika K, Hood VC, De Felipe C, Bester H, Hunt SP, Cruwys SC (2003) Inhibition of inflammation and hyperalgesia in NK-1 receptor knock-out mice. [Miscellaneous Article]. Neuroreport 14:2189-2192.

Kim JY, Zeng W, Kiselyov K, Yuan JP, Dehoff MH, Mikoshiba K, Worley PF, Muallem S (2006) Homer 1 Mediates Store- and Inositol 1,4,5-Trisphosphate Receptor-dependent Translocation and Retrieval of TRPC3 to the Plasma Membrane. Journal of Biological Chemistry 281:32540-32549.

Kimitsuki T, Nakagawa T, Hisashi K, Komune S, Komiyama S (1996) Gadolinium blocks mechano-electric transducer current in chick cochlear hair cells. Hear Res 101:75-80.

Kobayashi K, Fukuoka T, Obata K, Yamanaka H, Dai Y, Tokunaga A, Noguchi K (2005) Distinct expression of TRPM8, TRPA1, and TRPV1 mRNAs in rat primary afferent neurons with adelta/c-fibers and colocalization with trk receptors. J Comp Neurol 493:596-606.

Kobori T, Smith GD, Sandford R, Edwardson JM (2009) The transient receptor potential channels TRPP2 and TRPC1 form a heterotetramer with a 2:2 stoichiometry and an alternating subunit arrangement. J Biol Chem 284:35507-35513.

Kottgen M, Buchholz B, Garcia-Gonzalez MA, Kotsis F, Fu X, Doerken M, Boehlke C, Steffl D, Tauber R, Wegierski T, Nitschke R, Suzuki M, Kramer-Zucker A, Germino GG, Watnick T, Prenen J, Nilius B, Kuehn EW, Walz G (2008) TRPP2 and TRPV4 form a polymodal sensory channel complex. J Cell Biol 182:437-447.

Kretschmer T (2002) Clinical Article Accumulation of PN1 and PN3 Sodium Channels in Painful Human Neuroma-Evidence from Immunocytochemistry. Acta neurochirurgica 144:803.

Kumar N, Laferriere A, Yu JS, Poon T, Coderre TJ (2010) Metabotropic glutamate receptors (mGluRs) regulate noxious stimulus-induced glutamate release in the spinal cord dorsal horn of rats with neuropathic and inflammatory pain. J Neurochem 114:281-290.

Kunert-Keil C, Bisping F, Kruger J, Brinkmeier H (2006) Tissue-specific expression of TRP channel genes in the mouse and its variation in three different mouse strains. BMC Genomics 7:159.

Kwan KY, Allchorne AJ, Vollrath MA, Christensen AP, Zhang DS, Woolf CJ, Corey DP (2006) TRPA1 Contributes to Cold, Mechanical, and Chemical Nociception but Is Not Essential for Hair-Cell Transduction. Neuron 50:277-289.

Lai J, Gold MS, Kim CS, Bian D, Ossipov MH, Hunter JC, Porreca F (2002) Inhibition of neuropathic pain by decreased expression of the tetrodotoxin-resistant sodium channel, NaV1.8. Pain 95:143-152.

Larson AA, Brown DR, el-Atrash S, Walser MM (1986) Pain threshold changes in adjuvant-induced inflammation: a possible model of chronic pain in the mouse. Pharmacol Biochem Behav 24:49-53.

Lawson SN (2002) Phenotype and function of somatic primary afferent nociceptive neurones with C-, Adelta- or Aalpha/beta-fibres. [Review] [27 refs]. Experimental Physiology 87(2):239-44.

Lee HJ, Choi HS, Ju JS, Bae YC, Kim SK, Yoon YW, Ahn DK (2006) Peripheral mGluR5 antagonist attenuated craniofacial muscle pain and inflammation but not mGluR1 antagonist in lightly anesthetized rats. Brain Research Bulletin 70:378-385.

Leem JW, Willis WD, Chung JM (1993a) Cutaneous sensory receptors in the rat foot. J Neurophysiol 69:1684-1699.

Leem JW, Willis WD, Weller SC, Chung JM (1993b) Differential activation and classification of cutaneous afferents in the rat. J Neurophysiol 70:2411-2424.

Lembeck F, Donnerer J, Colpaert FC (1981) Increase of substance P in primary afferent nerves during chronic pain. Neuropeptides 1:175-180.

Lemonnier L, Trebak M, Putney JW, Jr. (2008) Complex regulation of the TRPC3, 6 and 7 channel subfamily by diacylglycerol and phosphatidylinositol-4,5-bisphosphate. Cell Calcium 43(5):506-14.

Lewin GR, Moshourab R (2004) Mechanosensation and pain. J Neurobiol 61:30-44.

Lewin GR, Ritter AM, Mendell LM (1993) Nerve growth factor-induced hyperalgesia in the neonatal and adult rat. J Neurosci 13:2136-2148.

Lewin GR, Rueff A, Mendell LM (1994) Peripheral and central mechanisms of NGF-induced hyperalgesia. Eur J Neurosci 6:1903-1912.

Li CY, Song YH, Higuera ES, Luo ZD (2004) Spinal Dorsal Horn Calcium Channel {alpha}2{delta}-1 Subunit Upregulation Contributes to Peripheral Nerve Injury-Induced Tactile Allodynia. J Neurosci 24:8494-8499.

Li HS, Xu XZ, Montell C (1999) Activation of a TRPC3-dependent cation current through the neurotrophin BDNF. Neuron 24(1):261-73.

Li Y, Jia YC, Cui K, Li N, Zheng ZY, Wang YZ, Yuan XB (2005) Essential role of TRPC channels in the guidance of nerve growth cones by brain-derived neurotrophic factor.[see comment]. Nature 434(7035):894-8.

Liedtke W, Choe Y, Marti-Renom MA, Bell AM, Denis CS, Sali A, Hudspeth AJ, Friedman JM, Heller S (2000) Vanilloid receptor-related osmotically activated channel (VR-OAC), a candidate vertebrate osmoreceptor. Cell 103:525-535.

Liedtke W, Tobin DM, Bargmann CI, Friedman JM (2003) Mammalian TRPV4 (VR-OAC) directs behavioral responses to osmotic and mechanical stimuli in Caenorhabditis elegans. Proc Natl Acad Sci U S A 100 Suppl 2:14531-14536.

Lievremont JP, Bird GS, Putney JW, Jr. (2004) Canonical transient receptor potential TRPC7 can function as both a receptor- and store-operated channel in HEK-293 cells. American Journal of Physiology - Cell Physiology 287(6):C1709-16.

Liu B, Linley JE, Du X, Zhang X, Ooi L, Zhang H, Gamper N (2010) The acute nociceptive signals induced by bradykinin in rat sensory neurons are mediated by inhibition of M-type K+ channels and activation of Ca2+-activated ClΓÇô channels. The Journal of Clinical Investigation 120:1240-1252.

Loot AE, Popp R+, Fisslthaler B, Vriens J, Nilius B, Fleming I (2008) Role of cytochrome P450-dependent transient receptor potential V4 activation in flow-induced vasodilatation. Cardiovascular Research 80:445-452.

Lu ZH, Books JT, Kaufman RM, Ley TJ (2003) Long targeting arms do not increase the efficiency of homologous recombination in the {beta}-globin locus of murine embryonic stem cells. Blood 102:1531-1533.

Lumpkin EA, Caterina MJ (2007) Mechanisms of sensory transduction in the skin. Nature 445:858-865.

Luo ZD, Chaplan SR, Higuera ES, Sorkin LS, Stauderman KA, Williams ME, Yaksh TL (2001) Upregulation of Dorsal Root Ganglion {alpha}2{delta} Calcium Channel Subunit and Its Correlation with Allodynia in Spinal Nerve-Injured Rats. J Neurosci 21:1868-1875.

Lussier MP, Cayouette S, Lepage PK, Bernier CL, Francoeur N, St-Hilaire M, Pinard M, Boulay G (2005) MxA, a Member of the Dynamin Superfamily, Interacts with the Ankyrin-like Repeat Domain of TRPC. Journal of Biological Chemistry 280:19393-19400.

MacIver MB, Tanelian DL (1993) Free nerve ending terminal morphology is fiber type specific for A delta and C fibers innervating rabbit corneal epithelium. J Neurophysiol 69:1779-1783.

Mansikka H, Pertovaara A (1995) Influence of selective [alpha]2-adrenergic agents on mustard oil-induced central hyperalgesia in rats. European Journal of Pharmacology 281:43-48.

Marcotti W, Geleoc GS, Lennan GW, Kros CJ (1999) Transient expression of an inwardly rectifying potassium conductance in developing inner and outer hair cells along the mouse cochlea. Pflugers Arch 439:113-122.

Marks PW, Arai M, Bandura JL, Kwiatkowski DJ (1998) Advillin (p92): a new member of the gelsolin/villin family of actin regulatory proteins. J Cell Sci 111:2129-2136.

McCarter GC, Reichling DB, Levine JD (1999) Mechanical transduction by rat dorsal root ganglion neurons in vitro. Neuroscience Letters 273:179-182.

McKemy DD, Neuhausser WM, Julius D (2002) Identification of a cold receptor reveals a general role for TRP channels in thermosensation. Nature 416(6876):52-8.

McMahon S, Koltzenburg M (1990a) The changing role of primary afferent neurones in pain. Pain 43:269-272.

McMahon SB, Koltzenburg M (1990b) Novel classes of nociceptors: beyond Sherrington. Trends in Neurosciences 13:199-201.

McNamara CR, Mandel-Brehm J, Bautista DM, Siemens J, Deranian KL, Zhao M, Hayward NJ, Chong JA, Julius D, Moran MM, Fanger CM (2007) TRPA1 mediates formalin-induced pain. Proc Natl Acad Sci U S A 104:13525-13530.

Meyer RA, Davis KD, Cohen RH, Treede RD, Campbell JN (1991) Mechanically insensitive afferents (MIAs) in cutaneous nerves of monkey. Brain Research 561:252-261.

Mobarakeh JI, Sakurada S, Katsuyama S, Kutsuwa M, Kuramasu A, Lin ZY, Watanabe T, Hashimoto Y, Yanai K (2000) Role of histamine H(1) receptor in pain perception: a study of the receptor gene knockout mice. Eur J Pharmacol 391:81-89.

Mobarakeh JI, Takahashi K, Sakurada S, Kuramasu A, Yanai K (2006) Enhanced antinociceptive effects of morphine in histamine H2 receptor gene knockout mice. Neuropharmacology 51:612-622.

Molliver DC, Snider WD (1997) Nerve growth factor receptor TrkA is down-regulated during postnatal development by a subset of dorsal root ganglion neurons. J Comp Neurol 381:428-438.

Molliver DC, Wright DE, Leitner ML, Parsadanian AS, Doster K, Wen D, Yan Q, Snider WD (1997) IB4-Binding DRG Neurons Switch from NGF to GDNF Dependence in Early Postnatal Life. Neuron 19:849-861.

Montell C (2005) The TRP superfamily of cation channels. Sci STKE 2005:re3.

Montell C, Rubin GM (1989) Molecular characterization of the Drosophila trp locus: a putative integral membrane protein required for phototransduction. Neuron 2(4):1313-23.

Moqrich A, Hwang SW, Earley TJ, Petrus MJ, Murray AN, Spencer KS, Andahazy M, Story GM, Patapoutian A (2005) Impaired thermosensation in mice lacking TRPV3, a heat and camphor sensor in the skin. Science 307:1468-1472.

Moriyama T, Higashi T, Togashi K, Iida T, Segi E, Sugimoto Y, Tominaga T, Narumiya S, Tominaga M (2005) Sensitization of TRPV1 by EP1 and IP reveals peripheral nociceptive mechanism of prostaglandins. Molecular Pain 1:3.

Munns C, AlQatari M, Koltzenburg M (2007) Many cold sensitive peripheral neurons of the mouse do not express TRPM8 or TRPA1. Cell Calcium 41:331-342.

Munsch T, Freichel M, Flockerzi V, Pape HC (2003) Contribution of transient receptor potential channels to the control of GABA release from dendrites. Proceedings of the National Academy of Sciences of the United States of America 100:16065-16070.

Nagata K, Duggan A, Kumar G, Garcia-Anoveros J (2005) Nociceptor and Hair Cell Transducer Properties of TRPA1, a Channel for Pain and Hearing. J Neurosci 25:4052-4061.

Nassar MA, Baker MD, Levato A, Ingram R, Mallucci G, McMahon SB, Wood JN (2006) Nerve injury induces robust allodynia and ectopic discharges in Nav1.3 null mutant mice. Mol Pain 2:33.

Nassar MA, Stirling LC, Forlani G, Baker MD, Matthews EA, Dickenson AH, Wood JN (2004) Nociceptor-specific gene deletion reveals a major role for Nav1.7 (PN1) in acute and inflammatory pain. Proceedings of the National Academy of Sciences of the United States of America 101:12706-12711.

Noguchi K, Kawai Y, Fukuoka T, Senba E, Miki K (1995) Substance P induced by peripheral nerve injury in primary afferent sensory neurons and its effect on dorsal column nucleus neurons. J Neurosci 15:7633-7643.

Oancea E, Wolfe JT, Clapham DE (2006) Functional TRPM7 Channels Accumulate at the Plasma Membrane in Response to Fluid Flow. Circulation Research 98:245-253.

Obata K, Katsura H, Mizushima T, Yamanaka H, Kobayashi K, Dai Y, Fukuoka T, Tokunaga A, Tominaga M, Noguchi K (2005) TRPA1 induced in sensory neurons contributes to cold hyperalgesia after inflammation and nerve injury. J Clin Invest 115:2393-2401.

Okada T, Inoue R, Yamazaki K, Maeda A, Kurosaki T, Yamakuni T, Tanaka I, Shimizu S, Ikenaka K, Imoto K, Mori Y (1999) Molecular and functional characterization of a novel mouse transient receptor potential protein homologue TRP7. Ca(2+)-permeable cation channel that is constitutively activated and enhanced by stimulation of G protein-coupled receptor. J Biol Chem 274:27359-27370.

Olsen UB, Eltorp CT, Ingvardsen BK, Jorgensen TK, Lundbaek JA, Thomsen C, Hansen AJ (2002) ReN 1869, a novel tricyclic antihistamine, is active against neurogenic pain and inflammation. Eur J Pharmacol 435:43-57.

Otsuka Y, Sakagami H, Owada Y, Kondo H (1998) Differential localization of mRNAs for mammalian trps, presumptive capacitative calcium entry channels, in the adult mouse brain. Tohoku J Exp Med 185:139-146.

Peier AM, Moqrich A, Hergarden AC, Reeve AJ, Andersson DA, Story GM, Earley TJ, Dragoni I, McIntyre P, Bevan S, Patapoutian A (2002a) A TRP channel that senses cold stimuli and menthol. Cell 108:705-715.

Peier AM, Reeve AJ, Andersson DA, Moqrich A, Earley TJ, Hergarden AC, Story GM, Colley S, Hogenesch JB, McIntyre P, Bevan S, Patapoutian A (2002b) A heat-sensitive TRP channel expressed in keratinocytes. Science 296:2046-2049.

Pesquero JB, Araujo RC, Heppenstall PA, Stucky CL, Silva JA, Jr., Walther T, Oliveira SM, Pesquero JL, Paiva AC, Calixto JB, Lewin GR, Bader M (2000) Hypoalgesia and altered inflammatory responses in mice lacking kinin B1 receptors.[see comment]. Proceedings of the National Academy of Sciences of the United States of America 97(14):8140-5.

Petes TD (2001) Meiotic recombination hot spots and cold spots. Nat Rev Genet 2:360-369.

Pfaffl MW (2001) A new mathematical model for relative quantification in real-time RT-PCR. Nucleic Acids Res 29:e45.

Phan PA, Tadros SF, Kim Y, Birnbaumer L, Housley GD (2010) Developmental regulation of TRPC3 ion channel expression in the mouse cochlea. Histochem Cell Biol 133:437-448.

Philipp S, Cavalie A, Freichel M, Wissenbach U, Zimmer S, Trost C, Marquart A, Murakami M, Flockerzi V (1996) A mammalian capacitative calcium entry channel homologous to Drosophila TRP and TRPL. EMBO J 15:6166-6171.

Philipp S, Hambrecht J, Braslavski L, Schroth G, Freichel M, Murakami M, Cavalie A, Flockerzi V (1998) A novel capacitative calcium entry channel expressed in excitable cells. EMBO J 17:4274-4282.

Philipp S, Trost C, Warnat J, Rautmann J, Himmerkus N, Schroth G, Kretz O, Nastainczyk W, Cavalie A, Hoth M, Flockerzi V (2000) TRP4 (CCE1) protein is part of native calcium release-activated Ca2+-like channels in adrenal cells. J Biol Chem 275:23965-23972.

Phillips AM, Bull A, Kelly LE (1992) Identification of a Drosophila gene encoding a calmodulin-binding protein with homology to the trp phototransduction gene. Neuron 8(4):631-42.

Price MP, Lewin GR, McIlwrath SL, Cheng C, Xie J, Heppenstall PA, Stucky CL, Mannsfeldt AG, Brennan TJ, Drummond HA, Qiao J, Benson CJ, Tarr DE, Hrstka RF, Yang B, Williamson RA, Welsh MJ (2000) The mammalian sodium channel BNC1 is required for normal touch sensation. Nature 407:1007-1011.

Price MP, McIlwrath SL, Xie J, Cheng C, Qiao J, Tarr DE, Sluka KA, Brennan TJ, Lewin GR, Welsh MJ (2001) The DRASIC Cation Channel Contributes to the Detection of Cutaneous Touch and Acid Stimuli in Mice. Neuron 32:1071-1083.

Priest BT, Murphy BA, Lindia JA, Diaz C, Abbadie C, Ritter AM, Liberator P, Iyer LM, Kash SF, Kohler MG, Kaczorowski GJ, MacIntyre DE, Martin WJ (2005) Contribution of the tetrodotoxin-resistant voltage-gated sodium channel NaV1.9 to sensory transmission and nociceptive behavior. Proc Natl Acad Sci U S A 102:9382-9387.

Rahman W, Suzuki R, Webber M, Hunt SP, Dickenson AH (2006) Depletion of endogenous spinal 5-HT attenuates the behavioural hypersensitivity to mechanical and cooling stimuli induced by spinal nerve ligation. Pain 123:264-274.

Ramsey IS, Delling M, Clapham DE (2006) An introduction to TRP channels. Annu Rev Physiol 68:619-647.

Raouf R, Quick K, Wood JN (2010) Pain as a channelopathy. J Clin Invest 120:3745-3752.

Rashid MH, Inoue M, Matsumoto M, Ueda H (2004) Switching of Bradykinin-Mediated Nociception Following Partial Sciatic Nerve Injury in Mice. J Pharmacol Exp Ther 308:1158-1164.

Ravenall SJ, Gavazzi I, Wood JN, Akopian AN (2002) A peripheral nervous system actin-binding protein regulates neurite outgrowth. European Journal of Neuroscience 15:281-290.

Regoli D, Barabe J (1980) Pharmacology of bradykinin and related kinins. Pharmacol Rev 32:1-46.

Reid G, Flonta M (2001a) Cold transduction by inhibition of a background potassium conductance in rat primary sensory neurones. Neurosci Lett 297:171-174.

Reid G, Flonta ML (2001b) Physiology. Cold current in thermoreceptive neurons. Nature 413:480.

Reid LH, Shesely EG, Kim HS, Smithies O (1991) Cotransformation and gene targeting in mouse embryonic stem cells. Mol Cell Biol 11:2769-2777.

Rexed B (1952) The cytoarchitectonic organization of the spinal cord in the cat. J Comp Neurol 96:414-495.

Riccio A, Mattei C, Kelsell RE, Medhurst AD, Calver AR, Randall AD, Davis JB, Benham CD, Pangalos MN (2002a) Cloning and functional expression of human short TRP7, a candidate protein for store-operated Ca2+ influx. J Biol Chem 277:12302-12309.

Riccio A, Medhurst AD, Mattei C, Kelsell RE, Calver AR, Randall AD, Benham CD, Pangalos MN (2002b) mRNA distribution analysis of human TRPC family in CNS and peripheral tissues. Brain Research Molecular Brain Research 109(1-2):95-104.

Rodriguez-Santiago M, Mendoza-Torres M, Jimθnez-Bremont JF, L≤pez-Revilla R (2007) Knockout of the trcp3 gene causes a recessive neuromotor disease in mice. Biochemical and Biophysical Research Communications 360:874-879.

Rosland JH (1991) The formalin test in mice: the influence of ambient temperature. Pain 45:211-216.

Rueff A, Mendell LM (1996) Nerve growth factor NT-5 induce increased thermal sensitivity of cutaneous nociceptors in vitro. Journal of Neurophysiology 76:3593-3596.

Safieh-Garabedian B, Poole S, Allchorne A, Winter J, Woolf CJ (1995) Contribution of interleukin-1 beta to the inflammation-induced increase in nerve growth factor levels and inflammatory hyperalgesia. Br J Pharmacol 115:1265-1275.

Saleh SN, Albert AP, Peppiatt CM, Large WA (2006) Angiotensin II activates two cation conductances with distinct TRPC1 and TRPC6 channel properties in rabbit mesenteric artery myocytes. J Physiol 577:479-495.

Sauer B, Henderson N (1988) Site-specific DNA recombination in mammalian cells by the Cre recombinase of bacteriophage P1. Proceedings of the National Academy of Sciences of the United States of America 85:5166-5170.

Schaefer M, Plant TD, Obukhov AG, Hofmann T, Gudermann T, Schultz G (2000) Receptor-mediated regulation of the nonselective cation channels TRPC4 and TRPC5. Journal of Biological Chemistry 275(23):17517-26.

Schafers M, Svensson CI, Sommer C, Sorkin LS (2003) Tumor Necrosis Factor-alpha Induces Mechanical Allodynia after Spinal Nerve Ligation by Activation of p38 MAPK in Primary Sensory Neurons. J Neurosci 23:2517-2521.

Schaible HG, Schmidt RF (1988) Time course of mechanosensitivity changes in articular afferents during a developing experimental arthritis. Journal of Neurophysiology 60(6):2180-95.

Schnitzler M, Storch U, Meibers S, Nurwakagari P, Breit A, Essin K, Gollasch M, Gudermann T (2008) Gq-coupled receptors as mechanosensors mediating myogenic vasoconstriction. EMBO J 27:3092-3103.

Schwenk F, Baron U, Rajewsky K (1995) A cre-transgenic mouse strain for the ubiquitous deletion of loxP-flanked gene segments including deletion in germ cells. Nucl Acids Res 23:5080-5081.

Selli C, Erac Y, Kosova B, Tosun M (2008) Post-transcriptional silencing of TRPC1 ion channel gene by RNA interference upregulates TRPC6 expression and store-operated Ca2+ entry in A7r5 vascular smooth muscle cells. Vascular Pharmacology 51:96-100.

Setoguchi M, Ohya Y, Abe I, Fujishima M (1997) Stretch-activated whole-cell currents in smooth muscle cells from mesenteric resistance artery of guinea-pig. Journal of Physiology 501 (Pt 2):343-53.

Settmacher B, Rheinheimer C, Hamacher H, Ames R, Wise A, Jenkinson L, Bock D, Schaefer M, K+Âhl J, Klos A (2003) Structure-function studies of the C3a-receptor: C-terminal serine and threonine residues which influence receptor internalization and signaling. Eur J Immunol 33:920-927.

Sharif-Naeini R (2008) TRP channels and mechanosensory transduction: insights into the arterial myogenic response. [Review] [107 refs].

Sharpe EF, Kingston AE, Lodge D, Monn JA, Headley PM (2002) Systemic pre-treatment with a group II mGlu agonist, LY379268, reduces hyperalgesia in vivo. Br J Pharmacol 135:1255-1262.

Shen J, Harada N, Kubo N, Liu B, Mizuno A, Suzuki M, Yamashita T (2006) Functional expression of transient receptor potential vanilloid 4 in the mouse cochlea. Neuroreport 17:135-139.

Shibata M, Ishii J, Koizumi H, Shibata N, Dohmae N, Takio K, Adachi H, Tsujimoto M, Arai H (2004) Type F Scavenger Receptor SREC-I Interacts with Advillin, a Member of the Gelsolin/Villin Family, and Induces Neurite-like Outgrowth. Journal of Biological Chemistry 279:40084-40090.

Sidi S, Friedrich RW, Nicolson T (2003) NompC TRP channel required for vertebrate sensory hair cell mechanotransduction. Science 301:96-99.

Simone DA, Kajander KC (1997) Responses of cutaneous A-fiber nociceptors to noxious cold. J Neurophysiol 77:2049-2060.

Singh BB, Liu X, Tang J, Zhu MX, Ambudkar IS (2002) Calmodulin Regulates Ca2+-Dependent Feedback Inhibition of Store-Operated Ca2+ Influx by Interaction with a Site in the C Terminus of TrpC1. Molecular Cell 9:739-750.

Singh BB, Lockwich TP, Bandyopadhyay BC, Liu X, Bollimuntha S, Brazer Sc, Combs C, Das S, Leenders AGM, Sheng ZH, Knepper MA, Ambudkar SV, Ambudkar IS (2004) VAMP2-Dependent Exocytosis Regulates Plasma Membrane Insertion of TRPC3 Channels and Contributes to Agonist-Stimulated Ca2+ Influx. Molecular Cell 15:635-646.

Sluka KA, Price MP, Breese NM, Stucky CL, Wemmie JA, Welsh MJ (2003) Chronic hyperalgesia induced by repeated acid injections in muscle is abolished by the loss of ASIC3, but not ASIC1. Pain 106:229-239.

Smith GD, Harmar AJ, McQueen DS, Seckl JR (1992) Increase in substance P and CGRP, but not somatostatin content of innervating dorsal root ganglia in adjuvant monoarthritis in the rat. Neurosci Lett 137:257-260.

Smithies O, Gregg RG, Boggs SS, Koralewski MA, Kucherlapati RS (1985) Insertion of DNA sequences into the human chromosomal [beta]-globin locus by homologous recombination. Nature 317:230-234.

Smyth JT, Lemonnier L, Vazquez G, Bird GS, Putney JW, Jr. (2006) Dissociation of regulated trafficking of TRPC3 channels to the plasma membrane from their activation by phospholipase C. Journal of Biological Chemistry 281(17):11712-20.

Snider WD, McMahon SB (1998) Tackling pain at the source: new ideas about nociceptors. Neuron 20:629-632.

Sommer C, Schmidt C, George A (1998) Hyperalgesia in experimental neuropathy is dependent on the TNF receptor 1. Exp Neurol 151:138-142.

Sommer C, Kress M (2004) Recent findings on how proinflammatory cytokines cause pain: peripheral mechanisms in inflammatory and neuropathic hyperalgesia. Neuroscience Letters 361:184-187.

Souslova V, Cesare P, Ding Y, Akopian AN, Stanfa L, Suzuki R, Carpenter K, Dickenson A, Boyce S, Hill R, Nebenuis-Oosthuizen D, Smith AJ, Kidd EJ, Wood JN (2000) Warm-coding deficits and aberrant inflammatory pain in mice lacking P2X3 receptors.[see comment]. Nature 407(6807):1015-7.

Southall MD, Vasko MR (2000) Prostaglandin E(2)-mediated sensitization of rat sensory neurons is not altered by nerve growth factor. Neurosci Lett 287:33-36.

Spassova MA, Hewavitharana T, Xu W, Soboloff J, Gill DL (2006) A common mechanism underlies stretch activation and receptor activation of TRPC6 channels. Proceedings of the National Academy of Sciences of the United States of America 103(44):16586-91.

Stanfa LCC, Dickenson AH (1994) Enhanced alpha-2 adrenergic controls and spinal morphine potency in inflammation. [Miscellaneous]. Neuroreport 5:469-472.

Staniland AA, McMahon SB (2008) Mice lacking acid-sensing ion channels (ASIC) 1 or 2, but not ASIC3, show increased pain behaviour in the formalin test. Eur J Pain.

Stirling LC, Forlani G, Baker MD, Wood JN, Matthews EA, Dickenson AH, Nassar MA (2005) Nociceptor-specific gene deletion using heterozygous NaV1.8-Cre recombinase mice. Pain 113:27-36.

Story GM, Peier AM, Reeve AJ, Eid SR, Mosbacher J, Hricik TR, Earley TJ, Hergarden AC, Andersson DA, Hwang SW, McIntyre P, Jegla T, Bevan S, Patapoutian A (2003) ANKTM1, a TRP-like channel expressed in nociceptive neurons, is activated by cold temperatures. Cell 112(6):819-29.

Strotmann R, Harteneck C, Nunnenmacher K, Schultz G, Plant TD (2000) OTRPC4, a nonselective cation channel that confers sensitivity to extracellular osmolarity. Nat Cell Biol 2:695-702.

Strubing C, Krapivinsky G, Krapivinsky L, Clapham DE (2001) TRPC1 and TRPC5 form a novel cation channel in mammalian brain. Neuron 29:645-655.

Strubing C, Krapivinsky G, Krapivinsky L, Clapham DE (2003) Formation of novel TRPC channels by complex subunit interactions in embryonic brain. Journal of Biological Chemistry 278(40):39014-9.

Stucky CL, Lewin GR (1999) Isolectin B4-Positive and -Negative Nociceptors Are Functionally Distinct. J Neurosci 19:6497-6505.

Suchyna TM, Johnson JH, Hamer K, Leykam JF, Gage DA, Clemo HF, Baumgarten CM, Sachs F (2000) Identification of a peptide toxin from Grammostola spatulata spider venom that blocks cation-selective stretch-activated channels.[erratum appears in J Gen Physiol 2001 Apr;117(4):371]. Journal of General Physiology 115(5):583-98.

Suchyna TM, Tape SE, Koeppe RE, Andersen OS, Sachs F, Gottlieb PA (2004) Bilayer-dependent inhibition of mechanosensitive channels by neuroactive peptide enantiomers.[see comment]. Nature 430(6996):235-40.

Suzuki M, Mizuno A, Kodaira K, Imai M (2003) Impaired Pressure Sensation in Mice Lacking TRPV4. J Biol Chem 278:22664-22668.

Suzuki R, Rygh LJ, Dickenson AH (2004) Bad news from the brain: descending 5-HT pathways that control spinal pain processing. Trends Pharmacol Sci 25:613-617.

Tabuchi K, Suzuki M, Mizuno A, Hara A (2005) Hearing impairment in TRPV4 knockout mice. Neurosci Lett 382:304-308.

Tadros SF, Kim Y, Phan PA, Birnbaumer L, Housley GD (2010) TRPC3 ion channel subunit immunolocalization in the cochlea. Histochem Cell Biol 133:137-147.

Taiwo YO, Goetzl EJ, Levine JD (1987) Hyperalgesia onset latency suggests a hierarchy of action. Brain Res 423:333-337.

Takesue EI, Schaefer W, Jukniewicz E (1969) Modification of the Randall-Selitto analgesic apparatus. J Pharm Pharmacol 21:788-789.

Takumida M, Anniko M (2009) Expression of canonical transient receptor potential channel (TRPC) 1ΓÇô7 in the mouse inner ear. Acta Oto-laryngologica 129:1351-1358.

Tanabe M, Ono K, Honda M, Ono H (2009) Gabapentin and pregabalin ameliorate mechanical hypersensitivity after spinal cord injury in mice. European Journal of Pharmacology 609:65-68.

Tang J, Lin YK, Zhang ZM, Tikunova S, Birnbaumer L, Zhu MX (2001) Identification of common binding sites for calmodulin and inositol 1,4,5-trisphosphate receptors on the carboxyl termini of Trp channels. J Biol Chem 276:21303-21310.

Tate S, Benn S, Hick C, Trezise D, John V, Mannion RJ, Costigan M, Plumpton C, Grose D, Gladwell Z, Kendall G, Dale K, Bountra C, Woolf CJ (1998) Two sodium channels contribute to the TTX-R sodium current in primary sensory neurons. Nat Neurosci 1:653-655.

Thilo F, Scholze A, Liu DY, Zidek W, Tepel M (2008) Association of transient receptor potential canonical type 3 (TRPC3) channel transcripts with proinflammatory cytokines. Archives of Biochemistry and Biophysics 471:57-62.

Thomas KR, Capecchi MR (1987) Site-Directed Mutagenesis by Gene Targeting in Mouse Embryo-Derived Stem-Cells. Cell 51:503-512.

Tiruppathi C, Freichel M, Vogel SM, Paria BC, Mehta D, Flockerzi V, Malik AB (2002) Impairment of store-operated Ca2+ entry in TRPC4(-/-) mice interferes with increase in lung microvascular permeability. Circ Res 91:70-76.

Todd AJ (2002) Anatomy of primary afferents and projection neurones in the rat spinal dorsal horn with particular emphasis on substance P and the neurokinin 1 receptor. Experimental Physiology 87:245-249.

Tolle T, Freynhagen R, Versavel M, Trostmann U, Young J (2008) Pregabalin for relief of neuropathic pain associated with diabetic neuropathy: A randomized, double-blind study. European Journal of Pain 12:203-213.

Tominaga M, Caterina MJ, Malmberg AB, Rosen TA, Gilbert H, Skinner K, Raumann BE, Basbaum AI, Julius D (1998) The cloned capsaicin receptor integrates multiple pain-producing stimuli. Neuron 21:531-543.

Trebak M, Bird GS, McKay RR, Putney JW, Jr. (2002) Comparison of human TRPC3 channels in receptor-activated and store-operated modes. Differential sensitivity to channel blockers suggests fundamental differences in channel composition. Journal of Biological Chemistry 277(24):21617-23.

Treede RD, Meyer RA, Raja SN, Campbell JN (1995) Evidence for two different heat transduction mechanisms in nociceptive primary afferents innervating monkey skin. The Journal of Physiology 483:747-758.

Tsuda M, Ueno S, Inoue K (1999) Evidence for the involvement of spinal endogenous ATP and P2X receptors in nociceptive responses caused by formalin and capsaicin in mice. Br J Pharmacol 128:1497-1504.

Uda R, Horiguchi S, Ito S, Hyodo M, Hayaishi O (1990) Nociceptive effects induced by intrathecal administration of prostaglandin D2, E2, or F2[alpha] to conscious mice. Brain Research 510:26-32.

Van HJ, Gybels JM (1972) Pain related to single afferent C fibers from human skin. Brain Res 48:397-400.

Vannier B, Zhu X, Brown D, Birnbaumer L (1998) The membrane topology of human transient receptor potential 3 as inferred from glycosylation-scanning mutagenesis and epitope immunocytochemistry. J Biol Chem 273:8675-8679.

Vazquez G, Wedel BJ, Kawasaki BT, Bird GS, Putney JW (2004) Obligatory Role of Src Kinase in the Signaling Mechanism for TRPC3 Cation Channels. Journal of Biological Chemistry 279:40521-40528.

Vazquez G, Wedel BJ, Trebak M, John Bird G, Putney JW, Jr. (2003) Expression Level of the Canonical Transient Receptor Potential 3 (TRPC3) Channel Determines Its Mechanism of Activation. J Biol Chem 278:21649-21654.

Venkatachalam K, Ma HT, Ford DL, Gill DL (2001) Expression of functional receptor-coupled TRPC3 channels in DT40 triple receptor InsP3 knockout cells. J Biol Chem 276:33980-33985.

Venkatachalam K, Montell C (2007) TRP channels. Annu Rev Biochem 76:387-417.

Viana F, De La PE, Belmonte C (2002) Specificity of cold thermotransduction is determined by differential ionic channel expression. Nat Neurosci 5:254-260.

Voets T, Nilius B (2003) The pore of TRP channels: trivial or neglected? Cell Calcium 33:299-302.

Waldmann R, Bassilana F, de WJ, Champigny G, Heurteaux C, Lazdunski M (1997) Molecular cloning of a non-inactivating proton-gated Na+ channel specific for sensory neurons. J Biol Chem 272:20975-20978.

Wall PD, Melzack R, McMahon SB, Koltzenburg M (2005) Wall and Melzack's Textbook of Pain. Churchill Livingstone.

Wang S, Dai Y, Fukuoka T, Yamanaka H, Kobayashi K, Obata K, Cui X, Tominaga M, Noguchi K (2008) Phospholipase C and protein kinase A mediate bradykinin sensitization of TRPA1: a molecular mechanism of inflammatory pain. Brain 131:1241-1251.

Watanabe H, Davis JB, Smart D, Jerman JC, Smith GD, Hayes P, Vriens J, Cairns W, Wissenbach U, Prenen J, Flockerzi V, Droogmans G, Benham CD, Nilius B (2002) Activation of TRPV4 Channels (hVRL-2/mTRP12) by Phorbol Derivatives. J Biol Chem 277:13569-13577.

Welsh DG, Morielli AD, Nelson MT, Brayden JE (2002) Transient receptor potential channels regulate myogenic tone of resistance arteries. Circulation Research 90(3):248-50.

Welsh DG, Nelson MT, Eckman DM, Brayden JE (2000) Swelling-activated cation channels mediate depolarization of rat cerebrovascular smooth muscle by hyposmolarity and intravascular pressure. Journal of Physiology 527 Pt 1:139-48.

West JW, Patton DE, Scheuer T, Wang Y, Goldin AL, Catterall WA (1992) A cluster of hydrophobic amino acid residues required for fast Na(+)-channel inactivation. Proc Natl Acad Sci U S A 89:10910-10914.

Wetzel C, Hu J, Riethmacher D, Benckendorff A, Harder L, Eilers A, Moshourab R, Kozlenkov A, Labuz D, Caspani O, Erdmann B, Machelska H, Heppenstall PA, Lewin GR (2007) A stomatin-domain protein essential for touch sensation in the mouse. Nature 445:206-209.

White TA, Xue A, Chini EN, Thompson M, Sieck GC, Wylam ME (2006) Role of Transient Receptor Potential C3 in TNF-{alpha}-Enhanced Calcium Influx in Human Airway Myocytes. Am J Respir Cell Mol Biol 35:243-251.

Winn MP, Conlon PJ, Lynn KL, Farrington MK, Creazzo T, Hawkins AF, Daskalakis N, Kwan SY, Ebersviller S, Burchette JL, Pericak-Vance MA, Howell DN, Vance JM, Rosenberg PB (2005) A mutation in the TRPC6 cation channel causes familial focal segmental glomerulosclerosis. Science 308:1801-1804.

Woolf CJ, Allchorne A, Safieh-Garabedian B, Poole S (1997) Cytokines, nerve growth factor and inflammatory hyperalgesia: the contribution of tumour necrosis factor alpha. Br J Pharmacol 121:417-424.

Woolf CJ, Safieh-Garabedian B, Ma QP, Crilly P, Winter J (1994) Nerve growth factor contributes to the generation of inflammatory sensory hypersensitivity. Neuroscience 62:327-331.

Worley PF, Zeng W, Huang GN, Yuan JP, Kim JY, Lee MG, Muallem S (2007) TRPC channels as STIM1-regulated store-operated channels. Cell Calcium 42:205-211.

Wu D, Huang W, Richardson PM, Priestley JV, Liu M (2007) TRPC4 in rat dorsal root ganglion neurons is increased after nerve injury and is necessary for neurite outgrowth. J Biol ChemM703177200.

Wu X, Zagranichnaya TK, Gurda GT, Eves EM, Villereal ML (2004) A TRPC1/TRPC3-mediated increase in store-operated calcium entry is required for differentiation of H19-7 hippocampal neuronal cells. Journal of Biological Chemistry 279(42):43392-402.

Xu GY, Huang LYM (2002) Peripheral Inflammation Sensitizes P2X Receptor-Mediated Responses in Rat Dorsal Root Ganglion Neurons. J Neurosci 22:93-102.

Xu H, Ramsey IS, Kotecha SA, Moran MM, Chong JA, Lawson D, Ge P, Lilly J, Silos-Santiago I, Xie Y, DiStefano PS, Curtis R, Clapham DE (2002) TRPV3 is a calcium-permeable temperature-sensitive cation channel. Nature 418(6894):181-6.

Yang X, Yang HB, Xie QJ, Liu XH, Hu XD (2009) Peripheral inflammation increased the synaptic expression of NMDA receptors in spinal dorsal horn. Pain 144:162-169.

Yang Y, Wang Y, Li S, Xu Z, Li H, Ma L, Fan J, Bu D, Liu B, Fan Z, Wu G, Jin J, Ding B, Zhu X, Shen Y (2004) Mutations in SCN9A, encoding a sodium channel alpha subunit, in patients with primary erythermalgia. J Med Genet 41:171-174.

Yuan JP, Zeng W, Huang GN, Worley PF, Muallem S (2007) STIM1 heteromultimerizes TRPC channels to determine their function as store-operated channels. Nat Cell Biol 9:636-645.

Yuan JP, Kiselyov K, Shin DM, Chen J, Shcheynikov N, Kang SH, Dehoff MH, Schwarz MK, Seeburg PH, Muallem S, Worley PF (2003) Homer Binds TRPC Family Channels and Is Required for Gating of TRPC1 by IP3 Receptors. Cell 114:777-789.

Zagranichnaya TK, Wu X, Villereal ML (2005) Endogenous TRPC1, TRPC3, and TRPC7 proteins combine to form native store-operated channels in HEK-293 cells. Journal of Biological Chemistry 280(33):29559-69.

Zeitz KP, Guy N, Malmberg AB, Dirajlal S, Martin WJ, Sun L, Bonhaus DW, Stucky CL, Julius D, Basbaum AI (2002) The 5-HT3 subtype of serotonin receptor contributes to nociceptive processing via a novel subset of myelinated and unmyelinated nociceptors. J Neurosci 22:1010-1019.

Zhang L, Lu Y, Chen Y, Westlund KN (2002) Group I Metabotropic Glutamate Receptor Antagonists Block Secondary Thermal Hyperalgesia in Rats with Knee Joint Inflammation. Journal of Pharmacology and Experimental Therapeutics 300:149-156.

Zhang P, Luo Y, Chasan B, Gonzalez-Perrett S, Montalbetti N, Timpanaro GA, Cantero MdR, Ramos AJ, Goldmann WH, Zhou J, Cantiello HF (2009) The multimeric structure of

polycystin-2 (TRPP2): structural-functional correlates of homo- and hetero-multimers with TRPC1. Hum Mol Genet 18:1238-1251.

Zhao J, Yuan G, Cendan CM, Nassar MA, Lagerstrom MC, Kullander K, Gavazzi I, Wood JN (2010) Nociceptor-expressed ephrin-B2 regulates inflammatory and neuropathic pain. Mol Pain 6:77.

Zhao J, Seereeram A, Nassar MA, Levato A, Pezet S, Hathaway G, Morenilla-Palao C, Stirling C, Fitzgerald M, McMahon SB, Rios M, Wood JN (2006) Nociceptor-derived brain-derived neurotrophic factor regulates acute and inflammatory but not neuropathic pain. Molecular and Cellular Neuroscience 31:539-548.

Zhong Y, Dunn PM, Bardini M, Ford APDW, Cockayne DA, Burnstock G (2001) Changes in P2X receptor responses of sensory neurons from P2X3 - deficient mice. European Journal of Neuroscience 14:1784-1792.

Zhou FW, Matta SG, Zhou FM (2008a) Constitutively active TRPC3 channels regulate basal ganglia output neurons. Journal of Neuroscience 28(2):473-82.

Zhou J, Du W, Zhou K, Tai Y, Yao H, Jia Y, Ding Y, Wang Y (2008b) Critical role of TRPC6 channels in the formation of excitatory synapses. Nat Neurosci 11:741-743.

Zhou L, Rowley DL, Mi QS, Sefcovic N, Matthes HW, Kieffer BL, Donovan DM (2001) Murine inter-strain polymorphisms alter gene targeting frequencies at the mu opioid receptor locus in embryonic stem cells. Mamm Genome 12:772-778.

Zhou X, Wang L, Hasegawa H, Amin P, Han BX, Kaneko S, He Y, Wang F (2010) Deletion of PIK3C3/Vps34 in sensory neurons causes rapid neurodegeneration by disrupting the endosomal but not the autophagic pathway. Proc Natl Acad Sci U S A 107:9424-9429.

Zhu CZ, Wilson SG, Mikusa JP, Wismer CT, Gauvin DM, Lynch JJ, III, Wade CL, Decker MW, Honore P (2004) Assessing the role of metabotropic glutamate receptor 5 in multiple nociceptive modalities. Eur J Pharmacol 506:107-118.

Zimmermann K, Leffler A, Babes A, Cendan CM, Carr RW, Kobayashi J, Nau C, Wood JN, Reeh PW (2007) Sensory neuron sodium channel Nav1.8 is essential for pain at low temperatures. Nature 447:855-858.

Zurborg S, Yurgionas B, Jira JA, Caspani O, Heppenstall PA (2007) Direct activation of the ion channel TRPA1 by Ca2+. Nat Neurosci 10:277-279.